Combination therapies in a patient-derived glioblastoma model

A STEP TOWARDS PRECISION MEDICINE

Lotte M.E. Berghauser Pont

Financial support
Financial support for the research conducted in this thesis was provided by the Foundation STOPhersentumoren.nl (Chapter 3 and 4). The research leading to the results of Chapter 3 has received funding from the European Community's Seventh Framework Programme (FP7/2007-2013) under grant agreement No. HEALTH-F2-2010-259893. Chapters 5 and 8 were financially supported by the Travel Fund of the Royal Dutch Wilhelmina Fund (KWF) and the Travel Fund of the EUR Trustfonds.

Financial support thesis printing
Printing of this thesis was kindly supported by the foundation STOPhersentumoren.nl, Promega, Zeiss, ErasmusMC, Ruben Dammers, Chipsoft and ABN AMRO.

Cover editing: Gijs Heuts
Cover photo: Geert Jan Jansen
Book layout: Zedline
Publisher: Berghauser Pont Publishing

ISBN 978-94-91930-39-3 (folio)
ISBN 978-94-91930-38-6 (digitaal)

Combination therapies in a patient-derived glioblastoma model

A STEP TOWARDS PRECISION MEDICINE

Combinatietherapieën in een uit patiënten afgeleid glioblastoommodel

EEN STAP RICHTING PRECISION MEDICINE

PROEFSCHRIFT

ter verkrijging van de graad van doctor aan de
Erasmus Universiteit Rotterdam
op gezag van de rector magnificus

Prof.dr. H.A.P. Pols

en volgens besluit van het College voor Promoties.
De openbare verdediging zal plaatsvinden op
woensdag 2 september 2015 om 15:30 uur

Lotte Marie Elise Berghauser Pont
geboren te Soest

Erasmus University Rotterdam

Erasmus

Promotoren:
Prof.dr. C.M.F. Dirven
Prof.dr. S. Leenstra

Copromotor:
Dr. M.L.M. Lamfers

Overige leden:
Prof.dr. M. J. van den Bent
Prof.dr. P. A. J. Robe
Prof.dr. R. Kanaar

Table of contents

Chapter 1 General introduction.....*1*

Chapter 2 Aims.....*9*

Part I New therapeutic regimens using drugs in combination or in single agent settings

Chapter 3 DNA damage response and anti-apoptotic proteins predict radiosensitization efficacy of HDAC-inhibitors SAHA and LBH589 in patient-derived glioblastoma cells.....*15*

Chapter 4 The Bcl2-inhibitor obatoclax overcomes resistance to histone deacetylase inhibitors SAHA and LBH589 as radiosensitizers in patient-derived glioblastoma stem-like cells.....*37*

Chapter 5 Screening of clinically -applicable drugs in patient-derived glioblastoma stem-like cells identifies amiodarone, clofazimine and triptolide as potential anti-glioma agents.....*57*

Part II Combination strategies for oncolytic adenovirus Delta24-RGD in glioblastoma

Chapter 6 Concentrations of antiepileptic drugs do not inhibit the activity of the oncolytic adenovirus Delta24-RGD in malignant glioma.....*81*

Chapter 7 The HDAC-inhibitors scriptaid and LBH589 combined with the oncolytic virus Delta24-RGD exert enhanced anti-tumor efficacy in patient-derived glioblastoma cells.....*97*

Chapter 8 *In vitro* screening of clinical drugs identifies sensitizers of oncolytic viral therapy in glioblastoma stem-like cells.....*121*

Chapter 9 General discussion.....*149*

Summary *157*

Nederlandse samenvatting *161*

Manuscripts on which this thesis is based *165*

Acknowledgements / Dankwoord *167*

PhD Portfolio *173*

Manuscripts other than this thesis *177*

About the author *179*

Chapter 1
General introduction

1.1 Glioblastoma

This thesis aims at finding new therapeutic strategies to treat the most malignant form of primary brain cancer, glioblastoma. The incidence of this tumor is about 4 in 100.000 annually.[1] Glioblastoma is the most frequent and malignant form of glioma[1] and originates from the supportive glial cells either astrocytes or oligodendrocytes. According to the World Health Organization glioblastoma is defined as a WHO grade IV glioma. Glioblastoma has a poor median survival of 14.6 months.[2] Patients with glioblastoma exhibit symptoms primarily caused by increased intracranial pressure or the mechanical pressure and infiltration of functional nervous tissue. The location and the size of the tumor determine additional symptoms, which may vary from general symptoms such as headache, nausea and vomiting or neurological deficits due to dysfunctional brain structures, such as aphasia, abnormal sensations and paretic limbs. The treatment options for these patients are always limited and consist of surgical resection followed by chemoradiation which is administration of the alkylating agent temozolomide during radiation treatment. Before and/or after surgery, symptoms due to the intracranial swelling are reduced by administration of dexamethasone.

1.2 Current treatment

The current paradigm for development of new treatments in medicine emphasizes the need for large randomized controlled trials, preferably in blinded and multicenter settings, which provide evidence that dictates decision making for doctors in clinical practice.[3] Placebo controlled trials are unethical in patients with malignancies, therefore trials in cancer patients include the standard of care as comparative treatment. Before the introduction of the treatment with temozolomide as an adjuvant to radiation,[4] radiation alone after surgery was the standard adjuvant treatment with reported median survival around twelve months.[5] The current therapy for glioblastoma is the result of a large study cohort including over 500 patients treated in two arms, one consisting of surgery and radiation, the other of surgery, radiation and temozolomide, performed by the European Organization for Research and Treatment of Cancer (EORTC) and the National Cancer Institute of Canada Clinical Trials Group.[2,5] This study confirmed the longer survival in patients treated with temozolomide as an adjuvant to surgery and radiotherapy, with a better prognosis in patients with a complete surgical resection in comparison to partial resection or biopsy only.[2,5] However, the combination treatment regimen still results in a poor overall median survival rate of 14.6 months.[2] Recurrent glioblastoma is treated with either another course of temozolomide, radiation or second line chemotherapy. Patients with recurrent tumors enter clinical trials in which cytostatic and targeted drugs are tested, such as bevacuzimab, carmustine and lomustine. Up till now, all have had limited effects.[6-9]

Importantly, the aforementioned EORTC study identified an important predictor of response to adjuvant temozolomide therapy, namely the methylation status of the promoter for the O-6-methylguanine-DNA methyltransferase *(MGMT)* gene.[2,5] It was shown that the methylation status of the promoter in a specific tumor is a predictor of therapeutic response.[10] The identification of this biomarker is an important step forward in the treatment of glioblastoma. For example, patients harboring a glioblastoma having an unmethylated *MGMT* promoter gene in which temozolomide is rather ineffective are nowadays selected for clinical trials.[11-13] These patients can be included in other trials to test novel drugs. Another important biomarker in glioblastoma is the isocitrate dehydrogenase-1

(IDH1) mutation, which is strongly related to prognosis and to a distinct molecular profile.[14] The identification of relevant biomarkers opens up new possibilities for patient first of tailored treatment options.

1.3 Precision medicine

The identification of the *MGMT* promoter methylation status as a predictor of response is an important step toward a personalized approach in therapy in glioblastoma. Developing biomarkers that predict outcome of treatment is now becoming a major focus of research in the field. The National Institutes of Health (NIH, USA) refers to it as precision medicine which is defined as:

"Precision medicine is an emerging approach for disease treatment and prevention that takes into account individual variability in genes, environment and lifestyle for each person."[15]

This approach takes the molecular characteristics of the tumor of the patient into account as a determinant of outcome in medical practice. Identifying prognostic factors allows us to treat patients more effectively, e.g. treating with effective drugs, at the best time, in the right sequence while minimalizing side effects. Improving diagnostic techniques on the molecular level goes in parallel with this development, since precision medicine is very much based on the knowledge gained from research on genetic alterations, gene expression profiling, proteomics and epigenetics.

1.4 Heterogeneity

Glioblastoma is a very heterogeneous tumor.[16] Various molecular subgroups can be found in glioblastoma including the segmentation by *MGMT* promoter status, IDH mutation status, tumor protein 53 *(TP53)* status, phosphatase and tensin homolog (PTEN) status and epidermal growth factor receptor *(EGFR)* amplifications.[1,17,18] These genes show a relation with survival and response to treatment. Another method of molecular subtyping includes classification in classical, proneural, neural and mesenchymal subtypes of Verhaak et al. which is based on gene expression profiling.[19] These subgroups are correlated with clinical outcome and specific gene alteration patterns based on several important genes such as platelet-derived growth factor receptor alpha *(PDGF(RA)), IDH1, EGFR* and neurofibromatose type 1 *(NF1)*.[19] The heterogeneity of the tumor, as expressed in the different number and type of genetic alterations within these tumors, makes it impossible to find a universal treatment.

Not only is heterogeneity observed between individuals; also intra-tumoral heterogeneity on the level of expression profiling exists and was recently demonstrated in a report in which the researchers analyzed tumor specimens resected from different regions of a single tumor.[20] Various stages of the tumor evolution were observed in the same tumor.[20] This underlines the complexity of finding an appropriate treatment for glioblastoma.

1.5 The patient-derived glioblastoma stem like cell model

To develop novel therapeutic strategies, a model is needed that resembles the original tumor and its heterogeneity. Preclinical studies aimed at finding new treatments for cancer need to take heterogeneity into account to bridge the translational gap to clinical practice. The models to be used, should resemble all of the genetic alterations that have been reported in glioblastoma patients. In part, such a model is provided by the patient-derived

glioblastoma stem like cell (GSC) model. The GSCs are tumor initiating cells that are drivers behind the resistance to treatment[21] and tumor propagation.[22] Tumor initiating cells often harbor CD133 on the cell surface, which is related to a defective DNA damage response pathway.[23] The GSCs also plays an important role in the recurrence of glioblastoma, the invasive character[24]as well as in the heterogeneity.[25]

The GSCs are isolated from fresh tumor tissue which has been acquired during surgery.[26] The tissue is dissociated mechanically and enzymatically.[26] Those cells are cultured in a serum free manner in addition with the growth factors EGF and bFGF.[26,27] These growth factors are essential for cell maintenance.[26,27] This method is used to preserve stem-like characteristics as can be demonstrated by the presence of various markers of stemness in the tumor cells, including Nestin, SOX2, Musashi-1 and Bmi-1.[28] Moreover, the heterogeneity between tumors derived from separate patients is reflected in this model in contrast with conventional commercially available cell lines.[26,27] Preliminary results show that the heterogeneity in response to temozolomide in these cultures very well reflects the response as observed in patients from which the parental tumor originates. Others also have observed that the *in vivo* predictive marker *MGMT* for temozolomide response, is also a predictive marker for the temzolomide response in the *in vitro* patient derived cell cultures.[29]

1.6 The epigenetically acting histone deacetylase inhibitors and clinical drugs

Single agent regimens are probably not a strategy that will lead to long term effects, as glioblastoma cells are known to circumvent therapeutic effects using multiple mechanisms of drug resistance.[30] As a consequence it is likely that combination treatments will show better results. However, the intra-tumoral heterogeneity within glioblastomas makes finding an effective treatment a challenge.[20]

Various reports have reported on the potential role of the anti-epileptic drug valproic acid (VPA) in the treatment for glioblastoma.[31,32] Apart from acting as an anti-epileptic drug, VPA also weakly inhibits histone deacetylases (HDACs).[33] HDACs remove acetyl groups of core histones of the chromatin and are regulating the epigenetic balance. Acetylated histones are associated with activated transcription and open chromatin, whereas deacetylated histones are often associated with gene silencing and compacted chromatin.[34] Apart from this function, HDACs also affect non-histone proteins that function as transcription factors, DNA repair proteins and inflammatory markers.[35] Other than VPA, there are stronger acting HDACi like SAHA (vorinostat) and LBH589 (panobinostat).[34] The testing of SAHA as an adjuvant to existing therapies has been completed in various studies. For LBH589 there are two active studies in glioblastoma.[13] The HDACi have various effects as combination agents: they have shown radiosensitizing capacity, influence the cell cycle and show apoptotic activity.[34] HDACi enhance gene expression and protein levels, affect (oncolytic) viral vectors and can alter the immune response.[36-39] Therefore, these drugs are interesting combination partners in a broad range of treatment strategies including chemotherapy, radiation therapy and immune related therapy including oncolytic virotherapy.[40]

In addition we have taken direction of drug repurposing for glioblastoma, by means of finding clinical agents that have the ´off´ target effect to inhibit glioblastoma stem-like cells.[41] The NIH has a clinical drug collection containing over 450 clinical drugs, most of which enter the central nervous system.[42] These drugs have a known toxicity profile and

have frequently been administered to patients for other conditions. Therefore, they are ideal candidates for fast-track implementation in the clinical setting. The development of patient-derived GSCs provides an *in vitro* drug screening model that resembles the tumor *in situ*, in terms of both genetic resemblance, tumor heterogeneity and resistance to therapy in the patient population.[26,27] Therefore, reevaluation of clinically available drugs for other indications using patient-derived GSCs can lead to the identification of novel anti-glioblastoma agents.[41]

1.7 Experimental therapy with oncolytic viruses

One of the difficulties in treating glioblastoma patients is the invasive character of this tumor, which prevents total tumor resection. It has been shown in autopsy cases that tumor cells can be found at a distance up to 2 cm or further from the resection cavity.[43] These cells are difficult to reach and to treat with therapeutics. A possible therapeutic modality to handle this phenomenon is oncolytic viral therapy, which makes use of tumor selective viruses that can efficiently kill tumor cells and that may have a wider spread throughout the brain than drugs.[44] The virus will elicit a general immune response that may also be directed against the remaining tumor cells. Oncolytic virotherapy is emerging and recently phase-I/II clinical trials have been performed, testing different types of tumor selective viruses among those the oncolytic adenovirus Delta24-RGD.[45] Treatment with Delta24-RGD has shown promising results in preclinical models[46] and has demonstrated therapeutic responses in a subset of patients.[45] Delta24-RGD specifically targets and replicates in cancer cells deficient in the retinoblastoma pathway by means of a 24-base pair deletion in the viral *E1A* gene. The insertion of the RGD-peptide into the fiber-knob facilitates viral entry through αvβ3/αvβ5 integrins into the glioma cell.[47] Delta24-RGD is therefore not dependent on entry via the coxsackie adenovirus receptor which is usually sparsely expressed in glioblastoma.[48] The recently conducted trials with oncolytic viruses show promising results, however it becomes clear that better and more efficient cell kill by the virus and more potent induction of the immune response will be needed in order to make OV an efficient and novel therapy for glioblastoma.[44]

References

1. Ohgaki H, Kleihues P. Population-based studies on incidence, survival rates, and genetic alterations in astrocytic and oligodendroglial gliomas. J Neuropathol Exp Neurol 2005;64:479-89.
2. Stupp R, Hegi ME, Mason WP, et al. Effects of radiotherapy with concomitant and adjuvant temozolomide versus radiotherapy alone on survival in glioblastoma in a randomised phase III study: 5-year analysis of the EORTC-NCIC trial. Lancet Oncol 2009;10:459-66.
3. Hart JT. Cochrane Lecture 1997. What evidence do we need for evidence based medicine? J Epidemiol Community Health 1997;51:623-9.
4. Brada M, Hoang-Xuan K, Rampling R, et al. Multicenter phase II trial of temozolomide in patients with glioblastoma multiforme at first relapse. Annals of oncology : official journal of the European Society for Medical Oncology / ESMO 2001;12:259-66.
5. Stupp R, Mason WP, van den Bent MJ, et al. Radiotherapy plus concomitant and adjuvant temozolomide for glioblastoma. The New England journal of medicine 2005;352:987-96.

6. Taal W, Oosterkamp HM, Walenkamp AM, et al. Single-agent bevacizumab or lomustine versus a combination of bevacizumab plus lomustine in patients with recurrent glioblastoma (BELOB trial): a randomised controlled phase 2 trial. Lancet Oncol 2014;15:943-53.
7. Rahman R, Hempfling K, Norden AD, et al. Retrospective study of carmustine or lomustine with bevacizumab in recurrent glioblastoma patients who have failed prior bevacizumab. Neuro Oncol 2014;16:1523-9.
8. Glas M, Happold C, Rieger J, et al. Long-term survival of patients with glioblastoma treated with radiotherapy and lomustine plus temozolomide. J Clin Oncol 2009;27:1257-61.
9. Hochberg FH, Linggood R, Wolfson L, Baker WH, Kornblith P. Quality and duration of survival in glioblastoma multiforme. Combined surgical, radiation, and lomustine therapy. JAMA 1979;241:1016-8.
10. Hegi ME, Diserens AC, Godard S, et al. Clinical trial substantiates the predictive value of O-6-methylguanine-DNA methyltransferase promoter methylation in glioblastoma patients treated with temozolomide. Clin Cancer Res 2004;10:1871-4.
11. Motomura K, Natsume A, Kishida Y, et al. Benefits of interferon-beta and temozolomide combination therapy for newly diagnosed primary glioblastoma with the unmethylated *MGMT* promoter: A multicenter study. Cancer 2011;117:1721-30.
12. Nabors LB, Fink KL, Mikkelsen T, et al. Two cilengitide regimens in combination with standard treatment for patients with newly diagnosed glioblastoma and unmethylated *MGMT* gene promoter: results of the open-label, controlled, randomized phase II CORE study. Neuro Oncol 2015;17:708-17.
13. Health NIo. Www.clinicaltrials.gov. last visited May 2015.
14. Aldape K, Zadeh G, Mansouri S, Reifenberger G, von Deimling A. Glioblastoma: pathology, molecular mechanisms and markers. Acta Neuropathol 2015.
15. About the Precision Medicine Initiative. 2015. at http://www.nih.gov/precisionmedicine/.)
16. Nicholas MK, Lukas RV, Chmura S, Yamini B, Lesniak M, Pytel P. Molecular heterogeneity in glioblastoma: therapeutic opportunities and challenges. Seminars in oncology 2011;38:243-53.
17. von Deimling A, Louis DN, Wiestler OD. Molecular pathways in the formation of gliomas. Glia 1995;15:328-38.
18. Hegi ME, Diserens AC, Gorlia T, et al. *MGMT* gene silencing and benefit from temozolomide in glioblastoma. The New England journal of medicine 2005;352:997-1003.
19. Verhaak RG, Hoadley KA, Purdom E, et al. Integrated genomic analysis identifies clinically relevant subtypes of glioblastoma characterized by abnormalities in PDGFRA, IDH1, EGFR, and NF1. Cancer Cell 2010;17:98-110.
20. Sottoriva A, Spiteri I, Piccirillo SG, et al. Intratumor heterogeneity in human glioblastoma reflects cancer evolutionary dynamics. Proc Natl Acad Sci U S A 2013;110:4009-14.
21. Bao S, Wu Q, McLendon RE, et al. Glioma stem cells promote radioresistance by preferential activation of the DNA damage response. Nature 2006;444:756-60.
22. Chen J, Li Y, Yu TS, et al. A restricted cell population propagates glioblastoma growth after chemotherapy. Nature 2012;488:522-6.
23. McCord AM, Jamal M, Williams ES, Camphausen K, Tofilon PJ. CD133+ glioblastoma stem-like cells are radiosensitive with a defective DNA damage response compared with established cell lines. Clin Cancer Res 2009;15:5145-53.

24. Jackson M, Hassiotou F, Nowak A. Glioblastoma stem-like cells: at the root of tumor recurrence and a therapeutic target. Carcinogenesis 2015;36:177-85.
25. Piccirillo SG, Colman S, Potter NE, et al. Genetic and functional diversity of propagating cells in glioblastoma. Stem Cell Reports 2015;4:7-15.
26. Balvers RK, Kleijn A, Kloezeman JJ, et al. Serum-free culture success of glial tumors is related to specific molecular profiles and expression of extracellular matrix-associated gene modules. Neuro Oncol 2013;15:1684-95.
27. Lee J, Kotliarova S, Kotliarov Y, et al. Tumor stem cells derived from glioblastomas cultured in bFGF and EGF more closely mirror the phenotype and genotype of primary tumors than do serum-cultured cell lines. Cancer Cell 2006;9:391-403.
28. Gursel DB, Shin BJ, Burkhardt JK, Kesavabhotla K, Schlaff CD, Boockvar JA. Glioblastoma stem-like cells-biology and therapeutic implications. Cancers 2011;3:2655-66.
29. Fouse SD, Nakamura JL, James CD, Chang S, Costello JF. Response of primary glioblastoma cells to therapy is patient specific and independent of cancer stem cell phenotype. Neuro Oncol 2014;16:361-71.
30. Haar CP, Hebbar P, Wallace GCt, et al. Drug resistance in glioblastoma: a mini review. Neurochemical research 2012;37:1192-200.
31. Van Nifterik KA, Van den Berg J, Slotman BJ, Lafleur MV, Sminia P, Stalpers LJ. Valproic acid sensitizes human glioma cells for temozolomide and gamma-radiation. J Neurooncol 2012;107:61-7.
32. Berendsen S, Broekman M, Seute T, et al. Valproic acid for the treatment of malignant gliomas: review of the preclinical rationale and published clinical results. Expert opinion on investigational drugs 2012;21:1391-415.
33. Chinnaiyan P, Cerna D, Burgan WE, et al. Postradiation sensitization of the histone deacetylase inhibitor valproic acid. Clin Cancer Res 2008;14:5410-5.
34. Lee JH, Choy ML, Marks PA. Mechanisms of resistance to histone deacetylase inhibitors. Advances in cancer research 2012;116:39-86.
35. Bezecny P. Histone deacetylase inhibitors in glioblastoma: pre-clinical and clinical experience. Med Oncol 2014;31:985.
36. Cody JJ, Markert JM, Hurst DR. Histone deacetylase inhibitors improve the replication of oncolytic herpes simplex virus in breast cancer cells. PLoS One 2014;9:e92919.
37. Alvarez-Breckenridge CA, Yu J, Price R, et al. The histone deacetylase inhibitor valproic acid lessens NK cell action against oncolytic virus-infected glioblastoma cells by inhibition of STAT5/T-BET signaling and generation of gamma interferon. J Virol 2012;86:4566-77.
38. Nguyen TL, Wilson MG, Hiscott J. Oncolytic viruses and histone deacetylase inhibitors--a multi-pronged strategy to target tumor cells. Cytokine & growth factor reviews 2010;21:153-9.
39. Hoti N, Chowdhury W, Hsieh JT, Sachs MD, Lupold SE, Rodriguez R. Valproic acid, a histone deacetylase inhibitor, is an antagonist for oncolytic adenoviral gene therapy. Mol Ther 2006;14:768-78.
40. Bieler A, Mantwill K, Dravits T, et al. Novel three-pronged strategy to enhance cancer cell killing in glioblastoma cell lines: histone deacetylase inhibitor, chemotherapy, and oncolytic adenovirus dl520. Hum Gene Ther 2006;17:55-70.
41. Triscott J, Rose Pambid M, Dunn SE. Concise review: bullseye: targeting cancer stem cells to improve the treatment of gliomas by repurposing disulfiram. Stem Cells 2015;33:1042-6.
42. http://nihclinicalcollection.com/. last visited september 2014.

43. Kelly PJ. Imaging features of invasion and preoperative and postoperative tumor burden in previously untreated glioblastoma: Correlation with survival. Surg Neurol Int 2010;1.
44. Kaufmann JK, Chiocca EA. Glioma virus therapies between bench and bedside. Neuro Oncol 2014;16:334-51.
45. Lang FF, Conrad C, Gomez-Manzano C, et al. First-in-human phase I clinical trial of oncolytic delta-24-rgd (dnx-2401) with biological endpoints: implications for viro-immunotherapy. Neuro Oncol 2014;16 Suppl 3:iii39.
46. Lamfers ML, Grill J, Dirven CM, et al. Potential of the conditionally replicative adenovirus Ad5-Delta24RGD in the treatment of malignant gliomas and its enhanced effect with radiotherapy. Cancer Res 2002;62:5736-42.
47. Suzuki K, Fueyo J, Krasnykh V, Reynolds PN, Curiel DT, Alemany R. A conditionally replicative adenovirus with enhanced infectivity shows improved oncolytic potency. Clin Cancer Res 2001;7:120-6.
48. Van Houdt WJ, Wu H, Glasgow JN, et al. Gene delivery into malignant glioma by infectivity-enhanced adenovirus: *in vivo* versus *in vitro* models. Neuro Oncol 2007;9:280-90.

Chapter 2
Aims

In this thesis, we analyze an extensive database of patient-derived glioblastoma stem-like cell cultures. Motivated by the concepts of personalized or precision medicine, we search for new therapeutic strategies, specifically the combination of drugs using current treatment modalities and experimental oncolytic virotherapy with Delta24-RGD in combination with other drugs. We search for molecular markers to predict responses at epigenetic, gene expression, and at protein level, in order to provide precision medicine.

2.1 Part I: New therapeutic regimens using drugs in combination or in single agent settings

Chapter 3. *Which HDAC inhibitors are the most effective sensitizers of radiation and in what percentage of patient-derived glioblastoma cultures? What is the best timing and sequence of combination therapy? Can we identify molecular markers in the DNA damage and the apoptotic pathway that predict therapeutic response?*

The HDACi SAHA, LBH589, Valproic Acid (VPA), Scriptaid and MS275 are well-studied drugs and effectively sensitize various tumor types to radiation as was shown in several *in vitro* and *in vivo* models including conventional glioma cell lines.[1-6] SAHA and LBH589 are currently tested in clinical trials as combination drugs for temozolomide or radiation in glioblastoma.[7] The mechanism of action of HDACi as radiosensitizers is a combination of chromatin relaxation, altered transcription of DNA damage repair genes and common cell death (apoptotic) pathway synergisms.[8] We compare the efficacy of SAHA, LBH589, VPA, MS275 and Scriptaid as radiosensitizers in the patient-derived glioblastoma model. In more detail, SAHA and LBH589 were evaluated to determine predictors of response. Various markers in the context of DNA damage repair, cell cycle arrest and the apoptotic pathway were studied in relation to response. In addition we analyzed the optimizing of timing and sequence of combination therapy.

Chapter 4. *Can the resistance of patient-derived GSCs to HDAC inhibitors as radiosensitizers be overcome when combined with drugs that inhibit the apoptotic Bcl-2 family proteins?*

Based on the results found in Chapter 3, we study the efficacy of SAHA/radiation and LBH589/radiation when manipulating Bcl-2 family proteins using the Bcl-2 inhibitor Obatoclax in patient-derived glioblastoma stem-like cell cultures. The relation between treatment response and various factors including Bcl-2 family protein levels, *MGMT* promoter methylation and recurrence status, as well as gene expression levels of the tumors were studied.

Chapter 5. *Are there clinically approved drugs available for other indications than cancer that may have anti-glioblastoma efficacy in the patient-derived glioblastoma model?*

We aim at finding new drugs that have anti-glioblastoma efficacy, which may be potential agents in future combination studies. Clinical implementation of new drugs can take years, therefore we screened 446 clinically approved drugs in twenty patient-derived GSCs which if effective may be implemented quickly compared to drugs that need extensive toxicity testing. Effects on viability, three-dimensional cell invasion and toxicity in normal human astrocytes were analyzed. Gene expression profiling, *in silico* analyses and mechanistic studies were performed to gain insights into the mechanisms of action.

The responses were related to *MGMT* promoter methylation status as well as recurrence status.

2.2 Part II: Combination strategies for oncolytic adenovirus Delta24-RGD in glioblastoma

Chapter 6. *Do frequently prescribed anti-epileptic drugs in glioblastoma patients interfere with the oncolytic activity of Delta24-RGD?*

Frequently prescribed anticonvulsants for patients with glioblastoma are the HDACi VPA, and two other drugs phenytoin and levetiracetam. The literature suggests that these may interfere with cellular mechanisms of cancer and with oncolytic virus activity. We investigate the direct effects of therapeutic doses of these drugs on Delta24-RGD infection, replication and on oncolytic activity in established glioma cell lines as well as patient-derived glioblastoma cultures.

Chapter 7. *Which HDAC inhibitors effectively synergize with Delta24-RGD and in which subset of patient-derived GSCs?*

HDAC inhibitors also affect integrins and share common cell death pathways with Delta24-RGD. We study the combination treatment effects of HDACi and Delta24-RGD in GSCs and we determined the most effective HDACi. SAHA, VPA, Scriptaid, MS275 and LBH589 were combined with Delta24-RGD in fourteen distinct cultures. We have related the response to therapy with gene expression profiles, mutations and glioblastoma subtypes.

Chapter 8. *Are there any already clinically approved drugs for other indications than cancer available that may have a synergistic effect on the working mechanism of oncolytic viruses?*

We address the feasibility of clinically applicable drugs to enhance the therapeutic potential of Delta24-RGD in glioblastoma. For this purpose we tested 446 drugs for their viral sensitizing properties in patient-derived GSCs *in vitro*. Mechanistic studies were undertaken to assess viability, replication efficacy, viral infection enhancement and cell death pathway induction in a selected panel of drugs. We have combined these agents with two other oncolytic viruses and in other solid tumors including breast carcinoma, ovarian carcinoma and colon carcinoma cell lines.

References

1. Thiemann M, Oertel S, Ehemann V, et al. In vivo efficacy of the histone deacetylase inhibitor suberoylanilide hydroxamic acid in combination with radiotherapy in a malignant rhabdoid tumor mouse model. Radiat Oncol 2012;7:52.
2. Deorukhkar A, Shentu S, Park HC, et al. Inhibition of radiation-induced DNA repair and prosurvival pathways contributes to vorinostat-mediated radiosensitization of pancreatic cancer cells. Pancreas 2010;39:1277-83.
3. Sonnemann J, Kumar KS, Heesch S, et al. Histone deacetylase inhibitors induce cell death and enhance the susceptibility to ionizing radiation, etoposide, and TRAIL in medulloblastoma cells. Int J Oncol 2006;28:755-66.

4. Chinnaiyan P, Vallabhaneni G, Armstrong E, Huang SM, Harari PM. Modulation of radiation response by histone deacetylase inhibition. Int J Radiat Oncol Biol Phys 2005;62:223-9.
5. Groselj B, Sharma NL, Hamdy FC, Kerr M, Kiltie AE. Histone deacetylase inhibitors as radiosensitisers: effects on DNA damage signalling and repair. Br J Cancer 2013;108:748-54.
6. Geng L, Cuneo KC, Fu A, Tu T, Atadja PW, Hallahan DE. Histone deacetylase (HDAC) inhibitor LBH589 increases duration of gamma-H2AX foci and confines HDAC4 to the cytoplasm in irradiated non-small cell lung cancer. Cancer Res 2006;66:11298-304.
7. Health NIo. Www.clinicaltrials.gov. last visited May 2015.
8. Shabason JE, Tofilon PJ, Camphausen K. Grand rounds at the National Institutes of Health: HDAC inhibitors as radiation modifiers, from bench to clinic. J Cell Mol Med 2011;15:2735-44.

Part I

New therapeutic regimens using drugs in combination or in single agent settings

Chapter 3

DNA damage response and anti-apoptotic proteins predict radiosensitization efficacy of HDAC-inhibitors SAHA and LBH589 in patient-derived glioblastoma cells

Lotte M.E. Berghauser Pont,[1] Kishan Naipal,[2] Jenneke J. Kloezeman,[1] Subramanian Venkatesan,[1] Martin van den Bent,[3] Dik C. van Gent,[2] Clemens M.F. Dirven,[1] Roland Kanaar,[2] Martine L.M. Lamfers,[1] Sieger Leenstra.[1,4]

Affiliations

1 Department of Neurosurgery, Brain Tumor Center, ErasmusMC, Rotterdam, The Netherlands
2 Department of Genetics, Dept. Radiation Oncology, Cancer Genomics Netherlands, ErasmusMC
3 Department of Neurology/Neuro-oncology, Brain Tumor Center, ErasmusMC Cancer Institute
4 Department of Neurosurgery, Elizabeth Medical Hospital, Tilburg, The Netherlands

Published in Cancer Lett. 2015 Jan 28;356(2 Pt B):525-35

PMID: 25305451

Abstract

HDAC inhibitors have radiosensitizing effects in established cancer cell lines. This study was conducted to compare the efficacy of SAHA, LBH589, Valproic Acid (VPA), MS275 and Scriptaid in the patient-derived glioblastoma model. In more detail, SAHA and LBH589 were evaluated to determine predictors of response. Acetylated-histone-H3, γH2AX /53BP1, (p)Chek2/ATM, Bcl-2/Bcl-XL, $p21^{CIP1/WAF1}$ and caspase-3/7 were studied in relation to response. SAHA sensitized 50% of cultures, LBH589 45%, VPA and Scriptaid 40% and MS275 60%. Differences after treatment with SAHA/RTx or LBH589/RTx in a sensitive and resistant culture were increased acetylated-H3, caspase-3/7 and prolonged DNA damage repair γH2AX /53BP1 foci. pChek2 was found to be associated with both SAHA/RTx and LBH589/RTx response with a positive predictive value (PPV) of 90%. Bcl-XL had a PPV of 100% for LBH589/RTx response. Incubation with HDACi 24 and 48hours pre-RTx resulted in the best efficacy of combination treatment. In conclusion a subset of patient-derived glioblastoma cultures were sensitive to HDACi/RTx. For SAHA and LBH589 responses were strongly associated with pChek2 and Bcl-XL, which warrant further clinical exploration. Additional information on responsiveness was obtained by DNA damage response markers and apoptosis related proteins.

3.1 Introduction

Glioblastoma is the most malignant form of primary brain tumor, originating from the supporting tissue of the brain, the glial cells. With the current standard treatment consisting of maximal safe surgical resection followed by temozolomide and radiation therapy (RTx) patients have a post-operative expected survival of 12 – 15 months.[1] Since glioblastoma is highly resistant to conventional anti-cancer regimens, new combined approaches are urgently needed to improve outcome. Histone deacetylase inhibitors (HDACi) are anti-cancer drugs that alter the epigenome by inhibiting histone deacetylases which are involved in the deacetylation of core histones. Hereby these drugs change gene expression, but they also affect non-histone proteins directly.[2,3] The HDACi SAHA, LBH589, Valproic Acid (VPA), Scriptaid and MS275 are well-studied drugs and effectively sensitize various tumor types to radiation (RTx) as was shown in several *in vitro* and *in vivo* models including conventional glioma cell lines.[4-9] SAHA and LBH589 are currently tested in clinical trials as combination drugs for temozolomide or RTx in glioblastoma.[10] The mechanism of action of HDACi as radiosensitizers is a combination of chromatin relaxation, altered transcription of DNA damage repair genes and common cell death pathway synergisms.[3]

In contrast to the established glioma cell lines, patient-derived glioblastoma cultures that are cultured under serum-free conditions, resemble the genotype of the parental tumor and as a consequence reflect the genetic heterogeneity between patients.[11] Therefore, this study investigated the responsiveness to various HDACi in combination with RTx in the patient-derived glioblastoma model. This representative model allows determination of tumor subtypes related to treatment response and identification of molecules related to response. In conventional cell lines, important molecules for the mechanism of action of HDACi were found to be acetylated histones, cell cycle regulatory proteins ($p21^{CIP1/WAF1}$), Bcl-2 family apoptotic proteins and the DNA damage response.[8,12-14] The objective of this study was to assess sensitivity of patient-derived glioblastoma cultures to five HDACi in combination with RTx. These HDACi included SAHA, LBH589, VPA, Scriptaid and MS275. Also, we identified molecules that were associated with response to the clinically

relevant HDACi SAHA and LBH589 as radiosensitizers. Furthermore, the optimal timing of HDACi/RTx was assessed, as well as the effects of fractionated radiation on combination treatment.

3.2 Materials and methods

Chemicals
The compounds SAHA and MS275 were obtained from Cayman chemicals (MI, USA),VPA from Sigma-Aldrich (MO, USA), LBH589 from Biovision (CA, USA), Scriptaid from Santa Cruz Biotechnology (CA, USA) and Staurosporin was obtained from BioMol (Germany). Stocks were prepared at 100mM (VPA) in sterile water and at 50mM (SAHA), 10mM (Scriptaid), 4mM (MS275) and 200 µM (LBH589) in dimethyl sulfoxide (Sigma-Aldrich) and stored at -20°C. The DMSO concentration was kept below 1% in the treatment dilutions.

Patient-derived glioblastoma stem-like cell cultures
Fresh tumor tissue specimens were obtained by surgical resection at the Department of Neurosurgery of the ErasmusMC (Rotterdam, The Netherlands) and Elisabeth Hospital (Tilburg, The Netherlands). Tumor material was obtained with patients' informed consent as approved by the institutional review board of the ErasmusMC. The tumor tissue specimens were dissociated, maintained as patient-derived glioblastoma cultures under serum-free conditions, and characterized as was described previously.[11] Twenty-two patient-derived glioblastoma cultures were used for the experiments. The (clinical) characteristics of the original tumors are shown in Table 1. These clinical characteristics were investigated for relation with the mean differences in viability of single agent treatment compared to either combination treatment (SAHA/RTx or LBH589/RTx).

Viability assays
Dose-response assays for the HDACi alone were performed to determine the IC_{50} values by using at least three different drug concentrations. The combination treatment was applied using at least two different HDACi concentrations, 24 hours before applying single dose RTx (3Gy, Cs-137 source). The concentrations of HDACi were (0.25)/0.5/1.0µM SAHA; (0.1)/0.3/0.6mM VPA; (0.35)/0.7/1.4µM Scriptaid; (0.05)/0.1/0.5µM MS275; (1)/5/20nM LBH589. These concentrations were based on the values determined in the dose-response assays in mono therapy, and the highest dose to be tested had to be between the average IC_{20} and IC_{50} of all cultures. This was used to determine enhancement in combination with 3Gy RTx. One dose of RTx was tested, as patients in the clinical setting receive a fixed dose of RTx daily. The dose of 3Gy RTx was chosen based on the initial screen of the panel of cultures. The latter showed that 3Gy was the only fixed dose where RTx still had a small effect on the most resistant culture, and where the most sensitive culture had enough viability (>25%) at day eight after treatment to be able to study enhancement. The 96-wells plates were coated with BD Matrigel (1:20, BD Biosciences, CA, USA) and seeded at 1x103 cells/well. Cell viability was measured on day eight by CellTiterGlo-assay[15] (Promega, WI, USA). The IC_{50} values were calculated by median effect equation.[16] To study the optimal sequence of HDACi/RTx, 0.75x103 cells/well were plated and treated with SAHA at 48 hours or 24 hours pre-RTx, simultaneously, or 24 hours post-RTx.

Western blot

The four patient-derived glioblastoma cultures GS79, GS160, GS186 and GS257 were treated with SAHA, LBH589, RTx or the combinations, according to the schedule used in the previous experiments. The cells were harvested 24 hours after RTx. For the experiment shown in figure 3C and 4A, the glioblastoma cultures were collected 30 minutes after RTx, together with corresponding untreated controls. Cells were washed with PBS and collected in a lysis buffer under protease and phosphatase inhibitory conditions. Protein concentrations were assessed by BCA Protein Assay Reagent Kit (Thermo Fisher Scientific, MA, USA). Separation was performed on a 10% Acrylamide/Bis gel (Bio-Rad, CA, USA) and blotted onto a PVDF membrane (Immobilon-P, Millipore, MA, USA) using the Mini-Protean Tetra Cell system (Bio-Rad). Membranes were blocked in a 5% non-fatty milk solution 0.5 hour at room temperature. The blots were probed with anti-acetylated histone H3 (anti-ac-H3), anti-β-actin (1:300; and 1:5,000, Millipore), anti-Bcl-2, anti-Bcl-XL (both 1:500; Cell Signaling), anti-$p21^{CIP1/WAF1}$ (1:500, BD Bioscience), anti-pChek2-Thr68, anti-Chek2, ATM, pATM-Ser1981 (1:500, Cell Signaling) in 5% BSA/TBS-T overnight. After washing, membranes were incubated with secondary anti-rabbit-HRP or anti-mouse-HRP (1:2000, Dako Denmark A/S, Denmark) 1 hour at room temperature. The blots were visualized using the ChemiDoc MP system (Bio-Rad), and analyzed with the ImageLab Software (Bio-rad).

Immunohistochemistry

The patient-derived glioblastoma cultures GS79 (responsive to HDACi/RTx) and GS257 (resistant to HDACi/RTx) were selected to study the DNA repair response. Double strand breaks were identified by quantifying 53BP1 and γH2AX foci. Cells were grown on cover slips glass coated with Matrigel (BD Bioscience) and were treated with SAHA or LBH589. After 24 hours the cells were irradiated with 3Gy. At 1 hour and 24 hours post-RTx the cells were fixed with PFA (4%), washed with PBS/0.1% Triton and stained with anti-53BP1 (rabbit, 1:500, Novus Biochemicals, CO, USA), and anti-γH2AX (mouse, 1:500, Rockland). The cells were stained with a secondary antibody against mouse (Alexa-488, Life Technologies) and anti-rabbit (Alexa-546, Life Technologies). Immunofluorescence-stained cover glasses were analyzed using the Zeiss (Zeiss, Jena, Germany) LSM 700 upright confocal laser scanning microscope. Z-stack confocal images were used for quantifying the DNA repair foci at a pixel resolution of 512x512 with a 63x objective with an optical slice of 1.0µm and an interval of 1.5µm (4.7 digital zoom). Comparisons were made between the foci count of the RTx treated cells at 1 hour, and the SAHA/RTx and LBH589/RTx treated cells at 1 hour. Also, the foci count of the RTx and HDACi/RTx treated cells at 24 hours were compared to the foci count of the RTx treated cells at 1 hour. Single agent treatments were observed as controls.

Caspase 3/7 assays

The patient-derived glioblastoma cultures GS79 and GS257 were seeded $5x10^3$ cells/well in a 96-well plate and treated with SAHA, LBH589 or RTx, or in combination. Apoptosis-inducer staurosporin (20nM) was used as a positive control. The cells were incubated with 5µM CellPlayer 96-Well Kinetic Caspase-3/7 Apoptosis Reagent[17] (Essen Bioscience, MI, USA). After applying RTx the plates were placed in an IncuCyte[18] (Essen BioScience) with a 10X objective at 37°C in a humid 95% air/5% CO2 chamber. Three fluorescent images/well were collected every 2 hours up to 24 hours post-RTx. The number of fluorescent foci indicated caspase-3/7 activity. The fluorescent foci were counted using the IncuCyte Software and the treatments were compared.

Statistical analysis
The viability experiments were performed in triplicate. The results were presented as mean percentage of controls ± standard error. The enhancement of the combination treatment was calculated as described by Chou[19] as the fold-enhancement of the effect of a single agent. The mean differences in effects[20] were provided, and the significance was tested using the Students' T-test. In case of >1.0 enhancement, and statistical significance ($p<0.05$) a culture was considered sensitive. The Western blots were analyzed using the ImageLab software and band intensities were calculated as percentage of non-treated controls, corrected for the relative β-actin levels. The DNA damage repair foci were counted of n>20 cells and the results were analyzed by a Student's T-test ($p<0.05$ was considered significant). The caspase-3/7 experiments were done in duplicate of which three pictures were taken per time point. The results are presented as the mean object counts/surface area ± standard error. The differences in treatment effects were analyzed by the two-way ANOVA and Tukey's Post-hoc Test. ($p<0.05$ was considered significant). For the correlation analysis of the clinical data age, Karnofsky performance score (KPS) and progression free survival (PFS) with the effect sizes (mean difference in single vs. combination treatments), the Spearman correlation test was performed for non-parametric data. For the differences between groups of *MGMT* promoter methylation status, gender and recurrence status, the Mann Whitney U-test for non-parametric data was used.

3.3 Results

Patient-derived glioblastoma cultures show different sensitivity to HDACi and HDACi/RTx
The various tested HDACi had varying IC_{50} values between eight different patient-derived glioblastoma cultures, ranging from 0.7-6.1μM for SAHA, 0.4-4.9μM for Scriptaid, 0.04-2.5μM for MS275, 8.2-40.9nM for LBH589 and 0.8-3.9mM for VPA (Figure 1A). Subsequently the effects of three concentrations of the HDACi, as single agents and as radiosensitizers, were evaluated on twelve patient-derived glioblastoma cultures. Later on, ten additional patient-derived glioblastoma cultures were evaluated for their sensitivity to two concentrations of SAHA and LBH589 in combination with RTx (Table 2). The concentrations HDACi and dose of RTx being used, were based on the results in the dose-response assays (see the Methods section for a detailed description) and the efficacy in the various patient-derived glioblastoma cultures. A large overlap in responsiveness to SAHA/RTx and LBH589/RTx treatment was observed. The HDACi that are currently under phase I/II investigation, SAHA and LBH589, both sensitized 11/22 cultures with mean differences (mono vs. combination) of 5-27% and 13-32% respectively. Figure 1B shows seven of the 22 tested patient-derived glioblastoma cultures including responsive and resistant cultures. VPA and Scriptaid both sensitized 40% (4/10) cultures and MS275 sensitized 60% (6/10) cultures, with absolute effects (mean differences of mono vs. combination treatment) ranging from 13–30%, 20%-34% and 12%-24% respectively. The cultures that were sensitized by both SAHA and LBH589 (overlap) were 9/11 (Table 2). In further detail, the sensitive cultures to SAHA/RTx and LBH589/RTx were compared to the cultures resistant to those treatments, in order to identify candidate predictive markers and markers for response monitoring.

Table 1. The characteristics of the twenty-two patient-derived glioblastoma cultures.
The clinical characteristics twenty-two patient-derived glioblastoma cultures that were tested for the response to SAHA/RTx and LBH589/RTx, and of which 12 were used for testing the effects of VPA/RTx, Scriptaid/RTx and MS275/RTx. MGMT status = MGMT promoter methylation status; M = methylated; UM = unmethylated; PFS = progression free survival (months); Gender, M = Male, F = Female; Age (yrs) in years at time of resection; KPS = Karnofsky Performance Scale; recurrent tumor = if original tumor of which culture was derived was recurrent (yes) or not (no); treated tumor = if original tumor was treated in case of recurrence, with temozolomide (TMZ) and/or radiation (RTx). *This data is unavailable.

GSC culture	MGMT status	PFS (mths)	Gender	Age (yrs) at resection	KPS pre-operative	Recurrent tumor	Treated tumor
GS102	M	5	M	68.0	90	No	No
GS160	UM	1,5	M	58.1	90	No	No
GS184	M	2.5	M	50.4	90	No	No
GS186	M	3	F	48.2	90	Yes	TMZ/RTx
GS203	M	7	M	64.0	100	No	No
GS216	UM	2.5	F	42.9	90	Yes	TMZ/RTx
GS224	M	3.5	M	58.5	80	Yes	TMZ/RTx
GS245	UM	5	M	69.0	70	No	No
GS257	UM	2	F	60.1	60	No	RTx
GS261	M	2.5	M	82.2	80	No	No
GS274	M	6	F	67.1	70	No	No
GS279	M	19	M	62.8	90	Yes	TMZ/RTx
GS289	UM	3	M	79.6	80	No	No
GS295	UM	7	M	50.1	90	No	No
GS330	M	0	F	77.1	70	No	No
GS335	UM	3	F	60.6	80	Yes	TMZ/RTx
GS357	M	3	M	56.9	90	No	No
GS359	M	14	M	69.7	90	No	No
GS365	UM	3.5	M	59.5	90	No	No
GS401	M	2.5	M	52.6	70	Yes	TMZ/RTx
GS423	M	*	M	65.0	90	No	No
GS79	UM	4	F	74.7	90	No	No

Table 2. Responses to HDACi/RTx treatments in 22 patient-derived GBM cultures.

Twenty-two patient-derived GBM cultures were tested for the response to SAHA/RTx and LBH589/RTx. Initially 12 were tested for response to radiation combined with VPA, Scriptaid or MS275. The enhancement factors and the mean differences in viability are displayed based on cell viability on day eight. Statistical significance was considered if $p<0.05$. Legend: EF = enhancement factor; mean difference = difference between group mono-treatment and combination treatment in cell viability; light grey = significant mean difference; dark grey = no significant mean difference.

GSC culture	EF SAHA	Mean difference	EF LBH589	Mean difference	EF VPA	Mean difference	EF Scriptaid	Mean difference	EF MS275	Mean difference
GS79	2.3	27%	2.3	32%	2.8	30%	3.2	34%	1.7	24%
GS102	2.2	26%	1.6	31%	1.1	12%	1.6	29%	1.6	20%
GS401	3.0	24%	1.9	18%						
GS330	1.8	19%	1.6	16%						
GS423	1.3	18%	1.3	18%						
GS257	1.5	15%	1.2	8%	0.8	-12%	1	-2%		
GS186	1.5	15%	1.7	28%	1.5	19%	1.2	6%	1.4	16%
GS261	1.5	14%	1.6	14%	1.4	13%	1.8	20%	1.8	20%
GS224	1.3	13%	1.2	10%	1.4	17%	1.3	9%	1	3%
GS289	1.2	9%	1.2	7%						
GS357	1.2	9%	1.3	14%						
GS184	1.4	8%	2.4	29%						
GS160	1.2	8%	1.3	10%	1.4	16%	1	0%	1.5	12%
GS216	1.2	8%	1.2	13%						
GS274	1.2	8%	1.1	3%	1.1	4%	1	0%	1.2	4%
GS245	1.4	7%	1.5	13%	0.9	-2%	1.2	4%	1.4	14%
GS295	1.2	6%	1.1	6%	1.1	6%	1.7	20%	1.5	10%
GS203	1.2	6%	1.5	19%						
GS359	1.7	5%	2.2	13%						
GS279	1.0	0%	1.2	12%						
GS335	1.0	-2%	0.8	-18%						
GS365	0.9	-5%	0.6	-18%						

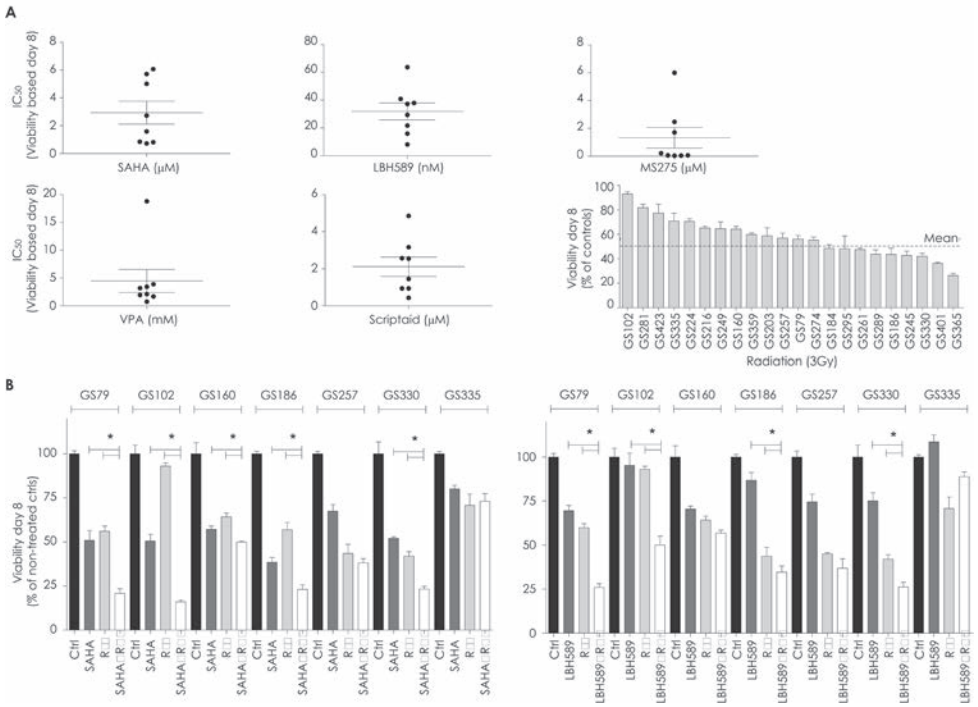

Figure 1. Differential responses to HDACi and to HDACi/RTx treatment.

(A) The IC_{50} values eight days post- treatment with the either of the five HDACi SAHA, LBH589, VPA, Scriptaid and MS275 were studied in eight different patient-derived glioblastoma cultures with CellTiter-Glo assay. The average IC_{50} values are displayed as the middle horizontal lines. The responses to a fixed dose of radiation (3Gy) are shown of the 22 cultures that were tested in the panel, as % viability of non-treated controls with the standard error, eight days post-treatment with 3Gy. **(B)** The radiosensitizing effects of SAHA, and LBH589 were determined by CellTiter Glo-assay in various patient-derived glioblastoma cultures. Seven representative cultures are shown, which included sensitive and resistant cultures to combination treatment. Cells were seeded 1x103 cells/well and treated with either 1μM SAHA or 20nM LBH589. After 24 hours the cells were irradiated with a single dose of 3Gy. At day eight the viability was measured by CellTiter Glo-assay. The results are presented as % viability of non-treated controls with the standard error. *Indicates significance at $p<0.05$.

HDACi increase histone-H3 acetylation in the sensitive glioblastoma culture

Since histone acetylation is an important mechanism of HDACi, the relation to radiosensitization efficacy by SAHA and LBH589 was studied pre- and post-treatment. By Western blot, the levels and alterations were initially assessed in two patient-derived glioblastoma cultures, one resistant and one sensitive to combination treatment. The acetylated histone-H3 levels were increased in the sensitive culture GS79 by both SAHA (657%), SAHA/RTx (505%) and in LBH589 (546%), LBH589/RTx (417%) as compared to non-treated controls and corrected for the β-actin levels (Figure 2A). In the resistant culture GS257, high baseline levels of acetylated histone-H3 were observed. The increase in levels was small in comparison to the sensitive culture: SAHA (129%), LBH589 (127%) and LBH589/RTx (115%). SAHA/RTx treated GS257 cells even had reduced histone-H3 acetylation levels (47%, Figure 2A).

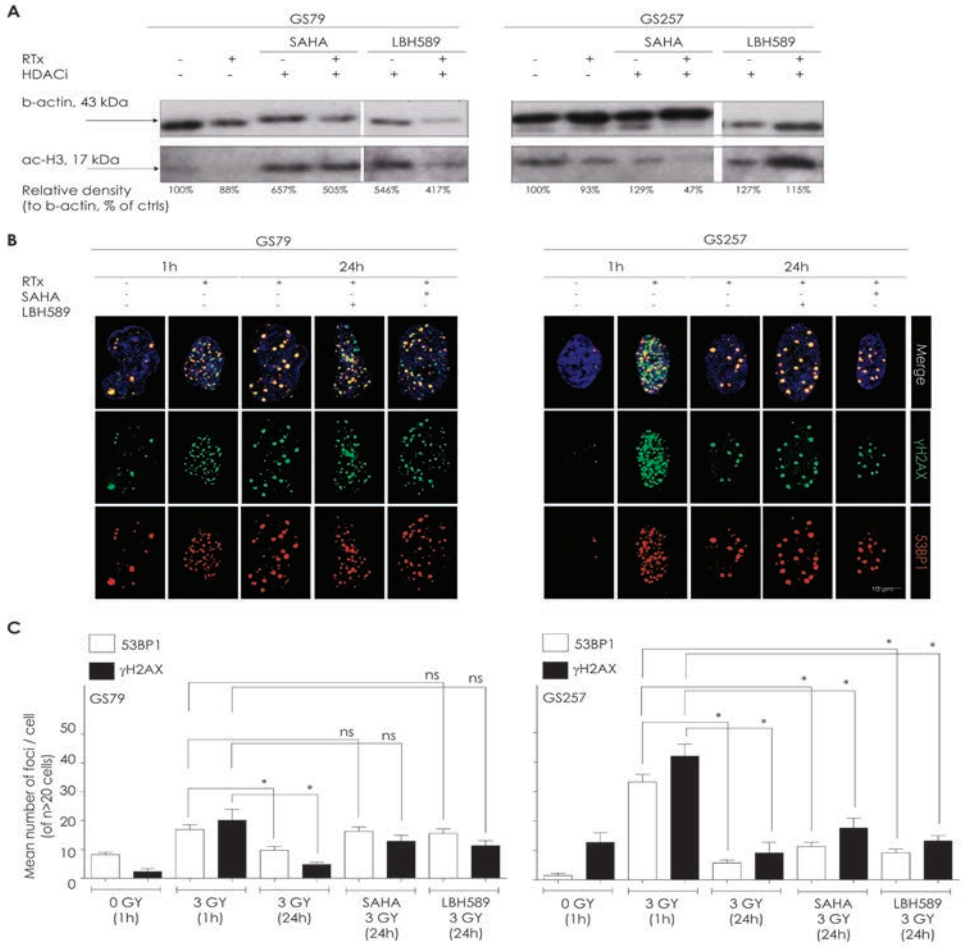

Figure 2. Differential effects on histone-H3 acetylation and DNA damage responses in the sensitive and resistant culture.

(A) Western blot detecting acetylation of histone-H3 in the patient-derived glioblastoma cultures GS79 and GS257 with HDACi and HDACi/RTx 24h after RTx. The relative densities corrected for β-actin levels are provided below the lanes. **(B)** DNA damage was analyzed in GS79 and GS257 by visualizing 53BP1 and γH2AX foci. Cells were incubated for 24 hours with 1μM SAHA or 20nM LBH589, and irradiated with 3Gy. Post-RTx (1 hour and 24 hours), the cells were fixed and stained with both antibodies and observed by confocal microscope. The drug-only figures are shown in Supplemental Figure 1, which did not differ for both drugs and both glioblastoma cultures at 1 hour and 24 hours post-treatment with the HDACi. **(C)** The graphs showing the 53BP1 and γH2AX DNA damage response foci in the patient-derived culture GS79 and GS257. The mean is shown of n>20 counted cells per sample slide with the standard error. The foci of the combination treatments were compared to the 3Gy induced foci at 1h. *Indicates significance at $p<0.05$.

SAHA and LBH589 prolonged the RTx induced DNA damage response in the sensitive glioblastoma culture

HDACi have been reported to influence the DNA damage repair response. Therefore the variations in DNA damage response were assessed in the sensitive and resistant culture

(GS79 and GS257). The DNA damage response proteins 53BP1 and γH2AX were stained. These proteins are known to localize at DNA damage sites. Particularly the duration of the foci presence was studied using the time-point of 24 hours, at which normally the RTx induced foci should have recovered to control levels. First of all, SAHA and LBH589 alone did not induce 53BP1/γH2AX foci in GS79 and GS257, at both 1 hour and 24 hours post-treatment (Supplemental Figure 1A). In both the responsive and resistant culture, both HDACi did not change the initial foci formation by RTx ($p>0.05$, Supplemental Figure 1B). In the sensitive culture, the RTx induced foci were normalized to control levels at 24 hours. At 24 hours, in the HDACi/RTx treated cells, the number of 53BP1 and the number of γH2AX foci were still comparable to the number of foci at 1 hour after RTx treatment (Figure 2B-C), meaning the foci were maintained in the presence of HDACi and the number of foci after 24 hours was higher in HDACi/RTx compared to RTx treated cells ($p<0.05$). In the resistant culture the number of RTx induced foci present at 1 hour post-RTx, was comparable to the combination treated cells, and at 24 hours all the treatment modalities had significantly decreased numbers of foci compared to RTx treated cells 1 hour post-treatment($p<0.05$). Thus, the level of foci induced by RTx at 1 hour was not maintained by HDACi in the resistant culture, contrary to the sensitive culture. The observed differences in 53BP1 and γH2AX clearance after 24 hours in the sensitive and resistant glioblastoma culture suggest differences in the DNA damage response.

Induction of apoptosis was related to responsiveness to HDACi/RTx

Next, cell-inhibition related mechanisms were studied in the sensitive and resistant patient-derived glioblastoma cultures. The cell cycle regulator $p21^{CIP1/WAF1}$, which is related to cell cycle arrest, was studied. In untreated cells, $p21^{CIP1/WAF1}$ was absent in the responsive culture GS79 and present in the resistant culture GS257. RTx increased $p21^{CIP1/WAF1}$ in the resistant culture (189%, upper band) but not in the sensitive culture (98%). SAHA and SAHA/RTx increased $p21^{CIP1/WAF1}$ levels in the sensitive culture (142% and 128% respectively). In the resistant culture the treatments did not alter $p21^{CIP1/WAF1}$ levels (SAHA 105%, SAHA/RTx 110% (upper band), LBH589 81% and LBH589/RTx 121%, Figure 3A). Thus, $p21^{CIP1/WAF1}$ levels were increased in the responsive culture by SAHA and by SAHA/RTx, whereas in the resistant culture, the RTx induced $p21^{CIP1/WAF1}$ levels, were lower in HDACi/RTx treatments. To assess whether decreased viability was associated to induction of apoptosis, the caspase-3/7 activity was assessed after treatment. Caspase-3/7 activity was increased ($p<0.0001$) in the sensitive glioblastoma culture by all the HDACi compared to RTx alone (Figure 3B). Combination treatment induced caspase-3/7 activity comparable to HDACi alone. In the resistant glioblastoma culture GS257, caspase-3/7 activity was significantly higher in the cells treated with HDACi only, however to a much lesser extent than in the sensitive culture. Also, the levels of the caspase-3/7 counts did not exceed the levels at 0 hours, meaning there was no up-regulation of caspase-3/7 activity, also not in the treated cells, but a smaller decrease of baseline levels over time. SAHA/RTx reduced caspase-3/7 activity and LBH589/RTx did not alter the levels. Thus, the caspase-3/7 levels increased compared to 0 hours by the HDACi and HDACi treatment, the levels of Bcl-2 were compared in both patient-derived glioblastoma cultures. The Bcl-2 protein was decreased in the sensitive culture by SAHA (46%), SAHA/RTx (60%), LBH589 (38%) and LBH589/RTx (84%) (Figure 3A). In the resistant glioblastoma culture Bcl-2 was increased by single dose RTx (89%) and maintained in HDACi and HDACi/RTx treated cells. Thus, the drugs had a pro-apoptotic effect and inhibited Bcl-2 in the sensitive culture, but not in the resistant culture. To establish these findings, we repeated this assay for the responsive culture

GS186, and the moderately responsive GS160 (low enhancement, only for SAHA). In GS186, HDACi reduced the Bcl-2 levels, whereas RTx induced Bcl-2 levels. These RTx-mediated increased Bcl-2 levels were suppressed by HDACi/RTx. In GS160, the HDACi did not affect the Bcl-2 levels in mono nor in combination treatment. These findings support our initial observations that Bcl-2 is inhibited by HDACi in sensitive cultures, whereas this protein is not affected in less responsive cultures, such as GS160.

Responses to HDACi/RTx correlated with clinical characteristics

Next, we studied whether the response to SAHA/RTx and LBH589/RTx was related to either clinical (Table 1) or molecular characteristics. The results show that for LBH589/RTx the enhancement was significantly higher in the glioblastoma cultures derived from *MGMT* promoter methylated tumors compared to *MGMT* promoter un-methylated tumors (17% vs. 6%, p=0.03). For SAHA/RTx, no differences in response were found between the two groups (Supplemental Figure 2A). No significant differences were found between cultures from male/female patients, and between recurrent and non-recurrent tumors (Supplemental Figure 2B-C). Spearman correlation showed that SAHA/RTx effect sizes were significantly negatively correlated with the PFS (Spearman r= -0.45, p=0.04, Supplemental Figure 2D). Age and KPS were not correlated to the response to both HDACi/RTx treatments (Supplemental Figure 2E-F). In conclusion, there may be an indication that *MGMT* promoter methylated tumors are more responsive to LBH589/RTx treatment, and that there exists a negative correlation between progression free survival and response to SAHA/RTx *in vitro*.

Response to HDACi/RTx correlate with levels of Chek2, pChek2, and Bcl-XL

Based on our *in vitro* comparisons of the sensitive and resistant patient-derived glioblastoma cultures, several proteins were evaluated as potential markers for response prediction and monitoring. The presence and activation of the early DNA damage response proteins Chek2 and ATM were assessed after RTx (first in five patient-derived cultures as pilot experiment and finally in all 22 cultures). The pilot experiment showed that baseline Chek2 levels were present in 2/2 sensitive cultures and in 1/3 resistant cultures. The Chek2 protein was only phosphorylated after RTx in the sensitive cultures. The pATM levels were not different between the two groups. In the resistant culture GS257 an extensive phosphorylation upon RTx was observed (Figure 3C). The other markers studied included acetylated histone-H3, Bcl-2 and Bcl-XL. To this end the 22 tested cultures were analyzed for these proteins and the results were used to calculate the positive predictive value (PPV) and negative predictive value (NPV). These values indicate precise the marker is in prediction, i.e. regarding false positivity and false negativity. Acetylated histone-H3 did not distinguish resistant from sensitive cultures. Regarding the early DNA damage response protein ATM, these levels were highly expressed in the sensitive and less in the resistant cultures. However ATM was present in almost all patient-derived glioblastoma cultures (Figure 4A). To identify potential markers for future evaluation in patients, a cut-off of 85% was considered (Figure 4B). The PPV for pChek2 was 90% for both HDACi/RTx. The PPV of Bcl-XL was 100% for LBH589/RTx. The values of the proteins that did not meet the cut-off of 85% are shown in Figure 4B, as well as their NPVs. Based on the data comparing the sensitive and resistant culture, a schematic representation of the possible response mechanism for SAHA and LBH589 as radiosensitizers was conceptualized (Figure 4C), for a pronounced sensitive and resistant culture.

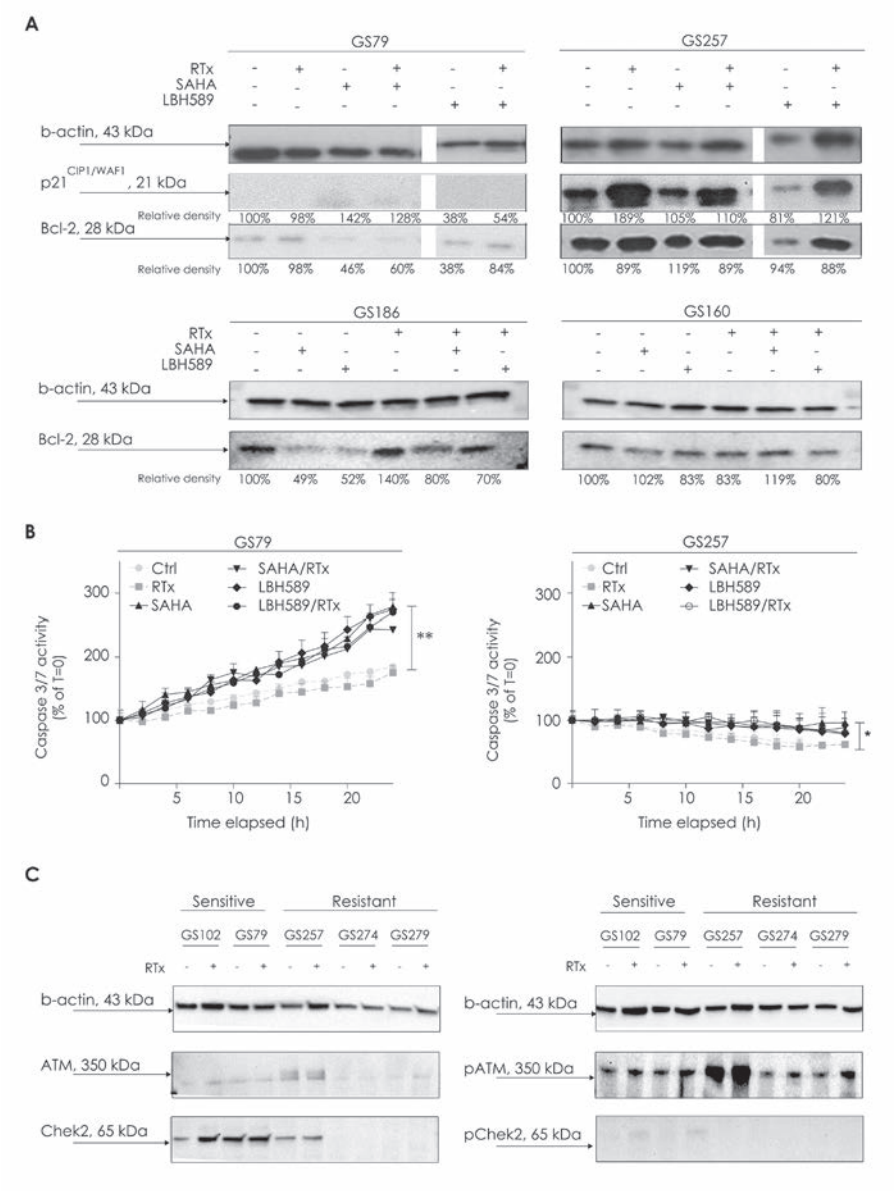

Figure 3. Differences in cell cycle regulation and apoptosis in a sensitive and resistant culture to HDACi/RTx treatment.

(A) Both glioblastoma cultures GS79 and GS257 were treated with HDACi/RTx and harvested 24 hours post-RTx. The levels of $p21^{CIP1/WAF1}$ and Bcl2 were determined by Western blot. The relative densities corrected for β-actin levels are provided below the lanes. Additionally, in the cultures GS160 (moderate responder) and GS186 (good responder), the experiments was repeated for the levels of Bcl-2. **(B)** Caspase-3/7 activity was determined by the Kinetic Caspase 3/7 assay and observed by an IncuCyte as fluorescent counts/mm2 up to 24 hours after RTx treatment. The results are shown as % of the level at 0 hours with the standard error. The time lapse was analyzed by using a two-way ANOVA. *Indicates significance at $p<0.05$. **(C)** Five patient-derived glioblastoma

cultures of which two were sensitive (GS102, GS79) and three were resistant (GS257, GS274, GS279) to combination treatment were analyzed for the DNA damage response at 0.5 hours after RTx. The levels of Chek2, ATM and the phosphorylation of these proteins after RTx were shown by Western blot.

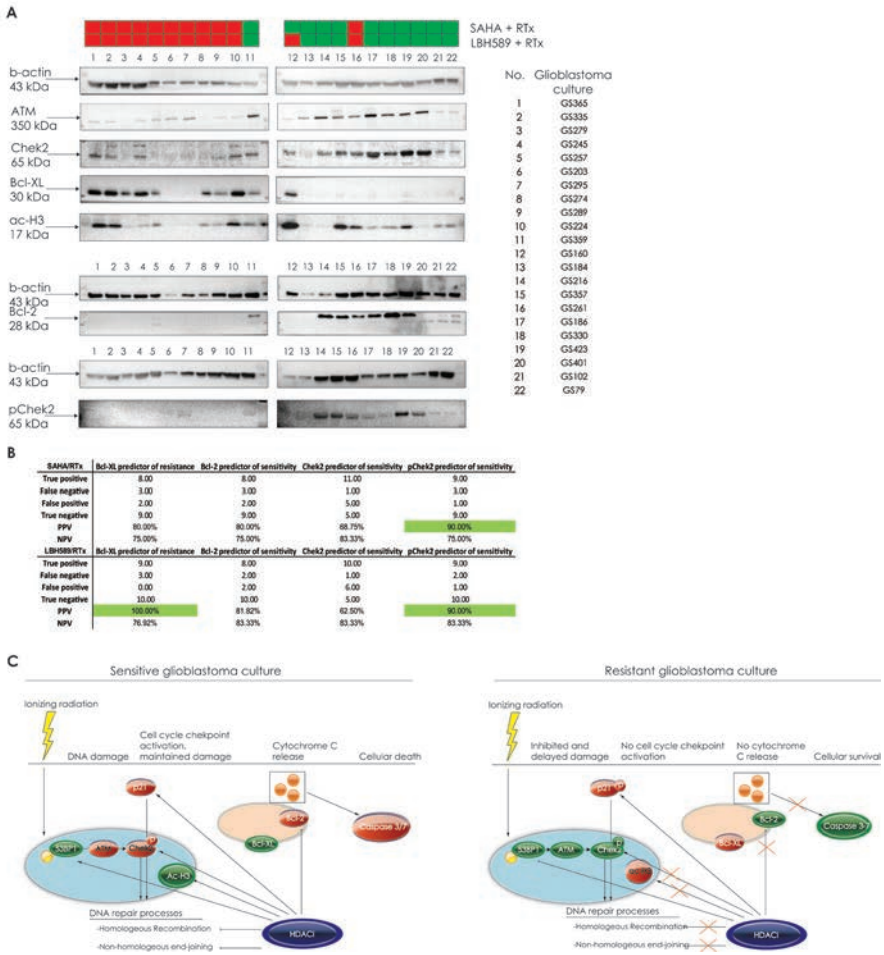

Figure 4. Predictors of response and monitoring response for HDACi/RTx and the proposed mechanism in sensitive and resistant glioblastoma cultures.

(A) Twenty-two glioblastoma cultures were analyzed for their relative protein levels of ATM, Chek2, Bcl-XL, acetylated histone-H3, Bcl-2 and the ability to phosphorylate Chek2 (pChek2) upon radiation by Western blotting. Cells were grown in culture flasks and harvested (controls) or radiated with 3Gy and harvested after 0.5 hours of incubation. **(B)** An overview of the potential response markers that were identfied in this study, showing the positive and negative predictive values to predict response *in vitro*. Some are candidate markers to determine response to SAHA/RTx and LBH589/RTx. **(C)** A schematic presentation of the sensitive and resistant patient-derived glioblastoma culture with regard to the different studied proteins and mechanisms. In a pronounced sensitive culture, histone-H3 is acetylated upon HDACi treatment. DNA damage foci are prolonged by HDACi/RTx treatment. In general the levels of ATM and Chek2 are relatively high and Chek2 is phosphorylated rapidly upon RTx. The DNA damage repair is inhibited by HDACi, finally leading to activation of caspase-3/7

and apoptosis. Since Bcl-XL is low it will not cause resistance to apoptosis. HDACi inhibit the high protein levels of Bcl-2, cytochrome C will be released and caspase-3/7 is activated. The resistant culture does not have altered levels of acetylated histone-H3 upon HDACi treatment. The DNA damage foci are not prolonged at 24 hours after HDACi/RTx. In general ATM and Chek2 levels are low and Chek2 is not phosphorylated upon RTx. Bcl-2 is present but is not inhibited, which also distinguished good responders from moderate responders or resistant cultures. Bcl-XL is highly present and prevents the cell from caspase-3/7 activation and apoptosis.

Time scheduling is crucial for combination effectiveness, single dose RTx application is not. Also, the importance of the time schedule of combination treatment for the effectiveness of HDACi was investigated. The results show that SAHA given pre-RTX enhanced RTx significantly better than the other regimens tested (Figure 5A). By administering the compound simultaneously with RTx, the radiosensitizing effects were absent in several cases and significantly smaller in other cases. The results of these experiments were comparable in a total of three patient-derived glioblastoma cultures (Figure 5B). Also the effects of fractionized RTx were evaluated, as is the standard of care for patients. The various RTx doses were applied in three fractions. Fractionized RTx did not affect the enhancement and efficacy of the combinations of SAHA/RTx in three patient-derived glioblastoma cultures (GS79, GS102, GS245). The efficacy was comparable to single dose treatment (Figure 5B shows the data of GS79 and GS102 treated by SAHA and LBH589).

3.4 Conclusion

This study shows that the HDACi SAHA, VPA, MS275, LBH589 and Scriptaid are radiosensitizers in a significant proportion of patient-derived glioblastoma cultures and have largely varying enhancement. The percentages of cultures responsive to the various HDACi, were comparable and in many cases overlapping for the glioblastoma cultures. The observed variations in sensitivity show a relationship with molecular characteristics of the specific cultures.[21] Regarding the clinically most relevant HDACi, SAHA and LBH589, differences in the DNA damage and apoptotic response were found between responsive and resistant cultures. Various identified associated molecules that warrant further exploration as candidate response markers are pChek2 for both SAHA/RTx and LBH589/RTx, and in addition Bcl-XL for LBH589/RTx. Although these molecules are promising candidates having PPVs of 90% and 100%, the 90% still has a false positive or negative rate of 10%. Therefore, these markers need further evaluation in the clinical setting, and using combinations of markers may increase predictive accuracy. Specifically for cultures that were moderately responsive to combination treatment, these markers need additional information provided by other assays: for example the levels of Bcl-2 after treatment with the drugs.

In addition, this study reveals that SAHA/RTx response *in vitro* was negatively related to the PFS of patients from which the cultures were derived. This finding may be clinically promising. Combination response was not related to *MGMT* promoter methylation status, which is usually a prognostic predictor. On the contrary, LBH589/RTx treatment response was related to *MGMT* promoter methylation status of the tumor; however, the differences in means between groups were found to be small.

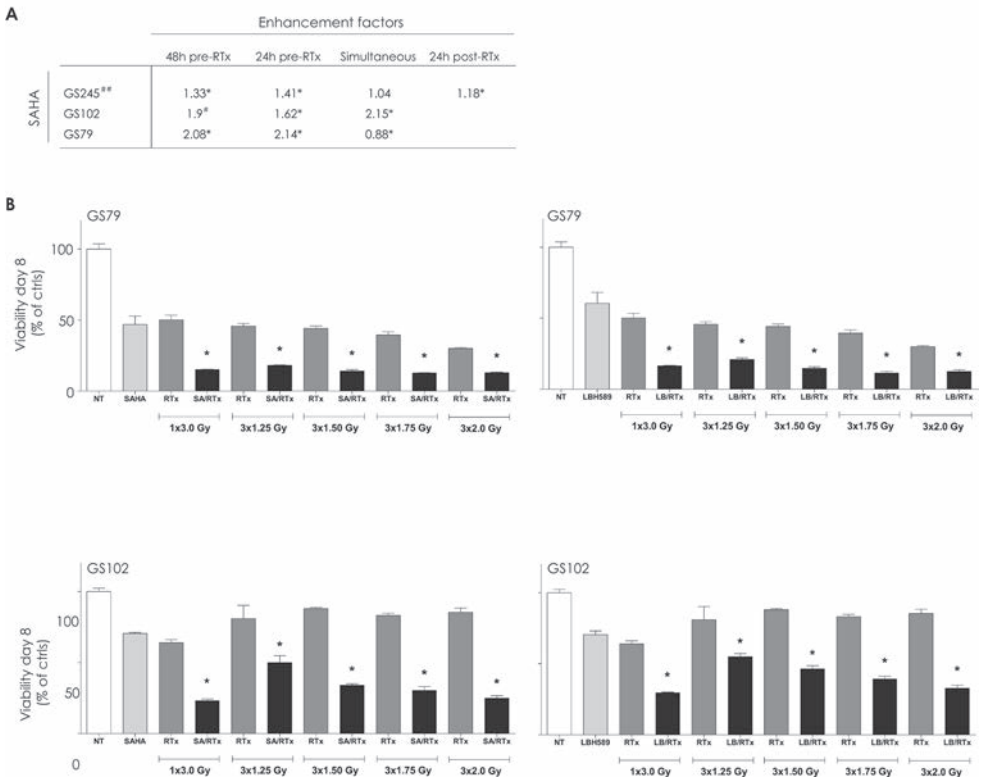

Figure 5. Timing and fractionation RTx in HDACi/RTx treatment.

(A) Cells were seeded 0.75 x10^3 cells/well and treated according different time schedules with 1μM SAHA and RTx (3Gy). Treatment schedules of applying HDACi differed from 48 hours pre-RTx to 24 hours post-RTx. After seven days of treatment, viability was measured by CellTiter-Glo-assay. Results are presented as enhancement factors. *Indicates significant difference between combination and mono treatment at $p<0.05$. #Indicates $p = 0.05$ for one of the treatments vs. combination treatment. ## Indicates data obtained from two independent experiments. **(B)** GS79 and GS102 were seeded 1x10^3 cells/well and treated with 1μM SAHA or 20nM LBH589. The cells were irradiated 24 hours after incubation with either a single dose of 3Gy or every 24 hours three fractions of 1.25Gy, 1.50Gy, 1.75Gy or 2Gy. The results were depicted as % of non-treated controls with the standard error.

3.5 Discussion

Differences in DNA damage response between patient-derived glioblastoma cultures are related to sensitivity to HDACi/RTx treatment

A recent review summarized the effects of HDACi on the DNA damage response including inhibition of the non-homologous end-joining and homologous recombination.[8] According to our data these effects are likely to occur in the sensitive and not in the resistant cultures. Firstly the DNA damage response (by 53BP1 and γH2AX) is prolonged in the sensitive culture by SAHA and LBH589 but not in the resistant culture. A prolonged increased level of DNA damage foci caused by HDACi has been reported earlier.[22] This study supports

that HDACi/RTx induces maintained high levels of DNA damage response markers. Since we have studied this phenomenon by using both a repair protein, γH2AX, that depends on dephosphorylation by Wip1[23] and one whose activity is independent of Wip1 dephosphorylation processes (53BP1), our data strongly suggest that prolonged foci are indeed the result of prolonged DNA damage. The findings thus point toward ineffective double stranded breaks repair. One possible explanation is that the breaks have been caused during a heterochromatin status. A second possible explanation is that the HDACi affect the DNA repair response as described above.[8] The resistant culture already harbored a high level of initial foci which is potentially due to pre-existing defects in the repair of residual breaks. DNA-PK defects for example can cause clustered DNA lesions in tumor cells.[24] Because of a continuously high level of chronic double stranded breaks, these cultures would potentially undergo other mutations that repress cell cycle checkpoints and apoptosis. Chek2 is a downstream checkpoint kinase and tumor suppressor which is activated in response to DNA damage and blocks cell cycle progression. Chek2 was associated with response to both SAHA/RTx and LBH589/RTx, but more strongly its phosphorylation (pChek2) upon RTx was associated with response. Mutations in the *CHEK2* gene have been described for glioblastoma.[25] In addition, a defective ATM/Chek2/p53 axis is associated with poor response to chemotherapy in other cancers.[26] ATM levels are higher in sensitive cultures but are present at lower levels in resistant cultures. The present study also supports that sensitivity and resistance are related to a differentially functioning ATM/Chek2 DNA damage response.

The levels of Bcl-2 family members differ between patient-derived glioblastoma cultures and are related to response to HDACi/RTx treatment

The apoptotic mechanism also plays an important role in the action of HDACi/RTx. Inactivation of the mitochondrial bound Bcl-2 anti-apoptotic proteins may lead to apoptosis.[27] Bcl-2 proteins can prevent the cell from caspase-dependent cell death[28] and are associated with resistance to HDACi.[12,13,29] This is consistent with the finding that Bcl-XL levels are high in the resistant cultures and Bcl-2 is maintained at baseline level in resistant cultures under HDACi treatment. In contrast Bcl-2 was shown to be down-regulated in the sensitive cultures GS186 and GS79. In addition, the culture with moderate responsiveness, but with 'responder-associated markers' of Chek2 and Bcl-XL, the regulation of Bcl-2 by the HDACi/RTx treatment showed a non-responsiveness pattern. This suggests that for the cultures with moderate response that express predictive markers, this assay may provide additional information about the final response to treatment. Caspase-3/7 is not significantly activated in resistant cells upon treatment, whereas in the sensitive culture caspase-3/7 is induced by HDACi, but independently of RTx. As there can be a lack of apoptosis induction as is debated in the literature,[30] in our samples the RTx alone did not induce apoptosis either. In the combination treatment, high Bcl-XL levels may contribute to the lack of apoptosis induction by the HDACi in the resistant cultures. Moreover, anti-apoptotic family members Mcl-1, Bcl-XL and Bcl-2 have roles in the DNA damage response as they are involved in cell cycle arrest upon DNA damage,[31] the NHEJ damage repair response,[32] chromosomal abnormalities in tumors and coordination of the DNA damage response.[33]

Furthermore, assessing the possibility of monitoring the *in vitro* response to HDACi/RTx by using acetylation of histone-H3 in tumors showed that this is not effective in this model. Hyper-acetylation was present in untreated resistant cultures and therefore using this characteristic as a marker could be misleading in monitoring the response. The use

of $p21^{CIP1/WAF1}$ as a response marker also seems limited. In established cell lines several HDACi have shown to cause increased $p21^{CIP1/WAF1}$.[14,34] In the comparison between sensitivity and resistance in this study, the regulation of $p21^{CIP1/WAF1}$ was not related to reduced viability as it was increased in both the resistant and sensitive culture.

The sequence of treatment application is crucial for the efficacy of HDACi/RTx treatment
The timing of the combination treatments shows increased effectiveness when HDACi are given 24 hours or 48 hours pre-RTx. This advantage is in accordance with another study that has demonstrated a better radio-enhancement when cells are exposed to HDACi 16 hours before RTx.[35] However, additional effects have also been reported when VPA is administered post-RTx.[36] This difference might be explained by the use of a different model or by differences in the used drug concentrations. A possible explanation for the time-dependent sensitization efficacy is that a certain time interval is required for altered transcription of DNA repair genes[37,38] and for inhibition of anti-apoptotic genes. Also the present study shows that fractionizing radiation did not alter the radio-sensitizing effects of HDACi and does not seem a drawback to achieve treatment effects. In conclusion this indicates that the timing of HDACi application before the initial dose of RTx is an important variable to achieve optimal treatment response and the fractionizing of RTx is not.

References

1. Stupp R, Mason WP, van den Bent MJ, et al. Radiotherapy plus concomitant and adjuvant temozolomide for glioblastoma. The New England journal of medicine 2005;352:987-96.
2. Stiborova M, Eckschlager T, Poljakova J, et al. The synergistic effects of DNA-targeted chemotherapeutics and histone deacetylase inhibitors as therapeutic strategies for cancer treatment. Current medicinal chemistry 2012;19:4218-38.
3. Shabason JE, Tofilon PJ, Camphausen K. Grand rounds at the National Institutes of Health: HDAC inhibitors as radiation modifiers, from bench to clinic. J Cell Mol Med 2011;15:2735-44.
4. Thiemann M, Oertel S, Ehemann V, et al. In vivo efficacy of the histone deacetylase inhibitor suberoylanilide hydroxamic acid in combination with radiotherapy in a malignant rhabdoid tumor mouse model. Radiat Oncol 2012;7:52.
5. Deorukhkar A, Shentu S, Park HC, et al. Inhibition of radiation-induced DNA repair and prosurvival pathways contributes to vorinostat-mediated radiosensitization of pancreatic cancer cells. Pancreas 2010;39:1277-83.
6. Sonnemann J, Kumar KS, Heesch S, et al. Histone deacetylase inhibitors induce cell death and enhance the susceptibility to ionizing radiation, etoposide, and TRAIL in medulloblastoma cells. Int J Oncol 2006;28:755-66.
7. Chinnaiyan P, Vallabhaneni G, Armstrong E, Huang SM, Harari PM. Modulation of radiation response by histone deacetylase inhibition. Int J Radiat Oncol Biol Phys 2005;62:223-9.
8. Groselj B, Sharma NL, Hamdy FC, Kerr M, Kiltie AE. Histone deacetylase inhibitors as radiosensitisers: effects on DNA damage signalling and repair. Br J Cancer 2013;108:748-54.

9. Geng L, Cuneo KC, Fu A, Tu T, Atadja PW, Hallahan DE. Histone deacetylase (HDAC) inhibitor LBH589 increases duration of gamma-H2AX foci and confines HDAC4 to the cytoplasm in irradiated non-small cell lung cancer. Cancer Res 2006;66:11298-304.
10. Health NIo. Www.clinicaltrials.gov. last visited May 2015.
11. Balvers RK, Kleijn A, Kloezeman JJ, et al. Serum-free culture success of glial tumors is related to specific molecular profiles and expression of extracellular matrix-associated gene modules. Neuro Oncol 2013;15:1684-95.
12. Lee JH, Choy ML, Marks PA. Mechanisms of resistance to histone deacetylase inhibitors. Advances in cancer research 2012;116:39-86.
13. Emanuele S, Lauricella M, Tesoriere G. Histone deacetylase inhibitors: apoptotic effects and clinical implications (Review). Int J Oncol 2008;33:637-46.
14. Xu J, Sampath D, Lang FF, et al. Vorinostat modulates cell cycle regulatory proteins in glioma cells and human glioma slice cultures. J Neurooncol 2011;105:241-51.
15. Sims JT, Plattner R. MTT assays cannot be utilized to study the effects of STI571/Gleevec on the viability of solid tumor cell lines. Cancer Chemother Pharmacol 2009;64:629-33.
16. Chou TC, Talalay P. Quantitative analysis of dose-effect relationships: the combined effects of multiple drugs or enzyme inhibitors. Advances in enzyme regulation 1984;22:27-55.
17. Cen H, Mao F, Aronchik I, Fuentes RJ, Firestone GL. DEVD-NucView488: a novel class of enzyme substrates for real-time detection of caspase-3 activity in live cells. Faseb J 2008;22:2243-52.
18. Thon JN, Devine MT, Jurak Begonja A, Tibbitts J, Italiano JE, Jr. High-content live-cell imaging assay used to establish mechanism of trastuzumab emtansine (T-DM1)--mediated inhibition of platelet production. Blood 2012;120:1975-84.
19. Chou TC. Theoretical basis, experimental design, and computerized simulation of synergism and antagonism in drug combination studies. Pharmacological reviews 2006;58:621-81.
20. Coe R. What effect size is and why it is important http://wwwleedsacuk/educol/documents/00002182htm 2002.
21. Verhaak RG, Hoadley KA, Purdom E, et al. Integrated genomic analysis identifies clinically relevant subtypes of glioblastoma characterized by abnormalities in PDGFRA, IDH1, EGFR, and NF1. Cancer Cell 2010;17:98-110.
22. Camphausen K, Burgan W, Cerra M, et al. Enhanced radiation-induced cell killing and prolongation of gammaH2AX foci expression by the histone deacetylase inhibitor MS-275. Cancer Res 2004;64:316-21.
23. Cha H, Lowe JM, Li H, et al. Wip1 directly dephosphorylates gamma-H2AX and attenuates the DNA damage response. Cancer Res 2010;70:4112-22.
24. Peddi P, Loftin CW, Dickey JS, et al. DNA-PKcs deficiency leads to persistence of oxidatively induced clustered DNA lesions in human tumor cells. Free radical biology & medicine 2010;48:1435-43.
25. Sallinen SL, Ikonen T, Haapasalo H, Schleutker J. CHEK2 mutations in primary glioblastomas. J Neurooncol 2005;74:93-5.
26. Knappskog S, Chrisanthar R, Lokkevik E, et al. Low expression levels of ATM may substitute for CHEK2 /TP53 mutations predicting resistance towards anthracycline and mitomycin chemotherapy in breast cancer. Breast Cancer Res 2012;14:R47.

27. Chen X, Wong P, Radany E, Wong JY. HDAC inhibitor, valproic acid, induces p53-dependent radiosensitization of colon cancer cells. Cancer Biother Radiopharm 2009;24:689-99.
28. Okuno S, Shimizu S, Ito T, et al. Bcl-2 prevents caspase-independent cell death. J Biol Chem 1998;273:34272-7.
29. Bolden JE, Peart MJ, Johnstone RW. Anticancer activities of histone deacetylase inhibitors. Nat Rev Drug Discov 2006;5:769-84.
30. Watters D. Molecular mechanisms of ionizing radiation-induced apoptosis. Immunol Cell Biol 1999;77:263-71.
31. Wang J, Beauchemin M, Bertrand R. Bcl-xL phosphorylation at Ser49 by polo kinase 3 during cell cycle progression and checkpoints. Cellular signalling 2011;23:2030-8.
32. Kumar TS, Kari V, Choudhary B, Nambiar M, Akila TS, Raghavan SC. Anti-apoptotic protein BCL2 down-regulates DNA end joining in cancer cells. J Biol Chem 2010;285:32657-70.
33. Jamil S, Stoica C, Hackett TL, Duronio V. MCL-1 localizes to sites of DNA damage and regulates DNA damage response. Cell Cycle 2010;9:2843-55.
34. Gui CY, Ngo L, Xu WS, Richon VM, Marks PA. Histone deacetylase (HDAC) inhibitor activation of p21WAF1 involves changes in promoter-associated proteins, including HDAC1. Proc Natl Acad Sci U S A 2004;101:1241-6.
35. Camphausen K, Cerna D, Scott T, et al. Enhancement of *in vitro* and *in vivo* tumor cell radiosensitivity by valproic acid. Int J Cancer 2005;114:380-6.
36. Chinnaiyan P, Cerna D, Burgan WE, et al. Postradiation sensitization of the histone deacetylase inhibitor valproic acid. Clin Cancer Res 2008;14:5410-5.
37. Munshi A, Tanaka T, Hobbs ML, Tucker SL, Richon VM, Meyn RE. Vorinostat, a histone deacetylase inhibitor, enhances the response of human tumor cells to ionizing radiation through prolongation of gamma-H2AX foci. Mol Cancer Ther 2006;5:1967-74.
38. Chen X, Wong P, Radany EH, Stark JM, Laulier C, Wong JY. Suberoylanilide hydroxamic acid as radiosensitizer through modulation of RAD51 protein and inhibition of homology-directed repair in multiple myeloma. Mol Cancer Res 2012.

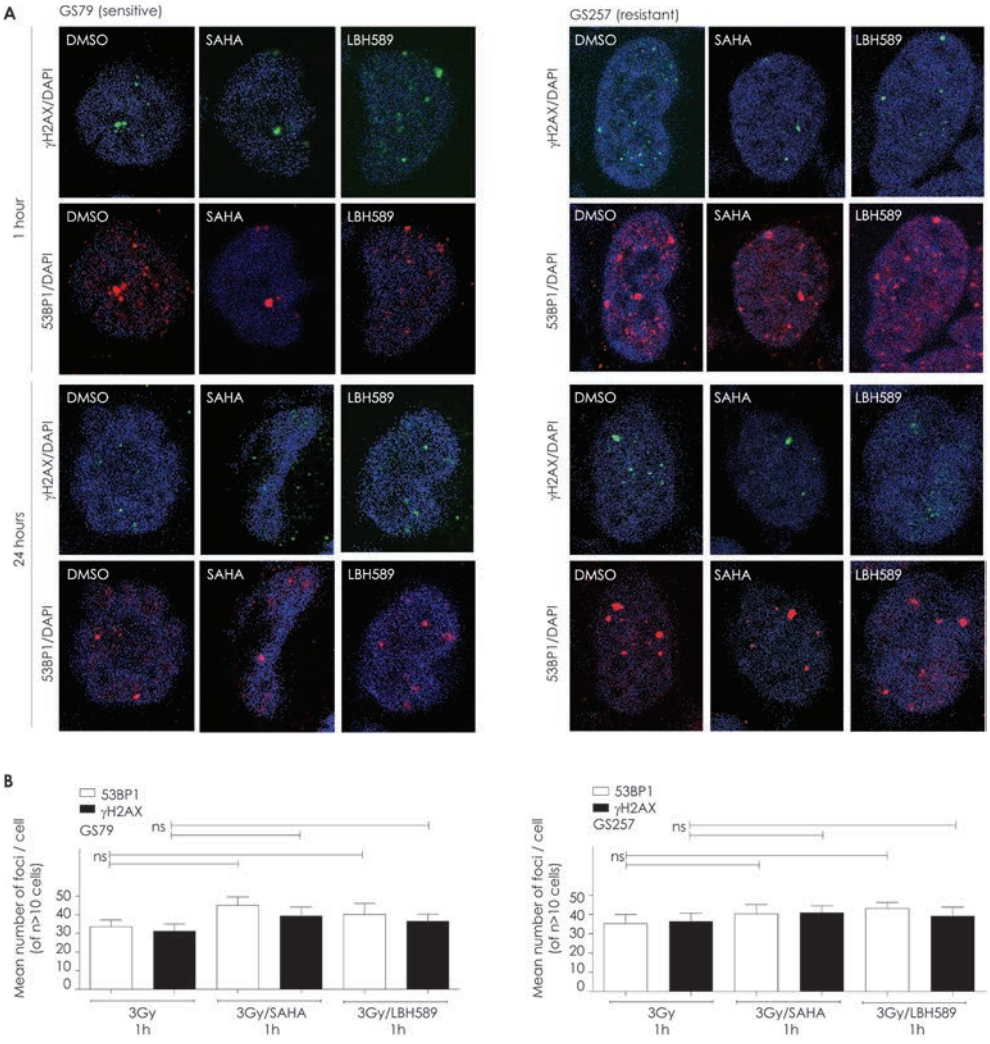

Supplemental Figure 1. The 53BP1 and γH2AX foci in HDACi only treated cells.

(A) The DNA damage response was analyzed in both patient-derived glioblastoma cultures GS79 and GS257, by visualizing 53BP1 and γH2AX foci. The drug-only figures corresponding to the experiment presented in Figure 2C. Cells were incubated with either 1μM SAHA or 20nM LBH589. At 1 hour and 24 hours post-RTx, the cells were fixed and stained with both antibodies and observed by confocal microscope. No difference were observed for both drugs in both glioblastoma cultures at 1 hour and 24 hour post-treatment with the HDACi alone. **(B)** The graphs show the 53BP1/γH2AX DNA damage response foci in the patient-derived culture GS79 and GS257 at 1 hour post-RTx. The mean is shown of n>10 counted cells per sample slide with the standard error. The foci of the combination treatments were compared to the 3Gy induced foci at 1 hour. No significant differences were observed.

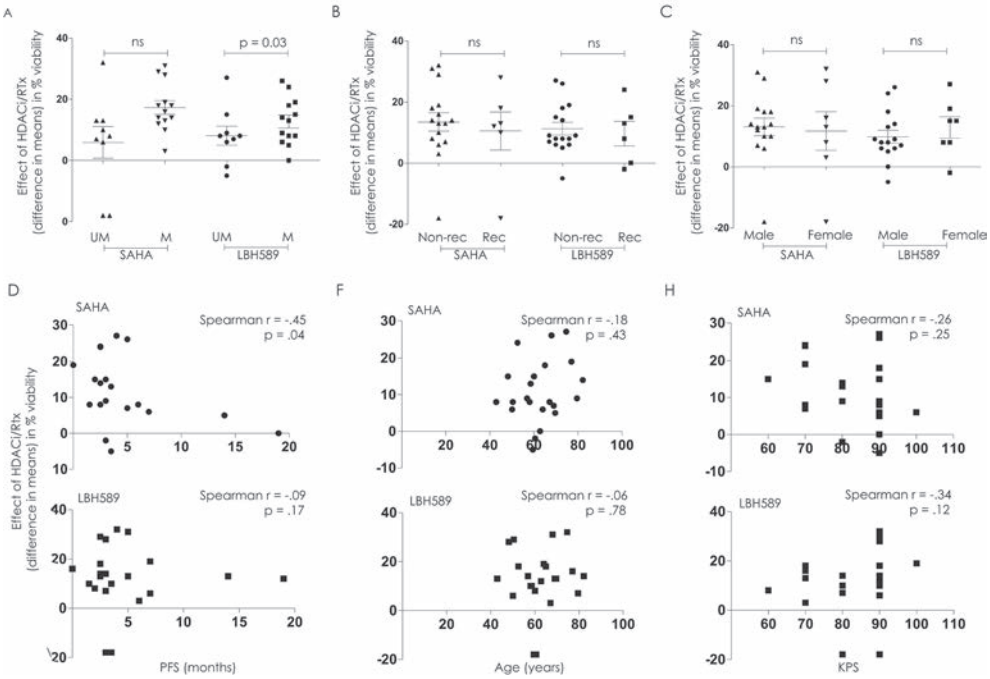

Supplemental Figure 2. The clinical characteristics of the patient-derived glioblastoma cultures and the relation with HDACi/RTx treatment.

The mean differences in effects of mono and combination treatments for SAHA/RTx and LBH589/RTx (effects) were compared between the **(A)** *MGMT* promoter methylated and *MGMT* promoter un-methylated culture, **(B)**, the non-recurrent and recurrent cultures and **(C)** the male derived and the female derived cultures, by using the Mann Whitney U-test. Significance was considered $p<0.05$. The mean differences in effects of mono and combination treatments for SAHA/RTx and LBH589/RTx (effects) were correlated with progression free survival (PFS in months), age at time of surgical resection (in years) and the pre-operative Karnofsky Performance Score (KPS) with the Spearman correlation test. Significance was considered $p<0.05$

Chapter 4

The Bcl2-inhibitor obatoclax overcomes resistance to histone deacetylase inhibitors SAHA and LBH589 as radiosensitizers in patient-derived glioblastoma stem-like cells

Lotte M.E. Berghauser Pont,[1] Jochem K.H. Spoor,[1] Subramanian Venkatesan,[1] Sigrid Swagemakers,[2] Jenneke J. Kloezeman,[1] Clemens M.F. Dirven,[1] Peter J. van der Spek,[2] Martine L.M. Lamfers,[1] Sieger Leenstra.[1,3]

Affiliations

1 Department of Neurosurgery, Brain Tumor Center, Erasmus MC
2 Department of Bio-informatics, Brain Tumor Center, Erasmus MC
3 Department of Neurosurgery, Elisabeth Medical Hospital

Published in Genes Cancer. 2014 Nov; 5(11-12): 445-59

PMID: 25568669

Abstract

Glioblastoma has shown resistance to histone deacetylase inhibitors (HDACi) as radiosensitizers in case of overexpression of Bcl-XL proteins. We study the efficacy of SAHA/RTx and LBH589/RTx when manipulating Bcl-2 family proteins using the Bcl-2 inhibitor Obatoclax in patient-derived glioblastoma stem-like cell cultures (GSC cultures) which in general have a deletion in phosphatase and tensin homolog (PTEN). Synergy was determined by the Chou Talalay method. The effects on apoptosis and autophagy were studied by measuring caspase-3/7, Bcl-XL, Mcl-1 and LC3BI/II proteins. The relation between treatment response and O6-Methylguanine-DNA methyltransferase (*MGMT*) promoter methylation status, recurrence and gene expression levels of the tumors were studied. Obatoclax synergized with SAHA and LBH589 and sensitized cells to HDACi/RTx. Over 50% of GSC cultures were responsive to Obatoclax with either single agent. Combined with HDACi/RTx treatment, Obatoclax increased caspase-3/7 and inhibited Bcl-2 family proteins Bcl-XL and Mcl-1 more effectively than other treatments. A set of predictive genes was identified for treatment response, including the F-box/WD repeat-containing protein-7 (FBXW7), which was previously related to Bcl-2 inhibition and HDACi sensitivity. In conclusion, we emphasize the functional relation between Bcl-2 family proteins and radiosensitization by HDACi and we herewith provide a target for increasing responsiveness in a model of PTEN deleted glioblastoma by using the novel Bcl-2 family inhibitor Obatoclax.

4.1 Introduction

Patients with glioblastoma have a poor prognosis.[1] Thus far, maximally safe surgical resection and radiation therapy (RTx) with adjuvant temozolomide (TMZ) gives a median survival of 14.7 months.[1] The O6-Methylguanine-DNA methyltransferase (MGMT) promoter methylation status is the most important biomarker that predicts response to current therapy.[2] Some of the causes of poor outcome lie in the heterogeneity of the tumor and the multiple escape pathways glioblastoma harbors.[3,4] Specifically targeting these resistance pathways using combination therapies may be an approach to achieve better treatment results in this disease. A novel therapy in glioblastoma that is currently under phase I/II investigation is the epigenetic modulatory treatment using histone deacetylase inhibitors (HDACi). These drugs affect multiple pathways including apoptosis, autophagy and DNA damage repair.[5] We reported earlier that a subset of patient-derived glioblastoma stem-like cell cultures (GSC cultures) showed resistance to the combination of RTx with the HDACi SAHA or LBH589.[6] Both over-expression of Bcl-XL proteins as well as the maintained Bcl-2 proteins post-HDACi treatment were related to this resistance.[6] Thus, regulation of Bcl-2 family members may be an important mechanism in the resistance to HDACi as radiosensitizers. Others have already shown that these proteins are important in resistance to HDACi as single agents.[7] The Bcl-2 family regulates the intrinsic cell death pathway by controlling permeability of the outer mitochondrial membrane.[8] In addition, by binding the endoplasmic reticulum, these proteins regulate autophagy by binding to Beclin-1.[9] Inhibiting these Bcl-2 family proteins may provide an effective strategy in overcoming resistance to HDACi.[10] A recent study has shown efficacy of the Bcl-2 inhibitor ABT-737 and SAHA in an immortalized glioma model. Efficacy was only observed in cell lines with an intact phosphatase and tensin homolog (PTEN) status. In our study, we aimed to inhibit the anti-apoptotic Bcl-2 pathway by using Obatoclax, to enhance the efficacy of SAHA and LBH589 as both single agents and as radiosensitizers in the PTEN deleted patient-derived GSC model.[11,12] Obatoclax is a Bcl-2 family inhibitor which has higher affinity than ABT-737 to inhibit Bcl-XL, Mcl-1

and to induce autophagy.[10,13,14] Obatoclax reduces Bak/Mcl-1-binding, up-regulates Bim and subsequently induces cytochrome-C release and caspase-3-activity.[15] The drug is currently being tested in clinical trials for hematological cancers, non-small cell lung carcinoma and extensive-stage small-cell lung carcinoma.[16-19] Our study provides novel insights into the efficacy of inhibiting the Bcl-2 family pathway by Obatoclax in overcoming resistance to HDACi as radiosensitizers. In addition, gene expression prediction profiles for treatment response to the various modalities were identified.

4.2 Materials and methods

Chemicals

Stocks of 50mM SAHA (Cayman chemicals, MI, USA), 200µM LBH589 (Biovision, CA, USA) and 60mM Obatoclax (Selleck Chemicals, Texas, USA) were prepared in dimethyl sulfoxide (DMSO, Sigma-Aldrich, MO, USA) and stored at -20°C. Staurosporin was obtained from BioMol, Germany.

Patient-derived glioblastoma stem-like cell cultures

Fresh glioblastoma tissue was obtained from patients undergoing surgery at the Department of Neurosurgery, ErasmusMC (Rotterdam, The Netherlands) after informed consent and approval by the institution's medical ethical board. The tissue was dissociated mechanically and enzymatically, after which the patient-derived GSC cultures were cultured under serum-free conditions in DMEM/F12 medium supplemented with 2% B27 (Life Technologies, UK), 20ng/ml bFGF, 20ng/ml EGF (Tebu-Bio, France), 5ug/ml heparin (Sigma-Aldrich, MO, USA) as was described previously.[11] These patient-derived GSC cultures, which were characterized and validated as previously reported.[11] The U373 cells were cultures under 10% serum conditions in DMEM medium. The cultures were stored at 37°C in a humid 95% air/5% CO_2 chamber. In total, nineteen patient-derived GSC cultures were used for the experiments.

Viability assays

Concentration-response assays were performed in order to determine IC_{50} values of Obatoclax. The cells of various GSC cultures were plated at $1x10^3$ cells/well in 96-wells plates. After incubation overnight, various drug concentrations in three-fold increments were applied to the cells. At five and eight days post-treatment cell viability was measured using the CellTiter-Glo assay (Promega, WI, USA). The results were plotted and the IC_{50} values were computed using the median effect equation.[20] The IC_{50} values of the HDACi SAHA and LBH59 in the GSC cultures GS79 and GS257 were derived from previous research.[6] Subsequently, Chou-Talalay assays were performed on the GSC cultures GS79 and GS257 for Obatoclax in combination with the HDACi to determine synergy.[20] After assessment of the combination effects in these two cultures, either two or four concentrations (10, 30, 100 and 225nM) were applied to the panel of patient-derived GSC cultures to determine the combination effects. From these concentrations, an estimated IC_{50} was calculated for each glioblastoma culture. The HDACi concentrations were always kept similar at 1µM SAHA and 20nM LBH589. The DMSO concentration was never above 1% in the dilutions. RTx (3Gy) was applied as single-fraction treatment from a Cesium-137 source 24 hours after drug application.

Western blot
Alteration of specific proteins post-treatment was determined by seeding cells of the GSC culture GS257 in culture flasks with 225nM Obatoclax, 1 µM SAHA and the combination. After 24 hours, the cells were irradiated with 3Gy. At 24 and 48 hours post-RTx, the cells were harvested, washed with PBS and collected in a 1% Triton-X100 (Sigma-Aldrich) buffer for protein isolation. Protein concentrations were measured with the BCA Protein Assay Reagent Kit (Thermo Fisher Scientific, MA, USA). Protein separation was performed on a 4-15% pre-casted gel (Bio-Rad, CA, USA), and blotted onto a PVDF membrane (Immobilon-P, Millipore, MA, USA) using the Mini-Protean Tetra Cell system (Bio-Rad). After blocking the membranes with 5% non-fatty milk solution for 30 minutes at room temperature, the blots were incubated with primary antibodies against Bcl-XL, LC3BI/II, Mcl-1 (1:375, Cell Signaling, MA, USA) and anti-β-actin (1:5,000, Millipore) in 5% BSA/TBS-T overnight. Membranes were washed with TBS-T 0.2% and incubated with secondary antibodies, anti-rabbit-HRP and anti-mouse-HRP (1:2000, Dako Denmark A/S, Denmark) 1½h at room temperature and detected by chemiluminescence using the Pierce ECL substrate (Thermo Fisher Scientific) and the ChemiDoc MP system (BioRad). The data were analyzed using the ImageLab software (Bio-rad).

Caspase-3/7 assay
The GS257 cells were seeded at $5x10^3$ cells/well in a black 96-wells plate and incubated with the treatment as performed in the viability and Western blot experiments (SAHA, Obatoclax, after 24 hours RTx). Immediately after RTx, the cells were incubated with 5µM of the kinetic apoptosis reagent of the CellPlayer 96-Well Kinetic Caspase-3/7 Apoptosis Assay (Essen Bioscience) and were live imaged by using the IncuCyte system (Essen BioScience) with a 10X objective at 37°C in a humid 95% air/5% CO_2 chamber. The apoptosis-inducer staurosporin (20nM) was used as a positive control. Three fluorescent images/well were collected up to 60 hours post-RTx. The caspase-3/7 activity was presented as counted objects/mm^2 as measured by the IncuCyte software.

Gene expression analysis
The RNA of the original glioblastoma tissue corresponding with the glioblastoma cultures was isolated with the RNeasy Mini kit (#74104, Qiagen Inc., CA, USA). The mRNA expression levels of were analyzed by the HumanHT-12 v4 Expression BeadChip microarray (Illumina, CA, USA). The raw intensity values of all the samples were normalized using quantile normalization with the Partek software, version 6.6 (Partek Inc., St. Louis, MO, USA). Subsequently, the Partek Batch Remover was used to remove the effect of the differences between the batches. The effect sizes of HDACi/Obatoclax, and RTx/Obatoclax in n=13 GSC cultures (mRNA expression data of GS102 did not meet quality standards) were correlated to the gene expression levels. The data were analyzed using the linear model function in R package 'stats' (version 2.15.3) to identify genes that correlate to treatment responses (Pearson's R correlations). The p-values were adjusted for multiple comparisons using the method of Benjamini & Hochberg.[21] The cut-off values for significantly expressed genes were the adjusted p-values ($p<0.05$). The initially identified genes that significantly correlated with response were validated using a sample set of five additionally treated GSC cultures ($p<0.05$). Heat maps of the genes were constructed by the OmniViz Treescape software. The functional and network analyses of the identified genes were performed using the QIAGEN's Ingenuity® Pathway Analysis (IPA®, QIAGEN Redwood City,www.qiagen.com/ingenuity).

Quantitative PCR on MGMT promoter methylation
The DNA of the various patient-derived GSC cultures was isolated and 100ng was used for the quantitative polymerase chain reaction (PCR). The DNA samples were modified with sodium bisulphite using the EZ DNA Methylation GoldTM kit (Zymo Research, Baseclear, The Netherlands) Primers specific for methylated and un-methylated *MGMT* promoter DNA were used as described by others.[22] Methylation specific primers were F: TTTCGACGTTCGTAGGTTTTCGC and R: GCACTCTTCCGAAAACGAAACG. The un-methylated specific primers were F: TTTGTGTTTTGATGTTTGTAGGTTTTTGT and R: AACTCCACACTCTTCCAAAAACAAAACAQ. The PCR conditions were used as described by others.[23] with annealing temperature of 59°C and 40 cycles of amplification yielding PCR products for methylated and un-methylated DNA of 80 and 93 base pairs, respectively. The PCR products were separated on a routine 2% agarose gel. As a methylated control the DNA isolated from FFPE human colorectal cancer cell line SW48 was used and FFPE human tonsil DNA was used as an un-methylated control. In addition, in each experiment a H_2O sample without DNA was used as a negative contamination control.

Statistical analysis
For the viability and caspase-3/7 assay experiments, the means of triplicates were plotted with the standard deviations. The Western blots were performed in singlicate. The results were presented as a percentage of non-treated controls. The differences between treatment effects were analyzed using the one-way ANOVA and a Tukey's Post-test for multiple conditions. The statistical significance was defined as $p<0.05$. The differences in mean cell viability between combinations were presented as effect sizes. In addition, we calculated the enhancement factor of combination treatments, as was described by Chou.[24] In case of an enhancement factors > 1 in combination with $p<0.05$, the combination was considered effective and the GSC was defined as a responder.

4.3 Results

Patient-derived GSC cultures show differential sensitivity to Obatoclax
The IC_{50} values of Obatoclax were determined in three patient-derived GSC cultures and in U373 glioma cells in order to find the right concentrations for further screening. Then, fourteen patient-derived glioblastoma cultures were screened for the combination treatments, after which validation of the results was performed in another five cultures. If the cultures were highly sensitive to Obatoclax, lower concentrations (10 and 30nM) of the drug were used. As the *MGMT* promoter methylation and recurrence status is the most established predictive marker of glioblastoma survival2, we evaluated whether treatment efficacy was related to these factors. Also, the relation between the IC_{50} values and Bcl-2/Bcl-XL protein levels was investigated (Figure 1A-D, Table 1). The results show that Obatoclax reduced in the nanomolar range. The IC_{50} values as approached by median effect equation, ranged from 17 – 562nM, varying per GSC culture. In total, eleven of nineteen GSC cultures had a methylated *MGMT* promoter status and seven cultures were derived from recurrent tumors. Neither of these parameters correlated to the IC_{50} values of Obatoclax ($p<0.05$). The protein level status of these cultures was retrieved from previous research.[6] The protein levels were categorized as high or low. In cultures with high levels of Bcl-2, the mean IC_{50} value is significantly higher than in other cultures ($p=0.017$). For Bcl-XL, we observed a trend that higher IC_{50} values occurred in cultures with lower Bcl-XL protein levels ($p=0.09$).

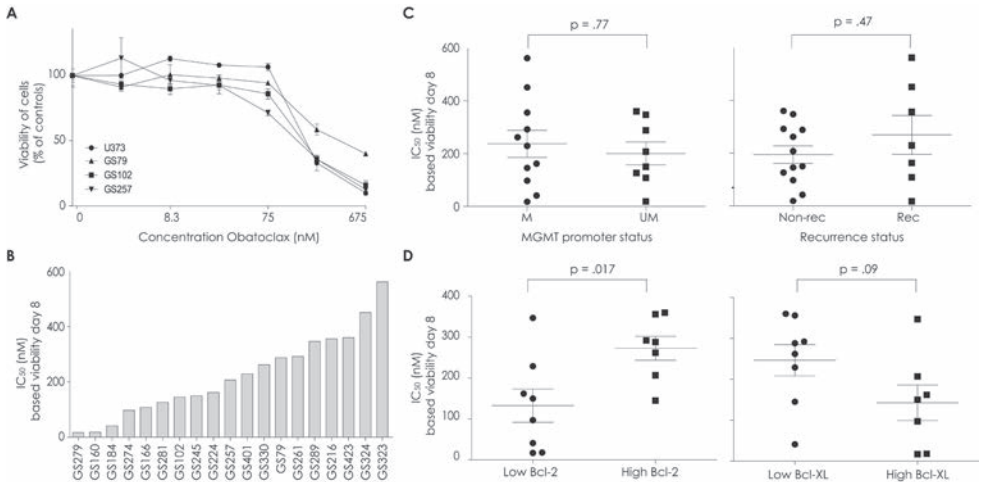

Figure 1A-D. Sensitivity of patient-derived GSC cultures to Obatoclax treatment.

(A) The immortalized glioma cell line U373 and the GSCs GS102, GS79 and GS257 were incubated with a concentration-range of Obatoclax and the IC_{50} values were calculated based on viability on day eight by median equation. Results show the viable percentage of cells compared to non-treated controls with standard errors. **(B)** Cells of patient-derived GSCs were treated with at least three different concentrations of Obatoclax in the nanomolar range. After eight days, viability was measured by CellTiterGlo-assay and the IC_{50} values were determined by median equation. The graph shows the results of nineteen screened patient-derived GSCs. **(C)** *MGMT* promoter and recurrence status of the patient-derived GSCs were related to the IC_{50} values of Obatoclax. **(D)** Bcl-2 and Bcl-XL levels were related to IC_{50} values of the cultures for which this status was known.

Obatoclax synergizes with HDAC inhibitors culture-dependently in patient-derived GSC cultures

To determine synergy between Obatoclax and the HDACi SAHA or LBH589, the Chou Talalay method was used in the patient-derived GSC cultures GS79 and GS257. Next, the panel of fourteen and five patient-derived GSC cultures were screened with the previously mentioned concentrations of Obatoclax, combined with SAHA and LBH589, and with or without RTx. Also, the *MGMT* promoter methylation and recurrence status of the tumors were related to responses to treatment. For both cultures GS79 and GS257, Obatoclax showed synergistic effects with SAHA and LBH589 with combination indices < 1 (Figure 2A). The combination efficacy widely varied in the panel of patient-derived GSC cultures: responders and non-responders were identified for all combination treatments (Table 1, Figure 3). In the first set of glioblastoma cultures (n=14) eight cultures responded to SAHA/Obatoclax treatment. In the validation set (n=5) four cultures responded to treatment. Enhancement factors ranged from 1.2 – 14.3 with effect sizes ranging from 5% – 35%. Seven of the fourteen cultures responded to LBH589/Obatoclax treatment and three of the five cultures in the validation set responded to treatment. The enhancement factors ranged from 0.9 – 4.9 with effect sizes of -6% – 26%. Obatoclax sensitized seven of fourteen GSC cultures to radiation, and all the GSC cultures in the validation set responded to this treatment. The enhancement factors ranged from 0.9–3.6 with effect sizes ranging from -5% – 26%. The

MGMT promoter methylation and recurrence status were not related to the effect sizes of the tested combination treatments (p>0.05) (Figure 2B).

Table 1. The characteristics and responses of the screened patient-derived GSC cultures.
The relevant characteristics are displayed, being the *MGMT* promoter methylation status, gender and whether or not the culture was obtained from a patient with a recurrent tumor. The combination of treatments of Obatoclax with either SAHA, LBH589 or radiation with 3Gy, shows differential responses in different patient-derived GSC cultures. Dark grey = non-responsive to the proposed treatment; light grey = responsive to the proposed treatment. Oba = Obatoclax. EF = enhancement factor; ES = effect size.

GSC culture	MGMT status	Recurrent	IC_{50} (nM)	SAHA/ Oba EF	SAHA/ Oba ES	LBH589/ Oba EF	LBH589/ Oba ES	Oba/ RTx EF	Oba/ RTx ES
GS102	M	No	145	1.56	20.25%	1.26	0.36%	1.69	23.80%
GS160	UM	No	18	1.51	19.68%	1.33	5.61%	1.43	23.36%
GS166	UM	Yes	108	1.4	8.07%	1.5	18.05%	1.25	15.67%
GS184	M	No	41	1.85	20.80%	1.77	26.10%	1.58	15.09%
GS216	M	Yes	356	2.05	21.46%	1.1	7.25%	1.89	19.74%
GS224	M	Yes	162	2.06	20.62%	1.74	17.07%	1.07	3.59%
GS245	UM	No	150	2.23	13.65%	1.39	6.93%	1.31	5.89%
GS257	UM	No	207	2.34	20.23%	1.3	8.24%	1.8	14.07%
GS261	M	No	292	14.3	21.39%	1.17	11.97%	3.61	16.63%
GS274	M	No	97	2.26	13.30%	1.49	7.86%	2	11.93%
GS279	M	Yes	17	1.41	13.93%	1.15	10.12%	1.59	26.24%
GS281	UM	No	126	1.42	14.74%	1.22	8.97%	0.91	-4.98%
GS289	UM	No	347	2.64	20.29%	1	-0.12%	2.82	21.08%
GS323	M	Yes	562	1.16	6.34%	1.19	7.65%	1.24	12.95%
GS324	M	Yes	451	1.17	8.56%	0.92	-6.09%	1.14	8.65%
GS330	M	No	262	1.29	4.78%	1.11	9.77%	1.19	13.40%
GS401	M	Yes	229	1.21	8.12%	1.34	16.99%	1.24	9.79%
GS423	UM	No	360	3.35	18.24%	1.1	8.22%	1.49	8.51%
GS79	UM	No	288	2.74	34.54%	4.88	26.08%	1.45	10.25%

Obatoclax overcomes resistance to HDAC inhibitors as radiosensitizers in patient-derived GSC cultures

To evaluate whether treatment with Obatoclax sensitizes patient-derived GSC cultures to HDACi as radiosensitizers, the nineteen patient-derived GSC cultures were evaluated (Figure 2C). The co-treatment with Obatoclax resulted in a significant reduction in cell viability compared to the combination treatment of RTx and SAHA without Obatoclax. However the effect sizes of triple treatment were small, since the ATP-levels at day eight show that either HDACi/Obatoclax, Obatoclax/RTx or HDACi/RTx already killed the largest part of the cell population. In the patient-derived GSC cultures GS257, GS274, GS224 and GS401, the effect sizes ranged from 5 – 9% and the enhancement factor ranged from 1.1 – 2.2 (GS257 and GS274 shown in Figure 2C). The addition of Obatoclax to the combination treatment of LBH589/RTx did not result in significant additional treatment effects.

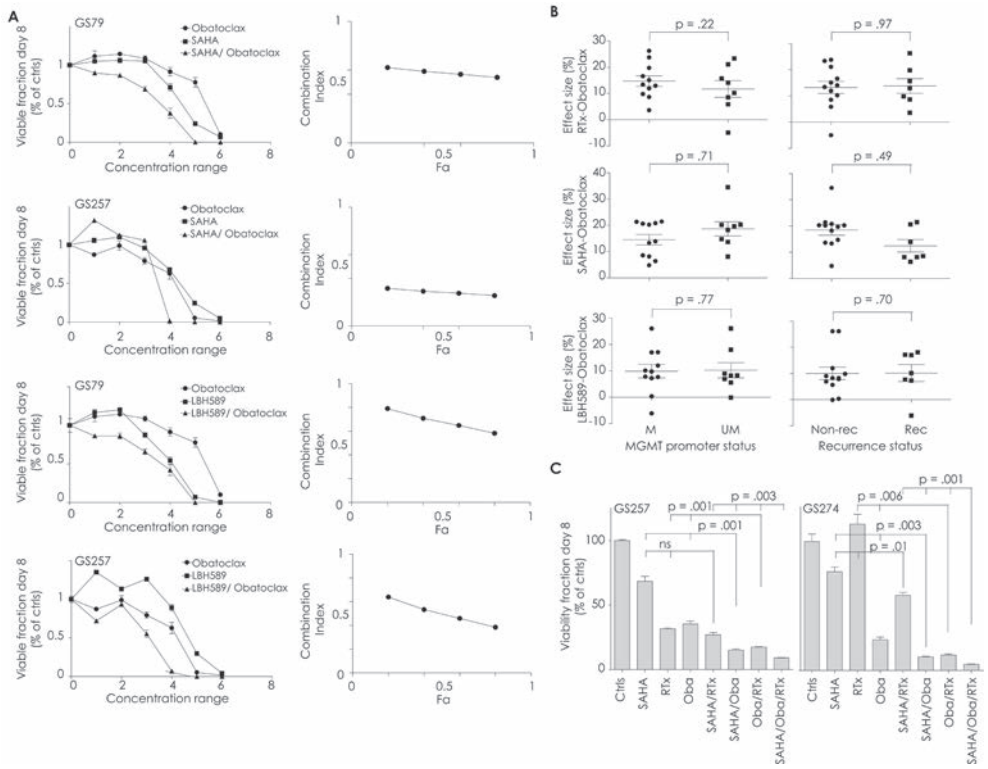

Figure 2A-C. The effect of Obatoclax on HDACi and radiation treatment in patient-derived GSC cultures.

(A) Left: Concentration-range assays to determine synergy between Obatoclax and SAHA and LBH589 were performed on GSCs GS79 (sensitive to HDACi/RTx treatment) and GS257 (resistant to HDACi/RTx). After eight days of incubation viability and synergism were determined. Means of triplicate tests are shown with the standard deviation. Right: The combination indices (CI) corresponding to the viability graphs in Figure 2A were calculated. Synergy was observed in both GSCs for the HDACi and Obatoclax with CI <1 (CI=1 corresponds to additive effects, CI>1 corresponds to antagonism). **(B)** The *MGMT* promoter and recurrence status of the GSCs were related to the effect sizes of the SAHA/Obatoclax, LBH589/Obatoclax or RTx/Obatoclax treatments. No significant relations were found. **(C)** The results on viability at day eight, of two patient-derived GSC cultures treated with Obatoclax combined with SAHA or LBH589, RTx and all possible combinations. O = Obatoclax, RTx = radiation. */**/***/**** Indicate significance at p<0.05 for the different combination treatments compared to as indicated in the graphs by the vertical lines.

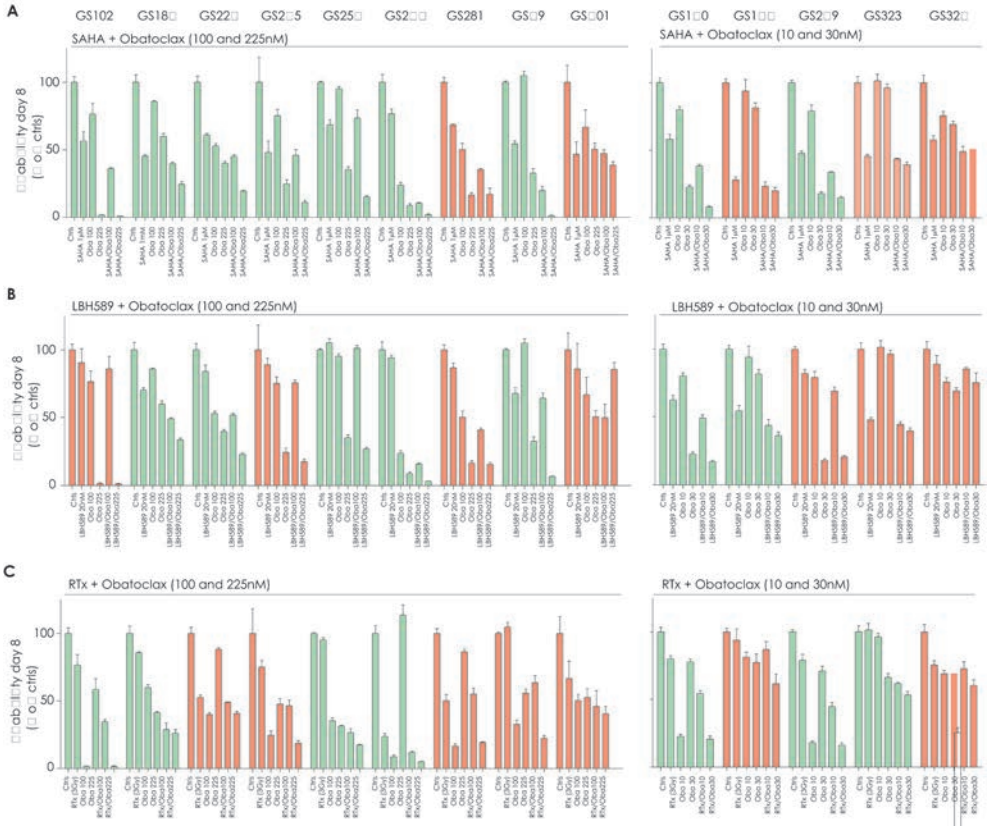

Figure 3A-C. The effects of Obatoclax on HDACi in patient-derived GSC cultures.

(A) Nine (left, high concentrations) and five (right, low concentrations) patient-derived GSC cultures were treated with two different concentrations of Obatoclax and SAHA (1μM). After eight days viability was measured by CellTiterGlo-assay. Responders (green bars) and non-responders (red bars) were identified. The color blue indicates significance at the p<0.05 level for one of the concentrations. **(B)** Nine (left, high concentrations) and five (right, low concentrations) patient-derived GSC cultures were treated with two different concentrations of Obatoclax and LBH589 (20nM). After eight days viability was measured by CellTiter-Glo assay. Responders (green bars) and non-responders (red bars) were identified. The color blue indicates significance at the p<0.05 level. **(C)** Nine (left, high concentrations) and five (right, low concentrations) patient-derived glioblastoma cultures were treated with two different concentrations of Obatoclax and RTx (3Gy). After eight days viability was measured by CellTiter-Glo assay. Responders (green bars) and non-responders (red bars) were identified. The color blue indicates significance at the p<0.05 level.

Obatoclax triggers apoptosis and induces autophagy in both HDAC inhibitor and HDACi/RTx combination treatment

The CellTiter-Glo assay at day eight may have underestimated the effects of triple treatment due to the lack of differentiation between the effective treatments. Also, we hypothesized that early treatment differences could be observed by studying the important cell death mechanisms of the Bcl-2 pathway: apoptosis and autophagy.[25] Therefore, we studied early caspase-3/7 activation, which could provide more insights into the difference in efficacy between triple and combination treatment. The activated caspase-3/7 levels

were monitored over time for SAHA concentrations at which additional effects after triple treatment were observed in the viability assay. The HDACi SAHA and the Bcl-2 family inhibitor Obatoclax activated the caspase-3/7 activity at both 48 and 60 hours post-treatment (Figure 4A). There was no additional caspase-3/7 activation in case of the combination treatment of SAHA and RTX, in comparison to single agents alone. Combination treatment of RTx/Obatoclax did not increase caspase-3/7 activity in comparison to single agent treatment either. In both SAHA/Obatoclax and SAHA/Obatoclax/RTx treated cells, increased caspase-3/7 activity was observed at 48 and 60 hours ($p<0.05$), with SAHA/Obatoclax/RTx being significantly more effective than SAHA/Obatoclax ($p<0.05$). As well as inducing caspase-dependent apoptosis, the Bcl-2 family proteins play a crucial role in autophagy and autophagosome formation which can be studied by conversion of LC3BI/II proteins. Treatment of GS257 cells with either SAHA, RTx and SAHA/RTx did not result in conversion of LC3I/LC3II at 48 and 72 hours post-treatment (Figure 4B). On the contrary, treatment with Obatoclax strongly induced autophagy at 48 hours post-treatment. Obatoclax increased both LC3I and LC3II in combination with RTx. In the SAHA/Obatoclax and Obatoclax/SAHA/RTx treated cells, LC3BI/II conversion (LC3II divided by LC3I) was observed at both 48 and 72 hours post-treatment. The triple treatment showed a higher ratio of LC3BI/II conversion.

Obatoclax combined with HDACi and HDACi/RTx effectively decreases Bcl-XL and Mcl-1

As increased autophagy and apoptosis were observed in both the combination and triple treatment, we related these effects to altered levels of the anti-apoptotic Bcl-2 proteins Bcl-XL and Mcl-1 in the patient-derived glioblastoma culture GS257 (Figure 4C). The protein levels of Bcl-XL were decreased by Obatoclax at 48 hours post-treatment, but after 72 hours the levels were similar to controls. The HDACi SAHA even induced Bcl-XL protein levels at 48 hours, whereas at 72 hours, these levels were again similar to controls. The combination treatments of SAHA/RTx and Obatoclax/RTx did not affect Bcl-XL protein levels, whereas SAHA/Obatoclax and SAHA/Obatoclax/RTx completely eliminated Bcl-XL protein levels after both 48 and 72 hours. For Mcl-1, the most important effects were observed 48 hours after RTx: the levels were decreased by Obatoclax/RTx, Obatoclax/SAHA and to a larger extent by Obatoclax/SAHA/RTx. All these treatments induced additional Mcl-1 bands on the Western blot at both 37kDa and 25 kDa. The Mcl-1 protein levels (37 and 40 kDa) of cells treated by the latter two treatments were relatively low compared to the other combination treatments at 72 hours. In addition, the two additional Mcl-1 bands were induced by these treatments at both 15 and 17 kDa. These bands may correspond to cleaved Mcl-1, which has been associated with activation of apoptosis.

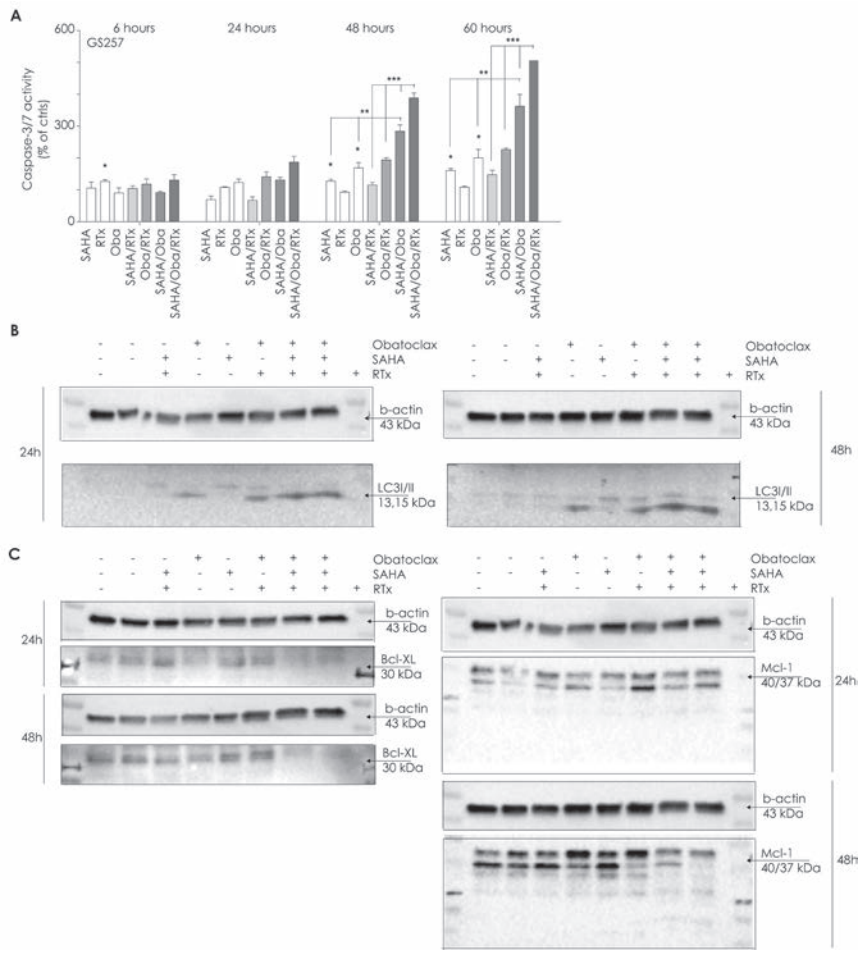

Figure 4A-C. The mechanisms involved in the efficacy of the combination treatments.

(A) Cells of the GSC GS257 were treated with Obatoclax (225nM), SAHA (1μM) and all possible combinations. After 24 hours, cells were radiated or not (controls) with 3Gy. Caspase-3/7 reagent was added to the wells, the plates were placed in an IncuCyte and followed for 60 consecutive hours. Fluorescence was measured using the IncuCyte software. *Indicates significance at p<0.05 compared to non-treated controls. **/***Indicate significance at p<0.05 of the treatments, compared to the treatments as indicated by the vertical bars. O=Obatoclax; RTx=radiation. **(B)** The GSC cultures GS257 were treated as in Figure 4A. Cells were collected either 24 or 48 hours post-treatment with RTx. The conversion of LC3BI/II, indicating autophagy was studied by using the Western blot analysis. **(C)** The cells of the GSC culture GS257 were treated as in Figure 4A. Cells were collected either 24 or 48 hours post-treatment with RTx. The anti-apoptotic Bcl-2 family proteins Bcl-Xl and Mcl-1 were studied by using the Western blot analysis.

Levels of specific genes correlate with response of GSC cultures to combination treatments with Obatoclax

In order to identify predictive markers for treatment response, the gene expression levels of the original tumor were related the treatment response of the fourteen patient-derived GSC cultures. The quality assessment of the gene expression array data showed that data of thirteen samples could be used for the analysis (GS102 was excluded). The validation of the identified genes that correlated with treatment response was performed in an independent set of five patient-derived GSC cultures. This resulted in a specific set of genes of which levels were related to treatment response in both the initial and validation set. For selection, at least a 1.5-fold change (log-2 scale) was the minimum difference in gene expression between the most and the least responsive patient-derived glioblastoma culture. The functions of the identified genes were analyzed using the QIAGEN's Ingenuity® Pathway Analysis. We focused on the functions and networks of the genes which were associated with the combination responses. Table 2A shows the gene lists per treatment, the correlation coefficient with the treatment effects and the fold-change difference in gene expression levels between the most and least sensitive corresponding glioblastoma culture. The responses to LBH589/Obatoclax treatment were related to gene expression levels of ten genes, being the non-coding RNA *NCRNA00086*, transmembrane protease serine 3 *(TMPRSS3)*, proto-cadherin gamma-subfamily B6 *(PCDHGB6)*, small integral membrane protein 21 *(LOC284274)*, forkhead box K1 *(LOC642782* or *FOXK1)*, vasoactive intestinal peptide *(VIP)*, zinc finger and SCAN domain containing 23 *(ZSCAN23)*, F-box and WD repeat domain containing 7, E3 ubiquitin protein ligase *(FBXW7)*, microRNA 325 *(MIR325)*, and G protein-coupled receptor 52 *(GPR52)* (Figure 5A,D). This set genes were found to be functioning in processes of cell cycle *(FBXW7, VIP, FOXK1)*, cell death and survival *(VIP, FBXW7, PCDHGB6)* and cell morphology *(FBXW7, VIP)* as top three gene functions (Table 2B). Another group recently showed that mutations in *FBXW7* were related to SAHA-induced cell death and Bcl-2 inhibition.[10] The genes that were related to responses to Obatoclax/RTx treatment were ST6 (alpha-N-acetyl-neuraminyl-2,3-beta-galactosyl-1,3)-N-acetylgalactosaminide alpha-2,6-sialyltransferase 5 *(ST6GALNAC5)*, EGF-like, fibronectin type III and laminin G domains *(EGFLAM)*, ABI family member 3 (NESH) binding protein *(ABI3BP)*, beta-carotene oxygenase 1 *(BCO1)* and DIRAS family GTP-binding RAS-like 1 *(DIRAS1)* (Figure 5B,E). These genes were involved in cellular development and cellular growth and proliferation *(DIRAS1)*, as well as lipid metabolism *(BCO1, ST6GALNAC5)*. Moreover, all the five genes were found to function in the same network, namely a cell cycle network (Table 2B). The responses to SAHA/Obatoclax treatment were related to one gene, namely ubiquilin 1 *(UBQLN1)* (Figure 5C). This gene is involved in cell morphology, cellular compromise and cell death and survival according to the functional analysis. In summary, we present a number of genes that is related to the responses of patient-derived glioblastoma cultures to combination treatments with Obatoclax, RTx and HDACi. Functional analysis showed that most of these genes were related to cell regulatory aspects including cell death and survival, as well as cycle regulatory processes.

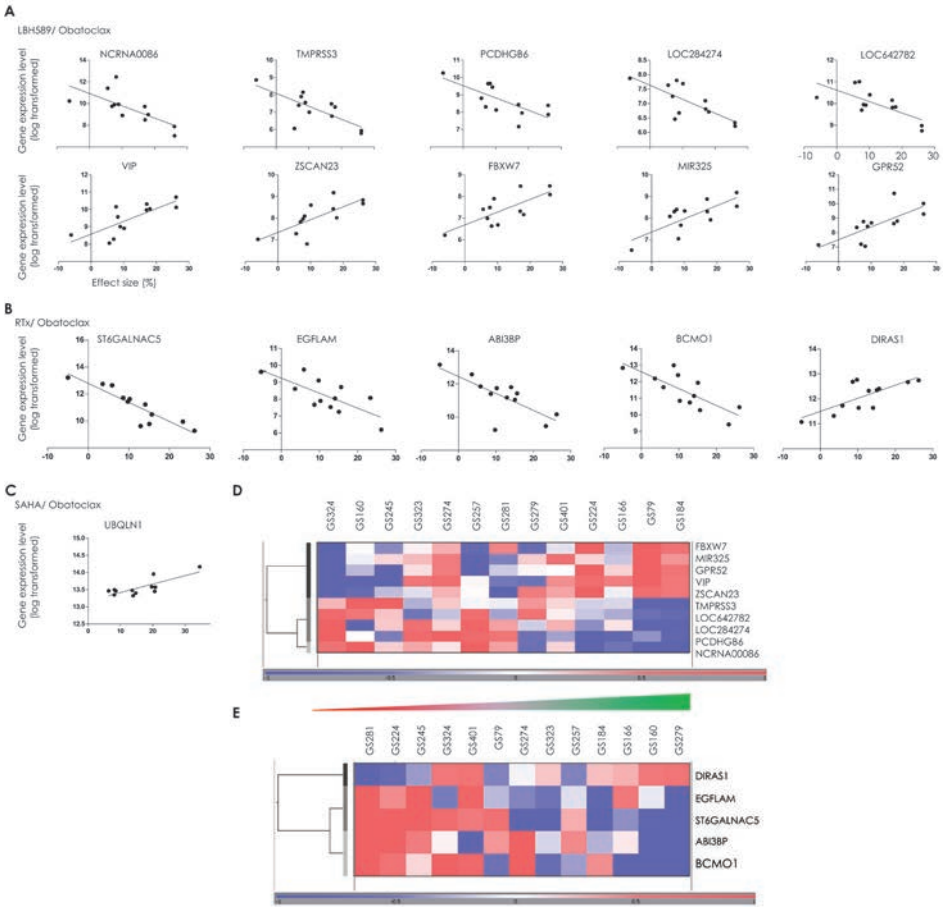

Figure 5A-E. Expression profiling of the response to treatment.

(A) The gene expression levels that were associated with the effect sizes to LBH589/Obatoclax treatment. Criteria were a p-value of <0.05, and a correlation coefficient of >0.5 or <-0.5. The gene expression intensity levels are displayed on log-2 scale. **(B)** The gene expression levels that are associated with the effect sizes to RTx/Obatoclax treatment. Criteria were a p-value of <0.05, and a correlation coefficient of >0.5 or <-0.5. The gene expression intensity levels are displayed on log-2 scale. **(C)** The gene expression levels that are associated with the effect sizes to SAHA/Obatoclax treatment. Criteria were a p-value of <0.05, and a correlation coefficient of >0.5 or <-0.5. The gene expression intensity levels are displayed on log-2 scale. (D,E) Heat map of the genes that correlated to the effect sizes of the combination treatments of LBH589/Obatoclax, RTx/Obatoclax and SAHA/Obatoclax Gene expression levels: red, up-regulated genes compared with the geometric mean; blue, down-regulated genes compared with the geometric mean. The color intensity correlates with the degree of change. The green-to-red intensity bar correlates with the degree of change in effect sizes of the corresponding GSC cultures.

Table 2. List of genes and functions related to the response of GSC cultures to Obatoclax combination treatments *in vitro*.

(A) The gene expression levels that were associated with the effect sizes of the several treatments with Obatoclax. The criteria were p-value of <0.05, a correlation coefficient of >0.5 or <-0.5. The intensity levels are displayed on log-2 scale. Corr. = correlation; FC = fold change between the least and most sensitive patient-derived GSC cultures. **(B)** The functions and networks of the specific genes derived from the Ingenuity Pathway Analysis.

Gene	LBH589/Oba		Corr.	Chrom. Locus	Least sensitive	Most sensitive	FC (log)
1	NCRNA00086	long intergenic non-protein coding RNA 86	-0.70	X	7.02	10.23	3.21
2	TMPRSS3	transmembrane protease, serine 3	-0.73	21	5.94	8.86	2.92
3	PCDHGB6	protocadherin gamma subfamily B, 6	-0.69	5	7.86	10.26	2.40
4	LOC284274	SMIM21 small integral membrane protein 21	-0.71	18	6.21	7.87	1.66
5	LOC642782		-0.71		8.74	10.28	1.53
6	VIP	vasoactive intestinal polypeptide	0.69	6	10.12	8.53	-1.59
7	ZSCAN23	zinc finger and SCAN domain containing 23	0.71	6	8.67	7.02	-1.65
8	FBXW7	F-box and WD repeat domain containing 7, E3 ubiquitin protein ligase	0.71		8.09	6.22	-1.87
9	MIR325	microRNA 325	0.70	X	8.55	6.52	-2.03
10	GPR52	G protein-coupled receptor 52	0.70	1	9.29	7.14	-2.14

Gene	SAHA/Oba		Corr.	Chrom. Locus	Least sensitive	Most sensitive	FC (log)
1	UBQLN1	ubiquilin 1	0.78	9	14.17	13.00	-1.16

Gene	RTx/Oba		Corr.	Chrom. Locus	Least sensitive	Most sensitive	FC (log)
1	ST6GALNAC5	ST6 (alpha-N-acetyl-neuraminyl-2,3-beta-galactosyl-1,3)-N-acetylgalactosaminide alpha-2,6-sialyltransferase 5	-0.74	1	9.27	13.21	3.94
2	EGFLAM	EGF-like, fibronectin type III and laminin G domains	-0.72	5	6.19	9.60	3.42
3	ABI3BP	ABI family, member 3 (NESH) binding protein	-0.70	3	10.16	13.16	3.00
4	BCMO1	beta-carotene 15,15'-monooxygenase	-0.72	16	10.47	12.83	2.36
5	DIRAS1	DIRAS family, GTP-binding RAS-L-1	0.73	19	12.75	11.08	-1.67

Table 2B. The top three functions and networks of the genes that are related to the response to Obatoclax combination treatments *in vitro*.

LBH589/Oba	
Function	**Gene**
Cell Cyle	FBXW7, VIP, FOXK1
Cell Death and survival	VIP, FBXW7, PCDHGB6
Cell Morphology	FBXW7, VIP

SAHA/Oba	
Function	**Gene**
Cell Morphology	UBQLN1
Cellular Compromise	UBQLN1
Cell Death and Survival	UBQLN1

RTx/Oba	
Function	**Gene**
Cellular Development	DIRAS1
Cellular Growth and Proliferation	DIRAS1
Lipid Metabolism	BCO1, ST6GALNAC5
Cell Cycle*	ABI3BP, BCO1, DIRAS1, EGFLAM, ST6GALNAC5

4.4 Conclusion

In summary, this study underlines the potential of inhibiting the Bcl-2 family proteins in combination treatment with HDACi and HDACi/RTx. Potential toxicities of combination therapies which may limit clinical use should be explored further. Examples could be thrombocytopenia by inhibition of Bcl-XL26 and HDACi.[27] Furthermore, we obtained predictive gene profiles that are associated with cellular regulatory functions for the combination treatments with Obatoclax. These gene sets may aid in further selecting the tumors most responsive to treatment.

4.5 Discussion

The present study emphasizes the efficacy of the Bcl-2 family pathway inhibition by Obatoclax in sensitizing patient-derived GSC cultures to HDACi/RTx, and hereby circumventing a tumor-related resistance mechanism to treatment. The Bcl-2 family proteins are heterogeneously expressed in glioblastoma as about 30%[28] to 60%[29] shows over-representation of these proteins.[29-31] Moreover, Bcl-XL levels in patient-derived glioblastoma cultures have shown a relationship with resistance to HDACi/RTx response.[6] Here, we demonstrate that Obatoclax acted synergistically with HDACi and show efficacy in a large set of patient-derived glioblastoma cultures. Hereby we confirm that this pathway is an adequate target to obtain treatment responses. The use of the serum-free patient-derived glioblastoma culture model allowed to study resistance and tumor response mechanisms in a more representative manner than in immortalized glioma cell lines.[11] Importantly, this

model provides a tool to develop predictive profiles of treatment response. The efficacy of down-regulation of Bcl-2 and Bcl-XL in inducing spontaneous cell death was already shown before.[32] This efficacy depended on neither *MGMT* promoter methylation status nor recurrence. A number of genes was found to be related to treatment response of patient-derived GSC cultures to combination treatments. Others showed that the gene *FBXW7* was related to SAHA-induced cell death and Bcl-2 inhibition.[10] This points to a biological rationale in Mcl-1 functioning to be predictive of treatment response to LBH589/Obatoclax. The use of these genes as potential markers for patient stratification or the functionality of these genes in sensitivity or resistance to combination treatments should be explored in future studies.

Others have studied the relationship between HDACi and Bcl-2 family proteins before. A recent study has shown that the intact *PTEN* immortalized malignant glioma cell lines are susceptible to the combination of SAHA and the Bcl-2 inhibitors ABT-737, whereas *PTEN* mutations were not.[33] They also showed that inhibition of the PTEN/PI3K pathway by BKM-120 sensitized glioma cells for ABT-737.[34] The patient-derived GSC model we used in this study is known to harbor *PTEN* deletions due to loss of chromosome 10q[11,12] and ensures that we tested the treatment efficacy in a setting of hyper-activation of the PIK3-pathway. Therefore, this suggests that Obatoclax may be a more potent combination partner for HDACi in the *PTEN* deleted tumors than ABT-737. The main differences between Obatoclax and ABT-737 are the stronger induction of autophagy[14] and the stronger inhibition of Mcl-1 by the first drug which may be underlying to the efficacy in *PTEN* deleted tumors.[13] Earlier, the efficacy of SAHA was related to Mcl-1 levels in acute myeloid leukemia.[35] Another study showed that in diffuse large B-cell lymphoma, over-expression of Bcl-2 and Bcl-XL triggered resistance to the HDACi SAHA and Trichostatin A, whereas the Bcl-2 family inhibitor ABT-737 increased sensitivity to SAHA treatment. Also, the latter study showed that the least sensitive cells to SAHA showed up-regulation of Bcl-XL and Mcl-1 proteins.[36] The loss of pro-apoptotic Bcl-2 family proteins Bax or Bax/Bak ratios are related to insensitivity to HDACi in Burkitt's lymphoma in a predictive and functional sense.[37] In mantle cell lymphoma, the efficacy of SAHA was enhanced by the BH-3 mimetic ABT-263.[38] In contrast, another study did not find HDACi efficacy to be related to Bcl-2 family proteins.[36] Thus, these relationships between Bcl-2 family proteins and HDACi responses may be either tumor type or HDACi specific. However, our study supports that inhibition of the Bcl-XL and Mcl-1 proteins by Obatoclax is related to efficacy of SAHA alone or in combination with RTx at multiple mechanistic levels. We observed restored levels of Bcl-2 family proteins Bcl-XL and Mcl-1, occurring at 72 hours after Obatoclax, HDACi and HDACi/RTx treatments. This observation indicates that Bcl-2 family members are restored relatively quickly if not inhibited effectively, which in turn may contribute to resistance to treatment.

As a mechanism of action, HDACi have shown to be able to down-regulate Bcl-2 family members, however not in all heterogeneous tumors including glioblastoma.[6] Others suggest that the up-regulation of pro-apoptotic members by HDACi are neutralized by high levels of anti-apoptotic members such as Bcl-2 and Bcl-XL.[39] In squamous cell carcinoma Mcl-1 was related to resistance to the BH3-mimetic ABT-737. The HDACi SAHA has the ability to sensitize tumor cells to this drug by shuttling the Bcl-2 family protein Bim from Mcl-1 to Bcl-2/Bcl-XL.[10]

Not only does Obatoclax enhance efficacy of HDACi/RTx, it also enhanced the efficacy of RTx as treatment alone. Thus, in many treatment modalities, including conventional glioblastoma treatment such as RTx, the Bcl-2 family members may play a crucial role. Others have shown already that Bcl-2 family members are determinants of responsiveness to treatment in glioblastoma. Bcl-XL levels were related to radioresistance in glioma[40] and Mcl-1 proteins regulate temozolomide efficacy in glioma independently of *MGMT* promoter methylation status.[41] Here, we found that *MGMT* promoter methylation status and tumor recurrence, which normally determine patient overall outcome,[2] were not related to the applied treatments either. Thus, our results are unlikely to be determined by these tumor statuses a priori.

The effect sizes of both SAHA and LBH589 in combination with Obatoclax correlated to expression levels of specific genes. Gene profiles may provide an opportunity to include predictive decision variables in treatment and patient selection. This may be of clinical relevance specifically for the *MGMT* un-methylated tumors. We need to point out immediately that these gene sets need further exploration in *in vivo* settings to be validated for their clinical value. Although these gene sets do not necessarily implicate mechanisms of action of the proposed treatments, they may provide insight into resistance mechanisms. *FBXW7*, the gene associated with LBH589/Obatoclax response, was shown to have a relationship with response to SAHA before, as well as to Bcl-2 inhibition. Both *FBXW7* and Bcl-2 inhibition were predictive for efficacy of SAHA in squamous cell carcinoma. Mutated *FBXW7* sensitized cells to HDACi and stabilized Mcl-1.[10] *FBXW7* encodes for the protein ubiquitin protein ligase and is positively related with the effect size of LBH589/Obatoclax in our study. Obatoclax has the potency to inhibit Mcl-1, and is more effective in combination with LBH589 in tumors that highly express *FBXW7*. Moreover, the whole gene set which was related to LBH589/Obatoclax response was associated with cell cycle and cell death and survival mechanisms, represented by the four genes *FBXW7, VIP, FOXK1* and *PCDHGB6*. This was also true for the gene ubiquilin 1 *(UBQLN1)*, which was associated to SAHA/Obatoclax response. This gene functions in cell death and survival as well. In addition, response to RTx/Obatoclax was associated to genes that function in the cell cycle and cellular proliferation as well. Basic studies should be performed to assess the direct relationship between the function of these genes and the success rate of Obatoclax, but the genes provide insights into the process of cellular responses. Our data on cell regulation by caspase-3/7 and autophagy are therefore potentially important mechanisms of action in the response to combination treatment.

References

1. Stupp R, Hegi ME, Mason WP, et al. Effects of radiotherapy with concomitant and adjuvant temozolomide versus radiotherapy alone on survival in glioblastoma in a randomised phase III study: 5-year analysis of the EORTC-NCIC trial. Lancet Oncol 2009;10:459-66.
2. Hegi ME, Diserens AC, Godard S, et al. Clinical trial substantiates the predictive value of O-6-methylguanine-DNA methyltransferase promoter methylation in glioblastoma patients treated with temozolomide. Clin Cancer Res 2004;10:1871-4.
3. Thaker NG, Pollack IF. Molecularly targeted therapies for malignant glioma: rationale for combinatorial strategies. Expert Rev Neurother 2009;9:1815-36.

4. Hegi ME, Sciuscio D, Murat A, Levivier M, Stupp R. Epigenetic deregulation of DNA repair and its potential for therapy. Clin Cancer Res 2009;15:5026-31.
5. Li Z, Zhu WG. Targeting Histone Deacetylases for Cancer Therapy: From Molecular Mechanisms to Clinical Implications. International journal of biological sciences 2014;10:757-70.
6. Berghauser Pont LM, Naipal K, Kloezeman JJ, et al. DNA damage response and anti-apoptotic proteins predict radiosensitization efficacy of HDAC inhibitors SAHA and LBH589 in patient-derived glioblastoma cells. Cancer Lett 2014.
7. Lee JH, Choy ML, Marks PA. Mechanisms of resistance to histone deacetylase inhibitors. Advances in cancer research 2012;116:39-86.
8. Dewson G, Kluck, R.M. Bcl-2 family-regulated apoptosis in health and disease. Cell Health and Cytoskeleton 2010;2:9-22.
9. Pattingre S, Tassa A, Qu X, et al. Bcl-2 antiapoptotic proteins inhibit Beclin 1-dependent autophagy. Cell 2005;122:927-39.
10. He L, Torres-Lockhart K, Forster N, et al. Mcl-1 and FBW7 control a dominant survival pathway underlying HDAC and Bcl-2 inhibitor synergy in squamous cell carcinoma. Cancer discovery 2013;3:324-37.
11. Balvers RK, Kleijn A, Kloezeman JJ, et al. Serum-free culture success of glial tumors is related to specific molecular profiles and expression of extracellular matrix-associated gene modules. Neuro Oncol 2013;15:1684-95.
12. Chen R, Nishimura MC, Bumbaca SM, et al. A hierarchy of self-renewing tumor-initiating cell types in glioblastoma. Cancer Cell 2010;17:362-75.
13. Nguyen M, Marcellus RC, Roulston A, et al. Small molecule obatoclax (GX15-070) antagonizes MCL-1 and overcomes MCL-1-mediated resistance to apoptosis. Proc Natl Acad Sci U S A 2007;104:19512-7.
14. Wroblewski D, Jiang CC, Croft A, Farrelly ML, Zhang XD, Hersey P. OBATOCLAX and ABT-737 Induce ER Stress Responses in Human Melanoma Cells that Limit Induction of Apoptosis. PLoS One 2013;8:e84073.
15. Trudel S, Li ZH, Rauw J, Tiedemann RE, Wen XY, Stewart AK. Preclinical studies of the pan-Bcl inhibitor obatoclax (GX015-070) in multiple myeloma. Blood 2007;109:5430-8.
16. www.clinicaltrials.gov. accessed 14.08.08.
17. Chiappori AA, Schreeder MT, Moezi MM, et al. A phase I trial of pan-Bcl-2 antagonist obatoclax administered as a 3-h or a 24-h infusion in combination with carboplatin and etoposide in patients with extensive-stage small cell lung cancer. Br J Cancer 2012;106:839-45.
18. Oki Y, Copeland A, Hagemeister F, et al. Experience with obatoclax mesylate (GX15-070), a small molecule pan-Bcl-2 family antagonist in patients with relapsed or refractory classical Hodgkin lymphoma. Blood 2012;119:2171-2.
19. Goard CA, Schimmer AD. An evidence-based review of obatoclax mesylate in the treatment of hematological malignancies. Core evidence 2013;8:15-26.
20. Chou TC, Talalay P. Quantitative analysis of dose-effect relationships: the combined effects of multiple drugs or enzyme inhibitors. Advances in enzyme regulation 1984;22:27-55.
21. Klipper-Aurbach Y, Wasserman M, Braunspiegel-Weintrob N, et al. Mathematical formulae for the prediction of the residual beta cell function during the first two years of disease in children and adolescents with insulin-dependent diabetes mellitus. Medical hypotheses 1995;45:486-90.

22. Esteller M, Garcia-Foncillas J, Andion E, et al. Inactivation of the DNA-repair gene *MGMT* and the clinical response of gliomas to alkylating agents. The New England journal of medicine 2000;343:1350-4.
23. Mollemann M, Wolter M, Felsberg J, Collins VP, Reifenberger G. Frequent promoter hypermethylation and low expression of the *MGMT* gene in oligodendroglial tumors. Int J Cancer 2005;113:379-85.
24. Chou TC. Preclinical versus clinical drug combination studies. Leuk Lymphoma 2008;49:2059-80.
25. Yu L, Liu S. Autophagy contributes to modulating the cytotoxicities of Bcl-2 homology domain-3 mimetics. Seminars in cancer biology 2013;23:553-60.
26. Davids MS, Letai A. ABT-199: taking dead aim at BCL-2. Cancer Cell 2013;23:139-41.
27. Bishton MJ, Harrison SJ, Martin BP, et al. Deciphering the molecular and biologic processes that mediate histone deacetylase inhibitor-induced thrombocytopenia. Blood 2011;117:3658-68.
28. Tirapelli LF, Bolini PH, Tirapelli DP, et al. Caspase-3 and Bcl-2 expression in glioblastoma: an immunohistochemical study. Arquivos de neuro-psiquiatria 2010;68:603-7.
29. Kraus JA, Wenghoefer M, Glesmann N, et al. TP53 gene mutations, nuclear p53 accumulation, expression of Waf/p21, Bcl-2, and CD95 (APO-1/Fas) proteins are not prognostic factors in de novo glioblastoma multiforme. J Neurooncol 2001;52:263-72.
30. Cartron PF, Loussouarn D, Campone M, Martin SA, Vallette FM. Prognostic impact of the expression/phosphorylation of the BH3-only proteins of the BCL-2 family in glioblastoma multiforme. Cell death & disease 2012;3:e421.
31. Abdullah JM, Ahmad F, Ahmad KA, et al. Molecular genetic analysis of BAX and cyclin D1 genes in patients with malignant glioma. Neurological research 2007;29:239-42.
32. Jiang Z, Zheng X, Rich KM. Down-regulation of Bcl-2 and Bcl-xL expression with bispecific antisense treatment in glioblastoma cell lines induce cell death. J Neurochem 2003;84:273-81.
33. Foster KA, Jane EP, Premkumar DR, Morales A, Pollack IF. Co-administration of ABT-737 and SAHA induces apoptosis, mediated by Noxa upregulation, Bax activation and mitochondrial dysfunction in PTEN-intact malignant human glioma cell lines. J Neurooncol 2014.
34. Jane EP, Premkumar DR, Morales A, Foster KA, Pollack IF. Inhibition of phosphatidylinositol 3-kinase/AKT signaling by NVP-BKM120 promotes ABT-737-induced toxicity in a caspase-dependent manner through mitochondrial dysfunction and DNA damage response in established and primary cultured glioblastoma cells. J Pharmacol Exp Ther 2014;350:22-35.
35. Pierceall WE, Lena RJ, Medeiros BC, et al. Mcl-1 dependence predicts response to vorinostat and gemtuzumab ozogamicin in acute myeloid leukemia. Leuk Res 2014;38:564-8.
36. Thompson RC, Vardinogiannis I, Gilmore TD. The sensitivity of diffuse large B-cell lymphoma cell lines to histone deacetylase inhibitor-induced apoptosis is modulated by BCL-2 family protein activity. PLoS One 2013;8:e62822.
37. Ierano C, Chakraborty AR, Nicolae A, et al. Loss of the proteins Bak and Bax prevents apoptosis mediated by histone deacetylase inhibitors. Cell Cycle 2013;12:2829-38.
38. Xargay-Torrent S, Lopez-Guerra M, Saborit-Villarroya I, et al. Vorinostat-induced apoptosis in mantle cell lymphoma is mediated by acetylation of proapoptotic BH3-only gene promoters. Clin Cancer Res 2011;17:3956-68.

39. Chen S, Dai Y, Pei XY, Grant S. Bim upregulation by histone deacetylase inhibitors mediates interactions with the Bcl-2 antagonist ABT-737: evidence for distinct roles for Bcl-2, Bcl-xL, and Mcl-1. Mol Cell Biol 2009;29:6149-69.
40. Streffer JR, Rimner A, Rieger J, Naumann U, Rodemann HP, Weller M. BCL-2 family proteins modulate radiosensitivity in human malignant glioma cells. J Neurooncol 2002;56:43-9.
41. Gratas C, Sery Q, Rabe M, Oliver L, Vallette FM. Bak and Mcl-1 are essential for Temozolomide induced cell death in human glioma. Oncotarget 2014.

Chapter 5

Screening of clinically -applicable drugs in patient-derived glioblastoma stem-like cells identifies amiodarone, clofazimine and triptolide as potential anti-glioma agents

Lotte M.E. Berghauser Pont,[1] Jenneke J. Kloezeman,[1] Maria. C. Speranza,[2] Sigrid Swagemakers,[3] Peter van der Spek,[3] Clemens M.F. Dirven,[1] Sieger Leenstra,[1,4] E. Antonio Chiocca,[2] Sean E. Lawler,[2] Martine L.M. Lamfers.[1]

Affiliations

1 Department of Neurosurgery, Brain Tumor Center, ErasmusMC
2 Department of Neurosurgery, Harvey Cushing Neuro-oncology Laboratories, Brigham and Women's Hospital, Harvard Medical School
3 Department of Bioinformatics, Erasmus MC
4 Department of Neurosurgery, Elisabeth Hospital, Tilburg

Submitted

Abstract

Glioblastoma is the most aggressive primary brain tumor and refractory to current therapies. Clinical implementation of new drugs can take years. Therefore we screened 446 clinically approved drugs in twenty patient-derived glioblastoma stem-like cultures (GSCs) to identify effective agents that allow faster implementation. Cell viability was assessed and 'hits' were validated. Effects on cell cycle inhibition, apoptosis and 3D-cell invasion were studied. Toxicity was determined in normal human astrocytes. In silico analysis on mechanisms was done using differences in gene expression that related to drug response. Drug response was related to tumor characteristics including O-6-methylguanine-DNA-methyltransferase (*MGMT*) promoter methylation and primary/recurrence status. Twenty-one effective agents were identified. Using efficacy and toxicity criteria, amiodarone, clofazimine and triptolide were selected and showed efficacy based on IC_{50} values in 20 distinct GSCs. The cytotoxic effects were higher in the GSCs than in human astrocytes. *MGMT* promoter methylation nor primary/recurrence status were related to drug response. Caspase-3/7 activity was induced by all drugs, amiodarone affected the cell cycle, and triptolide and amiodarone inhibited 3D-cell invasion. Amiodarone, clofazimine and triptolide are effective clinically-applicable anti-glioblastoma drugs in an extensive panel of genetically diverse GSCs and represent promising candidates for evaluation in preclinical models.

5.1 Introduction

Glioblastoma is a highly aggressive primary brain tumor which has a median survival of 14.7 months despite surgical resection, fractionated radiation and adjuvant chemotherapy.[1,2] The neuro-oncology field has developed a variety of novel treatment approaches, however, thus far these have not led to significant improvement in patient outcome.[3] Novel approaches based on the development of new agents can take many years to translate clinically. Among the strategies to reduce this time frame, efforts are now being undertaken to investigate drug repurposing.[4] With this approach, compounds available for a specific indication are evaluated for their therapeutic efficacy in other diseases, which could lead to fast-track implementation in the clinical setting.[5] Drug development research in glioblastoma has relied traditionally on established high-passage cell lines and *in vivo* models derived from these cells. With the development of patient-derived serum-free tumor stem-like cell cultures (GSCs), an *in vitro* drug screening model has become available that better recapitulates the tumor in situ, in terms of both genetic stability and tumor heterogeneity.[6,7] Therefore, re-evaluation of available compounds using patient-derived GSCs may lead to the identification of effective anti-glioblastoma agents that were not identified for this indication in the past. Moreover, it is expected that the use of this model in drug screening studies will potentially reduce false-positive 'hits', i.e., drugs that are effective only in conventional serum-cultured cell lines and that do not translate to clinical benefit. Finally, the representation of glioma inter-tumoral heterogeneity in the GSC model allows the correlation of drug sensitivity to the molecular characteristics of the tumor, as we have shown previously,[8] and can aid in the development of targeted and personalized treatments.

In the current study, we aimed to identify novel anti-glioblastoma therapeutics by using the NIH collection of 446 clinically applicable drugs.[9] All of these agents, prescribed for a broad range of therapeutic indications, are approved clinically and have known safety

profiles. After identification of potential effective drugs on two GSC cultures, we assessed efficacy in a panel of 20 distinct patient-derived GSCs. We assessed correlations between drug response and molecular markers such as *MGMT* promoter methylation and primary/recurrence status, as well as with whole genome gene expression levels. The identified molecular mechanisms associated with the drug response were studied both *in silico* and *in vitro*. The mechanisms of cell growth inhibition were studied, including apoptosis and cell cycle arrest, as well as the effects on neurosphere invasion. In addition, the drug toxicity was determined in normal human astrocytes. Together these studies led to the identification of three effective compounds for the treatment of glioblastoma, namely the anti-arrhythmic amiodarone, the antibiotic clofazimine and the anti-inflammatory triptolide.

5.2 Materials and methods

Clinical compounds

The NIH clinical collection of 446 clinically applicable agents was obtained from the NCI/DTP Open Chemical Repository (http://dtp.cancer.gov).[9] The compounds that were selected for further evaluation and validation were reordered from separate sources. These compounds included amiodarone, clofazimine, fluphenazine, tegaserod maleate, pitavastatin, and triptolide from Sigma-Aldrich (MO, USA), rimcazole, salmeterol (R&D Systems, MN, USA), and 5-nonyloxytryptamine, lacidipine, and perospirone (Sequoia Research Products Ltd, UK). The compounds were dissolved in 10mM in DMSO and stored at -20°C.

Glioblastoma stem-like cell cultures

The patient-derived GSCs used in this study (Table 1B; Table 2B) were derived from the brain tumor cell bank of the department of Neurosurgery, ErasmusMC. The use of patient tumor material was approved by the institutional review board of the Erasmus Medical Center, Rotterdam, The Netherlands. The patients' written informed consent was acquired for the use of patient material for our studies. The use of patient tumor material for the G9 cultures was approved by the Ohio state IRB.[10] All GSCs were prepared and cultured in serum-free medium, supplemented with B-27 Supplement (50X) minus antioxidants, EGF (Gibco, Life Technologies, Paisley, UK), bFGF (Sigma-Aldrich) and 1% penicillin/streptomycin (Gibco) as described previously.[11] The cultures were maintained at 37°C in a humidified 95% air/5% CO_2 chamber. The cytotoxicity experiments were performed on human astrocytes (ScienCell, CA, USA), which were cultured in EGF supplemented Astrocyte Medium (Gibco).

Viability assays

Patient-derived GSCs were seeded at $1x10^3$ cells/well in 96-well plates coated with growth factor-reduced Matrigel™ (BD Biosciences, CA, USA). After overnight incubation, the treatments were administered at different concentrations depending on the screen. The initial screen was performed at 100µM, the second screen was performed at 5 and 50µM and the third screen was performed at 1 and 10µM. The compound selection for the second screen was based on level of cytotoxicity in the initial screen. Cell viability was measured after five days with the ATP-based CellTiter-Glo assay (Promega, WI, USA). In cases where a compound reduced tumor viability by more than 75% compared to DMSO controls, it was tested in the subsequent screen at lower concentrations. The initial screening was done in singlicate in two patient-derived GSC cultures. After selection of drugs based on initial effects in both cultures, the compounds were validated. Validation was performed by

dose-response assessment in a twenty distinct patient-derived GSC cultures in triplicate using the CellTiter-Glo viability assay. IC_{50} values were calculated using Excel software.[12] The toxicity assays on primary human astrocytes were performed following the same regimen as mentioned for the patient-derived GSC cultures.

Quantitative PCR of MGMT promoter methylation and whole genome mRNA expression analysis

The *MGMT* promoter methylation status of the parental glioblastoma tissue corresponding to the cultures was done as described previously.[13] The parental tissues were also used for whole genome mRNA expression array using the HumanHT-12 v4 Expression BeadChip method (Illumina, San Diego, CA, USA). Data quantile normalization and removal of batch effects were done as previously described.[14] The IC_{50} values were correlated to gene expression using the linear model function in the R program and Pearson's R correlations were calculated. The method of Benjamini & Hochberg[15] was used to adjust p-values. The cut-off values for significantly expressed genes were the adjusted p-values, and considered $p<0.05$ combined with a correlation coefficient of <0.05 or >0.5. The heat maps were made in Omniviz software (Instem, Staffordshire, UK) and contain log2 transformed expression data of mRNA after calculation of the geometric mean. The functional annotation and biomarker analysis of the microarrays, as well as upstream regulator and network analyses were done using the QIAGEN's Ingenuity® Pathway Analysis (IPA®, QIAGEN Redwood City, CA, USA).

Invasion assays

Four-well chamber slides were coated with PureCol type I bovine collagen solution (Advanced BioMatrix, San Diego, CA, USA) and kept on a plate at 37°C until it hardened. Then, another layer of liquid collagen was added to the collagen layer, and patient-derived serum-free cultured glioblastoma neurospheres of *G9*, *GS79, GS184, GS257 and GS401* were seeded in three spheres per well. Then, the neurospheres were treated with the compounds amiodarone (1.5µM), clofazimine (1.5µM), and triptolide (10nM) and placed in a 37°C humified 95% air/5% CO_2 chamber. Every 24 hours, both fluorescent and phase-contrast pictures were made using a Nikon Eclipse Ti inverted microscope with a 4X magnification. Viability assessment at early time points for the concentrations used in the 3D-invasion assay was done using Cell-Titer-Glo (Promega) at 24, 48 and 72 hours after treatment. The images for morphological changes of the cells were made using a Zeiss Axio Observer D1 Fluorescence Microscope (Zeiss, Jena, Germany) using 40x magnification.

Cell cycle analysis

GS79 cells were seeded at $2.5x10^4$ cells/well 6-well plates and treated with the different compounds, amiodarone (1.5µM), clofazimine (5µM) and triptolide (10nM). After 24, 48 and 72 hours, the cells were collected and washed with PBS. The cells were prepared with the Muse® Cell Cycle Assay Kit (#MCH100106, Millipore, CA, USA) and G0/G1, S, and G2/M phase distributions were measured using the Muse Cell Analyzer (Millipore, USA). This assay is based on the whole-cell staining with propidium iodide (PI). The results were analyzed using the Muse Cell Analyzer and are displayed as fraction of cells in the specific cell cycle phases (G0/G1, S or G2/M) as a percentage of non-treated controls.

Caspase-3/7 assay
GS79, GS102 and GS257 cells were seeded at $5x10^3$ cells/well in GFR-Matrigel-coated black-walled 96-well plates. After 24 hours, the cells were treated with either amiodarone (1.5µM), clofazimine (5µM) or triptolide (10nM). Then, the CellPlayer™ Kinetic Caspase-3/7 Apoptosis Assay Kit (Essen Bioscience, Ann Arbor, MI, USA) was added at a concentration of 5µM in each well. The plates were placed in a fluorescence life-imaging microscope (Nikon, Tokyo, Japan) at a 4X magnification, measuring fluorescent spots for a period of 30 hours post-treatment. The experiments were performed in triplicate. ImageJ software (NIH) was used to count the fluorescent spots per well. The results are displayed as counts per image as percentage of non-treated controls ± standard error.

Statistical analysis
The experiments were performed in triplicate. The results were presented as mean percentage with the standard errors. To compare effects of different treatments between groups of *MGMT* promoter methylation or recurrence, the Student's T-test was used, and statistical significance was reached if $p<0.05$. Correlation analyses were performed using the Pearson R' correlation test. The caspase-3/7 data were analyzed using the two-way ANOVA with a Tukey´s Post-test, comparing the non-treated versus the treated cells over time. The therapeutic index of the drugs were calculated by dividing the IC_{50} value of the drug on primary human astrocytes, by the IC_{50} value of the drug on the various GSC cultures.

5.3 Results

Drug screening identifies 21 effective anti-glioblastoma agents in two patient-derived GSC cultures
An initial cell viability screen of 446 agents from the NIH Clinical Collection at multiple concentrations was performed in two distinct patient-derived GSCs; GS79 and GS102, which fall into the "classical" and "neural" transcriptionally defined glioblastoma subtypes, respectively.[16] This initial screen resulted in the identification of 21 agents, which reduced cell viability by more than 75% at concentrations up to 10µM in both GSCs (Table 1A). At 1µM, five agents were identified as potential anti-glioblastoma compounds, namely docetaxel, doxorubicin, epirubicin, idarubicin, and triptolide. At 5µM, nine agents were effective, namely 5-nonyloxytryptamine, clofazimine, rimcazole, salmeterol, tegaserod maleate, dactinomycin, homoharringtonine, vincristine and vindesine. At 10µM, seven drugs inhibited the viability of both cultures, namely amiodarone, cerivastatin, fluphenazine, itavastatin, lacidipine, perospirone, and 10H-phenothiazine. These compounds represented several distinct classes of drugs including anthracyclins, actinomycines, diterpenes, microtubule assembly-inhibitors, non-chemotherapeutic 3-hydroxy-3-methyl-glutaryl-CoA (HMG-CoA) reductase-inhibitors, serotonergic/dopaminergic drugs and ion-channel inhibitors. One of the anti-neoplastic drugs was doxorubicin, a well-known anti-glioma drug but which lacks the capability of penetrating the blood brain barrier. As we expected this drug to be a 'hit', this result serves as a validation of the screening procedure. After further selection, 12 of the 21 drugs (indicated in grey, Table 1A) were further evaluated *in vitro*. The selection was based on the efficacy at low concentrations in this patient-derived GSC model. There were 8 anti-neoplastic drugs that are already known to be ineffective or have clinical limitations in glioblastoma, and for one drug the chemical structure was not available. These drugs were therefore excluded from further validation.

Table 1A. The identified anti-glioblastoma agents after the initial drug screen.

Cell viability of GS79 and GS102 was measured after five days of incubation with the drug by CellTiter-Glo assay. The second column indicates molecular weight (Mw). The 'x' indicates the concentration at which effectiveness was observed: > 75% reduction of cell viability in both glioblastoma cultures. For each drug the clinical application is noted. The last column indicates whether currently there is a trial ongoing with this drug as anti-cancer agent in patients. The grey rows indicate the drugs that were investigated further on.

Drug name	MW	10µM	5µM	1µM	Clinical indication	Cancer trial
Triptolide	360			x	Antineoplastic; immuno-suppressive	(Minnelide)
Docetaxel	808			x	Antineoplastic	Yes
Doxorubicin Hcl	544			x	Antineoplastic; antibiotic	Yes
Epirubicin Hcl	544			x	Antineoplastic	Yes
Idarubicin Hcl	497			x	Antineoplastic	Yes
5nonyloxytryptamin	303		X		5-HT receptor agonist/antagonist	No
Clofazimine	473		X		Anti-inflammatory	No
Rimcazole	321		X		Antipsychotic; anticonvulsive	No
Salmeterol	415		X		Anti-asthmatic	No
Tegaserod Maleate	417		X		Anti-IBD/dyspepsia	No
Dactinomycin	1255		X		Antimycotic	Yes (glioma)
Homoharringtonine	546		X		Antineoplastic	Yes (CML; glioblastoma)
Vincristine sulfate	923		X		Antineoplastic	Yes
Vindesine sulfate	852		X		Antineoplastic	Yes
Amiodarone HCl	645	x			Antianginal; antiarrhythmic	No
Cerivastatin Na	459	x			Antihypercholesterolemia	No
Fluphenazine	474	x			Antipsychotic	Yes (M. Kahler)
Itavastatin Ca	881	x			Antihypercholesterolemia	No
Lacidipine	456	x			Antihypertensive	No
Perospirone Hcl	463	x			Antipsychotic	No
10H-phenothiazine	199	x			Antipsychotic; Antiprotozoal	No

Validation of the 12 selected compounds in a panel of patient-derived GSCs

To validate the efficacy of the compounds identified in the initial screen, the IC_{50} values of the 12 selected compounds were determined using an ATP-based viability assay in a panel of seven patient-derived glioblastoma cultures: GS79, GS102, GS184, GS335, GS357, GS359 and GS401 (Table 1B). Triptolide was effective at the lowest concentration (average IC_{50} = 10.00nM ± 0.01). The mean IC_{50} values for the other eleven drugs were 0.51µM ± 0.33 for cerivastatin, 0.88µM ± 2.24 for tegaserod maleate, 1.87µM ± 0.40 for 5-nonyloxytryptamine, 1.87µM ± 0.71 for clofazimine, 2.30µM ± 0.97 for amiodarone, 4.09µM ± 3.22 for pitavastatin, 4.5µM ± 1.15 for rimcazole, 6.0µM ± 0.37 for salmeterol, 6.32µM ± 2.01 for lacidipine, 6.42µM ± 3.83 for fluphenazine, and 6.98µM ± 5.10 for perospirone. Figure 1 depicts the viability data of the initially screened GSC cultures GS79 and GS102 after treatment with these twelve compounds. The IC_{50} values of the other GSC cultures are shown

in Table 1B. Six agents were selected for further studies, namely those that were effective at lower concentrations in all 7 cultures and showed little variability in response between the different cultures. The first to third interquartile ranges were taken for this purpose (Table 1B). These drugs were triptolide, amiodarone, clofazimine, 5-nonyloxytriptamine, tegaserod maleate and cerivastatin.

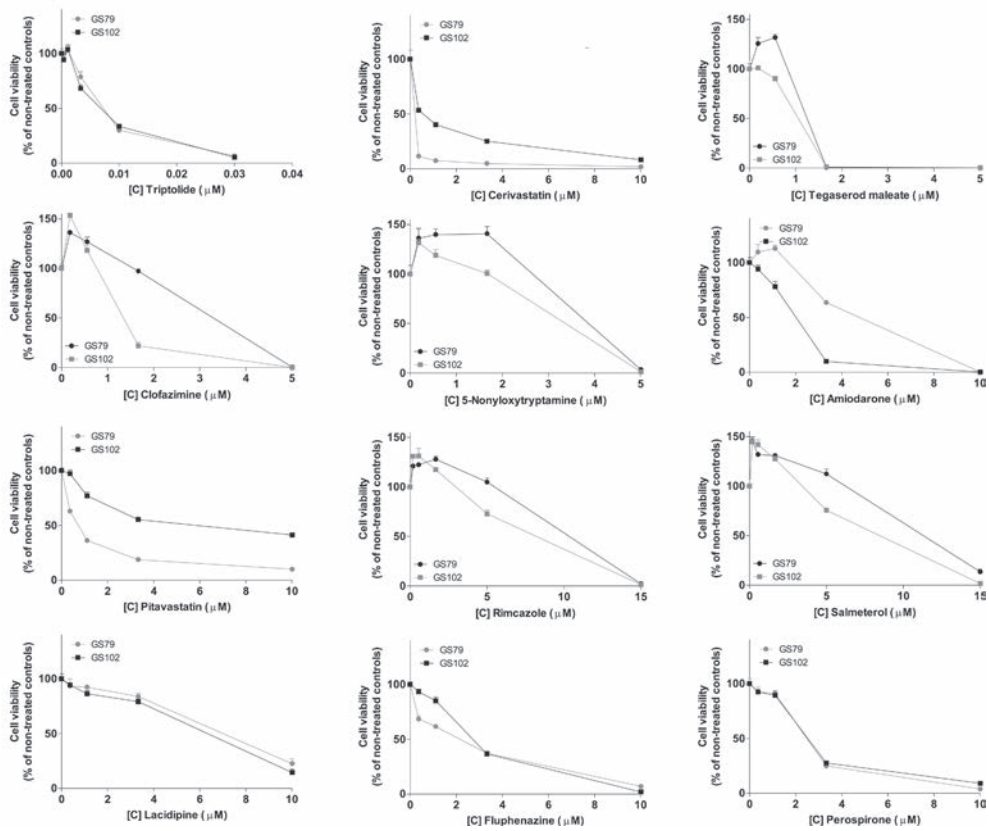

Figure 1. The effect of the twelve identified and selected anti-glioblastoma agents on the viability of patient-derived GSC cultures.

The serum-free cultured patient-derived GSCs GS79 and GS102, which were used for the initial screen, were treated with a dose range of the twelve identified compounds and viability was assessed after five days of incubation. Results are presented as percentage of non-treated controls with the standard error. IC_{50} values were calculated by median equation.

Table 1B. Validation of the 12 drugs in different patient-derived glioblastoma cultures.

The data revealed variability in IC_{50} values in the GS79, GS102, GS184, GS335, GS357, GS359 and GS401. The values indicate the IC_{50} in µM for all drugs. The drugs are ordered by the IC_{50} values. The column on the far right indicates the interquartile range Q75-Q25, which is taken as a measure for variability.

Drugs (µM)/ GSCculture	GS79	GS102	GS184	GS335	GS357	GS359	GS401	IC_{50} (mean)	Q75-Q25
Triptolide	0.004	0.004	0.013	0.027	0.008	0.004	0.012	0.01	0,023
Cerivastatin	0.09	0.56	0.43	0.56	1.17	0.17	0.59	0.51	1.08
Tegaserod maleate	0.78	1.2	0.62	1.22	0.84	0.58	0.92	0.88	0.64
Clofazimine	3.43	1.84	1.2	1.82	1.99	1.73	1.06	1.87	0.93
5-Nony-loxy-tryptamine	1.71	1.46	1.64	2.78	1.63	1.92	1.98	1.87	1.32
Amiodarone	4.52	1.45	2.03	2.44	2.34	1.69	1.61	2.30	0.99
Pitavastatin	0.6	7.19	2.74	7.06	1.97	0.35	8.73	4.09	8.38
Rimcazole	5.55	5.95	3.53	3.34	4.73	5.55	2.89	4.51	3.06
Salmeterol	5.8	5.87	6.54	5.96	6.33	5.32	6.2	6.00	1.22
Lacidipine	5.89	3.48	10.69	6.66	5.55	6.00	5.97	6.32	7.21
Fluphenazine	1.77	2.33	8.47	7.24	13.9	4.63	6.63	6.42	12.13
Perospirone	2.55	2.7	5.87	18.27	8.86	3.55	7.09	6.98	15.72

Human astrocytes are less sensitive to amiodarone, clofazimine and triptolide than GSCs

Next, we tested the selected drugs on low passage primary human astrocytes to gain insight into potential toxicity. This revealed that cerivastatin, 5-nonyloxytriptamine and tegaserod maleate were cytotoxic for human astrocytes at similar concentrations at which tumor cell viability reduction was reached (Table 2A). The IC_{50} values for the remaining three drugs on cultured human astrocytes were significantly higher than in the GSC lines, indicating potential tumor specificity. For amiodarone, clofazamine and triptolide IC_{50} values of 4.0µM, 3.1µM and 107.3nM were observed for human astrocytes, respectively. These values compared favorably to the toxicity of the drugs in an additional large panel of patient-derived GSCs as described below.

Table 2A. The three drugs that were excluded based on toxicity in normal human astrocytes.

The three drugs were added in three concentrations in micromolar (second column, C1, C2 and C3). Viability was measured by CellTiter-Glo assay at day 5 post-treatment are shown in the third column, as percentage of non-treated controls.

	Concentrations (µM)			Viability day 5		
Drug	[C1]	[C2]	[C3]	[C1]	[C2]	[C3]
Cerivastatin	0.17	0.51	1.53	10.26%	5.27%	1.08%
5-Nonyloxytryptamine	0.67	2.00	6.00	38.75%	0.17%	0.30%
Tegaserod maleate	0.33	1.00	3.00	85.21%	1.10%	0.10%

The effects of triptolide, clofazimine and amiodarone in twenty patient-derived GSC cultures

The effects of triptolide, clofazimine and amiodarone on tumor cell viability were then evaluated in twenty different patient-derived GSC cultures (Table 2B). In this panel of GSCs two sets of cultures, namely a primary and recurrent GSC culture originating from the same patient, were included. Heterogeneous responses to the drugs were observed. For amiodarone the IC_{50} values ranged more than 10-fold from 0.4 – 5.0μM (median=1.8μM; interquartile range (IQR)=1.5 – 2.3), for clofazimine the IC_{50} values ranged almost 20-fold from 0.6 – 9.8μM (median=2.0;IQR=1.1 – 3.4) and for triptolide the IC_{50} values ranged 15-fold from 4 – 60nM (median=11.6;IQR=7.7 – 16.9). Comparison of the IC_{50} values of the drugs in the normal human astrocytes with the IC_{50} values of the drugs in the panel of GSCs, revealed that astrocytes were relatively insensitive to amiodarone: 19/20 GSCs had a lower IC_{50} value than the astrocytes. Clofazimine showed less toxicity in six of 20 GSC cultures compared to the astrocytes, i.e. 14/20 cultures had a lower IC_{50} than the astrocytes. GSCs were considerably more sensitive to triptolide than astrocytes: the IC_{50} values in astrocytes were higher than the average IC_{50} value in the 19/20 GSCs (Figure 2B-C). The median of the therapeutic indices was 2.22 (IQR = 1.7 – 2.6) for amiodarone, 1.58 (IQR = 0.8 – 2.7) for clofazimine and 9.4 (IQR = 6.2 – 13.9) for triptolide.

Triptolide and amiodarone differentially affect GSC invasion

As glioblastomas grow highly invasively, the drugs were evaluated for their inhibitory effect on glioblastoma invasion *in vitro* by using the 3D-spheroid invasion assay. Collagen-embedded neurospheres of G9, GS79, GS184, GS257 and GS401 (Figure 3A-B) were selected based on their invasiveness and origin: G9, GS79 and GS257 are highly invasively-growing glioblastomas. GS184 and GS401 are derived from the same patient at different stages of disease progression, and were selected to study the differences in response between a primary and recurrent culture. The effects of the three drugs on neurosphere invasion were cell culture dependent. In G9 and GS79 cells, amiodarone (1.5μM) treatment significantly decreased invasion compared to non-treated controls at 24, 48 and 72 hours ($p<0.05$). Clofazimine (1.5μM) affected invasion of GS79 cells, and at multiple time points of G9 and GS401 cells. In general, the GSC neurosphere GS401, derived from the recurrent tumor of GS184, grew less invasively than its original counterpart (GS184) and was more susceptible to inhibition of invasion by clofazimine than GS184. Triptolide (10nM) inhibited invasion significantly ($p<0.05$) in G9 and GS79 neurospheres. As anti-invasive effects could potentially be attributed to cell viability reduction, we measured drug-induced cell death at 24, 48 and 72h (Figure 3C). Clofazimine moderately reduced viability at 48h and 72h post-treatment ($p<0.05$), whereas the other compounds did not, indicating that inhibitory effects on invasion were not caused by loss of viability at this dose. Figure 3D shows the limited morphological changes induced by the drug concentrations at the corresponding time points in GS79.

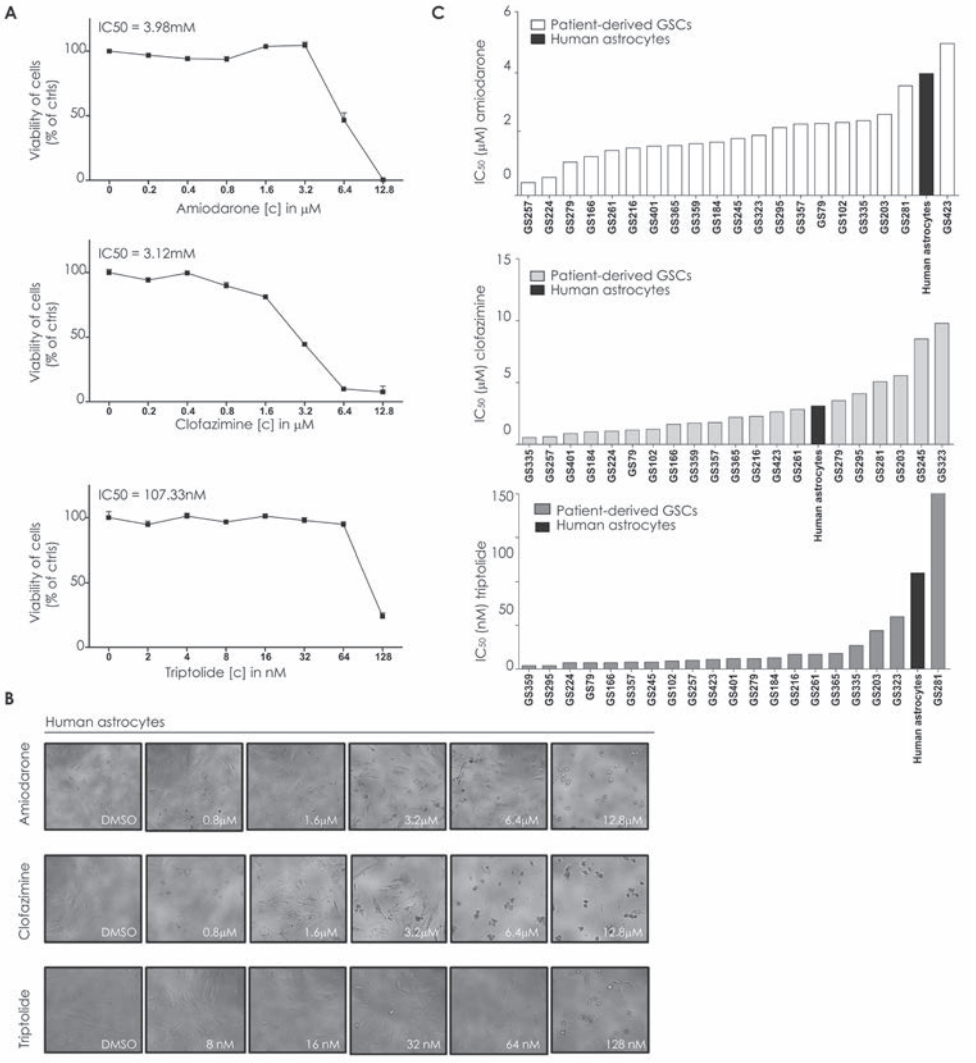

Figure 2. The effects of amiodarone, clofazimine and triptolide on human astrocytes.

(A) Primary human astrocytes were treated with a dose range of amiodarone, clofazimine and triptolide and viability was assessed after five days of incubation. Results are presented as percentage of non-treated controls. IC_{50} values were calculated by median equation and are shown in the respective graphs **(B)** Microscopic phase-contrast pictures of the human astrocytes showing effects on cell morphology at higher doses of the three compounds, (40X magnification). **(C)** The IC_{50} values of the three compounds on human astrocytes (black bars) in comparison to IC_{50} values of amiodarone (white bars), clofazimine (light grey bars) and triptolide (dark grey bars) on a panel of 20 distinct patient-derived GSC cultures

Table 2B. The three drugs screened on twenty patient-derived GSC cultures.

Cells were seeded $1x10^3$ and incubated for five days with the various drugs. Viability was measured using CellTiter-Glo assay. The IC_{50} were calculated in µM. The primary GSC culture characteristics including *MGMT* promoter methylation and recurrence status are depicted in the first two columns; M=methylated; UM=un-methylated; N=non-recurrent; Y=recurrent; TI = therapeutic index.

GSC	MGMT promoter status	Tumor recurrence status	Amiodarone IC_{50} (µM)	Clofazimine IC_{50} (µM)	Triptolide IC_{50} (µM)	Amiodarone TI	Clofazimine TI	Triptolide TI
GS79	UM	N	2.35	1.17	0.007	1.70	2.65	15.33
GS102	M	N	2.38	1.23	0.009	1.68	2.52	11.92
GS184	M	N	1.74	1.03	0.013	2.30	3.01	8.25
GS203	M	N	2.65	5.57	0.044	1.51	0.56	2.44
GS224	M	Y	0.59	1.08	0.007	6.78	2.87	15.33
GS261	M	N	1.47	2.84	0.017	2.72	1.09	6.31
GS279	M	Y	1.09	3.55	0.012	3.67	0.87	8.94
GS323	M	Y	1.96	9.78	0.06	2.04	0.32	1.79
GS357	M	N	2.33	1.77	0.008	1.72	1.75	13.41
GS359	M	N	1.69	1.73	0.004	2.37	1.79	26.83
GS401	M	Y	1.61	0.89	0.012	2.48	3.48	8.94
GS423	M	N	4.96	2.64	0.011	0.81	1.17	9.75
GS166	UM	Y	1.27	1.63	0.007	3.15	1.90	15.33
GS216	UM	Y	1.55	2.27	0.017	2.58	1.37	6.31
GS245	UM	N	1.86	8.52	0.008	2.15	0.36	13.41
GS257	UM	N	0.42	0.62	0.01	9.52	5.00	10.73
GS281	UM	N	3.58	5.07	1	1.12	0.61	0.11
GS295	UM	N	2.21	4.11	0.004	1.81	0.75	26.83
GS335	UM	Y	2.44	0.55	0.027	1.64	5.64	3.97
GS365	UM	N	1.63	2.19	0.018	2.45	1.42	5.96
Mean			1.80	1.98	0.01	2.22	1.58	9.35
IQR 1			1.53	1.15	0.01	1.70	0.84	6.22
IQR 3			2.36	3.69	0.02	2.62	2.70	13.89

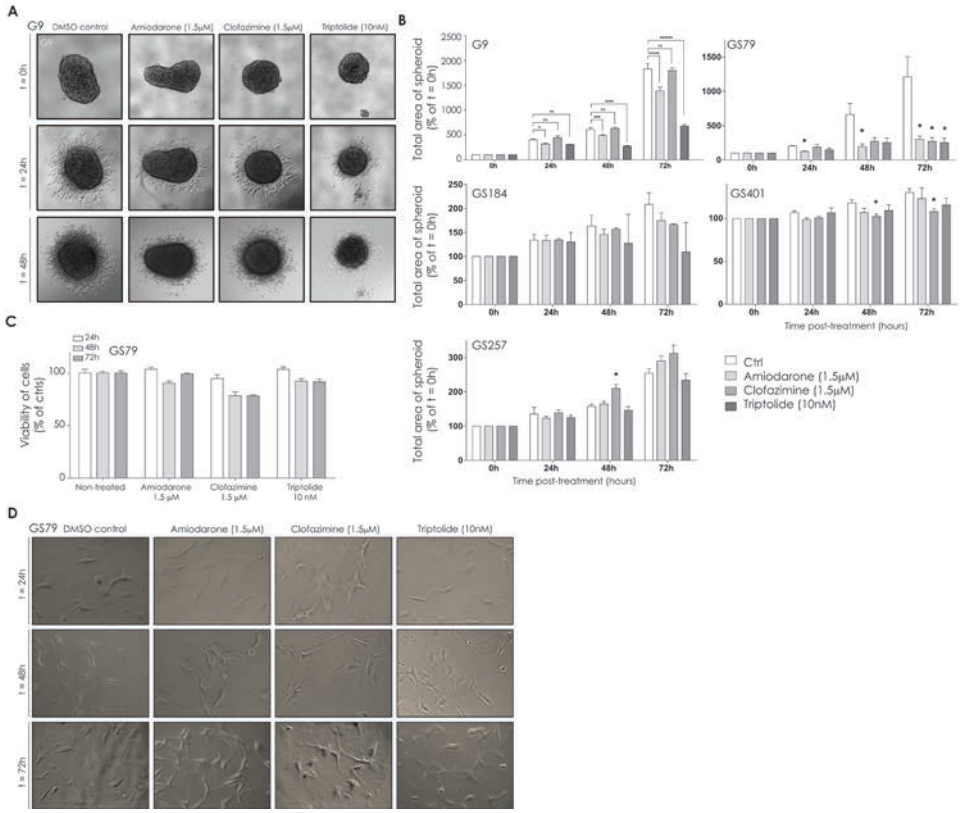

Figure 3. The effect of amiodarone, clofazimine and triptolide on invasion of patient-derived GSCs.

(A) Microscopic phase-contrast images of the tumor neurosphere invasion assay of patient-derived GSC culture G9. The tumor neurospheres were treated with amiodarone, clofazimine and triptolide and imaged immediately post-treatment (0 hour) and every 24 hours up to 72 hours (magnification 4X). **(B)** The results of the invasion assays for the patient-derived GSC neurospheres G9, GS401, GS79, GS257 and GS184 are displayed as total area of the neurosphere in time after treatment with the drugs at the indicated concentrations (mean total area with standard errors). *Indicates significance at $p<0.05$. **(C)** The drug concentrations used in the tumor neurosphere-invasion experiments were evaluated for effects on viability at these time points in GS79 cells. Cell viability was measured 24h, 48h and 72h post-treatment. The results are shown as % of non-treated controls with standard errors. **(D)** Microscopic images of GS79 cells at 24h, 48h and 72h post-treatment (40X magnification).

Molecular pathways and mechanisms related to response in patient-derived GSCs

The variability in sensitivity to the three drugs among the tested GSC cultures, prompted us to seek markers related to these responses. First, the three drugs under evaluation were studied in relation to known prognostic factors in glioblastoma. MGMT promoter methylation status is currently considered the main prognostic biomarker in glioblastoma and related to the standard of care therapy for glioblastoma, temozolomide.[17] Therefore we were specifically interested in the correlation between drug response and this marker. No correlation was found between the drug sensitivity of the 20 patient-derived GSCs and MGMT promoter methylation status of the parental tumor. Neither was there a correlation between primary/recurrence status (Table 2B) and drug responses. To identify potential mechanisms involved in drug response, the IC_{50} values were related to gene expression levels in the parental tumors of the GSC cultures used for the screening studies, which were determined by mRNA expression profiling (Figure 4B). A 'Functional Analysis' was done using Ingenuity® Pathway Analysis (IPA) software. We focused on the functions and networks of the genes, which were associated with drug response (Data on request, will become available online). The genes associated with amiodarone response were related to cell cycle regulation networks (3 in the top 10, Figure 4C, Supplemental Data 2) as well as to cell death and survival networks (Supplemental Data 1). Representative genes related to these functions were *AHR, BRAF, E2F1/E2F2/E2F3, BIRC5, BRCA2, CDC20/CDC25B, CASP9, FANCD2, RELN, and CDKN2D/CDKN2A*. Clofazimine response was related to functions involved networks of cellular growth and proliferation (Supplemental Data 1 and 2). Important genes involved in responsiveness were *BIRC2, CASP7, MAP2K7, TNF, CAMKK2, BCL2L12* and multiple collagens. Triptolide was associated with cell death and survival networks, and the genes were related to these mechanisms as well, including *CASP2, CLCN2, CPEB1, FANCC, FANCG, SNX7, KCNT2, DNM1, RAB40A* and *CREBL1*. Overall, these data provide a comprehensive set of genes that show associations with drug response and effects on cell regulatory pathways as identified by the *in silico* analysis.

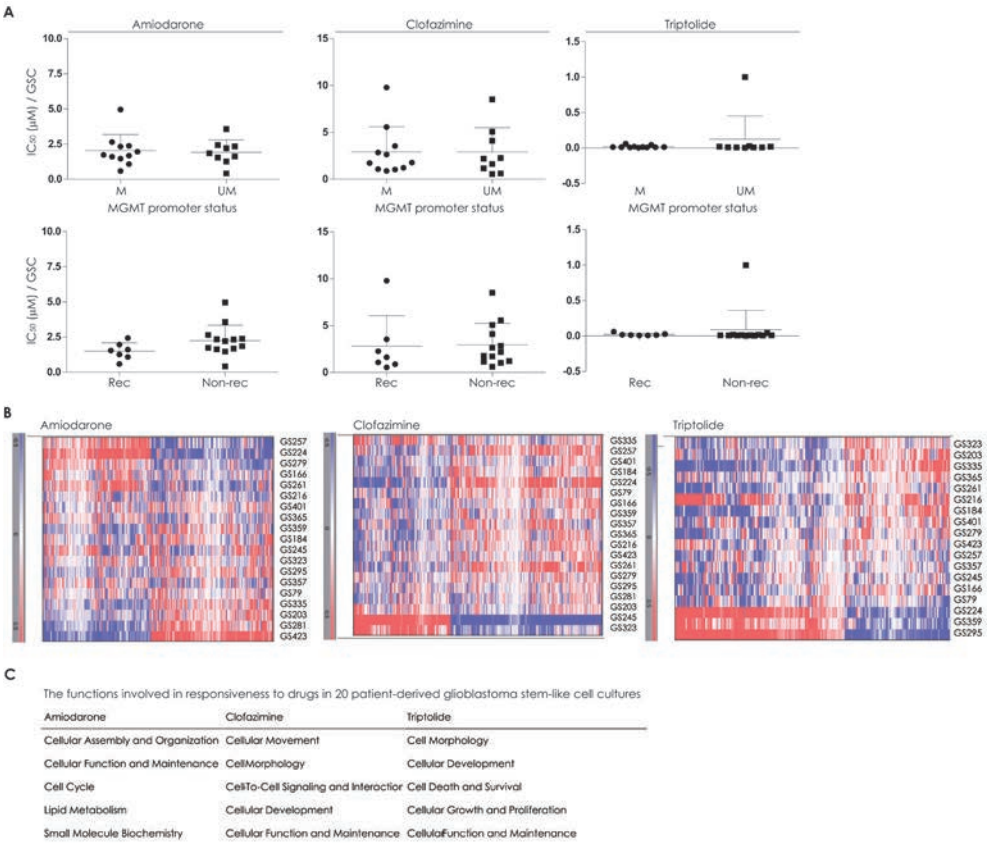

Figure 4. Correlation analysis of drug sensitivity with prognostic markers and mRNA gene expression profiles.

(A) Correlation analysis of the IC_{50} values for amiodarone, clofazimine and triptolide in the 20 GSC cultures with the *MGMT* promoter methylation status (M=methylated and UM=un-methylated) and for the recurrence status of the original tumor. No significant differences in IC_{50} values between groups were observed at $p<0.05$. **(B)** Heat maps of the mRNA gene expression analysis, in which expression levels were correlated to the drug responses. The data was analyzed with Partek Software and the heat maps were generated using OmniViz software. Gene expression levels: red, upregulated genes compared with the geometric mean; blue, down-regulated genes compared with the geometric mean. **(C)** The gene expression profiles of the original tumors were correlated to the response *in vitro* of the 20 GSC cultures. The identified genes had a significant correlation ($p<0.05$) and a correlation coefficient of < negative 0.5 or > 0.5. The genes were analyzed using the core analysis in the IPA software. The top five functions of the identified genes are shown.

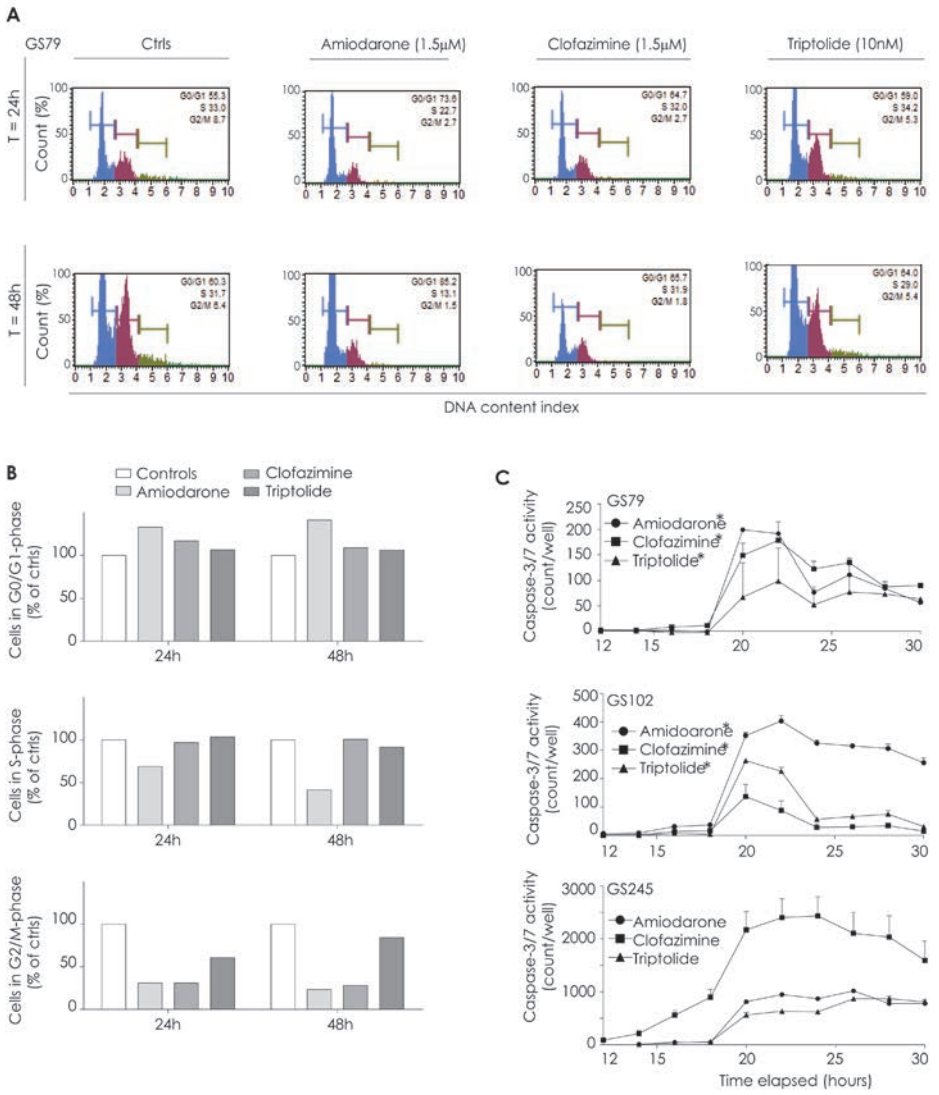

Figure 5. The effect of amiodarone, clofazimine and triptolide on the cell cycle progression and apoptosis.

(A) Flow cytometry was carried out to analyze the cell cycle of GS79 cells treated with amiodarone (1.5μM), clofazimine (1.5μM), and triptolide (10nM) for 24 and 48 hours. The DNA content indices are shown for each compound for each time point in the figure. **(B)** Quantification of flow cytometry data is depicted as percentage of treated cells in G0/G1, S and G2/M phase as percentage of control cells at 24 and 48 hours after post-treatment **(C)** The effects of the three compounds on caspase-3/7 activity were evaluated in three patient-derived GSCs GS79, GS102 and GS245, using the kinetic caspase-3/7 assay. After treatment with amiodarone (1.5μM), clofazimine (1.5μM) or triptolide (10nM) the plates were placed in a life-imaging microscope. Every two hours a fluorescence image was obtained at 4X magnification. The data were analyzed using ImageJ software and the results are presented as counts/well minus the background apoptotic activity of control cells with the standard error. *Indicates significance at $p<0.05$.

Amiodarone, clofazimine and triptolide differentially inhibit cell cycle progression and induce caspase-3/7 in patient-derived GSCs

To evaluate whether the mechanisms suggested by the gene expression and in silico analysis were affected by the drugs, the effects on caspase-3/7 activity and cell cycle distribution were studied in GS79 cells. The drugs were tested at one concentration based on the IC_{50} values in this culture (Table 2B). Cell cycle analysis by flow cytometry was performed at 24h and 48h post-treatment (Figure 5A-B). Amiodarone (1.5µM) increased the fraction of cells in the G0/G1-phase at both time points (133% and 141% of controls at 24 and 48 hours post-treatment). Both S-phase fraction and G2/M-phase fractions were reduced by amiodarone. Clofazimine (1.5µM) decreased the fraction of cells in the G2/M-phase. Triptolide (10nM) did not significantly affect cell fractions except G2/M fraction at 24h (Figure 5A-B). In conclusion, amiodarone and clofazimine induced accumulation of cells in G0/G1, amiodarone inhibited the fraction of cells in S-phase, whereas the proportion of cells in G2/M phase were affected. Next, the effects on apoptotic cell death were studied. Amiodarone, clofazimine and triptolide significantly increased caspase-3/7 activity compared to controls in GS79 cells (Figure 5C, $p<0.001$). Validation in GS102 and GS257 cells revealed comparable results as observed in GS79 (not shown). In conclusion, in addition to affecting the cell cycle, all three drugs also induced apoptosis in patient-derived glioblastoma cultures.

5.4 Discussion

With the aim of identifying effective and available drugs for glioblastoma treatment, we screened 446 clinical compounds using a representative *in vitro* model for glioblastoma. The patient-derived GSC model harbors genetic stability, *in vivo* resemblance of the glioblastoma, and in addition allows drug screening on large panels of distinct tumors at molecular level and analysis of the heterogeneity in response, as is often observed in glioblastoma.[6,7] The drugs were selected based on efficacy in GSC cultures and lack of toxicity in normal human astrocytes. This led to the identification of three clinical compounds that have potential for treating glioblastoma, namely the anti-arrhythmic amiodarone, the antibiotic clofazimine and the anti-inflammatory triptolide. Triptolide and clofazimine have previously been identified as potent inhibitors of growth in established glioma cell lines[18,19] but have not been studied yet in a large panel of the GSC cultures. Amiodarone is a novel candidate for glioblastoma treatment as single agent.

In our initial screen, several groups of compounds were identified as anti-glioblastoma agents. These groups include non-chemotherapeutic drug groups such as the HMG-CoA reductase inhibitors (cerivastatin, itavastatin), which have gained interest in the field of cancer research through their action against various hematological cancers,[20-22] serotonergic/dopaminergic drugs (5-nonyloxytryptamine, tegaserod maleate, perospirone and fluphenazine) which are central nervous system drugs previously reported to also possess anti-cancer activity.[23-25] Another study using a small-molecule compound screen of 30,000 agents, also found dopamine derivatives to be effective inhibitors of cell growth in glioblastoma cultures.[26] In addition we found ion-channel inhibitors to be effective, namely amiodarone, lacidipine, clofazimine. Ion channels are involved in cell cycle control and glioblastoma migration, invasion and proliferation.[27,28] Lastly, various agents we have identified are well-known anti-neoplastic agents, including vincristine which is (combined with procarbazine and lomustine; PCV) a beneficial therapeutic for low grade glioma,[29] and

doxorubicin which is currently under investigation using novel drug-delivery techniques to pass the blood-brain barrier in glioblastoma.[30,31]

We selected three drugs to study in more detail, amiodarone, clofazimine and triptolide, based on low-dose efficacy in the primary screens and lack of toxicity in normal human astrocytes. In a panel of twenty patient-derived GSC cultures, we confirmed the anti-tumor efficacy of the three drugs albeit with some degree of variability in response between the different GSC cultures. Importantly, neither the primary/recurrence status of the tumor nor the *MGMT* promoter methylation status was prognostic for the drug responses. This suggests that these drugs are effective in tumors, independent of known prognostic indicators. Our *in silico* analysis of the gene expression of the 20 glioblastomas in relation to response to the three drugs points toward apoptotic and cell cycle regulatory genes *(AHR, BIRC, CDKNs, CDCs, and E2F1-3)*, but also DNA repair proteins (FANC-genes) for amiodarone, apoptotic proteins *(CASP, BIRC* and *BCL2* genes*)* for clofazimine and caspases and DNA regulatory proteins *(FANC*-genes and *CASP2)* for triptolide. These molecular markers may also be potential biomarkers for response and need to be evaluated in a larger panel of cultures and preferably in *in vivo* settings. Our analysis of the effects of the three drugs on cell cycle distribution and apoptosis supported these findings.

The antibiotic clofazimine, a drug registered for leprosy, and amiodarone, have been reported as anti-glioblastoma agents[18,20,32] and in other tumors such as lung and breast carcinomas.[33-35] As a combination agent, amiodarone was shown to sensitize conventional glioma cells to TRAIL.[32] Also, synergy with conventional chemotherapeutics (cisplatin, docetaxel, doxorubicin) has been reported.[35] The present study demonstrates amiodarone efficacy as a single agent in the majority of patient-derived GSC cultures.

Mechanisms reported to play a role in clofazimine-induced apoptosis include effects on Wnt signaling,[34] and inhibition of the plasma membrane as well as the mitochondrial membrane potassium channels.[36] Indeed, Wnt-signaling has also been reported to play a role in maintenance and tumorigenicity of glioblastoma stem cells.[37] This potential selectivity for tumor stem cells, may also explain why lower IC_{50} values were found in our panel of GSC cultures (median IC_{50} of 1.98μM) than reported for established cancer cell lines, including the glioma lines U87, A172, LN443 and U118 (IC_{50} were 8.6 – 20.1).[18] These observations underline the importance of the use of the patient-derived GSC model in the initial drug screen and may explain discrepancies between identified agents in our screen and previously reported drug screens for glioma. In our study, triptolide, demonstrated high level cytotoxicity in the patient-derived GSCs. Triptolide is an extract of the herb Tripterygium wilfordii which is commonly used in China for various inflammatory and (auto)immune diseases.[38] Triptolide was previously shown to be an effective anti-glioma agent.[39] The reported mechanisms of action involve potassium channel inhibition,[40] induction of p53-independent apoptosis,[39] and RAS/ERK pathway attenuation.[39] There are strong indications in other cancers that triptolide exerts its effects through NFκB-inhibition[41] and that triptolide enhances temozolomide efficacy through regulation of NFκB.[42] The prodrug derivative of triptolide, Minnelide, which has an improved solubility and toxicity profile, is currently being evaluated in clinical trials for pancreatic and ovarian cancer.[43,44]

Another issue of importance to novel anti-glioblastoma drugs is the toxicity to primary human astrocytes, a question we have addressed. Triptolide and amiodarone are

relatively nontoxic to human astrocytes, and others have confirmed this for amiodarone.[32] median therapeutic indices were 2.2 for amiodarone, 1.6 for clofazimine and 9.[35] for triptolide. These therapeutic indices were in general above the value of 1, which indicates better efficacy in glioblastoma cultures than in normal brain cells. Moreover, clofazimine and amiodarone are widely prescribed drugs with known toxicity profiles in humans.

Our study was focused on the use of non-chemotherapeutic agents for the treatment of glioblastoma. Another drug screen that assessed drug-drug interactions found that for combination therapies in conventional glioma cell lines, similar drug (groups) as in our study were more effective in anti-glioblastoma activity compared to known chemotherapies. These drugs included serotonergic modulators, rimcazole and antioxidants.[45] These non-chemotherapeutic drugs usually have a known and acceptable toxicity profile, and combination therapies are therefore attractive. Future studies are thus recommended to further explore drug-drug interactions with our identified drugs. This may aid in lowering the effective dose of each compound and increasing the therapeutic index. Our study provides new avenues for monotherapy treatments, but as glioblastoma demonstrates rapid emergence of therapeutic resistance to single agents, using these drugs in combination may be required.

References

1. Stupp R, Hegi ME, Mason WP, et al. Effects of radiotherapy with concomitant and adjuvant temozolomide versus radiotherapy alone on survival in glioblastoma in a randomised phase III study: 5-year analysis of the EORTC-NCIC trial. Lancet Oncol 2009;10:459-66.
2. Stupp R, Mason WP, van den Bent MJ, et al. Radiotherapy plus concomitant and adjuvant temozolomide for glioblastoma. The New England journal of medicine 2005;352:987-96.
3. Minniti G, Muni R, Lanzetta G, Marchetti P, Enrici RM. Chemotherapy for glioblastoma: current treatment and future perspectives for cytotoxic and targeted agents. Anticancer Res 2009;29:5171-84.
4. Pantziarka P, Bouche G, Meheus L, Sukhatme V, Sukhatme VP. Repurposing drugs in your medicine cabinet: untapped opportunities for cancer therapy? Future oncology 2015;11:181-4.
5. Van Nuffel AM, Sukhatme V, Pantziarka P, Meheus L, Sukhatme VP, Bouche G. Repurposing Drugs in Oncology (ReDO)-clarithromycin as an anti-cancer agent. Ecancermedicalscience 2015;9:513.
6. Lee J, Kotliarova S, Kotliarov Y, et al. Tumor stem cells derived from glioblastomas cultured in bFGF and EGF more closely mirror the phenotype and genotype of primary tumors than do serum-cultured cell lines. Cancer Cell 2006;9:391-403.
7. Fouse SD, Nakamura JL, James CD, Chang S, Costello JF. Response of primary glioblastoma cells to therapy is patient specific and independent of cancer stem cell phenotype. Neuro Oncol 2014;16:361-71.
8. Pont LM, Naipal K, Kloezeman JJ, et al. DNA damage response and anti-apoptotic proteins predict radiosensitization efficacy of HDAC inhibitors SAHA and LBH589 in patient-derived glioblastoma cells. Cancer Lett 2015;356:525-35.
9. US National Institutes of Health. http://dtp.cancer.gov. 2014.

10. Williams SP, Nowicki MO, Liu F, et al. Indirubins decrease glioma invasion by blocking migratory phenotypes in both the tumor and stromal endothelial cell compartments. Cancer Res 2011;71:5374-80.
11. Balvers RK, Kleijn A, Kloezeman JJ, et al. Serum-free culture success of glial tumors is related to specific molecular profiles and expression of extracellular matrix-associated gene modules. Neuro Oncol 2013;15:1684-95.
12. Chou TC, Talalay P. Quantitative analysis of dose-effect relationships: the combined effects of multiple drugs or enzyme inhibitors. Advances in enzyme regulation 1984;22:27-55.
13. Berghauser Pont LM, Naipal K, Kloezeman JJ, et al. DNA damage response and anti-apoptotic proteins predict radiosensitization efficacy of HDAC inhibitors SAHA and LBH589 in patient-derived glioblastoma cells. Cancer Lett 2014.
14. Berghauser Pont LM, Spoor JK, Venkatesan S, et al. The Bcl-2 inhibitor Obatoclax overcomes resistance to histone deacetylase inhibitors SAHA and LBH589 as radiosensitizers in patient-derived glioblastoma stem-like cells. Genes Cancer 2014;5:445-59.
15. Klipper-Aurbach Y, Wasserman M, Braunspiegel-Weintrob N, et al. Mathematical formulae for the prediction of the residual beta cell function during the first two years of disease in children and adolescents with insulin-dependent diabetes mellitus. Medical hypotheses 1995;45:486-90.
16. Verhaak RG, Hoadley KA, Purdom E, et al. Integrated genomic analysis identifies clinically relevant subtypes of glioblastoma characterized by abnormalities in PDGFRA, IDH1, EGFR, and NF1. Cancer Cell 2010;17:98-110.
17. Hegi ME, Diserens AC, Gorlia T, et al. *MGMT* gene silencing and benefit from temozolomide in glioblastoma. The New England journal of medicine 2005;352:997-1003.
18. Jiang P, Mukthavaram R, Chao Y, et al. Novel anti-glioblastoma agents and therapeutic combinations identified from a collection of FDA approved drugs. J Transl Med 2014;12:13.
19. Zhang H, Zhu W, Su X, et al. Triptolide inhibits proliferation and invasion of malignant glioma cells. J Neurooncol 2012;109:53-62.
20. Wong WW, Dimitroulakos J, Minden MD, Penn LZ. HMG-CoA reductase inhibitors and the malignant cell: the statin family of drugs as triggers of tumor-specific apoptosis. Leukemia 2002;16:508-19.
21. Sehdev A, Shih YC, Huo D, Vekhter B, Lyttle C, Polite B. The Role of Statins for Primary Prevention in Non-elderly Colorectal Cancer Patients. Anticancer Res 2014;34:5043-50.
22. Ahern TP, Lash TL, Damkier P, Christiansen PM, Cronin-Fenton DP. Statins and breast cancer prognosis: evidence and opportunities. Lancet Oncol 2014;15:e461-8.
23. Roth BL, Craigo SC, Choudhary MS, et al. Binding of typical and atypical antipsychotic agents to 5-hydroxytryptamine-6 and 5-hydroxytryptamine-7 receptors. J Pharmacol Exp Ther 1994;268:1403-10.
24. Ishibashi T, Tagashira R, Nakamura M, Noguchi H, Ohno Y. Effects of perospirone, a novel 5-HT2 and D2 receptor antagonist, on Fos protein expression in the rat forebrain. Pharmacology, biochemistry, and behavior 1999;63:535-41.
25. Weninger S, Van Craenenbroeck K, Cameron RT, et al. Phosphodiesterase 4 interacts with the 5-HT4(b) receptor to regulate cAMP signaling. Cellular signalling 2014;26:2573-82.
26. Visnyei K, Onodera H, Damoiseaux R, et al. A molecular screening approach to identify and characterize inhibitors of glioblastoma stem cells. Mol Cancer Ther 2011;10:1818-28.

27. Molenaar RJ. Ion channels in glioblastoma. ISRN Neurol 2011;2011:590249.
28. Raphael M, Lehen'kyi V, Vandenberghe M, et al. TRPV6 calcium channel translocates to the plasma membrane via Orai1-mediated mechanism and controls cancer cell survival. Proc Natl Acad Sci U S A 2014.
29. van den Bent MJ, Erdem-Eraslan L, Idbaih A, et al. *MGMT*-STP27 methylation status as predictive marker for response to PCV in anaplastic Oligodendrogliomas and Oligoastrocytomas. A report from EORTC study 26951. Clin Cancer Res 2013;19:5513-22.
30. Battaglia L, Gallarate M, Peira E, et al. Solid lipid nanoparticles for potential doxorubicin delivery in glioblastoma treatment: preliminary *in vitro* studies. Journal of pharmaceutical sciences 2014;103:2157-65.
31. Kreuter J. Drug delivery to the central nervous system by polymeric nanoparticles: what do we know? Advanced drug delivery reviews 2014;71:2-14.
32. Kim IY, Kang YJ, Yoon MJ, et al. Amiodarone sensitizes human glioma cells but not astrocytes to TRAIL-induced apoptosis via CHOP-mediated DR5 upregulation. Neuro Oncol 2011;13:267-79.
33. Sri-Pathmanathan RM, Plumb JA, Fearon KC. Clofazimine alters the energy metabolism and inhibits the growth rate of a human lung-cancer cell line *in vitro* and *in vivo*. Int J Cancer 1994;56:900-5.
34. Koval AV, Vlasov P, Shichkova P, et al. Anti-leprosy drug clofazimine inhibits growth of triple-negative breast cancer cells via inhibition of canonical Wnt signaling. Biochem Pharmacol 2014;87:571-8.
35. Mitrakas AG, Kalamida D, Koukourakis MI. Effect of mitochondrial metabolism-interfering agents on cancer cell mitochondrial function and radio/chemosensitivity. Anticancer Drugs 2014.
36. Leanza L, O'Reilly P, Doyle A, et al. Correlation between potassium channel expression and sensitivity to drug-induced cell death in tumor cell lines. Current pharmaceutical design 2014;20:189-200.
37. Rheinbay E, Suva ML, Gillespie SM, et al. An aberrant transcription factor network essential for Wnt signaling and stem cell maintenance in glioblastoma. Cell reports 2013;3:1567-79.
38. Han R, Rostami-Yazdi M, Gerdes S, Mrowietz U. Triptolide in the treatment of psoriasis and other immune-mediated inflammatory diseases. British journal of clinical pharmacology 2012;74:424-36.
39. Lin J, Chen L, Lin Z, Zhao M. Inhibitory effect of triptolide on glioblastoma multiforme *in vitro*. The Journal of international medical research 2007;35:490-6.
40. So EC, Lo YC, Chen LT, Kao CA, Wu SN. High effectiveness of triptolide, an active diterpenoid triepoxide, in suppressing Kir-channel currents from human glioma cells. Eur J Pharmacol 2014;738:332-41.
41. Yinjun L, Jie J, Yungui W. Triptolide inhibits transcription factor NF-kappaB and induces apoptosis of multiple myeloma cells. Leuk Res 2005;29:99-105.
42. Sai K, Li WY, Chen YS, et al. Triptolide synergistically enhances temozolomide-induced apoptosis and potentiates inhibition of NF-kappaB signaling in glioma initiating cells. The American journal of Chinese medicine 2014;42:485-503.
43. Banerjee S, Nomura A, Sangwan V, et al. CD133+ tumor initiating cells in a syngenic murine model of pancreatic cancer respond to Minnelide. Clin Cancer Res 2014;20:2388-99.
44. Rousalova I, Banerjee S, Sangwan V, et al. Minnelide: a novel therapeutic that promotes apoptosis in non-small cell lung carcinoma *in vivo*. PLoS One 2013;8:e77411.

45. Schmidt L, Kling T, Monsefi N, et al. Comparative drug pair screening across multiple glioblastoma cell lines reveals novel drug-drug interactions. Neuro Oncol 2013;15:1469-78.

Supplemental Data 1. The networks involved in responsiveness to drugs in the twenty patient-derived GSC cultures.

The gene expression levels of the tumors were correlated to the response in vitro of the derived GSCs. The included genes had a significant correlation ($p<0.05$) and a correlation coefficient of <-0.5 or >0.5. The genes were analyzed using the core analysis in the IPA software. The top ten networks where the genes corresponded to are shown in this table. The whole set of genes and networks can be provided on request and will be published online.

Networks Amiodarone (top ten)	Networks Clofazimine (top ten)	Networks Triptolide (top ten)
Digestive System Development and Function, Skeletal and Muscular System Development and Function, Gene Expression	Cellular Growth and Proliferation, Connective Tissue Disorders, Cancer	Cell Morphology, Nervous System Development and Function, Cell-To-Cell Signaling and Interaction
Cardiovascular System Development and Function, Cellular Function and Maintenance, Tissue Development	Cellular Growth and Proliferation, Cellular Assembly and Organization, Cellular Function and Maintenance	Cell Death and Survival, Cellular Function and Maintenance, Organ Morphology
Cancer, Endocrine System Disorders, Gastrointestinal Disease	Cell Morphology, Cellular Assembly and Organization, Cellular Function and Maintenance	Cancer, Embryonic Development, Organismal Development
Cellular Assembly and Organization, Cellular Function and Maintenance, Cell Cycle	Cellular Movement, Skeletal and Muscular System Development and Function, Cancer	Immunological Disease, Inflammatory Disease, Inflammatory Response
Cancer, Cell Cycle, Gastrointestinal Disease	Auditory Disease, Hereditary Disorder, Neurological Disease	Cancer, Cell-To-Cell Signaling and Interaction, Connective Tissue Disorders
Cancer, Gastrointestinal Disease, Organismal Injury and Abnormalities	Drug Metabolism, Nucleic Acid Metabolism, Small Molecule Biochemistry	Cellular Assembly and Organization, Cellular Function and Maintenance, Cell Morphology
Gene Expression, Cell Morphology, Cellular Compromise	Cell Morphology, Cellular Assembly and Organization, Cellular Function and Maintenance	Cancer, Cardiovascular Disease, Cardiovascular System Development and Function
Cell Cycle, Cell Death and Survival, Cancer	Cellular Growth and Proliferation, Cancer, Cell Morphology	Cancer, Cell Morphology, Cellular Assembly and Organization
Gene Expression, Organismal Development, Energy Production	Cell-To-Cell Signaling and Interaction, Gene Expression, Cellular Movement	Cancer, Molecular Transport, Energy Production
Cell Cycle, DNA Replication, Recombination, and Repair, Developmental Disorder	Organismal Functions, Neurological Disease, Psychological Disorders	Cell Morphology, Cell-To-Cell Signaling and Interaction, Nervous System Development and Function

Part II

Combination strategies for oncolytic adenovirus Delta24-RGD in glioblastoma

Chapter 6

Concentrations of antiepileptic drugs do not inhibit the activity of the oncolytic adenovirus Delta24-RGD in malignant glioma

Jonas de Jonge,[1,2] Lotte M.E. Berghauser Pont,[1] Sander Idema,[2] Jenneke J. Kloezeman,[1] David Noske,[2] Clemens M.F. Dirven,[1] Martine L.M. Lamfers.[1]

Affiliations

1 Department of Neurosurgery, Brain Tumor Center, Erasmus MC
2 Department of Neurosurgery, VU Medical Center

Published in the J Gene Med. 2013 Mar-Apr;15(3-4):134-41

PMID: 23606319

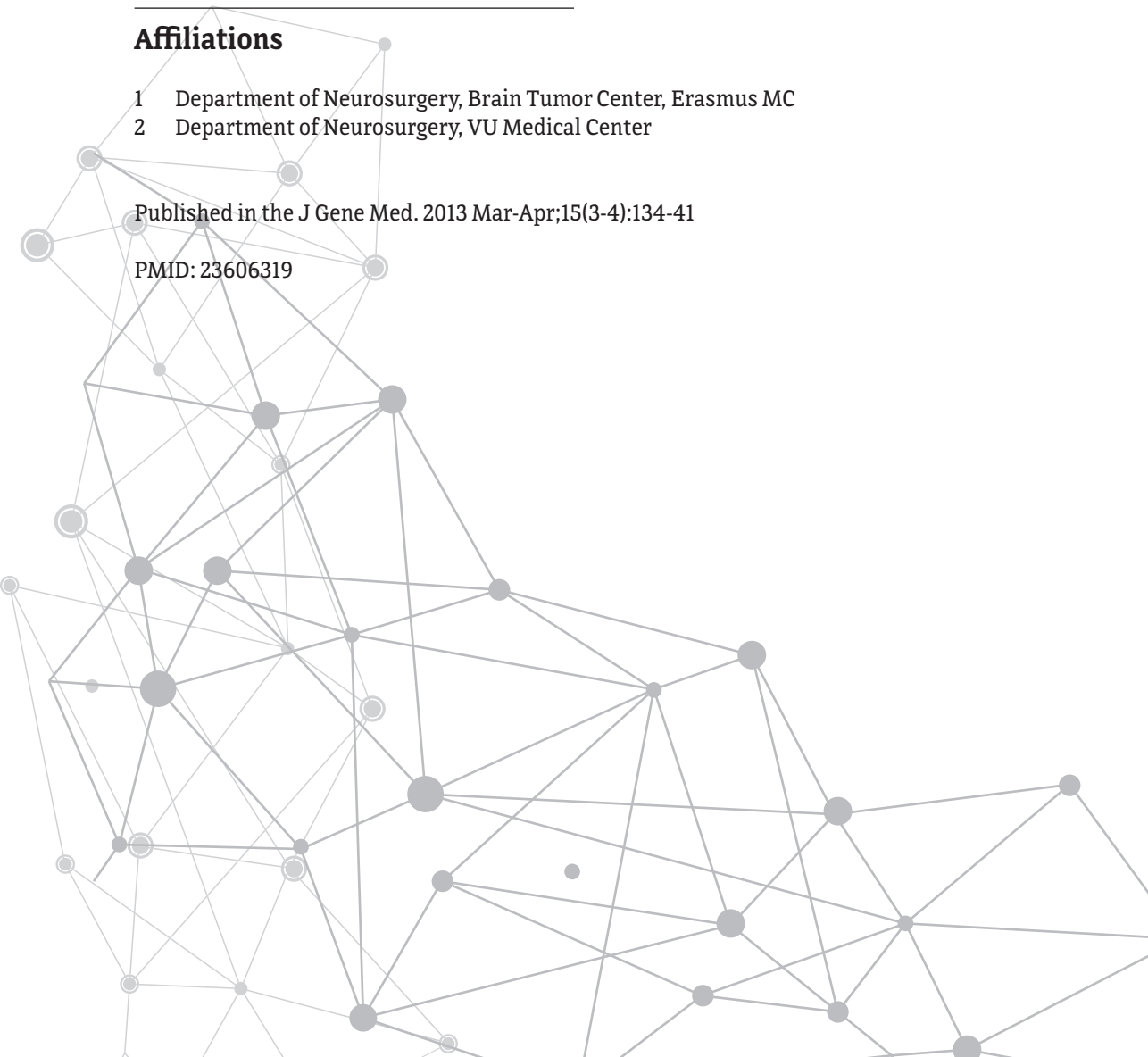

Abstract

The oncolytic adenovirus Delta24-RGD is currently being tested in phase I trials for the treatment of glioblastoma (GBM). Literature suggests that frequently prescribed anticonvulsants for these patients, phenytoin, valproic acid and levetiracetam, may interfere with cellular mechanisms of cancer or oncolytic virus activity. We therefore investigated the direct effects of these drugs on Delta24-RGD infection and oncolytic activity in established glioma cell lines as well as patient-derived glioblastoma cultures. IC_{50} values of the anti-epileptic drugs on the 4 glioma cell lines were far above clinically-relevant concentrations. At therapeutic concentrations, the anti-epileptics generally did not alter the infection efficiency of RGD-modified adenovirus, nor affect progeny production or oncolytic activity of Delta24-RGD. The only exception was found in U373 cells, where valproic acid slightly antagonized the oncolytic effect of Delta24-RGD (from 29% to 55% viability, $p<0.01$) as well as viral progeny production (60% decrease, $p<0.01$). Oncolysis by Delta24-RGD was not inhibited by the anti-epileptics in any of the patient-derived glioma cultures (n=6). In fact, in one culture a slight enhancement of viral oncolysis by PHE and LEV was found, from 89.7% viability to 76% and 62.4%, respectively ($p<0.01$).

These results indicate that therapeutic levels of valproic acid, phenytoin and levetiracetam do not negatively interfere with the infection efficiency or oncolytic activity of Delta24-RGD in patient-derived glioblastoma cells. Therefore, there is no indication that the choice of anticonvulsant for seizure control in glioma patients should take treatment with Delta24-RGD into account.

6.1 Introduction

Glioblastoma is the most aggressive form of brain cancer and its poor prognosis emphasizes the need for more effective treatment modalities. One approach encompasses the use of oncolytic viruses, designed to propagate selectively in tumor tissue.[1] The oncolytic adenovirus Delta24-RGD has shown promising preclinical anticancer efficacy in several tumor types including glioblastoma and is currently being tested in phase I/II trials for the treatment of glioblastoma.[2-6] It replicates selectively due to a 24 base-pair deletion in the adenoviral *E1A* gene, which abolishes the pRb binding capacity of the E1A protein and results in uninhibited viral replication in cells with lesions in the Rb pathway.[7] The Arg-Gly-Asp (RGD) motif insertion into the fiber knob allows the virus to attach to both αvβ3 and αvβ5 integrins. As most tumor cells express low levels of CAR this has greatly potentiated the oncolytic efficacy.[8,9] Epileptic seizures occur in 22 – 60% of glioma patients and are most commonly treated with valproic acid (VPA), phenytoin (PHE), or levetiracetam (LEV).[10,11] Whether these agents also directly affect cellular tumor mechanisms, is not fully understood. It has been described for VPA that it exerts anti-proliferative effects on glioma *in vitro*.[12,13] Moreover, a recent retrospective study in a large cohort of glioblastoma patients, revealed significantly improved survival rates in patients receiving VPA.[12] Effects of these anti-epileptics on oncolytic adenovirus infection and replication in glioblastoma, however, have not been reported thus far. In neuroblastoma and HeLa cells, VPA-induced weak histone deacetylase inhibition (HDACi), leading to enhanced adenoviral transgene expression.[14] Moreover, both the adenoviral receptor CAR as well as integrin expression have been reported to be affected by VPA[15-17] and antagonistic effects of VPA on adenoviral replication have also been described.[18] PHE is an antiepileptic that blocks voltage-dependent neuronal sodium channels; however, its mechanism of action is not fully

elucidated. The effect of PHE on oncolytic viruses has not been investigated thus far, but studies with PHE in glioma cells, report no significant inhibitory or stimulatory effects on tumor cell growth.[19,20] LEV has been reported to sensitize glioblastoma cells to temozolomide by enhancing p53-mediated *MGMT* inhibition via recruitment of the mSin3A/HDAC1 co-repressor complex.[21] Its major carboxylic acid metabolite 2-pyrrolidinone-n-butyric acid, has HDACi activity.[19] If the effects of these antiepileptic drugs on Delta24-RGD are elucidated, recommendations for antiepileptic therapy could be provided for glioblastoma patients treated with Delta24-RGD oncolytic viral therapy. Furthermore, the knowledge of possible interactions between these agents would aid in the interpretation of the results of current Delta24-RGD trials. Therefore, in view of the mechanisms of action of these drugs and the current clinical assessment of Delta24-RGD in glioblastoma patients, we studied the direct effects of the most frequently prescribed anticonvulsants on the infectivity, replication, and oncolytic activity of Delta24-RGD in *in vitro* glioma models.

6.2 Materials and methods

Cell cultures

Both established and human malignant glioblastoma cell cultures were used for the experiments. The human malignant glioma cell lines U87MG, U118MG, U251MG and U373MG were obtained from the American Type Culture Collection (Manassas, VA, USA). These cells were cultured in DMEM supplemented with 1% Pen/Strep and 5% fetal calf serum (Life Technologies, Paisley, United Kingdom). Patient-derived low passage glioblastoma cultures GS112, GS125, GS160, VU140, VU144 and VU214 were derived by mechanical dissociation from fresh tumor material collected during brain tumor surgery as described previously.[22] Patient tumor material was acquired with informed consent and approved by the Institutional Review Boards of the Erasmus Medical Center Rotterdam and VU medical center Amsterdam. The primary cell cultures included in this study were classified as glioblastoma by histological diagnosis and cultured in serum-free DMEM, supplemented with 1% antibiotics (Life Technologies, Paisley, United Kingdom), 2% B27 (Gibco, Life Technologies, Paisley, United Kingdom), 20 ng/ml bFGF (PeproTech, London, UK), 20 ng/ml EGF (PeproTech) and 5 ug/ml heparine (Sigma-Aldrich, St. Louis, MO).

Chemicals

Active pharmaceutical ingredients of PHE were kindly provided by Teva (Haarlem, The Netherlands). LEV was kindly provided by UCB Pharma (Breda, The Netherlands). Stock solutions of VPA (Sigma-Aldrich) and LEV were prepared at 200mM in sterile water and stock solution of PHE at 20mM in ethanol.

Recombinant adenovirus

The recombinant E1-deleted, replication-deficient adenovirus expressing the luciferase reporter gene, Ad.Luc, the integrin-targeted replication-deficient adenovirus expressing luciferase, Ad5LucRGD, and the conditionally replicating virus Delta24-RGD were a kind gift of Dr. D.T. Curiel (University of Alabama, Birmingham, AL). Viruses were plaque purified, propagated on 293 cells for replication-deficient vectors or A549 cells for Delta24-RGD, and purified by CsCl gradient according to standard techniques. Viral titers were determined by limiting dilution assay using the AdenoX rapid titer assay kit (Clontech, Mountain View, CA, USA).

Luciferase Assay

To assess the effects of anticonvulsants on adenovirus infection, glioma cell lines as well as patient-derived cell-cultures were plated sub-confluently at 1 x 10^4 cells per well in 96-well plates. After 24h, cells were infected at a multiplicity of infection (MOI) of 5 or 25 Ad.Luc or Ad.Luc-RGD, and primary cultures were infected with 25 MOI. Cells were co-treated with concentrations of VPA (0.3 and 0.6mM) , PHE (0.03 and 0.07mM) or LEV(0.05 and 0.1mM). The dosages were based upon the clinically relevant-concentrations according to the literature (VPA 0.04-0.7mM, PHE 0.02-0.08mM, and LEV 0.03-0.10mM).[23-27] After 48 hours, culture medium was aspirated and 50µl (primaries) or 100 µl (cell lines) lysis buffer was added to each well. After three cycles of freeze-thawing luciferase expression was assessed using the Luciferase Assay System (Promega, Madison, WI) and measured using a Lumat LB 9507 luminometer (EG&G Berthold, Bad Wildbad, Germany). The luciferase activities are presented as RLU (relative light units) per 50 or 100µL lysate.

Viability assays

Cells were plated subconfluently at 5 x 10^3 cells per well in 96-well plates to perform dose response assays for each anticonvulsant. A concentration range from 0.01-1.0mM was used, including two log steps and covering the clinically relevant concentrations. IC_{50}s were computed from the median effect equation five days after treatment. VPA and PHE have a relatively high protein binding in plasma, 70-92% and 82-92% respectively, in contrast to LEV (10%).[20,28] To limit the loss of drug activity due to protein binding in the serum-cultured cell lines, we used medium with 5% instead of the standard 10% fetal calf serum. For the combination experiments, Delta24-RGD was added to the wells in medium containing clinically-relevant concentrations of anticonvulsants, 24h after plating. Concentrations used were 0.1, 0.3 and 0.6 mM VPA, 0.003, 0.01 and 0.03 PHE and 0.01, 0.03 and 0.1 mM LEV. These concentrations were based on the IC_{50} determination experiment and therapeutic feasibility. The PHE concentration was chosen to be 0.03mM instead of 0.07mM, since this lower concentration of 0.03mM already showed tumor inhibiting properties at this value. MOIs applied to the different cell types were based on viral sensitivity of the specific cells. Established cell lines (U-lines) require the lower MOIs (0.125 - 0.5), whereas the patient-derived cells were less sensitive and were treated with higher MOI ranges (1 – 2). Viability was quantified on day 3, 5 and 7 after treatment using the tetrazolium salt WST-1 assay (Roche Diagnostics, Mannheim, Germany) as described by the manufacturer. Results are presented as percentage of non-treated controls.

Titration Assays

U87 and U373 cells were incubated with 0.6mM VPA and were infected with MOI 2 Delta-24-RGD 24h after plating. Supernatants and cell lysates were harvested on day 3 and 5 after infection to monitor viral production and release. Viral production in cells and media was assessed by endpoint dilution titration on cells using the AdenoX rapid titer assay kit (Clontech).

Statistical analysis

All experiments were performed in triplicate and means where plotted with their corresponding standard deviations. Treatment effects were compared by the two-tailed student's t-test. Statistical significance was defined as $p < 0.01$.

6.3 Results

Effects of anti-epileptics on glioma cell viability

The effect of the three anticonvulsants on the viability of glioma cell lines was determined by dose response assays. A concentration range from 0.01–1.0mM was used for each anticonvulsant and IC_{50} values were calculated. The IC_{50} values of PHE and VPA on glioma cell lines U87, U118, U251 and U373 are summarized in table 1 and are all far above therapeutic concentrations. Glioma cell line U87 exhibited the highest sensitivity for both anticonvulsive drugs. For LEV, no significant decrease in viability for this concentration range was observed and IC_{50} values hence not obtained.

Table 1. IC_{50} (R2) values for anticonvulsants on glioma cell lines.

The results are based on the viability after 5 days. IC_{50} = half maximal inhibitory concentration; mM = millimolar; PHE = phenytoin; VPA = valproic acid.

Glioma cell line	IC_{50} of PHE (mM) and (R^2)	IC_{50} of VPA (mM) and (R^2)
U87	1.805 (0.945)	1.43 (0.993)
U118	3.17 (0.995)	3.54 (0.998)
U251	2.96 (1.000)	4.98 (0.998)
U373	2.96 (0.993)	4.82 (0.950)

Effects of anti-epileptics on infection efficiency

To assess whether treatment with anticonvulsants interferes with the infection efficiency of Delta24-RGD, experiments were conducted using the luciferase-encoding replication-deficient vector Ad.Luc-RGD. Two concentrations of each drug (0.3mM and 0.6 mM VPA, 0.05mM and 0.1mM LEV, 0.03mM and 0.07mM PHE) were combined with MOI 5 and 25 Ad.Luc-RGD. These are clinically-relevant serum concentrations in anticonvulsant therapy. Glioma cell lines U87 and U373 were used for the experiments. The control vector Ad.Luc was used in parallel to determine if effects found were related to the RGD modification of the vector. As shown in figure 1, viral infection efficacy of Ad.Luc-RGD was not significantly affected by therapeutic concentrations of VPA, LEV and PHE. Similarly, no significant effects on Ad.Luc infectivity were found (not shown).

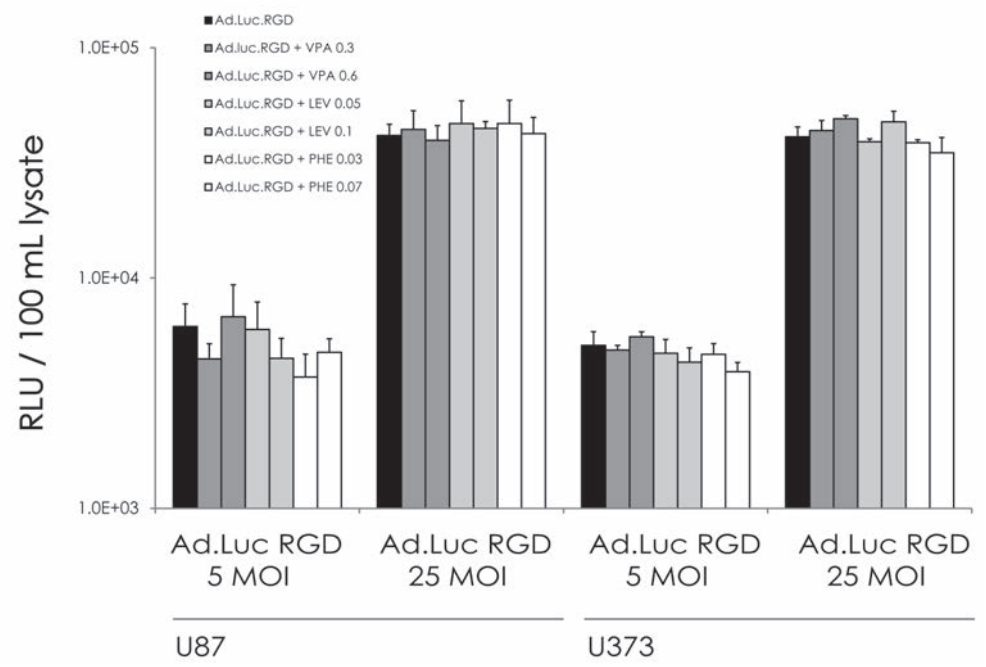

Figure 1.

Luciferase expression in glioma cells lines U87 and U373 infected with Ad.Luc.RGD (MOI 5 and 25) combined with incubation with anticonvulsants. Luciferase expression was determined 48h after infection. Results are presented as relative light units (RLU) per 100 µL cell lysate. Experiments were performed in triplicate. Data plots, mean percentages; bars ± SD; *p < 0.01 compared to controls.

Effects of antiepileptic drugs on Delta24-RGD oncolytic activity

To examine whether anticonvulsants interact directly with the oncolytic capacity of Delta-24-RGD, combination experiments with anticonvulsants were performed in 4 glioma cell lines. The results of U251 and U373 are shown in figure 2. Overall, therapeutic concentrations of VPA, PHE and LEV did not inhibit the oncolytic activity of Delta24-RGD. Only VPA slightly antagonized the oncolytic effect of Delta24-RGD in U373 cells on day 7, from 29% to 55% viability (p=0.01). This antagonistic effect was not observed with PHE or LEV. Table 2A shows the results of U87 and U118, as well as parallel experiments using lower and higher concentrations of virus or anticonvulsants, which resulted in similar outcome.

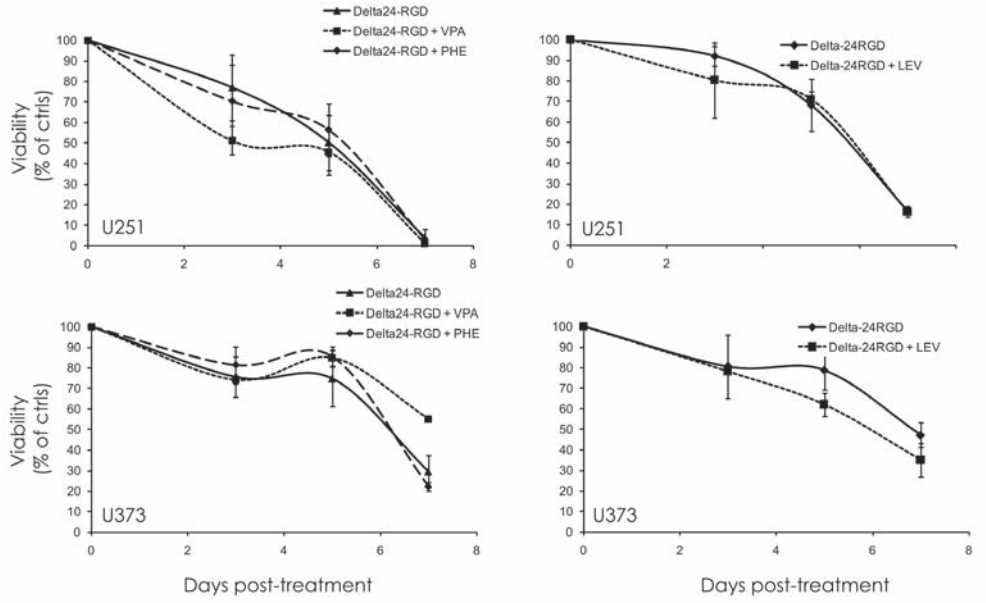

Figure 2.

Effects of anticonvulsants (0.6 mM VPA, 0.03 mM PHE, 0.1 mM LEV) in combination with Delta24-RGD (MOI 0.5) on viability of U251 and U373 during 7 days. PHE and VPA shared the same control. Experiments were performed in triplicate. Data are presented as mean percentage of non-treated same day controls ± SD; * $p < 0.01$ compared to infected controls without anticonvulsant.

Table 2A. Overview of all glioma cell lines tested with Delta24-RGD and the anticonvulsants VPA, PHE and LEV. Data are presented as mean percentage viability of non-treated controls on day 7 post-treatment; *p< 0.01 compared to infected controls without anticonvulsant.

U251	MOI 0	p value	MOI 0.125	p value	MOI 0.5	p value
Delta24RGD	100.0%		34.5%		4.0%	
VPA 0.06 mM	101.2%	0.40	52.3%	0.44	3.8%	0.96
VPA 0.2 mM	101.7%	0.29	37.0%	0.91	1.8%	0.40
VPA 0.6 mM	98.7%	0.45	12.9%	0.23	1.0%	0.26
Delta24RGD	100.0%		34.5%		4.0%	
PHE 0.003mM	100.7%	0.74	40.2%	0.74	4.4%	0.88
PHE 0.01mM	97.8%	0.15	47.6%	0.47	3.6%	0.89
PHE 0.03mM	100.3%	0.85	38.8%	0.80	3.1%	0.74
Delta24RGD	100.0%		29.6%		16.5%	
LEV 0.03mM	97.1%	0.56	22.7%	0.17	15.0%	0.58
LEV 0.1mM	104.3%	0.19	22.3%	0.16	16.2%	0.89
LEV 0.3mM	100.9%	0.78	23.9%	0.35	15.7%	0.57
U87	**MOI 0**	**p value**	**MOI 0.125**	**p value**	**MOI 0.5**	**p value**
Delta24RGD	100.0%		96.5%		97.1%	
VPA 0.06 mM	90.0%	0.65	91.8%	0.84	98.2%	0.90
VPA 0.2 mM	91.7%	0.49	98.9%	0.93	107.4%	0.40
VPA 0.6 mM	91.3%	0.53	96.3%	0.99	103.3%	0.47
Delta24RGD	100.0%		96.5%		97.1%	
PHE 0.003mM	100.9%	0.96	109.6%	0.68	109.6%	0.30
PHE 0.01mM	105.8%	0.76	101.1%	0.80	106.0%	0.50
PHE 0.03mM	122.9%	0.10	117.6%	0.26	102.4%	0.57
Delta24RGD	100.0%		94.3%		87.9%	
LEV 0.03mM	91.0%	0.35	89.4%	0.79	81.6%	0.18
LEV 0.1mM	92.3%	0.26	87.7%	0.71	86.7%	0.73
LEV 0.3mM	91.7%	0.53	87.9%	0.74	84.7%	0.38
U118	**MOI 0**	**p value**	**MOI 0.125**	**p value**	**MOI 0.5**	**p value**
Delta24RGD	100.0%		55.9%		26.0%	
VPA 0.06 mM	97.5%	0.55	80.1%	0.07	18.3%	0.18
VPA 0.2 mM	94.1%	0.41	59.0%	0.77	12.1%	0.04
VPA 0.6 mM	98.0%	0.57	56.6%	0.96	23.2%	0.69
Delta24RGD	100.0%		55.9%		26.0%	
PHE 0.003mM	105.8%	0.30	75.3%	0.18	25.8%	0.97
PHE 0.01mM	112.0%	0.02	52.2%	0.81	27.1%	0.86
PHE 0.03mM	112.5%	0.06	79.9%	0.06	22.8%	0.46
Delta24RGD	100.0%		82.4%		65.9%	
LEV 0.03mM	103.4%	0.28	79.6%	0.68	55.4%	0.15
LEV 0.1mM	104.1%	0.29	79.3%	0.52	71.5%	0.33
LEV 0.3mM	100.4%	0.94	78.9%	0.44	66.5%	0.90

U373	MOI 0	p value	MOI 0.125	p value	MOI 0.5	p value
Delta24RGD	100.0%		71.5%		29.4%	
VPA 0.06 mM	96.7%	0.55	68.9%	0.28	42.1%	0.39
VPA 0.2 mM	95.7%	0.37	81.5%	0.03	47.6%	0.16
VPA 0.6 mM	78.0%	0.01	81.9%	0.01	55.0%	0.01
Delta24RGD	100.0%		90.2%		29.4%	
PHE 0.003mM	97.2%	0.58	92.8%	0.89	29.5%	0.99
PHE 0.01mM	98.7%	0.93	84.7%	0.78	36.0%	0.48
PHE 0.03mM	88.7%	0.52	72.6%	0.50	22.1%	0.22
Delta24RGD	100.0%		84.2%		47.2%	
LEV 0.03mM	100.0%	0.99	83.8%	0.99	43.1%	0.34
LEV 0.1mM	99.7%	0.99	72.2%	0.57	35.0%	0.11
LEV 0.3mM	104.1%	0.78	71.7%	0.52	37.5%	0.13

Effects of anti-epileptics on Delta24-RGD replication

Based on the small antagonistic effect of VPA observed in U373, we assessed whether this effect was due to decreased viral progeny production of Delta24-RGD. U373 and U87 cells were treated with 0.6mM VPA and infected with MOI 2 Delta24-RGD. Cells and supernatants were collected 3 and 5 days later for virus titration. On day 5, U373 cells had produced 60% ($p<0.01$) less virus than controls, whereas no effects were seen in U87 cells (figure 3).

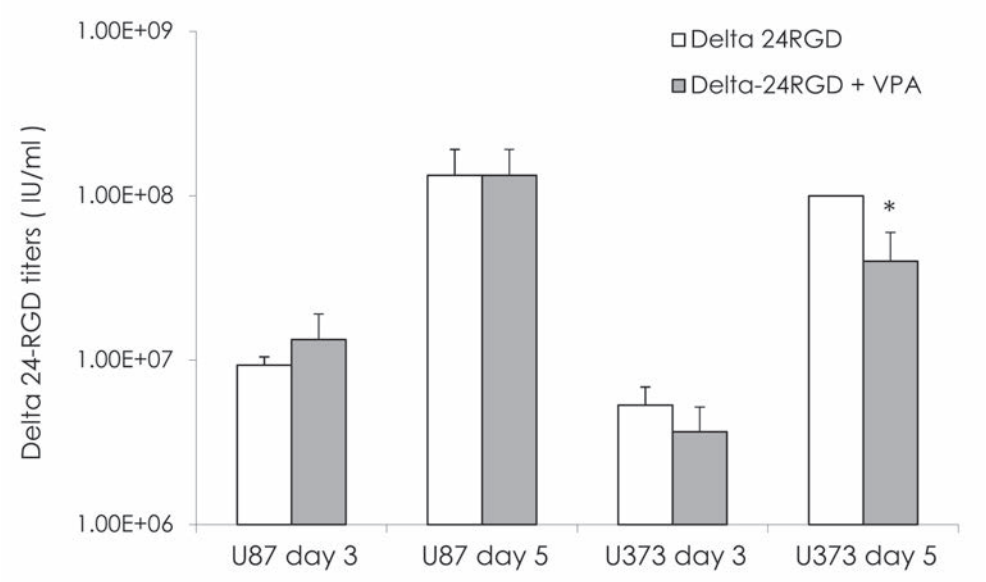

Figure 3.

Effects of 0.6 mM VPA on Delta24-RGD replication in U87 and U373 cells. Viral titers were determined by endpoint titration on day 3 and 5 and are expressed as infectious units (IU) per mL. Experiments were performed in triplicate. Bars (IU/mL) ± SD; *$p<0.01$ compared with infected controls without VPA.

Effects of anti-epileptics on infection efficiency and oncolysis of Delta24-RGD in patient-derived serum-free glioma cultures.

As serum-free cultures of patient-derived tumor closely resemble the genotype of the parental tumor, they are considered more representative of clinical glioblastoma.[22,29] Therefore, the infection and oncolysis experiments were repeated in patient-derived glioblastoma cultures. To determine whether anticonvulsants alter adenovirus infection efficiency, GS112, GS125 and GS160 cells were infected with Ad.Luc-RGD and Ad.Luc and analyzed for luciferase expression. As depicted in figure 4, no significant effects of anticonvulsants on Ad.Luc-RGD infection were observed. Similarly, no effects on Ad.Luc infection were found (not shown).

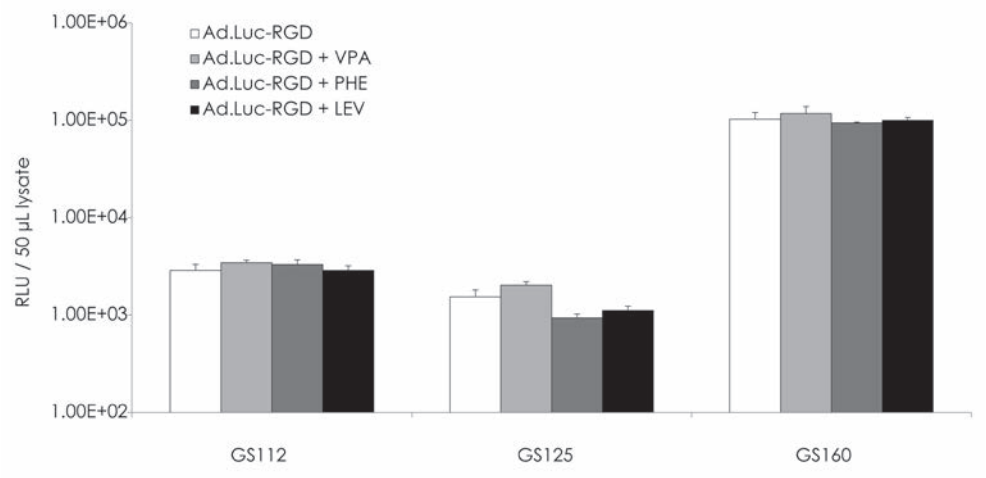

Figure 4.

Effects of the anticonvulsants (0.6 mM VPA, 0.03 mM PHE, 0.1 mM LEV) on the infection efficiency of MOI 25 Ad.Luc-RGD in patient-derived GSCs: GS112, GS125, and GS160. Experiments were performed in triplicate. Luciferase expression was determined 48 h post-infection and is presented as relative light units (RLU) per 50 µL lysate. Bars ± SD; *p< 0.01 compared to controls.

Oncolysis experiments were performed using a dose-range of Delta24-RGD in combination with the three anti-epileptics on a panel of six patient-derived glioma cells (GS112, GS125, GS160, VU140, VU144 and VU214). Results of all combination treatments in these cells are summarized in Table 2B. Monotherapy using the three anticonvulsants at clinically relevant concentrations did not significantly affect cell viability of these primary cultures with the exception VU140, which showed a slight decrease in viability after VPA and LEV monotherapy (to 87.5% and 84.9%, respectively, $p<0.01$). In general, there were no significant differences in viability observed between virus and combination treated cells (figure 5/Table 2B). Only VU214 appeared susceptible to virosensitization by the anti-epileptics PHE and LEV (89.7% versus 76.0% and 62.4%, respectively, at MOI 2, $p<0.01$).

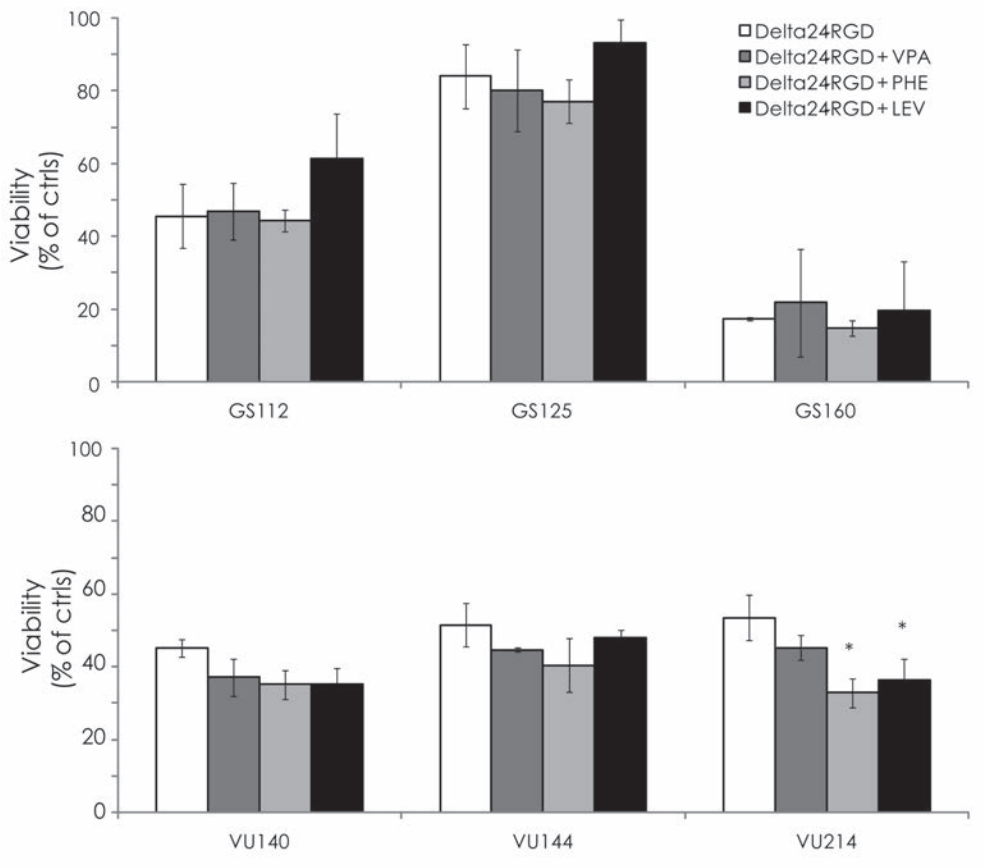

Figure 5.

Effects of anticonvulsants in combination with Delta24-RGD (MOI 2) on viability of 6 patient-derived glioma cell cultures on day 7 post-infection. Cells were incubated with Delta24RGD (MOI 2) with and without 0.03 mM PHE, 0.6 mM VPA and 0.1 mM LEV, respectively. Experiments were performed in triplicate. Data are presented as mean percentage of non-treated controls ± SD, * $p<0.01$ compared to infected controls without anticonvulsant.

Table 2B. Overview of all patient-derived glioblastoma cultures tested with Delta24-RGD and the anticonvulsants VPA, PHE and LEV.

Data are presented as mean percentage viability of non-treated controls on day 7 post-treatment; *p< 0.01 compared to infected controls without anticonvulsant.

EMC85	MOI 0	p value	MOI 1	p value	MOI 2	p value
Delta24RGD	100.0%		82.6%		45.6%	
VPA 0.6mM	64.8%	0.03	70.6%	0.92	46.8%	0.14
PHE 0.03mM	72.4%	0.03	78.9%	0.17	44.4%	0.06
LEV 0.1mM	101.2%	0.10	81.6%	0.89	61.4%	0.08
EMC96						
Delta24RGD	100.0%		83.1%		84.1%	
VPA 0.6mM	85.9%	0.18	82.5%	0.53	80.1%	0.80
PHE 0.03mM	86.9%	0.07	87.3%	0.06	77.2%	0.65
LEV 0.1mM	109.1%	0.74	98.8%	0.03	93.2%	0.07
EMC115						
Delta24RGD	100.0%		30.8%		17.4%	
VPA 0.6mM	98.1%	0.18	32.8%	0.53	21.9%	0.80
PHE 0.03mM	100.0%	0.07	26.0%	0.06	15.0%	0.65
LEV 0.1mM	105.8%	0.74	33.7%	0.03	19.8%	0.07

VU140	MOI 0	p value	MOI 1	p value	MOI 2	p value
Delta24RGD	100.0%		96.5%		81.7%	
VPA 0.6mM	87.5%	0.01	83.5%	0.03	68.5%	0.14
PHE 0.03mM	86.7%	0.07	78.7%	0.04	64.9%	0.10
LEV 0.1mM	84.9%	0.00	79.3%	0.02	61.5%	0.03
VU144						
Delta24RGD	100.0%		85.6%		84.8%	
VPA 0.6mM	93.6%	0.48	78.4%	0.26	72.4%	0.02
PHE 0.03mM	90.3%	0.13	83.4%	0.70	79.5%	0.39
LEV 0.1mM	83.1%	0.04	70.0%	0.06	78.6%	0.26
VU214						
Delta24RGD	100.0%		96.9%		89.7%	
VPA 0.6mM	104.9%	0.12	82.8%	0.11	77.9%	0.04
PHE 0.03mM	99.5%	0.87	75.3%	0.02	76.0%	0.00
LEV 0.1mM	105.5%	0.16	78.0%	0.03	62.4%	0.00

6.4 Discussion

The present study was designed to identify possible interaction between anticonvulsants and Delta24-RGD oncolytic viral therapy in glioblastoma cells. In general, our data from a panel of glioma cell lines and patient-derived cell cultures illustrate that therapeutic levels of the most frequently prescribed anticonvulsants valproic acid, phenytoin and levetiracetam do not negatively influence the oncolytic activity of Delta24-RGD.

Dose-response studies demonstrated that IC_{50} values of the tested anticonvulsants were all far above the clinical therapeutic concentrations. Combination experiments with Delta24-RGD in 4 glioma cell lines found no interaction between these agents with the exception of U373, in which slight inhibition of oncolysis was found by VPA. The reduced oncolysis in U373 also translated to reduced viral progeny production in these cells but was not caused by reduced infection efficiency as shown by Ad.Luc-RGD infection of VPA-treated cells. Interestingly, VPA effects on adenoviral replication have also been observed in prostate cancer cells. Hőti et al. described an inhibitory effect of VPA on adenoviral replication in the late phase of the viral life cycle18, and this was suggested to be based on HDAC inhibition,[13,30] thereby affecting viral transcription and inducing cell cycle regulator $p21^{WAF1/CIP1}$.[18] VPA-induced up-regulation of levels of cell surface integrin α and β subtypes as well as the adenovirus receptor CAR have also been reported.[17,31] Such effects would have been expected to result in enhanced infection efficiency by Delta24-RGD, however, these effects were not observed in our experiments. Effects of VPA therefore appear dose- and cell type dependent.[17]

The relevance of the antagonistic effect of VPA on Delta24-RGD in U373 cells was assessed by repeating the infection and oncolysis experiments in a panel of 6 patient-derived serum-free glioma cultures. In general, therapeutic levels of antiepileptic drugs did not affect the infection efficiency or oncolysis of Delta24-RGD, with the exception of a slight enhancement of viral oncolysis by PHE and LEV in VU-214. The patient-derived serum-free cell culture model has been shown to resemble the genotype and gene expression profiles of the original glioblastoma more closely than conventional glioma cell lines.[29] The results of these experiments are therefore more representative of combination effects expected in glioblastoma patients. However, since this is an *in vitro* study, conclusions for clinical application should always be drawn with prudence. We have not investigated the immune-related effects of the antiepileptic drugs in combination with Delta24-RGD. HDACi have been suggested to suppress the innate immune response against virotherapy. They have the ability to enhance vesicular stomatitis virus Δ51 oncolytic activity in multiple animal models.[32] Such potential immune-related effects of the HDACi VPA cannot be excluded to play a role in Delta24-RGD therapy in patients.

Taken together, these *in vitro* data support that therapeutic levels of the most frequently administered anticonvulsants valproic acid, phenytoin and levetiracetam do not negatively modulate the intrinsic sensitivity of patient-derived glioma cells for Delta24-RGD activity. Based on the experiments performed in the primary cell cultures, there is no suggestion that the choice of anticonvulsant for seizure control in glioma patients should take treatment with Delta24-RGD into account.

References

1. Parato KA, Senger D, Forsyth PA, Bell JC. Recent progress in the battle between oncolytic viruses and tumours. Nature reviews Cancer 2005;5:965-76.
2. Bauerschmitz GJ, Kanerva A, Wang M, et al. Evaluation of a selectively oncolytic adenovirus for local and systemic treatment of cervical cancer. Int J Cancer 2004;111:303-9.
3. Jiang H, Gomez-Manzano C, Lang FF, Alemany R, Fueyo J. Oncolytic adenovirus: preclinical and clinical studies in patients with human malignant gliomas. Current gene therapy 2009;9:422-7.
4. Fueyo J, Alemany R, Gomez-Manzano C, et al. Preclinical characterization of the antiglioma activity of a tropism-enhanced adenovirus targeted to the retinoblastoma pathway. J Natl Cancer Inst 2003;95:652-60.
5. Jiang H, Gomez-Manzano C, Aoki H, et al. Examination of the therapeutic potential of Delta-24-RGD in brain tumor stem cells: role of autophagic cell death. J Natl Cancer Inst 2007;99:1410-4.
6. Lamfers ML, Grill J, Dirven CM, et al. Potential of the conditionally replicative adenovirus Ad5-Delta24RGD in the treatment of malignant gliomas and its enhanced effect with radiotherapy. Cancer Res 2002;62:5736-42.
7. Fueyo J, Gomez-Manzano C, Alemany R, et al. A mutant oncolytic adenovirus targeting the Rb pathway produces anti-glioma effect *in vivo*. Oncogene 2000;19:2-12.
8. Fuxe J, Liu L, Malin S, Philipson L, Collins VP, Pettersson RF. Expression of the coxsackie and adenovirus receptor in human astrocytic tumors and xenografts. Int J Cancer 2003;103:723-9.
9. Huang KC, Altinoz M, Wosik K, et al. Impact of the coxsackie and adenovirus receptor (CAR) on glioma cell growth and invasion: requirement for the C-terminal domain. Int J Cancer 2005;113:738-45.
10. Lote K, Stenwig AE, Skullerud K, Hirschberg H. Prevalence and prognostic significance of epilepsy in patients with gliomas. European journal of cancer 1998;34:98-102.
11. Oberndorfer S, Schmal T, Lahrmann H, Urbanits S, Lindner K, Grisold W. [The frequency of seizures in patients with primary brain tumors or cerebral metastases. An evaluation from the Ludwig Boltzmann Institute of Neuro-Oncology and the Department of Neurology, Kaiser Franz Josef Hospital, Vienna]. Wien Klin Wochenschr 2002;114:911-6.
12. Weller M, Gorlia T, Cairncross JG, et al. Prolonged survival with valproic acid use in the EORTC/NCIC temozolomide trial for glioblastoma. Neurology 2011;77:1156-64.
13. Knupfer MM, Pulzer F, Schindler I, Hernaiz Driever P, Knupfer H, Keller E. Different effects of valproic acid on proliferation and migration of malignant glioma cells *in vitro*. Anticancer Res 2001;21:347-51.
14. Fan S, Maguire CA, Ramirez SH, et al. Valproic acid enhances gene expression from viral gene transfer vectors. J Virol Methods 2005;125:23-33.
15. Segura-Pacheco B, Avalos B, Rangel E, Velazquez D, Cabrera G. HDAC inhibitor valproic acid upregulates CAR *in vitro* and *in vivo*. Genet Vaccines Ther 2007;5:10.
16. Lin KT, Yeh SH, Chen DS, Chen PJ, Jou YS. Epigenetic activation of alpha4, beta2 and beta6 integrins involved in cell migration in trichostatin A-treated Hep3B cells. J Biomed Sci 2005;12:803-13.
17. Wedel S, Hudak L, Seibel JM, et al. Inhibitory effects of the HDAC inhibitor valproic acid on prostate cancer growth are enhanced by simultaneous application of the mTOR inhibitor RAD001. Life Sci 2011;88:418-24.

18. Hoti N, Chowdhury W, Hsieh JT, Sachs MD, Lupold SE, Rodriguez R. Valproic acid, a histone deacetylase inhibitor, is an antagonist for oncolytic adenoviral gene therapy. Mol Ther 2006;14:768-78.
19. Eyal S, Yagen B, Sobol E, Altschuler Y, Shmuel M, Bialer M. The activity of antiepileptic drugs as histone deacetylase inhibitors. Epilepsia 2004;45:737-44.
20. Stander M, Dichgans J, Weller M. Anticonvulsant drugs fail to modulate chemotherapy-induced cytotoxicity and growth inhibition of human malignant glioma cells. J Neurooncol 1998;37:191-8.
21. Bobustuc GC, Baker CH, Limaye A, et al. Levetiracetam enhances p53-mediated *MGMT* inhibition and sensitizes glioblastoma cells to temozolomide. Neuro Oncol 2010;12:917-27.
22. Balvers RK, Kleijn A, Kloezeman JJ, et al. Serum-free culture success of glial tumors is related to specific molecular profiles and expression of extracellular matrix-associated gene modules. Neuro Oncol 2013;15:1684-95.
23. Karkar KM, Thio LL, Yamada KA. Effects of seven clinically important antiepileptic drugs on inhibitory glycine receptor currents in hippocampal neurons. Epilepsy Res 2004;58:27-35.
24. Loscher W. Effects of the antiepileptic drug valproate on metabolism and function of inhibitory and excitatory amino acids in the brain. Neurochemical research 1993;18:485-502.
25. Madeja M, Margineanu DG, Gorji A, et al. Reduction of voltage-operated potassium currents by levetiracetam: a novel antiepileptic mechanism of action? Neuropharmacology 2003;45:661-71.
26. Margineanu DG, Klitgaard H. Inhibition of neuronal hypersynchrony *in vitro* differentiates levetiracetam from classical antiepileptic drugs. Pharmacol Res 2000;42:281-5.
27. Vajda FJ, Williams F, Davies DS. Measurement of plasma concentrations of tolbutamide by simplified gas-liquid chromatography. Med J Aust 1974;2:64-5.
28. Patsalos PN. Pharmacokinetic profile of levetiracetam: toward ideal characteristics. Pharmacol Ther 2000;85:77-85.
29. Lee J, Kotliarova S, Kotliarov Y, et al. Tumor stem cells derived from glioblastomas cultured in bFGF and EGF more closely mirror the phenotype and genotype of primary tumors than do serum-cultured cell lines. Cancer Cell 2006;9:391-403.
30. Shao Y, Gao Z, Marks PA, Jiang X. Apoptotic and autophagic cell death induced by histone deacetylase inhibitors. Proc Natl Acad Sci U S A 2004;101:18030-5.
31. Sachs MD, Ramamurthy M, Poel H, et al. Histone deacetylase inhibitors upregulate expression of the coxsackie adenovirus receptor (CAR) preferentially in bladder cancer cells. Cancer Gene Ther 2004;11:477-86.
32. Shulak L, Beljanski V, Chiang C, et al. Histone deacetylase inhibitors potentiate vesicular stomatitis virus oncolysis in prostate cancer cells by modulating NF-kappaB-dependent autophagy. J Virol 2014;88:2927-40.

Chapter 7

The HDAC-inhibitors scriptaid and LBH589 combined with the oncolytic virus Delta24-RGD exert enhanced anti-tumor efficacy in patient-derived glioblastoma cells

Lotte M.E. Berghauser Pont,[1] Anne Kleijn,[1] Jenneke J. Kloezeman,[1] Wouter van den Bossche,[1] Johanna K. Kaufmann,[2] Jeroen de Vrij,[3] Sieger Leenstra,[1,4] Clemens M.F. Dirven,[1] Martine L.M. Lamfers.[1]

Affiliations

1 Department of Neurosurgery, Brain Tumor Center, ErasmusMC
2 Harvey Cushing Neuro-Oncology Laboratories, Department of Neurosurgery, Brigham & Women's Hospital and Harvard Medical School
3 Department of Neurosurgery, Utrecht University Medical Center
4 Department of Neurosurgery, Elisabeth Hospital

Published in PLoS One. 2015 May 18;10(5):e0127058

PMID: 25993039

Abstract

A phase I/II trial for glioblastoma with the oncolytic adenovirus Delta24-RGD was recently completed. Delta24-RGD conditionally replicates in cells with a disrupted retinoblastoma-pathway and enters cells via αvβ3/5 integrins. Glioblastomas are differentially sensitive to Delta24-RGD. HDAC inhibitors (HDACi) affect integrins and share common cell death pathways with Delta24-RGD. We studied the combination treatment effects of HDACi and Delta24-RGD in patient-derived glioblastoma stem-like cells (GSC) and we determined the most effective HDACi. SAHA, Valproic Acid, Scriptaid, MS275 and LBH589 were combined with Delta24-RGD in fourteen distinct GSCs. Synergy was determined by Chou Talalay method. Viral infection and replication were assessed using luciferase and GFP encoding vectors and hexon-titration assays. Coxsackie adenovirus receptor and αvβ3 integrin levels were determined by flow cytometry. Oncolysis and mechanisms of cell death were studied by viability, caspase-3/7, LDH and LC3B/p62, phospho-p70S6K. Toxicity was studied on normal human astrocytes. *MGMT* promoter methylation status, TCGA classification, Rb-pathway and integrin gene expression levels were assessed as markers of responsiveness. Scriptaid and LBH589 acted synergistically with Delta24-RGD in approximately 50% of the GSCs. Both drugs moderately increased αvβ3 integrin levels and viral infection in responding but not in non-responding GSCs. LBH589 moderately increased late viral gene expression, however, virus titration revealed diminished viral progeny production by both HDACi, Scriptaid augmented caspase-3/7 activity, LC3B conversion, p62 and p-p70S6K consumption, as well as LDH levels. LBH589 increased LDH and p70S6K consumption. Responsiveness correlated with expression of various Rb-pathway genes and integrins. Combination treatments induced limited toxicity to human astrocytes. LBH589 and Scriptaid combined with Delta24-RGD revealed synergistic anti-tumor activity in a subset of GSCs. Both HDACi moderately augmented viral infection and late gene expression, but slightly reduced progeny production. The drugs differentially activated multiple cell death pathways. The limited toxicity on astrocytes supports further evaluation of the proposed combination therapies.

7.1 Introduction

Patients with the malignant brain tumor glioblastoma have a prognosis of 12–15 months despite maximum therapy.[1] More effective therapies than the current approach of surgery, radiation and temozolomide are urgently needed. One option is oncolytic virotherapy with Delta24-RGD, which has recently completed phase I/II clinical evaluation[2] and has shown promising results *in vitro* and *in vivo*.[3,4] Delta24-RGD is a genetically modified serotype-5 adenovirus which induces several cellular responses including necrosis, autophagy and caspase-dependent apoptosis.[5,6] Delta24-RGD conditionally replicates in tumors with a deregulated retinoblastoma (Rb) pathway, due to a 24-base pair deletion in the E1A gene. An arginine-glycine-aspartic acid (RGD) domain was inserted into the viral fiber knob domain, redirecting attachment to αvβ3 and αvβ5 integrins on the cell surface.[7] Despite these modifications glioblastomas are not equally susceptible to Delta24-RGD treatment.[8] Combination strategies that facilitate viral infection, replication and oncolysis are therefore necessary to improve this therapeutic option. Such a combination treatment may utilize histone deacetylase inhibitors (HDACi), which are novel anti-cancer drugs that act through inhibition of HDACs. This results in alterations in the transcription of oncogenes and tumor suppressor genes.[9,10] These drugs also affect non-histone targets including genes involved in cell cycle regulation, apoptosis and autophagy.[9,11] HDACi

are reported to enhance oncolytic adenoviral therapy,[12] however the effects of a panel of HDACi in patient-derived glioblastoma stem-like cells (GSC), a model that recapitulates the original tumor,[13] have not been evaluated yet. Previous studies provide a rationale to systematically investigate the efficacy of HDACi as enhancers for Delta24-RGD in glioblastoma. In this study we compared the *in vitro* effects of the five HDACi SAHA, LBH589, Scriptaid, MS-275 and Valproic Acid (VPA) on Delta24-RGD-induced oncolysis in fourteen patient-derived GSC cultures. We identify the most effective HDACi in combination treatment in this relevant model for glioblastoma. The effects on cell viability, viral infectivity, viral replication, as well as cellular autophagy, necrosis and apoptosis are studied. The differences between responding and resistant GSCs to combination treatment are charted. Specifically, the novel agent Scriptaid and the clinically applied LBH589, activate a variety of mechanisms including apoptosis, autophagy and necrosis, and induce viral gene expression over time. These effects were associated with up-regulation of αvβ3 integrins in responding cultures, however, viral progeny production was not increased. The effects of the combination treatment were studied in normal human astrocytes and toxicity was found to be very limited.

7.2 Materials and Methods

Chemicals

The HDACi tested were SAHA and MS275 (Cayman chemicals, MI, USA), VPA (Sigma-Aldrich, MO, USA), LBH589 (Biovision, CA, USA), and Scriptaid (Santa Cruz Biotechnology, CA, USA). Stocks were prepared at 100mM (VPA) in sterile water and at 50mM (SAHA), 10mM (Scriptaid), 4 mM (MS275), and 200μM (LBH589) in dimethyl sulfoxide (Sigma-Aldrich) and stored at -20°C. Staurosporin was obtained from BioMol (Hamburg, Germany).

Viruses

The construction of Delta24-RGD has been described previously.[14] The adenoviral construct has a 24-base pair deletion in the viral E1A gene, which disrupts the Rb-binding capacity of this protein and facilitates selective replication in cells with a dysfunctional Rb-pathway. The RGD peptide allows the virus to bind and enter the cell through cell surface integrins αvβ3/5.[15] The Delta24-RGD-GFP virus was constructed for the purpose of monitoring late viral gene expression over time and was used to evaluate the viral behavior by fluorescent imaging. The virus contains a GFP-expression cassette under control of the E3-promoter and was constructed, produced, purified and titrated as described previously.[16] The replication-deficient adenoviral vector Ad.luc.RGD, kindly provided by Dr. D.T. Curiel, (University of Alabama, Birmingham, Al, USA), was used for the infectivity experiments.

Patient-derived serum-free cultured glioblastoma stem-like cells

Fresh tumor material was obtained from surgical resection at the Department of Neurosurgery of the ErasmusMC (Rotterdam, The Netherlands). The tumors were classified as WHO grade IV (glioblastoma) by histopathological assessment. This entire study including the use of patient tumor material for the current study was approved by the institutional review board of the ErasmusMC. The patients' written informed consent was acquired for the use of patient material for our studies. The tumors were dissociated mechanically and enzymatically as described previously.[17] Both the primary cultures and parental tumors

were characterized and subtyped as described previously.[17] Fourteen patient-derived GSCs were used in the experiments and are summarized in Table 1. The cells were cultured as tumor neurospheres in serum-free DMEM/F12, supplemented with 1% penicillin/streptomycin, 2% B27, 20ng/ml bFGF, 20ng/ml EGF (Life Technologies, Paisley, UK), and 5µg/ml heparin (Sigma-Aldrich). For the experiments, the cell culture plates were coated with Cultrex™ (Trevigen, MD, USA) allowing attachment and monolayer formation for reproducible *in vitro* analysis. The cultures were maintained at 37°C in a humidified chamber (95% air/5% CO_2).

Table 1. Overview of the patient-derived GSC cultures tested for combination treatment

Fourteen patient-derived GSC cultures were tested for the responsiveness to the five HDACi and Delta-24-RGD. The MGMT promoter methylation status and the molecular TCGA characterizations are depicted. The enhancement factors are shown for the various treatment modalities if EF >1, and if there was a significant difference of the combination treatment compared to the monotreatments ($p<0.05$). NR indicates non-responsiveness to the proposed combination treatment. Legends: UM = unmethylated; M = methylated; CLA = classical; NEU = neural; PRO = proneural; MES = mesenchymal; ND = not determined.

GSC culture	MGMT status	Molecular subtype	Scriptaid	LBH589	SAHA	VPA	MS275
GS289	UM	CLA	2.12	1.58	NR	NR	1.27
GS245	UM	NEU	NR	NR	NR	NR	NR
GS160	UM	CLA	NR	1.26	NR	1.35	1.22
GS184	M	CLA	1.31	NR	NR	1.48	NR
GS224	M	CLA	1.78	4.4	2.71	NR	1.63
GS102	M	NEU	1.66	2.49	1.33	NR	NR
GS257	UM	CLA	2.9	NR	NR	NR	NR
GS79	UM	CLA	NR	NR	NR	NR	1.16
GS209	UM	PRO	1.23	1.37			
GS249	M	CLA	NR	NR			
GS274	M	ND	NR	NR			
GS335	M	CLA	NR	1.22			
GS359	M	MES	1.28	1.39			
GS368	UM	CLA	1.38	NR			

Viability assays

Primary GSC cultures and normal human astrocytes (Sciencell, CA, USA) were seeded at $1x10^3$ cells per well in 96-well plates. The cells were treated with the HDACi SAHA, Scriptaid, LBH589, MS275, and VPA in dose-increasing concentrations concomitantly with the Delta24-RGD infection. The tested virus doses were 5, 10, 25 and 50 infectious virus particles/ cell (multiplicity of infection; MOI) to ensure a viral dose that corresponded with the IC_{10} – IC_{50} value of the treatment, the optimal dosages for studying combination effects. Cell viability was assessed seven days post-treatment using the CellTiter-Glo cell viability assay (Promega, WI, USA). At least three MOIs of the virus were used for these assays and the IC_{50} values were determined by median equation. Next, the stringent approach to determine synergy between compounds, the Chou Talalay assay,[18] was used for the most

effective HDACi in combination with Delta24-RGD. The combination index of the two agents was calculated by using this method. The experiments were performed in triplicate and results are shown as percentage of non-treated controls ± standard deviation. In addition, primary human astrocytes were analyzed for viability as well as cell confluence after five days of combination treatment. These results are also shown as percentage of non-treated controls ± standard deviation. Microscopic images were obtained using the IncuCyte imaging system (Essen Bioscience, Ann Arbor, MI, USA) and are presented in phase-contrast at 10X magnification.

Gene expression analysis, TP53 mutation status, and MGMT promoter methylation status.

The *TP53* mutation status was available of ten GSCs, and was derived from next-generation DNA sequencing using an AB SOLiD sequencer on the fresh frozen parental tissues of the primary GSCs. In addition, molecular subtyping was done using available mRNA expression data[17] according to the transcriptionally-defined TCGA classification.[19] The *MGMT* promoter methylation status of the patient-derived GSCs was determined as described previously.[20] The mRNA of the parental glioblastoma tissue of the GSCs was isolated with the RNeasy Mini kit (#74104, Qiagen Inc., CA, USA) The expression levels were analyzed by the HumanHT-12 v4 Expression BeadChip microarray (Illumina, CA, USA), as we have described previously.[21] The normalization and batch effect removal was done as described previously by using Partek software, version 6.6 (Partek Inc., St. Louis, MO, USA). The expression data was used to subtype the tumors to the transcriptionally-defined glioblastoma classification of the TCGA.[19] We looked for patterns between responsiveness and molecular subtype. The average expression levels of specific genes of responders and non-responders to treatment were compared and the fold change was calculated including the p-value by Student's T-test. The KEGG pathways were used for identifying Rb-pathway genes.

Adenoviral infection experiments

The patient-derived GSC cultures GS102, GS224, GS289, GS79, GS245 and GS249 were seeded at $5x10^3$ cells per well in 96-well plates. After 24 hours the cells were treated with the concentrations of Scriptaid (1.5μM) and LBH589 (15nM) at which synergy with Delta-24-RGD was measured. Ad.Luc.RGD was applied to the cells at MOI25. After 24 hours the supernatant was removed and the cells were lysed using 0.9% Triton-X100. The plates were frozen and infectivity was quantified by using the Luciferase Assay System (Promega) according to manufacturer's instructions. Luminescence was measured with a Tecan Infinite® Reader (Tecan Group Ltd., Mannedorf, Switzerland). The experiments were performed in triplicate and the results are shown as mean absolute luciferase signal ± standard deviations.

Flow cytometric analysis of integrin and CAR expression

The cells of GS102, GS289, GS79 and GS245 were seeded in 6-well plates at $5x10^4$ cells per well and treated with Scriptaid (0.5 and 1.5μM) or with LBH589 (5nM, 15nM, or 45nM). The cells were harvested after 6 and 24 hours, were washed and incubated for 15 minutes with FACS buffer (PBS/0.25% bovine serum albumin (BSA)/0.05% NaN3/0.5mM Ethylene-di-amine-tetra-acetic acid (EDTA)/2% human serum) containing primary antibodies against integrin αvβ3 (mouse anti-CD51/CD61, 1:50, Abcam) and CAR (rabbit anti-CAR, H-300, 1:50, Santa Cruz). After washing with FACS buffer, the cells were incubated with

secondary antibodies Alexa-488 anti-rabbit and PE-anti mouse (Life Technologies). After staining and fixing with BD FACS lysing buffer (BD Biosciences, San Jose, California) a minimum of $3x10^4$ events were acquired on a FACS Canto II (Becton Dickinson, San Jose, California). The analysis of the flow cytometry data was done using Infinicyt software (Cytognos, Salamanca, Spain). Debris and doublets were removed using FSC-H and FSC-A after which expression was plotted for the remaining events.

Monitoring late viral gene expression by fluorescence imaging
The cells of the GSCs GS102, GS224 and GS289 were at $2.5x10^3$ cells per well in a 96-wells plate. After 24 hours the cells were treated with LBH589 or Scriptaid and the Delta24-RGD-GFP virus. Fluorescence intensity was detected by the IncuCyte imaging system for 120 hours post-infection, and was quantified by the IncuCyte software as intensity per mm^2 and by ImageJ fluorescent count per well. The experiments were performed in triplicate and are presented ± standard deviations.

Viral titration assay
The cells of GS102, GS224, GS79 and GS245 were seeded at $5x10^4$ cells per well. After 24 hours the cells were treated with Delta24-RGD in combination with Scriptaid or LBH589. After 48 and 96 hours the cells and supernatants were collected. The samples underwent three freeze-thaw cycles and were centrifuged at $1.5x10^3$ rpm for 3 minutes to remove cell debris. Supernatants were added in serial dilutions in a titration setting to A549 lung adenocarcinoma cells (ATCC, VA, USA), which were seeded at 1x103 cells per well. After 48 hours the cells were fixed with ice-cold methanol, washed in in PBS/0,05% Tween-20 (Sigma-Aldrich) and stained with primary mouse anti-hexon antibody in PBS/1% BSA from the Adeno-X™ Rapid Titer Kit (#632250, Clontech, CA, USA). After counting the hexon plaques under a microscope, the viral titers were calculated. The results are displayed as the mean viral titers of triplicates. Significant different titers were considered as such in case of $p<0.05$.

Caspase-3/7 apoptosis assay
The cells of GS102, GS224 and GS289 were seeded at $5x10^3$ cells per well in a 96-well plate and incubated with the concentrations of Scriptaid (1.5µM) and LBH589 (15nM) at which synergy was detected. Virus was added at MOI15 or MOI25 followed by the addition of 5µM of reagent of the CellPlayer 96-Well Kinetic Caspase-3/7 Apoptosis Assay (Essen Bioscience). The plates were placed in the IncuCyte imaging system at 37°C in a humidified 95% air/5% CO_2 chamber. Three images/well were taken every two hours in both phase-contrast and fluorescence for 60 hours. Caspase-3/7 activity is presented as counts per well. Experiments were performed in triplicate and means are plotted as percentages of non-treated controls ± standard deviations.

Western blot analysis
Western blot analysis was performed on protein extracts from the cells of the primary GSC culture GS102, treated with LBH589 and Scriptaid in combination with Delta24-RGD at the synergistic concentrations. The cells were seeded and treated with HDACi/Delta4-RGD. At 72 hours after treatment cells were harvested, washed with PBS and lysed with RIPA lysis buffer (Sigma-Aldrich). Protein concentrations were measured using the BCA Protein Assay Reagent Kit (Roche, Basel, Switzerland). Protein separation was performed on pre-casted 4–15% sodium dodecyl sulphate-polyacrylamide gel electrophoresis (SDS-PAGE) gels (Bio-Rad, CA, USA) and blotted onto a polyvinylidene fluoride membrane

(Immobilon-P, Millipore). Blocking was carried out with 5% non-fatty milk in Tris-Buffered Saline-Tween 20 (TBS-T) for 45 min at room temperature. Membranes were incubated overnight with primary antibodies against β-actin (1:5,000, Millipore, MA, USA), LC3BI/II, (1: 500, Cell Signaling), p62 (1:500, # ab56416, Abcam, Cambridge, UK), phospho-p70S6K (1:500, Cell Signaling) in 5% BSA/TBS-T. The membranes were washed with TBS-T and incubated with secondary antibody for 1.5 hour at room temperature (anti-rabbit-HRP, anti-mouse-HRP; 1:2000, Dako Denmark A/S, Glostrup, Denmark). Staining of β-actin was used as protein loading control. Proteins were visualized by the Pierce ECL kit (Roche), ChemiDoc MP (Bio-Rad) and ImageLab version 4.1 (Bio-Rad).

Lactate dehydrogenase assay
The cells of GS102, GS224 and GS289 were seeded at $1.5x10^3$ cells per well in a 96-well plate and incubated with two concentrations of Scriptaid and LBH589 and Delta24-RGD. The cells were incubated for five days after which the amount of LDH in the supernatant was determined using the CytoTox-One assay (Promega) according to the manufacturer's protocol. The fluorescence was measured in a Tecan Reader. The results are presented as LDH levels per viable unit as calculated from the percentage viability of non-treated controls. The experiments were performed in triplicate. The means are plotted ± standard deviations.

Statistical analysis
Patient-derived GSC cultures were classified as sensitive to therapy (responder) when the enhancement[22] was > 1, and the combination treatment was significantly better than either monotherapy ($p<0.05$). The samples that did not meet these criteria were defined as resistant to combination treatment (non-responders). The experiments were performed in triplicate and the results are presented as mean percentage of the non-treated controls ± standard deviation. Student's T-test was used to determine differences, which were considered significant if $p<0.05$. The time-based assays were analyzed by comparing single treatment to combination treatment cells by one-way ANOVA and a Tukey's Post-Test.

7.3 Results

HDAC inhibitors enhance Delta24-RGD oncolysis in a subset of GSC cultures
The combination assays with the five HDACi Scriptaid, LBH589, MS275, SAHA and VPA combined with Delta24-RGD were performed on eight *GSCs*. Delta24-RGD and drug treatment were applied simultaneously. At least two drug concentrations with two virus MOIs were tested per culture. The combinations of Scriptaid and LBH589 with Delta24-RGD were most effective. Scriptaid and LBH589 both enhanced the oncolytic activity of Delta-24-RGD in 5/8 and 4/8 (Figure 1A-B) of the tested GSCs with enhancement factors ranging from 1.2 – 2.9 for Scriptaid and 1.2 – 4.4 for LBH589, respectively (Table 1). SAHA and VPA were less effective than MS275, LBH589 and Scriptaid in enhancing viral oncolysis. In 2/8 of the patient-derived cultures SAHA/Delta24-RGD had additional effects (Figure 1C), enhancing 1.3-fold and 2.7-fold (Table 1). Furthermore, 2/8 GSCs responded to VPA/Delta-24-RGD treatment (Figure 1D) with enhancing effects of 1.4 and 1.5 (Table 1). The MS275/Delta24-RGD combination showed benefit in 5/8 GSCs (Figure 1E) with enhancing factors of 1.2 – 1.6 (Table 1). Based on the enhancement factors as well as the percentage of GSCs that were sensitized by the drug, Scriptaid and LBH589 were selected for further evaluation in combination with Delta24-RGD in six additional GSCs. Scriptaid and LBH589

showed combined additive effects with Delta24-RGD effects in 8/14 and 9/14 of the tested GSCs, respectively (Table 1, Supportive Information S1).

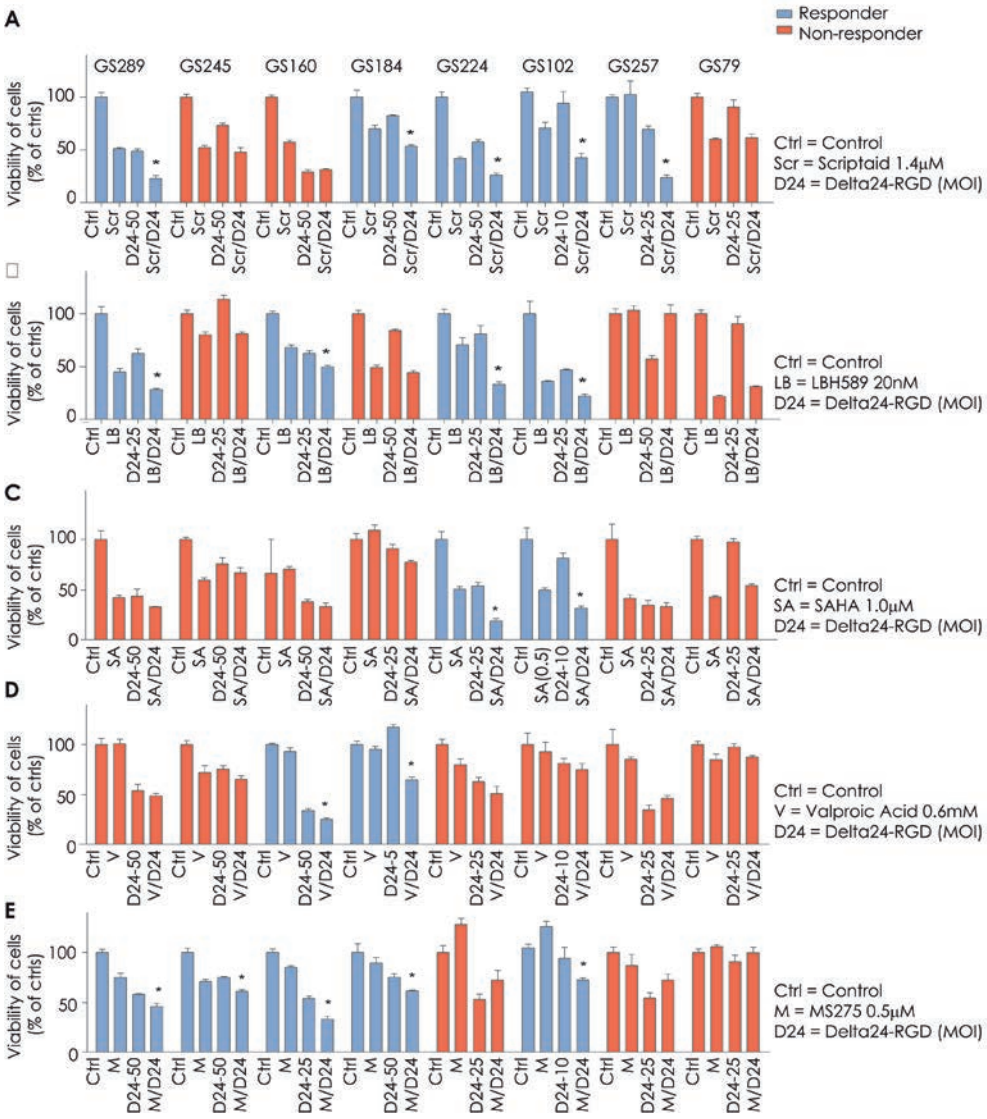

Figure 1. Delta24-RGD combined with various HDACi in patient-derived GSC cultures.

(A-E) The eight patient-derived GSC cultures that were treated according to a simultaneous treatment schedules of HDACi and Delta24-RGD at indicated concentrations and MOIs, respectively. The treatments were added concomitantly to the cells. Results are shown for one dose of drug and one dose of oncolytic virus, for Scriptaid **(A)**, LBH589 **(B)**, SAHA**(C)**, VPA **(D)** and MS275 **(E)**. Response was defined as a reduction in viability, which was significantly different from both mono-treatments ($p<0.05$), and is indicated in the graph by the blue bars (responders). If not meeting these criteria, the culture was defined as resistant (red bars). The results are displayed by the mean viability % ± standard deviations of triplicates. *Indicates significance of combination treatment compared to HDACi or Delta24-RGD alone, $p<0.05$.

Correlation of molecular characteristics with HDACi/Delta24-RGD treatment response
We evaluated whether specific molecular characteristics of the various GSCs were associated with HDACi/Delta24-RGD response (Supportive Information S2). A variety of molecular parameters were evaluated as markers for response, including the *TP53* status, the tumors' HDAC, Rb-pathway and integrin gene expression levels, *MGMT* promoter methylation (Table 1) and the molecular subtyping classification according to the TCGA (Table 1). None of the markers except for three Rb-pathway genes and integrin expression levels, showed a significant relationship with responses to combination treatments at the p>0.01 level. For LBH589/Delta24-RGD, expression of the Rb-pathway genes mitotic arrest deficient-like 2 (*MAD2L2*, FC = 1.23, p=0.001), E2F transcription factor 2 (*E2F2*, FC = 1.63, p=0.007) and *CDC16* (FC = -0.44, p=0.008) were related to response. Integrin expression levels of αv *(ITGAV)* were related to Scriptaid/Delta24-RGD response (FC = 0.48, p=0.003). However, these relationships showed small fold-changes. In conclusion, weak correlations were found between response to combination treatment and Rb-pathway gene and integrin expression levels.

LBH589 and Scriptaid synergize dose-dependently with Delta24-RGD
Combination assays using the Chou Talalay method[18] were performed on three responsive GSCs, GS102, GS224 and GS289, to evaluate synergy between the HDACi Scriptaid or LBH589 and Delta24-RGD. First the IC_{50} values of Scriptaid, LBH589 and Delta24-RGD were determined by median-equation calculation and subsequently the combination assays were performed. The results revealed that both Scriptaid and LBH589 enhanced the oncolytic effects of Delta24-RGD in a synergistic manner (Figure 2A-B) with combination indices below 1 (Figure 2C). Scriptaid significantly sensitized for Delta24-RGD in the concentration range 0.2 – 14μM. LBH589 significantly sensitized for Delta24-RGD in the concentration range 1.8 – 48nM. Thus, the HDACi Scriptaid and LBH589 both acted synergistically with Delta24-RGD in all three responsive GSCs.

LBH589 and Scriptaid increase RGD-mediated adenovirus infection in GSC cultures
To determine whether the combination effects of Delta24-RGD and HDACi were associated with enhanced viral infection, six different GSCs were infected with the replication-deficient vector Ad.luc.RGD in combination with Scriptaid and LBH589. Three of these GSCs were responsive to HDACi/Delta24-RGD treatment (GS102, GS224 and GS289) and three cultures were resistant (GS79, GS245 and GS359). The concentrations used were in the range at which synergy was detected in the Chou Talalay assays, namely 15nM for LBH589 and 1.5μM for Scriptaid. Luciferase expression was determined as a measure of infection efficiency (Figure 3A). The results show that LBH589 significantly enhanced the Ad.luc-RGD-mediated luciferase expression (p<0.05) in all three responders, GS102 (p<0.01), GS224 (p=0.03) and GS289 (p=0.04, Figure 3A). Similarly, Ad.luc.RGD combined with Scriptaid also resulted in significantly higher luciferase levels compared to Ad.luc. RGD alone in GS102 (p<0.01), GS224 (p=0.03) and GS289 (p<0.01). The two HDACi did not enhance the Ad.luc.RGD-mediated luciferase expression in the resistant glioblastoma cultures. In fact, for GS79 even a decrease of infection efficacy was observed (p<0.05). To summarize, the HDACi increased viral infection in the three responsive GSCs but not in the three resistant GSCs.

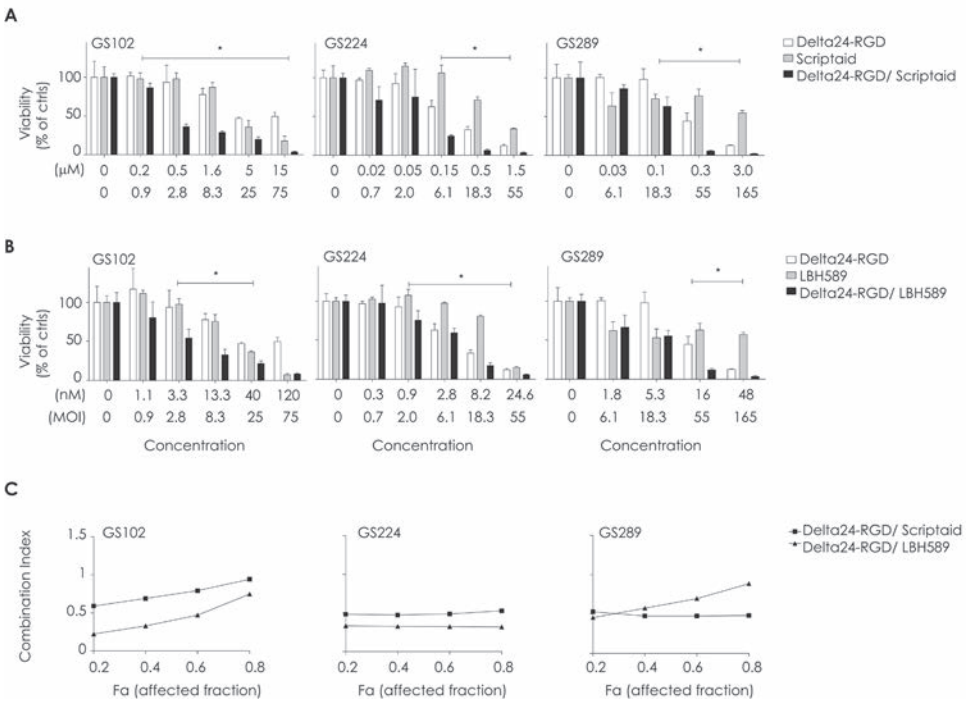

Figure 2. Scriptaid and LBH589 synergize with Delta24-RGD oncolysis in patient-derived GSC cultures.

(A) Chou Talalay assays were performed for Scriptaid (μM) and Delta24-RGD (MOI) to determine synergy in the GSCs GS102, GS224 and GS289. The treatments were added concomitantly to the cells. The results were depicted as viable fraction (0 – 100) compared to non-treated controls ± standard deviation for three replicates. *Indicates significant difference between combination and single agent treatments alone at $p<0.05$ level. **(B)** Chou Talalay assays were performed for LBH589 (nM) and Delta24-RGD (MOI)to determine synergy in the responsive GSCs GS102, GS224 and GS289. The treatments were added concomitantly to the cells. The results were depicted as viable fraction compared to non-treated controls ± standard deviation for three replicates. *Indicates significant difference between combination and single agent treatments alone at $p<0.05$ level. **(C)** The combination indices (CI) for both drugs and Delta24-RGD were calculated and shown in the same graph per GSC. A CI of < 1 indicates synergy between the two agents.

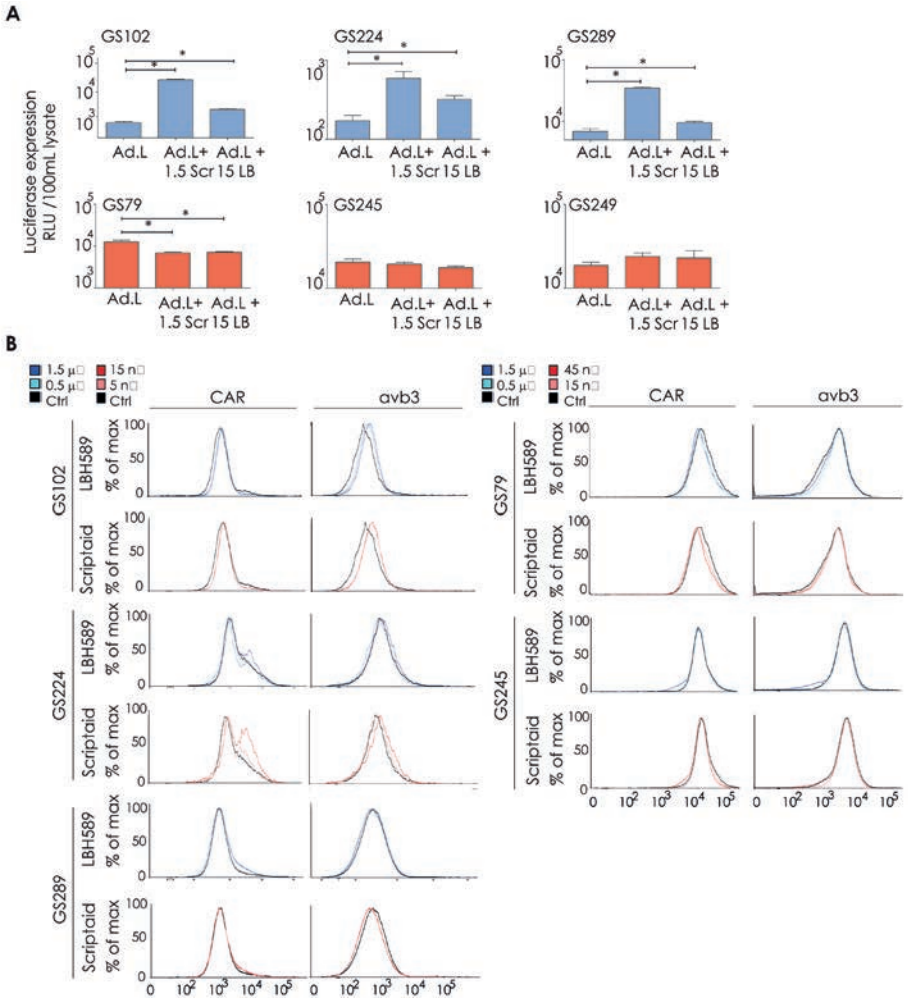

Figure 3. Increased Ad.luc.RGD infection and integrin levels by HDACi treatment in responding patient-derived GSC cultures.

(A) Responsive GSC cultures (blue, GS102, GS224 and GS289) and resistant cultures (red, GS79, GS245 and GS249) were treated with LBH589 (LBH, 15nM) or Scriptaid (Scr, 1.5µM) and concomitantly infected with the luciferase expressing vector Ad.luc.RGD. Luciferase expression was measured after 24 hours post-infection. The results are presented as relative luciferase units (RLU)/100 µL lysate. *Indicates significance of combination treatment compared to virus alone ($p<0.05$). **(B)** The cells of three responders (left, GS102, GS224 and GS289) and two non-responders (right, GS79 and GS245) were treated with LBH589 (blue) and Scriptaid (red) as indicated. After 6 hours (Supportive Information S3) and 24 hours (shown) the cells were harvested and the integrin αvβ3 (left) and CAR (right) levels were determined by flow cytometry analysis.

LBH589 and Scriptaid moderately increase αvβ3 integrin levels in responsive cultures

As a next step, we evaluated whether the increased infection efficacy in the HDACi-treated responsive cultures was related to increased levels of the Delta24-RGD binding sites.

Therefore flow cytometric analysis of surface expression of the coxsackie adenovirus receptor (CAR) and αvβ3 integrins was performed on three responsive GSCs, GS102, GS224 and GS289, as well as two resistant cultures, GS79 and GS245 (Figure 3B). The cells were treated with two concentrations of HDACi as in previous experiments. At 6 hours post-treatment, LBH589 and Scriptaid increased CAR and integrin levels in the responsive GS102. In GS289, LBH589 did not affect cell surface receptor levels and only the high concentration of Scriptaid increased CAR and integrin levels (Supportive Information S3). At 24 hours the αvβ3 levels were elevated in GS102 and GS224 by Scriptaid and in GS102 also by LBH589. CAR levels had returned to baseline levels in GS102. On the contrary, in GS289 and in the resistant GSCs, GS79 and GS245, no alterations were observed in αvβ3 or CAR levels. To summarize, HDACi primarily increased integrin levels in responders and not in non-responders. The results suggest that up-regulation of the important cell surface receptor for Delta24-RGD, namely αvβ3 integrin, plays a role in the increased cytotoxicity of Delta24-RGD/HDACi treatment.

LBH589 and Scriptaid increase late viral expression but decrease progeny production

We studied the effects of HDACi on the pattern of late viral gene expression using the GFP-encoding variant of the virus, Delta24-RGD-GFP, which has the GFP under the control of the adenoviral E3 promoter. This virus allows *in vitro* real-time monitoring of late viral gene expression as a marker for viral replication (Figure 4A-B). The results in responders GS102 and GS289, show that combination treatment with LBH589 or Scriptaid increased the GFP expression compared to Delta24-RGD-GFP alone ($p<0.05$). In GS102, Scriptaid led to a delayed onset of GFP intensity increase compared to Delta24-RGD-GFP and increased the GFP expression between 100 – 150 hours post-infection ($p<0.05$). There was no significant increase in GFP expression by the HDACi in GS224. To evaluate whether increased levels of late viral gene expression translate to increased viral progeny production, we performed viral titration experiments for the Delta24-RGD/HDACi combination treatments on two responder (GS102 and GS224) and two non-responder (GS79 and GS245) GSCs (Figure 4C). Analysis of lysates of treated cells did not reveal an increase in titers of infectious viral particles at 48 or 96 hours post-treatment, but a decrease in both responsive and non-responsive cultures ($p<0.05$).

Both HDACi enhance necrosis, whereas Scriptaid also enhances apoptosis and autophagy.

Next, we assessed whether enhanced viral oncolytic activity by HDACi could be attributed to activation of the cell death-associated mechanisms apoptosis, autophagy or necrosis, which are all known to be relevant in oncolytic viral therapy. Figure 5A shows the caspase 3/7 activity, a marker for apoptosis, for the three responsive cultures GS102, GS289 and GS224. Caspase-3/7 activity was increased by Scriptaid in two of three cultures. Delta-24-RGD induced caspase activity in all three GSCs. The caspase activity was further augmented by co-incubation with Scriptaid ($p<0.05$) in GS102. In contrast, LBH589 did not effectively alter virus-induced caspase-3/7 activity.

For detection of autophagy, Western blotting was performed to visualize the conversion of the LC3BI to the LC3BII protein as well the consumption of the p62 protein (sequestosome-1) and phospho-p70S6kinase (Figure 5B). In GS102 cells Scriptaid as well as Delta24-RGD/Scriptaid increased the LC3BII levels at 72 hours post-treatment. This increase in conversion was less evident for the single and combination treatment with LBH589. In

support of the effects of Scriptaid on autophagy induction, both p62 and phospho-p70S6K levels were decreased by Scriptaid in both mono and combination therapies (Figure 5B), whereas p62 was consumed more in the combination modality. The cell death marker LDH was studied to evaluate whether necrotic response occurred after combination treatment. Five days post-treatment, the LDH levels were elevated in all three responsive GSCs, after combination treatment with Scriptaid/Delta24-RGD (Figure 5C). This also occurred after combination treatment of LBH589/Delta24-RGD in GS224 and GS289. The degree of LDH increase varied between the different GSC cultures. In conclusion, the combination effects of HDACi/Delta24-RGD appear based, at least partly, on the induction of caspase-3/7-mediated apoptosis, and of autophagic and necrotic cell death.

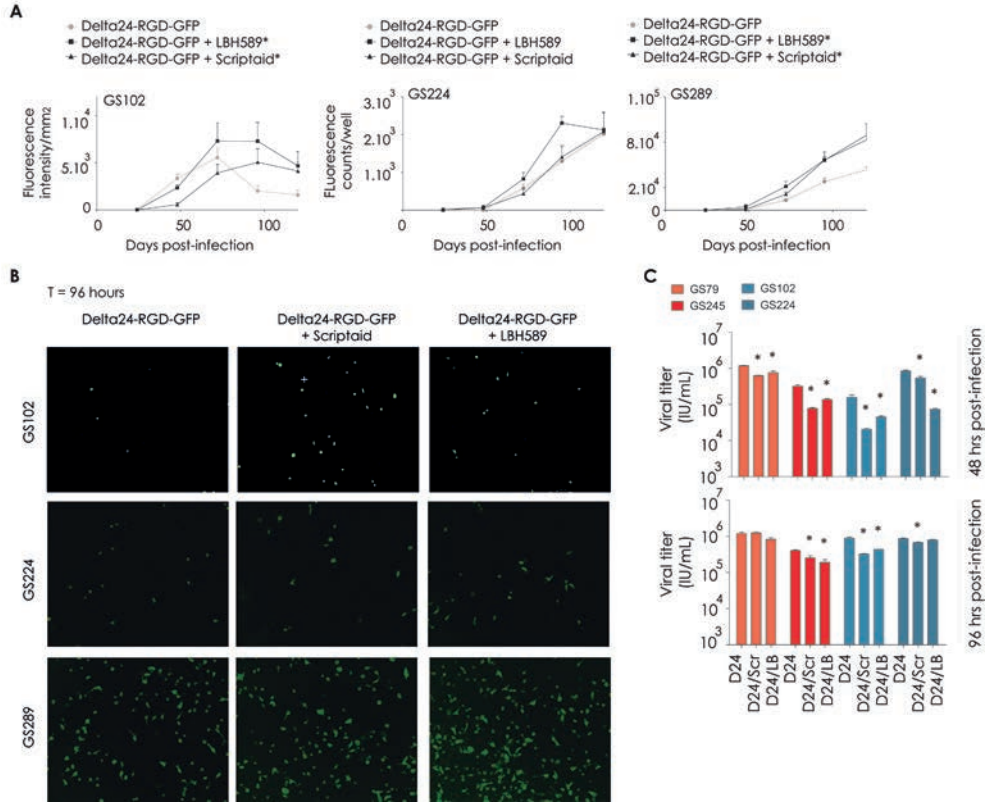

Figure 4. The effects of HDACi on viral transgene expression, replication and production.

(A) GS102, GS224 and GS289 cells were concomitantly treated with LBH589 or Scriptaid and Delta24-RGD-GFP virus. In a time-lapse, fluorescence intensity per mm^2 and counts per well were measured and analyzed using the IncuCyte system and Image J, respectively. The results were plotted graphically as means ± standard deviation. *Indicates significance of the combination treatments compared to Delta24-RGD alone ($p<0.05$). **(B)** Representative fluorescence images acquired by the IncuCyte system at 96 hours are shown of GS102, GS224 and GS289 (magnification 10X) . **(C)** Cells of the responsive GSCs GS102 and GS224 (blue), and cells of the non-responsive GSC cultures GS79 and GS245 (red) were concomitantly treated with Delta24-RGD and LBH589 or Scriptaid. The viral titers in the cell extracts that were obtained at 48h and 96h post-treatment are shown. *Indicates significant difference in the viral titers of Delta24-RGD alone compared to the combination treatments with HDACi and Delta24-RGD ($p<0.05$).

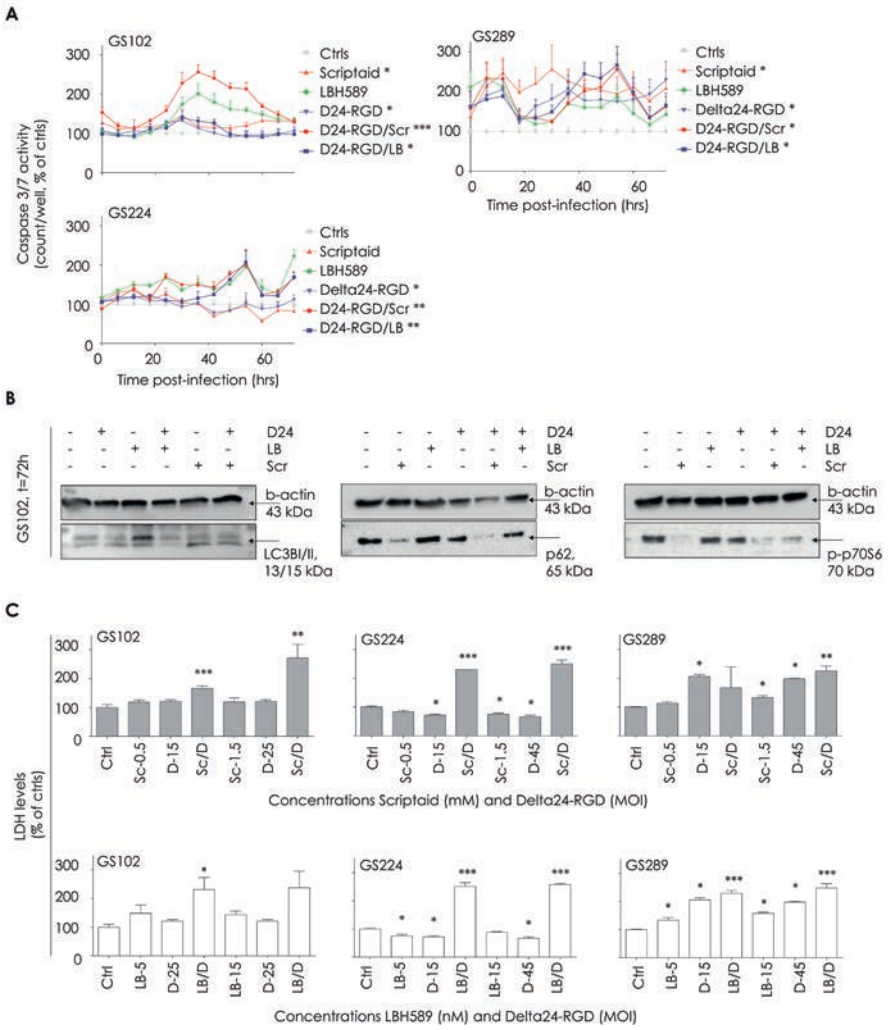

Figure 5. Affected cell death mechanisms in HDACi/Delta24-RGD treatment.

(A) The cells of GS102, GS224 and GS289 cells were concomitantly treated with HDACi and Delta24-RGD. Caspase-3/7 activity was measured using caspase-3/7 apoptosis assay and the IncuCyte system and counts/well are shown *Indicates significance at $p<0.05$ for single treatments compared to non-treated controls ± standard deviation; and **/*** Indicates significance at $p<0.05$ for the combination treatments compared to controls (**) and the two single agent treatments (***). **(B)** The cells of GS102 were concomitantly treated with HDACi and Delta24-RGD. After 72 hours, the cells were harvested and LC3BI/II, p62 and phospho-p70SK levels were determined by Western blot analysis. Beta-actin was detected as a loading control. **(C)** The cells of GS102, GS224 and GS289 cells were concomitantly treated with Scriptaid (upper panel, grey) or LBH589 (lower panel, white) and Delta24-RGD. The LDH levels were determined using the CytoTox-One Assay reagent at five days post-treatment. Fluorescence was measured with the Tecan reader. The LDH levels are presented as percentage of non-treated controls ± standard deviation, corrected for viability. * Indicates significance at $p<0.05$ for the combination treatments compared to controls (**) and the two single agent treatments.(***)

Primary human astrocytes are insensitive to HDACi and Delta24-RGD

In addition to the viability experiments on GSCs, we tested the drugs in combination with Delta24-RGD on normal human astrocytes to gain insight into toxicity of these regimens. The normal human astrocytes were treated with various concentrations of drugs, virus and the combination of both. Phase contrast images obtained at 120 hours and did not reveal any morphological changes as depicted in Figure 6A. Moreover, cell growth confluence data derived from this time course experiment detected no significant effects of any of the tested treatment combinations (Supportive Information S4). Viability assessment by CellTiter-Glo assay showed very limited toxicity, with less than 20% reduction in cell viability (Figure 6B). No additive effects of the combination treatments were detected for any of the tested concentrations.

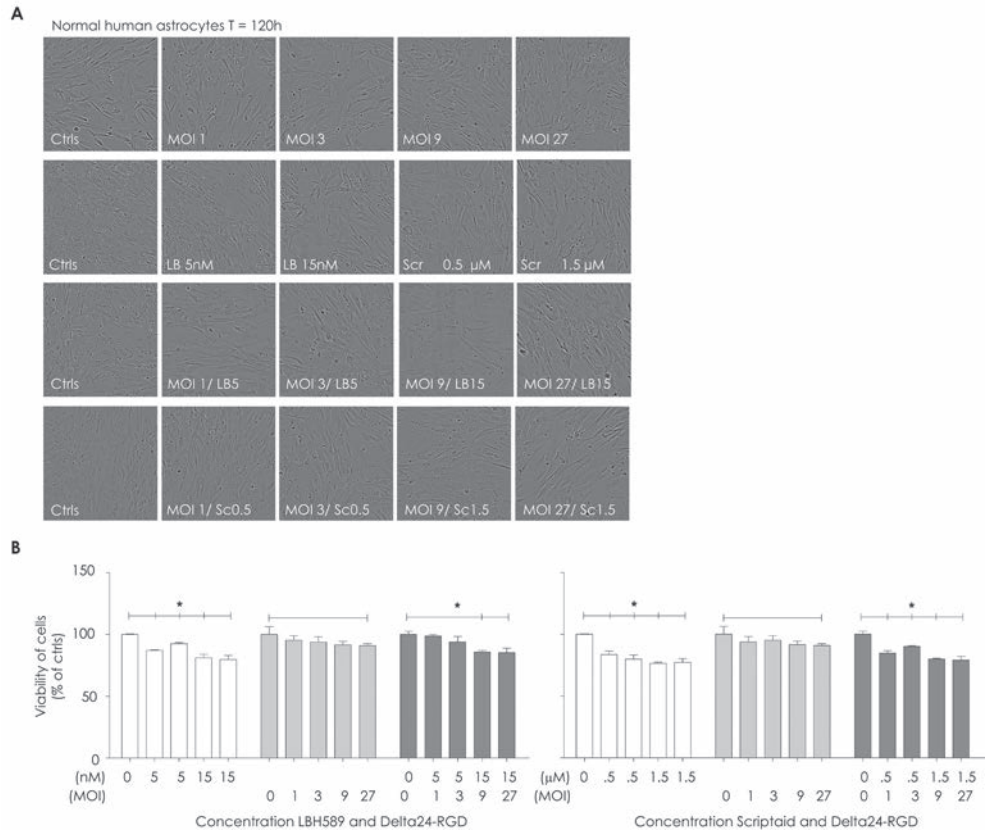

Figure 6. The effects of HDACi/Delta24-RGD on normal human astrocytes.

(A) Normal human astrocytes were concomitantly treated with a dose range of HDACi and Delta24-RGD and monitored for morphological changes using the IncuCyte imaging system. Representative images at day five are depicted (10X magnification) for the tested conditions. **(B)** Viability of the cells was measured at day five post-treatment using the CellTiter-Glo assay, and the results are shown as percentage of non-treated control cells ± standard deviation. *Indicates significance at $p<0.05$ of the treated cells compared to the non-treated control cells.

7.4 Discussion

In the current study we show that HDACi, in particular the novel pan-HDACi Scriptaid and LBH589 are effective sensitizers for the oncolytic virus Delta24-RGD in a subset of patient-derived GSC cultures. The limited toxicity to normal human astrocytes makes these drugs interesting candidates for further investigation for combination treatment with Delta24-RGD. These two HDACi have not been reported in combination with oncolytic virus therapy thus far. Notably, our data obtained on patient-derived GSCs, indicate that response to HDACi and Delta24-RGD combination treatment varies between the types of HDACi and between the different GSCs, with distinct responders and non-responders. Although we aimed at correlating the treatment efficacy to tumor subtype or profile by various methods, no clear relationships were observed between specific molecular markers and Scriptaid/Delta24-RGD or LBH589/Delta24-RGD responsiveness. An exception is the potential relationship between expression levels of Rb-pathway genes and LBH589/Delta24-RGD response, and αv integrin expression and Scriptaid/Delta24-RGD response. Larger patient-derived culture panels are required to substantiate this. Reports by others indicate that HDACi interact differentially with the activity of various oncolytic viruses: VPA was found to be an effective sensitizer of oncolytic herpes virus,[23] adenovirus[24,25] and vaccinia virus.[26] In contrast, VPA acted antagonistically with an oncolytic adenovirus.[27] In our previous study testing anti-epileptic drugs in combination with Delta24-RGD, the effects of VPA were very moderate and enhanced Delta24-RGD oncolysis only in a small subset of tumors.[8] Together, these reports underscore the variability in response with dependencies on tumor cell (sub)type, HDACi, and oncolytic virus strain.

In the present study, the two most effective HDACi, Scriptaid and LBH589, were further investigated in an additional panel of six GSCs. Over 50% of the total of fourteen distinct GSCs responded to Scriptaid-induced viral sensitization and 50% responded to LBH589-induced viral sensitization. Efficacy was related to HDACi-induced up-regulation of αvβ3 integrin expression and consequential increased infection efficiency of Delta24-RGD. Both HDACi asserted this effect in responding, but not in non-responding GSCs. Our data suggest that combined efficacy of HDACi and Delta24-RGD is at least partially determined by improved viral attachment and infection. The finding that responders have higher baseline gene expression levels of integrins than the non-responders may suggest that if gene expression is relatively high, these cells are able to further increase integrin production, whereas in non-responders, where gene production is already low or disturbed, this cannot be increased by the HDACi. VPA has previously been reported to alter integrin expression on the tumor cell surface.[28] Likewise, the HDACi TSA and sodium butyrate enhanced CAR levels and oncolytic adenoviral efficacy.[29,30] In our study, CAR was not consistently up-regulated in the patient-derived GSCs, which further supports that HDACi effects are cell type and time-dependent. The αvβ3 integrin expression can be partially regulated by the transcription factor Sp1,[31] which was previously reported to be induced by HDACi.[32]

The fact that the increased viral infection and late viral gene expression in our study, did not translate to increased viral yield, suggests that combination therapy supports early cell killing instead of viral replication. We hypothesize that the activation of cell death mechanisms by the HDACi interferes with the final stage of the viral lytic cycle, and hampers the assembly of new viral particles, a process that requires active cellular machineries. Indeed, we found that there were relatively more dead cells at 48 and 96 hours, as apoptosis, autophagy and necrosis markers were elevated compared to the

monotherapies. Apoptosis,[5] autophagy[6] and necrosis-like cell death[5] are important mechanisms in Delta24-RGD adenoviral oncolysis.[6,33] Autophagy and necrosis play a major role in the immunogenic cell death.[34] With regard to the effects of HDACi, not only cell death is important but also the reported induction of the cell cycle arrest proteins p21 and p27,[35] which induce cell cycle inhibition and dormancy in cellular replication machineries. These effects of HDACi can explain the limited effects, despite the increased infection, on nett viral replication and production.

We found that multiple mechanisms occur simultaneously in combination therapy. First of all, early (0 – 60 hours) apoptosis plays a role specifically in Scriptaid combination treatment. Secondly, autophagy plays a role for both HDACi (72 hours) as was observed by p62 consumption and LC3B conversion, as well as by phospho-p70S6K inhibition. Third, the LDH induction by degraded cells cannot be explained only by apoptosis and autophagy, which suggest that other cell death mechanisms are active, including necrosis. The observed effects of the HDACi, whether that is Scriptaid enhancing apoptosis, autophagy and necrosis, or LBH589 supporting autophagy and necrosis, can offer an advantage in boosting therapeutic efficacy by multiple mechanisms simultaneously. Moreover, enhancement of immunogenic cell death may offer the additional value of boosting the virus-induced anti-tumor immune response, known to play a key role in oncolytic viral therapy *in vivo*.[36-38] HDACi have been reported to induce antigen presentation and MHC-I induction, which could potentially contribute to T-cell activation and *in vivo* efficacy of the combination treatment.[39] Therefore, further studies into these aspects of HDACi/Delta24-RGD treatment are warranted.

7.5 Conclusion

The novel pan-HDACi Scriptaid and LBH589 in combination with Delta24-RGD exert enhanced anti-tumor activity in patient-derived GSCs. The HDACi induced slight up-regulation of cell surface integrins, facilitating adenoviral entry and leading to increased levels of viral gene expression. Moreover, the HDACi (differentially) induced cell death pathways in the GSCs, thereby accelerating the virus-induced killing of the infected cells but slightly hampering the production of progeny virus. The concerted action of these two treatment modalities leads to improved anti-tumor efficacy in patient-derived GSCs and shows very limited toxicity in normal human astrocytes. Taken together, Scriptaid and LBH589 offer opportunities potential candidates for future Delta24-RGD combination studies.

References

1. Stupp R, Hegi ME, Mason WP, et al. Effects of radiotherapy with concomitant and adjuvant temozolomide versus radiotherapy alone on survival in glioblastoma in a randomised phase III study: 5-year analysis of the EORTC-NCIC trial. Lancet Oncol 2009;10:459-66.
2. Lang FF, Conrad C, Gomez-Manzano C, et al. First-in-human phase I clinical trial of oncolytic delta-24-rgd (dnx-2401) with biological endpoints: implications for viro-immunotherapy. Neuro Oncol 2014;16 Suppl 3:iii39.
3. Lamfers ML, Grill J, Dirven CM, et al. Potential of the conditionally replicative adenovirus Ad5-Delta24RGD in the treatment of malignant gliomas and its enhanced effect with radiotherapy. Cancer Res 2002;62:5736-42.

4. Singh N. Apoptosis in health and disease and modulation of apoptosis for therapy: An overview. Indian journal of clinical biochemistry : IJCB 2007;22:6-16.
5. Abou El Hassan MA, van der Meulen-Muileman I, Abbas S, Kruyt FA. Conditionally replicating adenoviruses kill tumor cells via a basic apoptotic machinery-independent mechanism that resembles necrosis-like programmed cell death. J Virol 2004;78:12243-51.
6. Jiang H, Gomez-Manzano C, Aoki H, et al. Examination of the therapeutic potential of Delta-24-RGD in brain tumor stem cells: role of autophagic cell death. J Natl Cancer Inst 2007;99:1410-4.
7. Cripe TP, Dunphy EJ, Holub AD, et al. Fiber knob modifications overcome low, heterogeneous expression of the coxsackievirus-adenovirus receptor that limits adenovirus gene transfer and oncolysis for human rhabdomyosarcoma cells. Cancer Res 2001;61:2953-60.
8. de Jonge J, Berghauser Pont LM, Idema S, et al. Therapeutic concentrations of anti-epileptic drugs do not inhibit the activity of the oncolytic adenovirus Delta24-RGD in malignant glioma. J Gene Med 2013;15:134-41.
9. Grant S, Dai Y. Histone deacetylase inhibitors and rational combination therapies. Advances in cancer research 2012;116:199-237.
10. Monneret C. Histone deacetylase inhibitors for epigenetic therapy of cancer. Anticancer Drugs 2007;18:363-70.
11. Gammoh N, Lam D, Puente C, Ganley I, Marks PA, Jiang X. Role of autophagy in histone deacetylase inhibitor-induced apoptotic and nonapoptotic cell death. Proc Natl Acad Sci U S A 2012;109:6561-5.
12. Kim DR, Park MY, Lim HJ, et al. Combination therapy of conditionally replicating adenovirus and histone deacetylase inhibitors. Int J Mol Med 2012;29:218-24.
13. Lee J, Kotliarova S, Kotliarov Y, et al. Tumor stem cells derived from glioblastomas cultured in bFGF and EGF more closely mirror the phenotype and genotype of primary tumors than do serum-cultured cell lines. Cancer Cell 2006;9:391-403.
14. Suzuki K, Fueyo J, Krasnykh V, Reynolds PN, Curiel DT, Alemany R. A conditionally replicative adenovirus with enhanced infectivity shows improved oncolytic potency. Clin Cancer Res 2001;7:120-6.
15. Pasqualini R, Koivunen E, Ruoslahti E. Alpha v integrins as receptors for tumor targeting by circulating ligands. Nature biotechnology 1997;15:542-6.
16. Balvers RK, Belcaid Z, van den Hengel SK, et al. Locally-delivered T-cell-derived cellular vehicles efficiently track and deliver adenovirus delta24-RGD to infiltrating glioma. Viruses 2014;6:3080-96.
17. Balvers RK, Kleijn A, Kloezeman JJ, et al. Serum-free culture success of glial tumors is related to specific molecular profiles and expression of extracellular matrix-associated gene modules. Neuro Oncol 2013;15:1684-95.
18. Chou TC, Talalay P. Quantitative analysis of dose-effect relationships: the combined effects of multiple drugs or enzyme inhibitors. Advances in enzyme regulation 1984;22:27-55.
19. Verhaak RG, Hoadley KA, Purdom E, et al. Integrated genomic analysis identifies clinically relevant subtypes of glioblastoma characterized by abnormalities in PDGFRA, IDH1, EGFR, and NF1. Cancer Cell 2010;17:98-110.
20. Berghauser Pont LM, Naipal K, Kloezeman JJ, et al. DNA damage response and anti-apoptotic proteins predict radiosensitization efficacy of HDAC inhibitors SAHA and LBH589 in patient-derived glioblastoma cells. Cancer Lett 2014.

21. Berghauser Pont LM, Spoor JK, Venkatesan S, et al. The Bcl-2 inhibitor Obatoclax overcomes resistance to histone deacetylase inhibitors SAHA and LBH589 as radiosensitizers in patient-derived glioblastoma stem-like cells. Genes Cancer 2014;5:445-59.
22. Chou TC. Drug combination studies and their synergy quantification using the Chou-Talalay method. Cancer Res 2010;70:440-6.
23. Otsuki A, Patel A, Kasai K, et al. Histone deacetylase inhibitors augment antitumor efficacy of herpes-based oncolytic viruses. Mol Ther 2008;16:1546-55.
24. Sasaki Y, Negishi H, Idogawa M, et al. Histone deacetylase inhibitor FK228 enhances adenovirus-mediated p53 family gene therapy in cancer models. Mol Cancer Ther 2008;7:779-87.
25. Goldsmith ME, Aguila A, Steadman K, et al. The histone deacetylase inhibitor FK228 given prior to adenovirus infection can boost infection in melanoma xenograft model systems. Mol Cancer Ther 2007;6:496-505.
26. MacTavish H, Diallo JS, Huang B, et al. Enhancement of vaccinia virus based oncolysis with histone deacetylase inhibitors. PLoS One 2010;5:e14462.
27. Hoti N, Chowdhury W, Hsieh JT, Sachs MD, Lupold SE, Rodriguez R. Valproic acid, a histone deacetylase inhibitor, is an antagonist for oncolytic adenoviral gene therapy. Mol Ther 2006;14:768-78.
28. Wedel S, Hudak L, Seibel JM, et al. Molecular targeting of prostate cancer cells by a triple drug combination down-regulates integrin driven adhesion processes, delays cell cycle progression and interferes with the cdk-cyclin axis. BMC Cancer 2011;11:375.
29. Ma J, Zhao J, Lu J, et al. Coxsackievirus and adenovirus receptor promotes antitumor activity of oncolytic adenovirus H101 in esophageal cancer. Int J Mol Med 2012;30:1403-9.
30. Sachs MD, Ramamurthy M, Poel H, et al. Histone deacetylase inhibitors upregulate expression of the coxsackie adenovirus receptor (CAR) preferentially in bladder cancer cells. Cancer Gene Ther 2004;11:477-86.
31. Wu W, Dong YW, Shi PC, et al. Regulation of integrin alphaV subunit expression by sulfatide in hepatocellular carcinoma cells. J Lipid Res 2013;54:936-52.
32. Simboeck E, Sawicka A, Zupkovitz G, et al. A phosphorylation switch regulates the transcriptional activation of cell cycle regulator p21 by histone deacetylase inhibitors. J Biol Chem 2010;285:41062-73.
33. Alonso MM, Jiang H, Yokoyama T, et al. Delta-24-RGD in combination with RAD001 induces enhanced anti-glioma effect via autophagic cell death. Mol Ther 2008;16:487-93.
34. Kepp O, Tesniere A, Schlemmer F, et al. Immunogenic cell death modalities and their impact on cancer treatment. Apoptosis 2009;14:364-75.
35. Newbold A, Salmon JM, Martin BP, Stanley K, Johnstone RW. The role of p21(waf1/cip1) and p27(Kip1) in HDACi-mediated tumor cell death and cell cycle arrest in the Emu-myc model of B-cell lymphoma. Oncogene 2014;33:5415-23.
36. Kleijn A, Kloezeman J, Treffers-Westerlaken E, et al. The In Vivo Therapeutic Efficacy of the Oncolytic Adenovirus Delta24-RGD Is Mediated by Tumor-Specific Immunity. PLoS One 2014;9:e97495.
37. Jiang H, Clise-Dwyer K, Ruisaard KE, et al. Delta-24-RGD oncolytic adenovirus elicits anti-glioma immunity in an immunocompetent mouse model. PLoS One 2014;9:e97407.
38. Tong AW, Senzer N, Cerullo V, Templeton NS, Hemminki A, Nemunaitis J. Oncolytic viruses for induction of anti-tumor immunity. Current pharmaceutical biotechnology 2012;13:1750-60.

39. Woan KV, Sahakian E, Sotomayor EM, Seto E, Villagra A. Modulation of antigen-presenting cells by HDAC inhibitors: implications in autoimmunity and cancer. Immunol Cell Biol 2012;90:55-65.

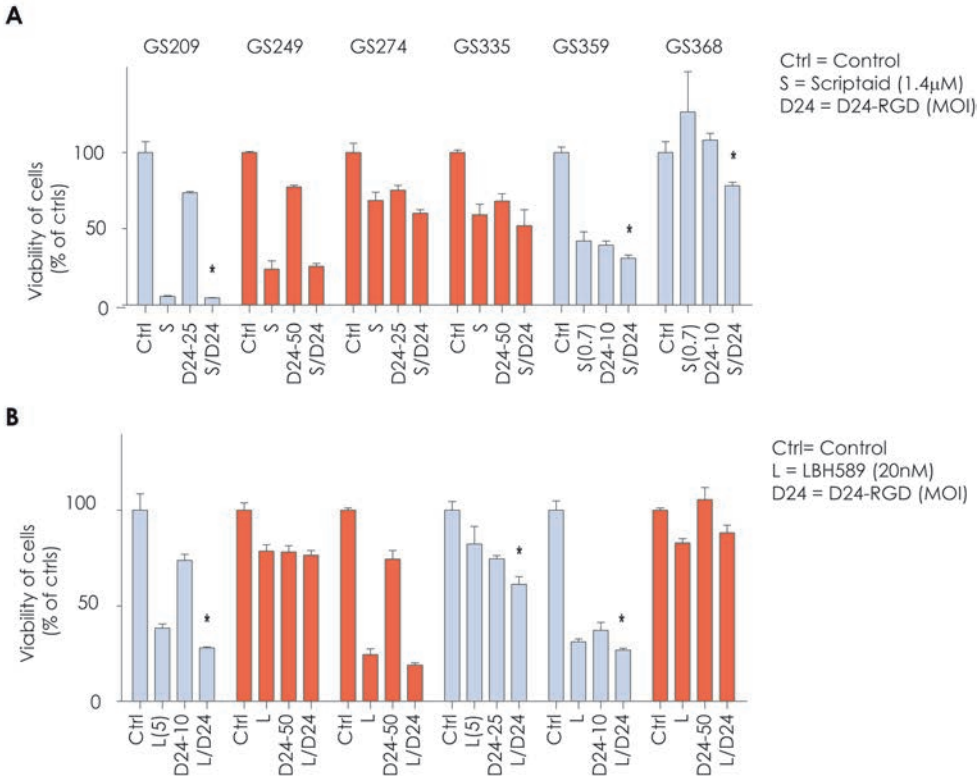

Supportive Information S1.

Six additional GSC cultures were tested for combination effects of HDACi and Delta24-RGD. Results are shown for one dose of the drugs Scriptaid and LBH589 and one dose of the oncolytic virus, as indicated. Response was defined as an enhancement factor >1 (Table 1), which was significantly different from both single agents ($p<0.05$). The red bars indicate resistant GSCs to combined treatment whereas the blue bars indicate sensitive GSCs to combined treatment. The results are displayed by the mean viability percentage compared to non-treated controls with the standard deviations. *Indicates significance of combination treatment compared to drug or Delta24-RGD alone, $p<0.05$.

Supportive Information S2.

The correlation data of responses to HDACi/Delta24-RGD and molecular characteristics of the patient-derived GSC cultures, including TP53 mutation status, HDAC gene expression, Rb-pathway gene expression, and integrin gene expression levels.

Scriptaid/Delta24-RGD		
Probe Illumina	**FC NR - R**	**p value**
HDAC9	-0,81	0,031
HDAC9	-1,45	0,064
HDAC5	0,60	0,073
HDAC9	-0,67	0,107
HDAC8	-0,47	0,202
HDAC7A	0,38	0,207
HDAC10	0,48	0,298
HDAC3	-0,14	0,298
HDAC1	-0,20	0,341
HDAC9	-0,24	0,444
HDAC2	-0,12	0,504
HDAC7A	-0,20	0,563
HDAC9	-0,16	0,691
HDAC2	0,19	0,736
HDAC4	-0,05	0,772
HDAC6	-0,09	0,785
HDAC11	0,14	0,827
HDAC5	0,10	0,861
HDAC7	-0,02	0,956
HDAC7	-0,02	0,958

LBH589/Delta24-RGD		
Probe Illumina	**FC NR - R**	**p-value**
HDAC6	-0,142	0,672
HDAC9	0,155	0,699
HDAC7A	-0,111	0,718
HDAC1	0,072	0,741
HDAC7A	-0,115	0,746
HDAC4	-0,053	0,763
HDAC8	0,023	0,951
HDAC11	0,000	0,999

Scriptaid/Delta24-RGD		
Gene	**FC R - NR**	**p value**
ABL1	1,065	0,016
CDK6	0,953	0,019
ANAPC11	0,381	0,031
CDC16	-0,074	0,031
GADD45A	0,640	0,033
PTTG1	0,718	0,041
PRKDC	0,115	0,044
PTTG2	-0,667	0,045
CCNA2	0,827	0,048

LBH589/Delta24-RGD		
Probe Illumina	**FC NR - R**	**p-value**
HDAC3	-0,247	0,049
HDAC9	-0,505	0,213
HDAC9	-0,466	0,280
HDAC9	-0,847	0,304
HDAC2	-0,175	0,332
HDAC2	-0,453	0,405
HDAC9	-0,244	0,439
HDAC7	0,178	0,539
HDAC5	0,219	0,543
HDAC7	0,232	0,554
HDAC5	0,268	0,651
HDAC10	-0,203	0,669

LBH589/Delta24-RGD		
Gene	**FC R - NR**	**p value**
MAD2L2	1,229	0,001
E2F2	1,626	0,007
CDC16	-0,437	0,008
CDC16	-0,177	0,011
CDKN2C	2,912	0,012
MCM7	0,350	0,012
CCNE1	0,852	0,019
CDC16	-0,227	0,021
CCNE1	1,019	0,024
CDKN2C	1,796	0,026
CDC25B	0,585	0,028
ZBTB17	0,354	0,031

LBH589/Delta24-RGD		
Gene	**FC R - NR**	**p value**
CDK6	1,274	0,033
MCM7	2,269	0,033
CCNB1	1,074	0,033
CDC25C	2,320	0,034
MCM5	1,166	0,034
TTK	1,877	0,034
PTTG1	1,100	0,039
CDKN2B	2,146	0,040
ATM	-1,292	0,044
RBL1	-0,264	0,045

Scriptaid /Delta24-RGD		
Gene	**FC (R - NR)**	**p value**
ITGAV-Scriptaid	0,483	0,003
ITGB3- Scriptaid	2,053	0,019

LBH589 /Delta24-RGD		
Gene	**FC (R - NR)**	**p value**
ITGAV-LBH589	0,363	0,034

GSC culture	TP53 Status	Scriptaid / Delta24RGD
GS160	ND	NR
GS257	ND	R
GS368	ND	R
GS79	ND	NR
GS102	TP53Δ	R
GS184	TP53Δ	R
GS209	TP53Δ	R
GS249	TP53Δ	NR
GS224	WT	R
GS245	WT	NR
GS274	WT	R
GS289	WT	R
GS335	WT	NR
GS359	WT	NR

GSC culture	TP53 Status	LBH589 / Delta24RGD
GS160	ND	R
GS257	ND	NR
GS368	ND	NR
GS79	ND	NR
GS102	TP53Δ	R
GS184	TP53Δ	NR
GS209	TP53Δ	R
GS249	TP53Δ	NR
GS224	WT	R
GS245	WT	NR
GS274	WT	R
GS289	WT	R
GS335	WT	R
GS359	WT	NR

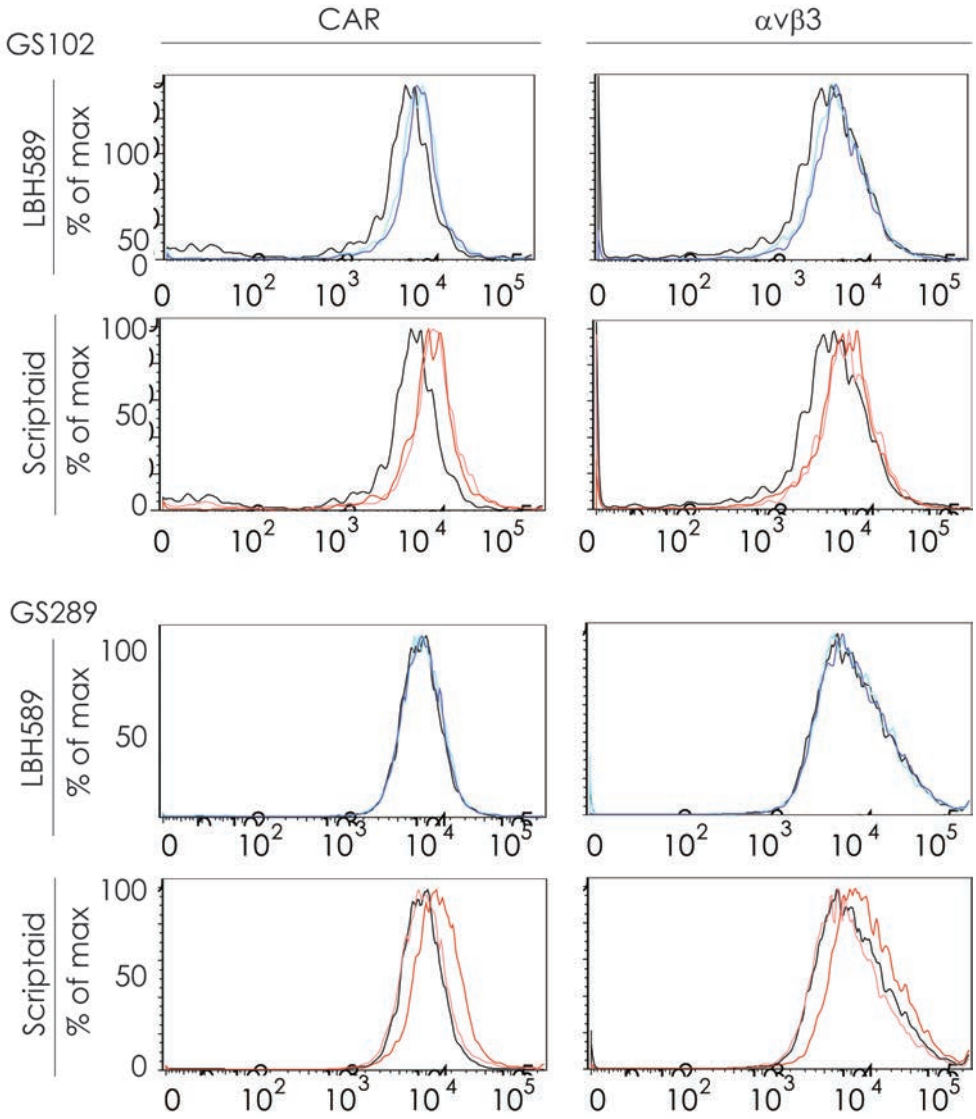

Supportive Information S3.

The cells of the two responsive GSCs GS102 and GS289, were treated with LBH589 and Scriptaid as indicated. After 6 hours of treatment, the cells were harvested and the integrin αvβ3 (left) and CAR (right) levels were determined by flow cytometry analysis.

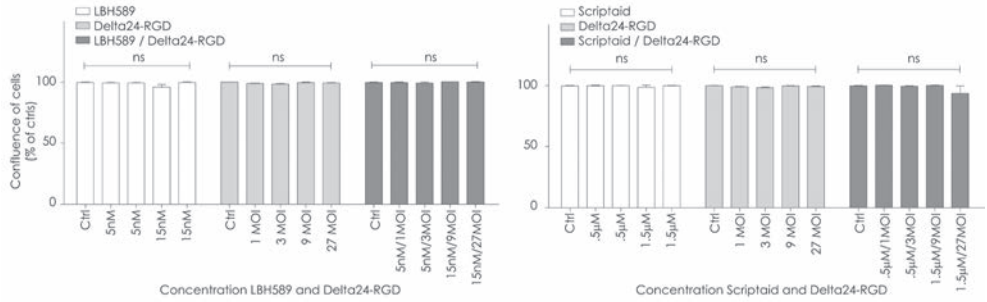

Supportive Information S4.

Confluence of the cells was measured at day five post-treatment by the IncuCyte imaging system and software, and is presented as percentage of non-treated control cells ± standard deviation. *Indicates significance at $p<0.05$ of the treated cells compared to the non-treated control cells.

Chapter 8

In vitro screening of clinical drugs identifies sensitizers of oncolytic viral therapy in glioblastoma stem-like cells

Lotte M.E. Berghauser Pont,[1] Rutger K. Balvers,[1] Jenneke J. Kloezeman,[1]
Michal O. Nowicki,[2] Wouter van den Bossche,[1,3] Andreas Kremer,[4] Hiroaki Wakimoto,[5]
Bernadette G. van den Hoogen,[6] Sieger Leenstra,[1,7] Clemens M.F. Dirven,[1]
E. Antonio Chiocca,[2] Sean E. Lawler,[2] Martine L.M. Lamfers.[1]

Affiliations

1 Department of Neurosurgery, Brain Tumor Center ErasmusMC, Rotterdam
2 Harvey Cushing Neuro-oncology Laboratories, Brigham and Women's Hospital, Harvard Medical School, Boston
3 Department of Immunology, ErasmusMC, Rotterdam
4 Department of Bioinformatics, ErasmusMC, Rotterdam
5 Department of Neurosurgery, Massachussets General Hospital, Harvard Medical School, Boston
6 Department of Viroscience, ErasmusMC, Rotterdam
7 Department of Neurosurgery, Elisabeth Hospital, Tilburg

Published in Gene Therapy. 2015

Abstract

Oncolytic viruses (OV) have broad potential as an adjuvant for the treatment of solid tumors. The present study addresses the feasibility of clinically applicable drugs to enhance the oncolytic potential of the OV Delta24-RGD in glioblastoma. In total, 446 drugs were screened for their viral sensitizing properties in glioblastoma stem-like cells (GSCs) *in vitro*. Validation was done for ten drugs to determine synergy based on the Chou Talalay assay. Mechanistic studies were undertaken to assess viability, replication efficacy, viral infection enhancement and cell death pathway induction in a selected panel of drugs. Four viral sensitizers (fluphenazine, indirubin, lofepramine and ranolazine) were demonstrated to reproducibly synergize with Delta24-RGD in multiple assays. After validation we underscored general applicability by testing candidate drugs in a broader context of a panel of different GSCs, various solid tumor models and multiple OVs.

Overall this study identified four viral sensitizers which synergize with Delta24-RGD and two other strains of oncolytic viruses. The viral sensitizers interact with infection, replication and cell death pathways to enhance efficacy of the OV.

8.1 Introduction

Patients newly diagnosed with glioblastoma have a median survival of 14.7 months despite surgery and radiation combined with adjuvant chemotherapy using temozolomide.[1,2] Hence, studies into more effective alternatives are warranted. An approach which is currently under phase-I/II clinical investigation is the use of the oncolytic adenovirus Delta24-RGD.[3] Treatment with Delta24-RGD has shown promising results in preclinical models4 and has demonstrated therapeutic responses in a subset of patients.[3] This is similar to results of other oncolytic virus (OV) trials.[5] Delta24-RGD was engineered to specifically target and replicate in cancer cells deficient in the Rb pathway by means of a 24-base pair deletion in the viral E1A gene. Insertion of the RGD-peptide into the fiber-knob enhances viral entry by attachment to $\alpha v\beta 3/\alpha v\beta 5$ integrins.[6] Delta24-RGD is therefore not dependent on entry via the coxsackie adenovirus receptor (CAR), which is usually sparsely expressed in glioblastoma.[7]

In OV therapy heterogeneous responses have been shown both in preclinical models as well as in patients.[3,8,9] Therefore such treatment strategies require enhancement of OV efficacy in order to be potentially curative. This can be achieved by enhancing replication, attenuating cellular defense mechanisms to infection, enhancing viral lysis or altering the immune response.

The current study is aimed at the identification of sensitizers of oncolysis mediated by Delta24-RGD using the National Institutes of Health (NIH) clinical collection.[10] One of the advantages of this drug library is the favorable toxicity profile of the drugs as these agents are routinely prescribed for a wide spectrum of clinical indications. Also, the pharmacological properties are known for most of these agents. These factors make these drugs suitable for rapid translation into clinical trials after *in vitro* confirmation. Potential heterogeneity in response to the newly identified combination therapies was studied utilizing a well-characterized panel of patient-derived glioblastoma stem-like cell cultures (GSCs).[11,12] This model is known to preserve the original phenotypic and genotypic tumor characteristics.[11,12] We characterize the identified viral sensitizers with regard to important aspects in

glioblastoma treatment, including synergistic interactions and viral mechanistic enhancement such as viral infectivity, protein production, expression and replication. Moreover, we study the cellular induction of apoptosis and necrosis.

In addition, we present data on the general applicability of the identified drugs as viral sensitizers in other types of neoplasms and in combination with other types of OVs. The effects of Delta24-RGD are also enhanced by the identified viral sensitizers in triple negative breast cancer, ovarian carcinoma and colon carcinoma. Finally, the identified viral sensitizers enhanced the efficacy of both the HSV-1-based OV G47Δ-mcherry[13] as well as the naturally occurring oncolytic Newcastle disease virus (NDV)[14] in the GSC model.

8.2 Materials and methods

Clinical drugs
The NIH clinical collection which contains 446 drugs was obtained from the NCI/DTP Open Chemical Repository (http://dtp.cancer.gov). All drugs were dissolved in DMSO at 10mM. For validation, the hereafter named drugs were purchased individually, dissolved in DMSO and stored at -20°C. Anagrelide (37.5mM), rabeprazole (250mM) and Amlodipine (500mM) were obtained from Sequoia Research Products Ltd. (UK). Ebselen (50mM), fenoldopam mesylate (100mM), fluphenazine diHCl (100mM), indirubin (37.5mM), lofepramine (50mM), stiripentol (400mM), sumatriptan succinate (100mM), ranolazine diHCl (100mM) from Sigma-Aldrich (MO, USA).

Viruses
The oncolytic virus Delta24-RGD was used for the viability experiments and the titration experiments. This virus has been described previously 6 and includes both a 24-base pair deletion (E1A region) for selective replication in Rb-pathway deregulated tumor cells, and an RGD peptide insertion for cell binding and entry using αv integrins.[15] The replication-deficient adenoviral vector Ad.luc.RGD was used for assessment of infectivity and was kindly provided by Dr. D.T. Curiel, (University of Alabama, Birmingham, Al, USA). The Delta24-RGD-GFP was constructed for monitoring viral replication using fluorescent imaging and contains a GFP expression cassette under the E3-promotor. This virus was produced, purified and titrated as previously described.[16] The Newcastle disease virus (NDV) has been described previously.[14] The Herpes Simplex Virus-1 based OV G47Δ-mCherry was constructed as described previously.[13]

Patient-derived serum-free cultured glioblastoma stem-like cells
The patient-derived GSCs used for the experiments included a panel of cultures that were established and maintained under serum-free conditions. The tumor specimens were acquired with patients' informed consent and with approval of the institutional review board of the ErasmusMC. The fresh resection material was dissociated mechanically and enzymatically as described previously.[11] The applied method has been demonstrated to 1) retain genetic stability after passaging;[11,17] 2) to recapitulate the phenotypic characteristics of the original tumor[11,12] and 3) to preserve markers of stemness in glioblastoma cells.[18] The cells were maintained under serum-free conditions in DMEM/F12 medium supplemented with 1% penicillin/streptomycin, 2% B27, 20ng/ml bFGF, 20ng/ml EGF (Life Technologies, Paisley, UK), and 5µg/ml heparin (Sigma-Aldrich), at 37°C in a humid 95% air/5% CO_2 chamber. The parental tumors and the cell cultures were molecularly characterized as

has been described previously.[11] The GSCs were classified as glioma World Health Organization (WHO) guidelines grade IV by histopathological assessment of the parental tumor. The passages used were between p8 – p22.

Cell lines

The A549 lung adenocarcinoma cell line and SKOV3 ovarian carcinoma cells were obtained from ATCC (VA, USA). The HCT-116 colon carcinoma cells were obtained from Sigma-Aldrich. The triple negative breast carcinoma cell lines MB-MDA-231 was kindly provided by K. Naipal, MD, of the Department of Genetics, ErasmusMC, Rotterdam, The Netherlands. The cells were cultured in DMEM medium conditions with 10% FBS and 1% penicillin/streptomycin. The cell lines were maintained at 37 °C in a humid 95% air/5% CO_2 chamber.

Viability assays and screening method

Patient-derived GSCs and the cell lines of the other tumor types were seeded at $1x10^3$ cells/well in 96-well plates. After 24 hours of incubation the cells were treated with the drugs at a concentration of 100μM, and combined with Delta24-RGD (MOI 50). Cell viability was measured using the CellTiter-Glo assay (Promega, WI, USA) after five days of incubation. For all drugs the combination drug effects were compared to single agent effects, with DMSO as controls. In cases where cell viability was reduced by more than 75% by the drug alone, the drug was re-screened at 10μM and 1μM. If the drug and the combination treatment did not affect viability in this screen (<25% reduction of non-treated controls), i.e. concentrations were too low, then the drug was tested in the third experiment at 50μM and 5μM). Potent viral sensitizers had to meet the criteria of 1) an enhancement factor (explained in the 'statistical analysis' section) of >2 in viability reduction in both of the tested GSCs, and an absolute enhancement of >25% in one the cultures, and 2) the viability of cells treated with the monotherapies had to be >25% compared to controls, as additional effects are difficult to distinguish below this threshold. After identification of the drugs that met these criteria, the drugs were further evaluated for available data on the blood-brain barrier penetration.

The validation of identified drugs was performed using the Chou-Talalay assays, to determine synergy between Delta24-RGD and the drugs by median effect equation calculation.[19] For the Chou-Talalay assay, the IC_{50} values were determined via a concentration-range of 3-fold steps, ensuring no effect on the one end, and complete cell kill on the other end of the concentration-range. Similarly, combination effects were determined using a concentration range of the drug with a concentration range of the virus. Viability was measured by CellTiter-Glo. The assays were performed in triplicate using the glioblastoma culture GS79. The same cell culture as in the original drug screen was used for the Chou Talalay experiments. The combination index was calculated for every combination and considered synergistic if <1, additive if =1 and antagonistic if >1. The screen on a panel of GSCs was performed according to a same treatment regimen, by using two drug concentrations, namely the IC_{50} value as determined in GS79 and a 2-fold step lower doses. Two MOIs of Delta24-RGD were used (MOI 25 and MOI 75). The results are presented as percentage of non-treated controls with standard error.

Viral infection assays
The effects of the selected drugs on viral infection were assessed using the non-replicating vector Ad.luc.RGD as described previously.[8] GS79 and GS102 cells were seeded at $5x10^3$ cells/well in a 96-wells plate and kept overnight in an incubator. The cells were treated with one concentration of the four drugs and infected with Ad.Luc.RGD. Post-infection, the cells were incubated for 24 hours and permeabilized by a freeze/thaw cycle in Triton X-100 (0.9% v/v). Steady-Glo substrate (Promega) was added and luciferase was measured with an Infinite M200 plate reader (Tecan, Switzerland). The results are presented from three independent experiments as percentage of Ad.Luc-RGD only treated cells with standard error.

Viral protein expression and viral titration assays by hexon staining
The viral protein expression in Delta-24RGD infected cells was determined by direct staining for viral hexon protein at 48 hours post-infection of GS79 cells. The cells were seeded $1x10^3$ cells/well in 96-wells plates and after 24 hours, the cells were treated with Delta24-RGD (Figure 1) or with Delta24-RGD and one of the viral sensitizers (Figure 3). After 48 hours cells were fixed with cold methanol and stained as described below. The results are displayed as mean counts/well of triplicates with standard deviation.

Viral titration assays were performed to determine progeny viral particle production. For this, GS79 cells were seeded at $5x10^4$ cells per well and after 24h were treated with Delta24-RGD in combination with each of the four drugs. At both 48h and 96h the cells and supernatants were harvested. Three freeze-thaw cycles were performed, the cells were centrifuged at 1500 rpm for 3 minutes to remove cell debris, and the supernatants were collected. Supernatants were added in serial dilution to $1x10^3$ cells per well of the A549 lung adenocarcinoma cell line. At 48h cells were fixed using ice-cold methanol and washed in PBS/0,05% Tween-20 (Sigma-Aldrich). Staining was done using the primary mouse anti-hexon antibody in PBS/1% BSA (Adeno-X™ Rapid Titer Kit, #632250, Clontech, CA, USA). The hexon plaques were quantified and viral titers were calculated in triplicate. The results are shown as mean of the three viral titers and were considered significant if $p<0.05$ (using the Students´ T-test)

Late viral transgene expression using Delta24-RGD-GFP
Late viral transgene expression was studied by evaluating GFP expression from a Delta-24-RGD-GFP virus. GFP expression was monitored over time. GS79 cells were seeded at $2.5x10^3$ cells/well in 96-well plates and were incubated with the identified drugs and/or Delta24-RGD-GFP at concentrations at which synergy had been detected by Chou Talalay analysis. The plates were placed in an IncuCyte real-time cell imaging incubator (Essen Bioscience) and GFP was measured for five consecutive days. The experiment was performed in duplicate and fluorescence was measured every two hours and graphically displayed as mean object counts/mm^2.

Flow cytometry on integrin αvβ3 and CAR expression
GS79 cells were seeded at $5x10^4$ cells per well in 6-well plates. After 24 hours the cells were treated with fluphenazine, indirubin, lofepramine and ranolazine at the concentrations shown in the results. At 4, 8 and 24 hours the cells were harvested, washed and incubated for 15 minutes in FACS buffer (PBS/0.25%, BSA/0.05%, NaN3/0.5mM, EDTA/2% human serum) using primary mouse anti-CD51/CD61 (1:50, Abcam (Cambridge, UK)) and primary

rabbit anti-CAR (H-300, 1:50, Santa Cruz (Dallas, TX, USA)). After a washing step the cells were incubated with Alexa-488 anti-rabbit and PE-anti mouse secondary antibodies (Life Technologies). Next, the cells were fixed in BD FACS lysing buffer (BD Biosciences, CA, USA). In the flow cytometry analysis, a minimum of $3x10^4$ events was obtained on a FACS Canto II (BD Bioscience). Flow cytometry data were analyzed by using the Infinicyt software (Cytognos, Salamanca, Spain), where debris and doublets were removed with FSC-H and FSC-A. The expression was plotted for the remaining events.

In silico analysis of pathways and target molecules

The Ingenuity Pathway Analysis (IPA) software was used for *in silico* analyses on the drugs of interest. We aimed to find mechanisms related to the efficacy of combination therapy, by analyzing downstream molecules influenced by the four drugs, fluphenazine, indirubin, lofepramine and ranolazine. We investigated overlapping functions of the four drugs to detect common pathways of interaction (IPA, Sept 2014). Firstly, molecules of common pathways were identified for fluphenazine, indirubin, lofepramine and ranolazine by *in silico* connection using the 'build' algorithm and addition of downstream direct and indirect molecules. The results were projected in a network for the four drugs (Figure S2). Furthermore, the 'comparison analysis' in the IPA software was used to analyze common pathways of the four drugs and discover potential novel drugs with the same mechanism of action. The top ten common pathways were considered significant if the p-value <0.05. The analysis was based on the first and second level of downstream affected molecules of the various drugs.

Caspase-3/7 activity

To evaluate Caspase-3/7 activity, cells were seeded $5x10^3$ cells/well in a black-walled 96-well plate. The cells were treated with the four drugs as single treatment, virus alone, or in combination with Delta24-RGD, at a concentration at which synergy was observed in the Chou Talalay assays. Staurosporine (Sigma Aldrich, 20nM) was used as a positive control. The CellPlayer 96-Well Kinetic Caspase-3/7 Apoptosis Assay (Essen Bioscience) was added to the wells and, the caspase-3/7 activity was tracked by fluorescent images over a time period of 60 hours with the IncuCyte system using a 10X magnification at 37°C. Two fluorescent images/well of triplicates were collected every two hours up to sixty hours and displayed as object counts/mm^2.

Lactate dehydrogenase assay

GS79 cells were seeded at $1.0x10^3$ cells/well in a 96-well plate. After 24 hours, cells were incubated with two concentrations of the drugs fluphenazine, indirubin, lofepramine and ranolazine in the range at which synergy was detected and two concentrations of virus (MOI 100 and MOI 50). The cells were incubated for five days and placed at 37°C in a humidified 95% air/5% CO_2 incubator. After this period, the amount of LDH in the supernatant was determined using the CytoTox-One assay (Promega). Fluorescence was measured in a Tecan Reader. Cell viability was measured by CellTiter-Glo assay to calculate the ratio of LDH per number of living cells. The results were presented as LDH per viable unit as percentage of non-treated controls with the standard errors. The experiments were performed in triplicate.

Statistical analysis

In the primary compound screens, the "Enhancement" was calculated according to the description of Chou,[20] namely the viability of the most effective monotherapy divided by the viability of the combination therapy. The criterion for designating a drug as potential viral sensitizer was as follows: an enhancement of >2 in both tested cultures, and an absolute reduction of the single drug treatment with >25% viability in at least one culture. The "Absolute Difference" is the viability of the most effective monotherapy minus the viability of the combination therapy, which determines the absolute reduction in viability of cells in the combination treatment compared to the single agent treatment.[20] The drug alone had to reduce viability by no more than 75% as below 25% viability combination effects are difficult to detect. The Chou-Talalay method was performed as described19 and means were plotted with standard deviations. To compare effects of different treatments, the Student's T-test was used, and statistical significance was reached if $p<0.05$. The caspase-3/7 activity was calculated as objects counts/well. The caspase-3/7 activity and Delta24-RGD-GFP over time were analyzed by a two-way ANOVA with a Tukey's Post-Test. The treatment effect was compared to the controls, and combination treatments to both single agent treatments.

8.3 Results

GSCs demonstrate heterogeneous susceptibility to Delta24-RGD

The therapeutic efficacy of Delta24-RGD is heterogeneous between glioblastoma patients.[3,9] Therefore, investigations into potential viral sensitizers should be designed to yield insights both from responsive and resistant models. To achieve this, we screened eight GSCs for their responsiveness to Delta24-RGD. The non-replicating vector Ad.Luc.RGD was used to assess infectivity and the results show substantial variation between the eight GSCs (Figure 1a). GS79 was relatively resistant whereas GS359 was very sensitive to adenoviral infection. The remaining cultures GS401, GS245 GS184, GS102, GS281 and GS295 were intermediately sensitive. Next, the viral protein production of Delta24-RGD during the first replication cycle was determined by staining for the adenoviral capsid protein hexon (Figure 1b) at 48 hours. The number of hexon counts at this time point revealed a similar pattern to the luciferase expression data of Figure 1a, with the most resistant GS79 having the lowest hexon counts and the most sensitive GS359 having the highest counts. Two cultures were selected for the subsequent drug screen to investigate which drugs sensitize glioblastoma to OV therapy with Delta24-RGD. Based on the infection and viral protein production assays, GS79 was picked as the "resistant" sample and GS102 as the "intermediate resistant" sample. Accordingly, the IC_{50} values of Delta24-RGD in GS79 and GS102 were found to be high compared to the MOIs observed in conventional cell lines;[8] MOI200 for GS79 and MOI70 for GS102 (Figures 1c-d).

Clinical drug screening identifies potential sensitizers of OV therapy with Delta24-RGD

In order to identify viral sensitizers of OV therapy with Delta24-RGD in GSCs, the NIH clinical collection was explored (Figure S1a[10]). This collection contains 446 drugs most of which have been approved by the FDA for use in humans for a wide spectrum of clinical indications.[21] A third of these are central nervous system (CNS) drugs, including antiepileptics, antidepressants, antipsychotics. The drug screening strategy is illustrated in a flow-chart (Figure S1b). The primary screen was performed on the two mentioned cultures GS79 and GS102 at a drug concentration of 100µM. Potential viral sensitizers were defined

as described in the methods section, which resulted in two arms. The first arm consisted of 332 drugs for which monotherapy reduced viability between 25-75%. Of those drugs, six had viral sensitizing effects in both GS79 and GS120. The second arm consisted of drugs for which monotherapy at 100µM decreased GSC viability by more than 75% (n=114 drugs), since this is incompatible with a reliable evaluation of additive effects with Delta24-RGD. Therefore these drugs were titrated for combination therapy activity at 50, 10, 5 or 1µM, which resulted in the identification of four viral sensitizers with enhancement effect at a dosage of 10 or 5µM. In total ten drugs had a viral sensitizing effect in both GSCs. Table 1 provides an overview of these drugs which are; amlodipine, anagrelide, ebselen, fenoldopam, fluphenazine, indirubin, lofepramine, ranolazine, stiripentol and sumatriptan succinate.

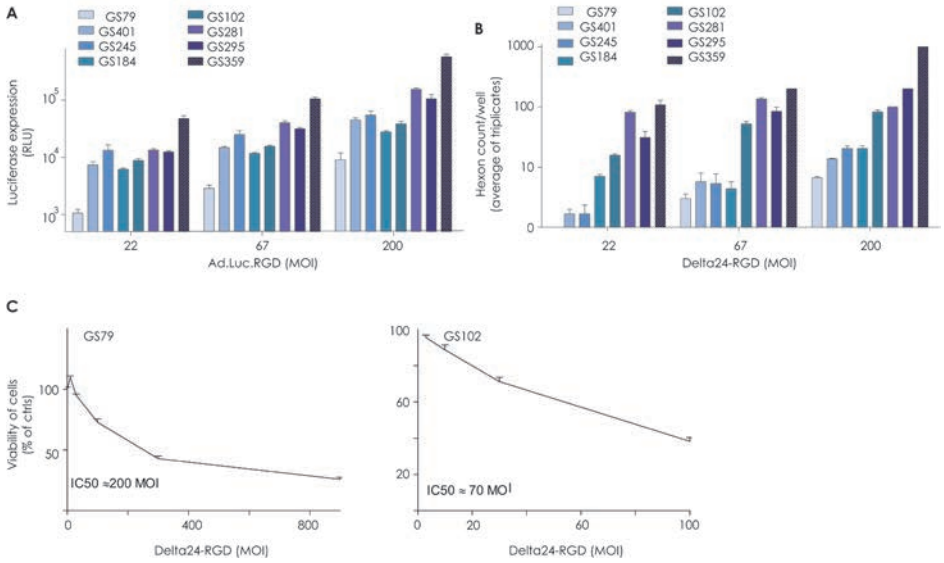

Figure 1. GSCs display heterogeneous susceptibility to oncolytic adenovirus *in vitro.*

(A) GSCs from eight individual patient samples were tested for susceptibility to adenovirus infection using the luciferase expressing non-replicating vector Ad.luc.RGD. The data are shown as RLU in a log10 scale with standard deviation for the three different MOIs of the virus. Read out was performed after 24 hours post-infection. **(B)**. Variability in adenoviral replication was assessed by staining for adenovirus hexon protein at 48 hours post-infection with three different MOIs Delta24-RGD. The data is presented as hexon counts/well (average of triplicate) in a log10 scale with standard deviation. **(C)** Dose-response curves for Delta24-RGD on GS79 (relatively low infection and replication) and GS102 (relatively intermediate infection and replication). The data are presented as viability of cells (percentage of non-treated controls) with standard deviation and IC_{50} values are depicted as calculated by linear regression.

Synergy was detected for six of the potential viral sensitizers

The ten identified viral sensitizers were validated and tested for synergistic activity in GS79 cells according to the Chou-Talalay methods.[19] The IC_{50} values were determined by concentration-response assays (displayed in Table 1). The combination assays were performed and the combination indices (CIs) were calculated. Four of the ten identified drugs were synergistic (CI<1) and two were additive (CI=1) when combined with Delta24-RGD.

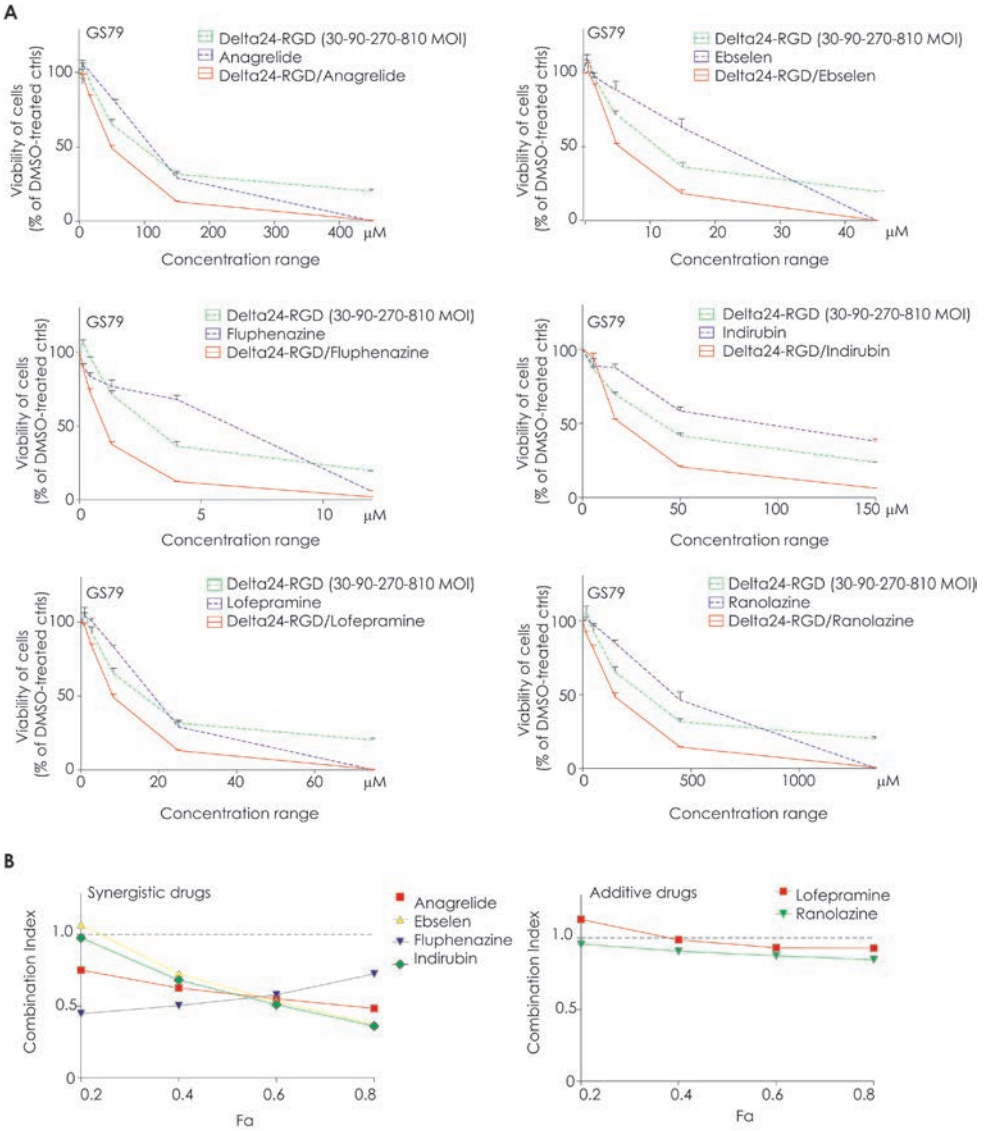

Figure 2. Chou-Talalay synergy analysis on the potential viral sensitizers.

(A) Dose-response assays were performed on GS79 cells using the Chou-Talalay method to determine synergy between Delta24-RGD and ten different drugs that were identified by the initial screen. The results are shown for the six drugs that were classified by this method as synergistic or additive. Results are presented as percentage of controls with standard deviation. Read out was performed at five days post-infection. **(B)** The combination index (CI) for each drug in combination with Delta24-RGD was calculated by the Chou-Talalay method. A CI of <1 is classified as synergy, a CI of = 1 as additive and a CI >1 as antagonism. The synergistically acting drugs (anagrelide, fluphenazine, indirubin and ranolazine) are shown in the left CI/Fa-plot, whereas additively acting drugs (lofepramine and rabeprazole) are plotted in the right CI/Fa-plot.

These were anagralide, ebselen, fluphenazine, indirubin, lofepramine and ranolazine (Figures 2a-b, Table 1). The other drugs (amlodipine, fenoldopam, stiripentol and sumatriptan) failed to reproduce enhancement in the wider concentration range of *in vitro* testing and were therefore excluded from further validation. In addition, the literature was searched for the ability of the six drugs to cross the blood brain barrier *in vivo*.[22-26] Anagrelide was excluded from further studies because it has not been reported to penetrate the blood-brain barrier *in vivo* (Table 1), whereas this has been reported for the other drugs.

Viral sensitizers increase adenoviral infection and replication efficacy

To determine whether the drugs improved the efficacy of viral infection, the luciferase expression of the Ad.Luc.RGD-infected GSCs was determined 24 hours after combination treatment with ebselen, fluphenazine, indirubin, lofepramine and ranolazine. The dosages at which synergy was observed were applied in these experiments. Fluphenazine, indirubin and lofepramine significantly increased Ad.Luc.RGD infection in both GS79 and GS102 (Figure 3a, $p<0.05$). Ranolazine increased viral infection only in GS102. Ebselen decreased luciferase expression in both GSCs ($p<0.05$ in GS79 and GS102). Triggered by the effect of these viral sensitizers on infection efficacy it was hypothesized that these drugs may alter the expression of viral entry receptors CAR and integrin $\alpha v\beta 3$. Flow cytometry was performed to investigate the expression of CAR and integrin $\alpha v\beta 3$ before and after treatment with the viral sensitizers (Figure 3b). Both indirubin and lofepramine were demonstrated to influence the adenoviral receptor expression at 4 and 8 hours post-treatment. We did not find up-regulation of entry receptors by fluphenazine although the viral infectivity was increased as shown in Figure 3a. For ranolazine, no effects on the surface receptors were observed. In summary, fluphenazine, indirubin, and lofepramine increased viral infection. For lofepramine and indirubin this was associated with increased levels of CAR and slightly increased levels of $\alpha v\beta 3$ integrins.

Table 1. Sensitizers to Delta24-RGD therapy identified by drug screening

The results are shown for all drug concentrations of the NIH clinical collection that were screened in vitro. This table (Part I) shows the 'hits' that were selected for validation. The combinations of these drugs with Delta24-RGD were more effective than virus alone in both GS79 and GS102 cells at the indicated concentrations (column 2-4). The molecular weight of the agent is indicated (column 5), and the drug category and therapeutic indication are provided (columns 6 and 7). The results are shown of the absolute difference in viability between single and combination treatment as well as the enhancement factor of the combination therapy in the two GSC cultures (Part II). The results of the validation experiments in GS79 are provided in the 'Chou Talalay' column and in Part II of the table. Results of a literature search for blood-brain barrier penetration of the drugs is listed in column 14. Legend: Mw kDa = molecular weight in kDa; absolute difference = mean difference between single agent and combination treatment; enhancement = fold increase of viability loss due to combination treatment; blanc = not tested; NO = no effect observed.

PART I

Drug	100 µM	10 µM	5 µM	Mw kDa	Category	Application	Chou Talalay	Cross BBB
Amlodipine base		NO	X	409	Ca+-channel-blocker	Hypertension	Antagonism	ND
Anagrelide HCl	X			254	Platelet aggregation inhibitor	Essential thrombocythemia, CML	Synergy	Not reported
Ebselen		NO	X	274	Anti-oxidant	Ulcer, inflammation	Synergy	*In vivo/ in vitro*
Fenoldopam mesylate	X			305	Dopamine-receptor1 agonist	Hypertension	Antagonism	ND
Fluphenazine		X	X	437	Dopamine-receptor-antagonist	Psychosis	Synergy	*In vivo*
Indirubin	X			262	Anti-neoplastic, anti-inflammatory	Cancer, inflammation	Synergy	*In vivo*
Lofepramine HCl		X	X	418	Tricyclic antidepressant	Depression	Additive	*In vivo*
Ranolazine diHcl	X			427	Na+-/ Ca+-channel affector	Angina	Additive	*In vivo*
Stiripentol	X			234	GABA-agonist	Convulsions	Antagonism	ND
Sumatriptan succinate	X			295	5HT1-receptor-agonist	Migraine	Antagonism	ND

PART II

Drug	Abs dif. % GS79	Abs dif. % GS102	Enh. GS79	Enh. GS102	IC_{50} (µM) in GS79
Amlodipine base	3.50%	41.20%	35.56	28.39	12
Anagrelide HCl	60.70%	25.10%	607.5	252.4	142
Ebselen	26.30%	13.30%	264.24	7.34	15
Fenoldopam mesylate	73.30%	26.90%	12.42	1.87	62
Fluphenazine	29.00%	1.40%	3.5	15.17	4
Indirubin	71.60%	61.20%	9.73	612.59	110
Lofepramine HCl	41.90%	32.10%	2.29	2.24	19
Ranolazine diHcl	36.50%	61.00%	2.56	23.09	431
Stiripentol	78.70%	18.00%	75.87	1.39	263
Sumatriptan succinate	77.60%	59.00%	36.23	13.2	622

Effects of the drugs on Delta24-RGD early viral replication, late viral gene expression and progeny production

We investigated the Delta24-RGD viral hexon production during the first viral cycle as a measure of replication efficacy after combination therapy with the viral sensitizers. At MOI 60, the four drugs increased the number of hexon spots at 48 hours ($p<0.05$). Ebselen slightly decreased the number of hexon counts/well ($p<0.01$). Fluphenazine, lofepramine, and ranolazine all increased viral protein production by 2 to 3-fold and indirubin was most effective, increasing the hexon counts by 3.7-fold ($p<0.01$) At the higher virus concentration of MOI 125, only indirubin and ranolazine were still significantly increased compared to control (Figure 3c).

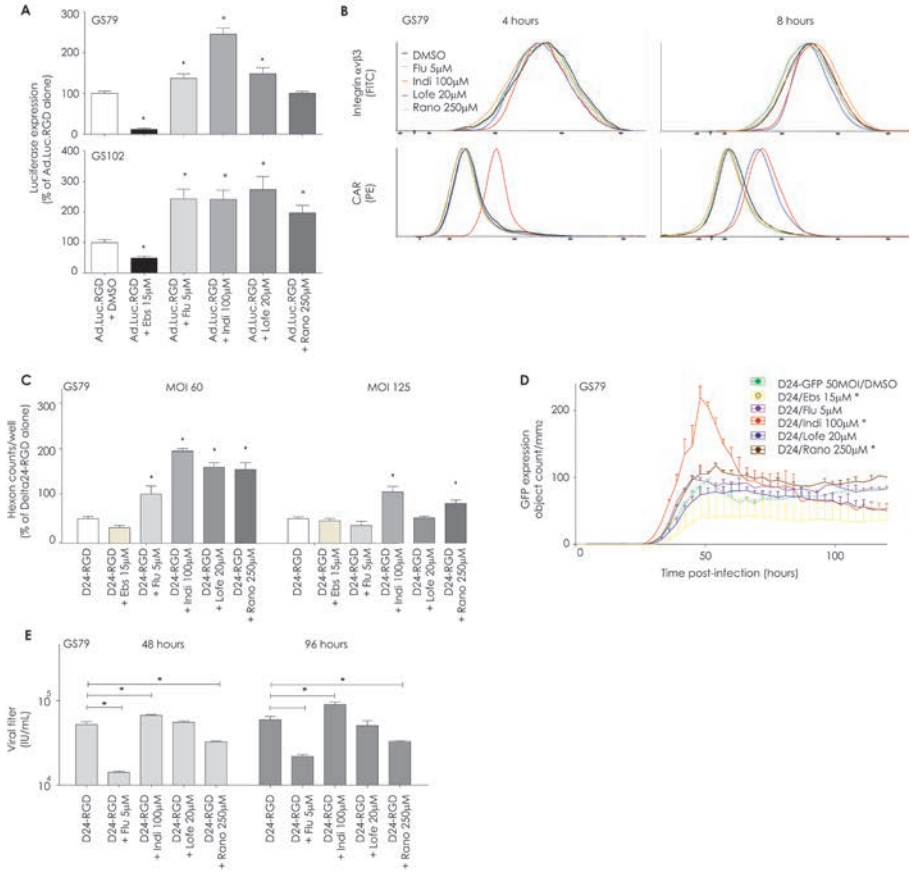

Figure 3. Viral sensitizers increase adenoviral infectivity and replication.

(A) GS79, GS102 and GS245 cells were treated with the indicated drugs and infected with Ad.Luc.RGD. Luciferase expression was measured at 24 hours post-infection. The results are presented as a percentage of DMSO/Ad.Luc-RGD-infected samples with the standard deviation. *Indicates significance difference between Ad.Luc.RGD alone and Ad.Luc.RGD/drug at the p<0.05 level. **(B)** GS79 cells were treated with indicated drugs. After 4 hours, 8 hours and 24 hours (not shown), the cells were harvested and both CAR and integrin levels were analyzed for differences between the Delta24-RGD alone and Delta24-RGD/drug treated samples. Flow cytometry histograms are presented. **(C)** GS79 cells were treated with three different MOIs of Delta24-RGD and the four viral sensitizers. The adenoviral replication in the first viral cycle was measured as indicated by hexon counts which are plotted as a percentage of DMSO/Delta24-RGD treated controls with standard deviations. *Indicates significance at p<0.05 level of combination treatment compared to Delta24-RGD alone. **(D)** GS79 cells were treated with the four drugs and infected with Delta24-RGD-GFP. The fluorescence intensity was measured and analyzed with the IncuCyte software. GFP expression was counted as object count/mm^2 per time point. The results are shown as means with the standard deviation. *Indicates significance at p<0.01 level of the combination treatments compared to Delta24-RGD alone.**(E)** GS79 cells were concomitantly treated with Delta24-RGD and each of the four drugs, as indicated. The infectious viral particle titers in the cell extracts and supernatants at 48 and 96 hours post-infection were determined by viral titration assay and are displayed graphically. *Indicates significant difference in the viral titers of Delta24-RGD alone compared to the combination treatments with drugs and Delta24-RGD (p<0.05).

To measure the effects of the four drugs on the viral cycle in a longitudinal manner, we performed time-lapse fluorescence imaging of Delta24-RGD-GFP infected cells. GFP is expressed late in the replication cycle (Figure 3d). Indirubin, ranolazine and fluphenazine peaked earlier than controls suggesting more efficient replication and lysis. The GFP data was in line with the results of the hexon staining. Both indirubin and ranolazine enhanced Delta24-RGD-GFP expression ($p<0.01$ and $p<0.001$ respectively). Differences in the kinetics were observed, namely indirubin increased peak levels of GFP expression whereas ranolazine increased the fluorescence levels consistently over time without evidently enhancing peak levels. In accordance with the previous findings, ebselen reduced viral replication of Delta24-RGD-GFP ($p<0.05$). Due to the pronounced inhibitory effects of ebselen in both the viral infection and replication assays this drug was not further evaluated.

To assess whether the enhancement of early and late viral protein production translates to increased viral progeny production, viral titration assays were performed (Figure 3e). Only indirubin increased the viral progeny production in GS79 cells at both 48 and 96 hours post-infection from 5.2x104 to 6.7x104 ($p<0.05$) and from 5.9x104 to 9.0x104 ($p<0.05$), respectively, compared to Delta24-RGD alone. Interestingly, fluphenazine and ranolozine achieved the opposite effect from indirubin: a decrease in viral progeny production at both time points ($p<0.05$). Lofepramine did not significantly alter the viral progeny production. In summary, the viral progeny production was increased by indirubin and was decreased by both fluphenazine and ranolazine.

The viral sensitizers increase Delta24-RGD-induced oncolysis by enhancing apoptosis and necrosis

We performed an *in silico* analysis using the Ingenuity Pathway Analysis (IPA) software (Figure S2, IPA, September 2014) to identify which pathways are activated or inhibited by the four viral sensitizers. Next, we evaluated whether identified cell death pathways are relevant for viral oncolysis. Fluphenazine targets the dopamine receptor, indirubin targets the aryl hydrocarbon receptor and the apoptotic signaling molecules Bcl-2, BIRC5 and NFκB, lofepramine affects pro-apoptosis associated SMPD1 and ranolazine affects the adrenergic receptor. The top ten of overlapping functions of the downstream molecules of these drugs included relevant mechanisms for viral oncolysis such as cell death, apoptosis and necrosis. Others have found cell death pathways to be affected by OV therapy.[27,28] Since oncolysis induced by the adenovirus is reported to be associated with both apoptosis and necrosis, we investigated the role of the viral sensitizers in both cellular responses. A longitudinal assessment of caspase-3/7 activity was performed to study the role of the viral sensitizers on apoptosis. All four viral sensitizers induced caspase 3/7 activity at early time points post-treatment (Figure 4a). Infection with Delta24-RGD led to a delayed onset of caspase 3/7 activity. Combination treatments of Delta24-RGD with each of the four viral sensitizers also led to a delayed onset of caspase 3/7 expression but with a higher peak activity level for indirubin at 9 – 15 hours and prolonged higher caspase 3/7 activity for fluphenazine, lofepramine and ranolazine at 30-60 hours ($p<0.05$).

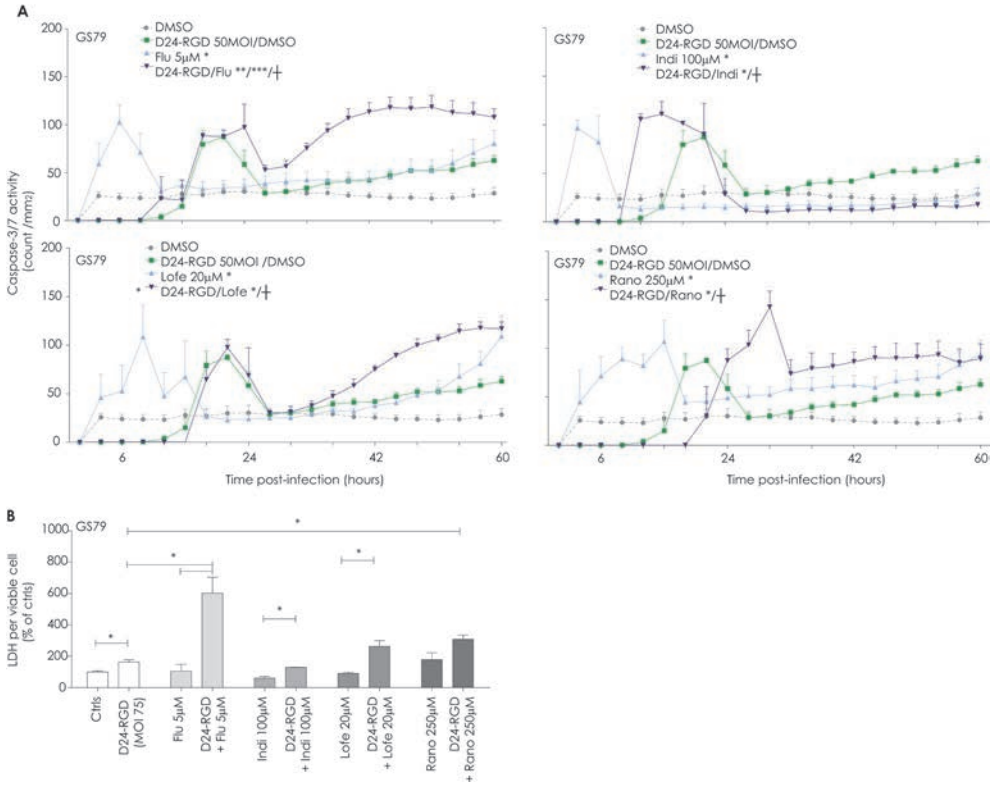

Figure 4. The selected viral sensitizers increase Delta24-RGD oncolytic efficacy by enhancing apoptosis and/or necrosis.

(A) GS79 cells were treated with the four drugs and Delta24-RGD. The caspase-3/7 activity levels were measured during a time lapse of 60 hours. The fluorescent spots were counted and are shown as count/mm^2. *Significance at p<0.05 combination vs. DMSO-controls;**Significance at p<0.05 combination vs. Delta24-RGD; ***Significance at p<0.05 combination vs. drug. (two-way ANOVA over whole episode). ┼In the graph indicates significance at p<0.05 using the Students' T-test of combination vs. both single agent treatments at single time points. **(B)** GS79 cells were treated with the four drugs and two MOIs of Delta24-RGD. LDH activity was measured at five days post-incubation. Fluorescence and viability were measured, to correct for the amount of viable cells. The LDH levels are presented as percentage of DMSO-controls with standard deviation, and corrected for viability. *Significance at p<0.05 level of combination vs. Delta24-RGD or agent alone.

To determine necrotic cell death, a lactate dehydrogenase (LDH) assay was used. This assay measures the release of LDH in the culture medium, which serves as a dynamic marker for loss of cellular membrane integrity, an early event in necrotic cell death. (Figure 4b). Delta24-RGD (MOI 75) monotherapy increased LDH levels five days post-infection (p<0.05 compared to controls). Fluphenazine was the only viral sensitizer that increased LDH levels in combination with the virus compared to both single agents (p<0.05). Indirubin and lofepramine combined with the virus increased LDH levels compared to the drugs alone, whereas ranolazine increased LDH compared to the virus alone (p<0.05). In conclusion, viral sensitizers combined with Delta24-RGD effectively induced both apoptotic and necrotic cell death *in vitro*. The four drugs interacted with apoptotic cell death as derived

from caspase-3/7 activity. Enhanced necrosis was demonstrated using ranolazine and fluphenazine.

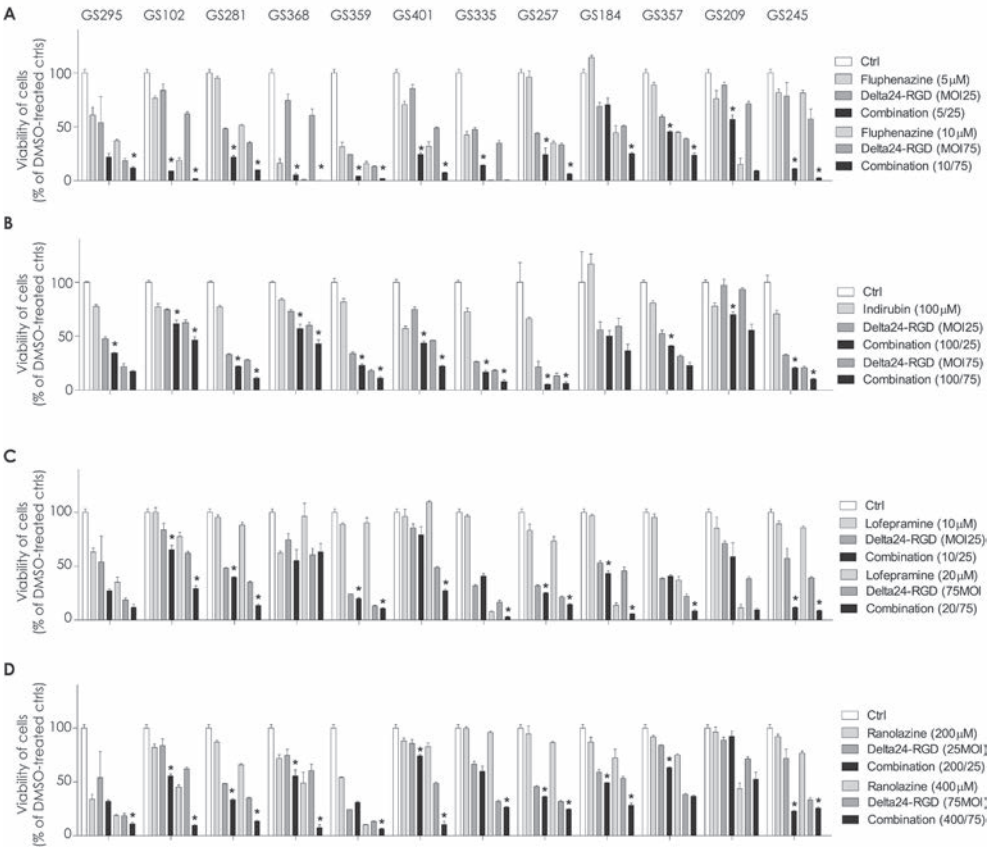

Figure 5. Viral sensitizers enhance Delta24-RGD efficacy in a broad panel of distinct.

Twelve patient-derived GSCs were tested with two different concentrations of the drugs in combination with two different MOIs of the virus. The viability is shown as percentage of DMSO-controls with the standard deviation. Fluphenazine/Delta24-RGD combination therapy demonstrated enhancement in all GSCs tested **(a)**, indirubin/Delta24-RGD in 11/12 GSCs **(b)**, lofepramine/Delta24-RGD in 9/12 GSCs and **(c)** ranolazine/Delta24-RGD in 11/12 GSCs **(d)**. *Indicates significance at the $p<0.05$ level for the combination treatment compared to both single agent treatments.

Viral sensitizers are effective in a broad panel of heterogeneously responding patient-derived GSCs

Glioblastoma is a heterogeneous tumor, which has profound consequences for efficacy of therapeutics. To place the viral sensitizing ability of the four drugs in the context of this molecular heterogeneity, a broader panel of GSCs was employed to investigate their general applicability. Table 2 shows the molecular characteristics of the panel of GSC cultures indicating that all TCGA-defined subtypes are represented as well as both methylated and unmethylated *MGMT* promoter subtypes. The viral sensitizers were combined with Delta24-RGD in the GSCs that were used in the initial infectivity studies (Figures 1a-b) and expanded with an additional set amounting to a total of twelve GSC cultures. The four viral

sensitizers were applied in two different concentrations in combination with two MOIs of Delta24-RGD (Figures 5a-d). Significant enhancement was considered if the combination therapy decreased the viability compared to both single agents therapies ($p<0.05$). Fluphenazine was effective in enhancing Delta24-RGD oncolysis in all twelve patient-derived GSCs. Indirubin was effective in 11/12 GSCs. Lofepramine was effective in 9/12 cultures mainly at the higher concentration of 20μM and ranolazine was effective in 11/12 cultures. Overall, these data confirm that the four drugs that were identified as potential viral enhancers by a screen on GS79 are effective in a broader panel of patient-derived GSCs, which bears distinct molecular characteristics and shows differential sensitivity to Delta24-RGD. These findings suggest that the identified sensitizers could be effective in enhancing Delta24-RGD oncolytic therapy in a broader context of heterogeneous glioblastomas.

Table 2. Molecular subtypes of the panel of GSC cultures.

Twelve patient-derived GSC cultures were used for the screening of the identified viral sensitizers in a larger panel. The culture used for the initial experiments (GS79) is also included in the table. The molecular characteristics are shown, including the molecular subtype according to The Cancer Genome Atlas (TCGA) and the MGMT promotor methylation status.

Primary GSC culture	Molecular subtype	MGMT methylation status
GS79	CLA	UM
GS102	NEU	M
GS184	CLA	M
GS209	PRO	UM
GS245	NEU	UM
GS257	CLA	UM
GS281	MES	UM
GS295	MES	UM
GS335	CLA	M
GS357	CLA	M
GS359	MES	M
GS368	CLA	UM
GS401	PRO	M

General applicability of the drugs: enhancement in other tumor cell lines and enhancement of other viruses

The applicability of the four drugs as viral sensitizers was subsequently investigated in a broader perspective. We tested the combination of Delta24-RGD and the viral sensitizers in other tumor cell lines, namely the breast carcinoma cell line MB-MDA-231, the ovarian cancer cell line SKOV3 and the colon carcinoma cell line HCT-116 (Figure 6a; Supplemental Figure 3-4). Chou-Talalay assays were performed to determine synergy, additivity or antagonism. The results reveal that fluhpenazine, indirubina and ranolazine show synergy in all three cell lines, however there are large differences in the actual enhancement. Lofepramine showed additive enhancement in HCT-116 and synergy in SKOV3 and

MB-MDA-231 cell lines. Ranolazine showed synergy at low concentrations in SKOV3 cells, at high concentrations in MB-MDA-231 cells and at all concentrations in HCT-116 cells. In summary, the four drugs, and in specific, ranolazine and indirubin are effective sensitizers of Delta24-RGD in other tumor cell lines including those originating from triple negative breast carcinoma, colon carcinoma and ovarian carcinoma. The extent of the enhancement could be tumor type dependent. In addition, we assessed the sensitizing effects of the four compounds on two other OVs, the Newcastle disease virus (NDV) and the Herpes Simplex Virus-based G47Δ-mcherry in GS79 and GS102 (Figure 6b; Figure S4). The results show that fluphenazine, indirubin and lofepramine effectively synergized with G47Δ-mcherry in both GSCs. All four drugs were effective in combination with NDV, where ranolazine was the least effective drug. Also, the extent of the enhancement depended on both the virus and the cell culture . In summary, fluphenazine, indirubin and lofepramine are effective viral sensitizers for the OVs based on NDV and HSV vectors.

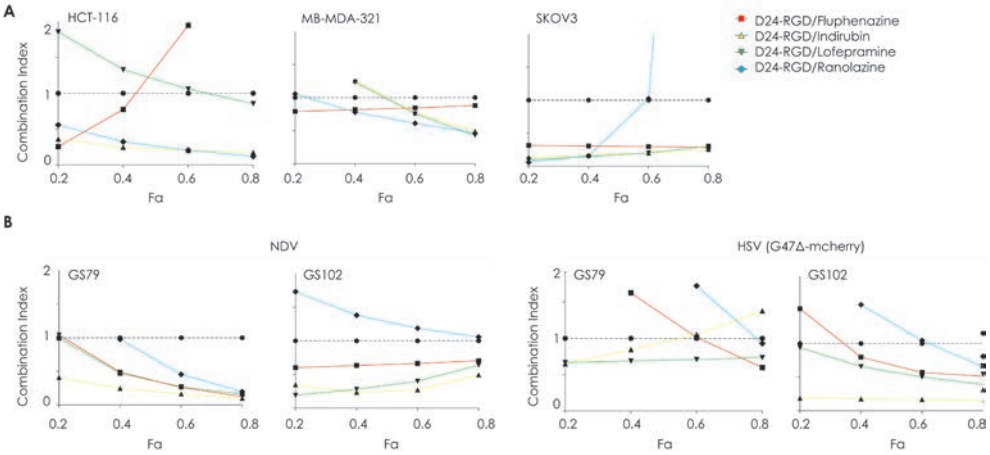

Figure 6. Drug/virus combination effects in different tumor cell lines and with different OVs.

(A) Dose-response combination assays were performed using Chou-Talalay analysis to study interaction between Delta24-RGD and the four viral sensitizers in three tumor cell lines, being triple negative breast, ovarian and colon carcinoma cells. Viability was measured at day five post-treatment. The combination indices (CI) were calculated and are shown for the various treatment combinations in these cell lines. **(B)** Dose-response combination assays were performed using Chou-Talalay assays to study interaction between the four viral sensitizers and oncolytic HSV and NDV in the GSCs GS79 and GS102. Viability was measured at day five post-treatment. The combination indices (CI) are shown for the various treatment combinations in these cell lines.

8.4 Discussion

The present study has identified four clinical approved viral sensitizers for the oncolytic adenovirus Delta24-RGD in patient-derived GSCs, namely fluphenazine, indirubin, lofepramine and ranolazine. Mechanistic studies attributed the synergistic activity with the virus partly to enhanced infection, replication or both. Not in the least, the induction of programmed cell death through apoptosis and or necrosis, was found to be increased and accelerated. As such, we conclude that these four viral sensitizers are potentially promising adjuvants to virotherapy for glioblastoma.

Previously, we have reported the strength of implementing a panel of GSCs for the assessment of combination therapy for glioblastoma *in vitro*.[9,29-31] The NIH clinical compound library has been applied to GSCs before[32,33] which resulted in the identification of numerous GSC specific compounds, and established the use of GSCs as a useful tool for drug screening experiments. Interestingly, Pollard et al., identified fluphenazine as a monotherapeutic agent in three GSC cultures as well. We here performed the first systematic drug screen to identify clinically approved drugs that enhance oncolytic adenovirus potency. Others have identified synergizing compounds in a mechanism driven strategy,[34,35] or by combining the current clinical standard therapeutics[36-38] and radiation therapy.[4,39,40] Compound screenings for oncolytic HSV, myxoma and VSV have been reported using other chemical libraries.[41-43] The strategy to detect viral sensitizers through high throughput screening, as implemented in this study, results in the unbiased detection of very potent FDA approved compounds.

One of the advantages of screening panels of GSCs is the identification of responders and non-responders, which grants the opportunity to investigate underlying mechanisms.[30] Accordingly we have observed that the response to Delta24-RGD therapy is heterogeneous[8] and may be driven by cell-entry receptors, autophagy mediated lysis and cellular anti-viral response.[27,44,45] Viral sensitization by these four compounds was reproduced in a panel of twelve GSCs, which suggests applicability of combination therapy in both intrinsically resistant and susceptible glioblastoma patients. Furthermore, viral sensitizing by the four drugs was not restricted to Delta24-RGD; both NDV and HSV virotherapy synergized with these compounds, nor was is restricted to glioblastoma, as viral sensitizing was observed in cell lines derived from other tumors. These results suggest that a more general mechanism of action underlies these combination therapies.

The combination of the *in vitro* drug screen and the *in silico* pathway analysis on the identified compounds was shown to be a powerful tool to predict mechanisms of action. As indicated by the *in silico* analysis, the four compounds converge on cell death pathway enhancement, which we could substantiate in the validation experiments. The pathways identified were of specific interest for combination treatment with Delta24-RGD, as apoptosis and necrosis have been shown to be involved in oncolytic cell death.[46-48]

The identified viral sensitizers have been sparsely investigated in the context of OV therapy. Below, we discuss the four viral sensitizers individually with regard to the mechanism of action, the reported effects in combination with viruses and their known effects on the immune response. The immune response is crucial for Delta24-RGD efficacy *in vivo*.[49]

Fluphenazine is a neuroleptic drug used for the treatment of psychosis and has not been previously identified as a viral enhancer. The drug enhanced infection, viral protein synthesis as well as oncolysis in the whole panel of patient-derived GSC cultures. Interestingly the viral progeny yield was decreased which may be related to the enhanced apoptotic and necrotic cell death possibly interfering with efficient viral particle production. Earlier fluphenazine was reported to inhibit leukemia and brain tumor cells,[32,50,51] which may be related to the inhibition of calmodulin that contributes to apoptosis through caspase-8 and Akt-pathway inhibition.[52]

Indirubin is used in Chinese medicine as an antipsoriatic[53] and anti-leukemia drug.[54] In OV therapy using Delta24-RGD, we showed that indirubin increases infection, CAR and integrin expression, viral protein production during the first cycle, viral gene expression over time and viral progeny production. Increased viral activity by indirubin has thus far not been reported. Indeed, indirubin derivatives have been shown to affect viral activities. Indirubin-3'-monoxime was effective in increasing viral transduction of an adeno-associated viral vector.[55] Another derivative was shown to inhibit viral replication of H5N1,[56] cytomegalovirus,[57] and the pseudorabies virus.[58] These reports and the results within this study, suggest that the effects of indirubin on viral replication may depend on the indirubin-derivative used, and/or on type of virus investigated. In our study, indirubin consistently augmented adenoviral oncolysis in multiple GSC cultures and other cancer cell lines, as well as the oncolytic activity of two other viruses, NDV and HSV. The downstream molecules of indirubin are associated with apoptosis,[59] which was confirmed by our *in vitro* studies. Indirubins may also have specific effects on the immune system as indirubin-3'-monoxime has been reported to induce immunosuppressive and anti-inflammatory effects on dendritic cells.[60] Moreover, inhibition of the indirubin target GSK-3 reduces microglial inflammatory responses.[61] Additional studies are warranted to investigate the effects on the immune response by indirubin in combination with Delta24-RGD.

The anti-depressant lofepramine has not previously been identified as an enhancer of viral efficacy. We show that this drug increases viral infection, which was associated with up-regulation of viral entry receptors, and enhances viral replication. The *in silico* pathway analysis revealed that lofepramine as a monotherapy affects downstream molecules related to apoptosis. This was translated to the combination therapy as well, as we confirmed *in vitro*. As a single drug treatment, lofepramine has been reported to block leukemia cell proliferation and to sensitize cells to apoptosis.[62]

The anti-anginal drug ranolazine is a sodium-channel blocker that has not been studied in combination with oncolytic viruses. Ranolazine enhanced the viral infection (culture specific) and viral protein production during the first viral cycle. However, viral progeny production was decreased, which is possibly related to enhanced induction of apoptosis and necrosis. Ranolazine has not been reported to possess direct tumor killing activity, however, a role for this drug in sodium channel–mediated breast cancer invasiveness has been reported.[63] The current study reveals novel mechanisms associated with this drug, which were not previously identified. Neither ranolazine nor lofepramine have been studied in the context of the immune system.

In conclusion, our study identified four effective viral sensitizers for Delta24-RGD oncolytic therapy in glioblastoma. These drugs include fluphenazine, indirubin, lofepramine and ranolazine. This study reveals the interaction of the drugs with important viral oncolytic cell death mechanisms, as shown *in silico* and *in vitro*. The identified drugs are not only applicable in glioblastoma but show synergy with Delta24-RGD in multiple cancer types. Moreover, all drugs except ranolazine act synergistically with other oncolytic viruses as well. Although the identified viral sensitizers are clinically applicable, future studies should focus on finding the optimal administration to achieve maximal effects *in vivo*. Moreover, *in vivo* studies with these agents are required to interrogate their effects on the immune response to OV therapy, a factor known to play a pivotal role in therapeutic outcome of these therapies.

References

1. Stupp R, Hegi ME, Mason WP, et al. Effects of radiotherapy with concomitant and adjuvant temozolomide versus radiotherapy alone on survival in glioblastoma in a randomised phase III study: 5-year analysis of the EORTC-NCIC trial. Lancet Oncol 2009;10:459-66.
2. Stupp R, Mason WP, van den Bent MJ, et al. Radiotherapy plus concomitant and adjuvant temozolomide for glioblastoma. The New England journal of medicine 2005;352:987-96.
3. Lang FF, Conrad C, Gomez-Manzano C, et al. First-in-human phase I clinical trial of oncolytic delta-24-rgd (dnx-2401) with biological endpoints: implications for viro-immunotherapy. Neuro Oncol 2014;16 Suppl 3:iii39.
4. Lamfers ML, Grill J, Dirven CM, et al. Potential of the conditionally replicative adenovirus Ad5-Delta24RGD in the treatment of malignant gliomas and its enhanced effect with radiotherapy. Cancer Res 2002;62:5736-42.
5. Kaufmann JK, Chiocca EA. Oncolytic virotherapy for gliomas: steps toward the future. CNS oncology 2013;2:389-92.
6. Suzuki K, Fueyo J, Krasnykh V, Reynolds PN, Curiel DT, Alemany R. A conditionally replicative adenovirus with enhanced infectivity shows improved oncolytic potency. Clin Cancer Res 2001;7:120-6.
7. Fuxe J, Liu L, Malin S, Philipson L, Collins VP, Pettersson RF. Expression of the coxsackie and adenovirus receptor in human astrocytic tumors and xenografts. Int J Cancer 2003;103:723-9.
8. de Jonge J, Berghauser Pont LM, Idema S, et al. Therapeutic concentrations of anti-epileptic drugs do not inhibit the activity of the oncolytic adenovirus Delta24-RGD in malignant glioma. J Gene Med 2013;15:134-41.
9. Berghauser Pont LM, Kleijn A, Kloezeman JJ, et al. The HDAC Inhibitors Scriptaid and LBH589 Combined with the Oncolytic Virus Delta24-RGD Exert Enhanced Anti-Tumor Efficacy in Patient-Derived Glioblastoma Cells. PLoS One 2015;10:e0127058.
10. US National Institutes of Health. http://dtp.cancer.gov. 2014.
11. Balvers RK, Kleijn A, Kloezeman JJ, et al. Serum-free culture success of glial tumors is related to specific molecular profiles and expression of extracellular matrix-associated gene modules. Neuro Oncol 2013;15:1684-95.
12. Lee J, Kotliarova S, Kotliarov Y, et al. Tumor stem cells derived from glioblastomas cultured in bFGF and EGF more closely mirror the phenotype and genotype of primary tumors than do serum-cultured cell lines. Cancer Cell 2006;9:391-403.
13. Cheema TA, Wakimoto H, Fecci PE, et al. Multifaceted oncolytic virus therapy for glioblastoma in an immunocompetent cancer stem cell model. Proc Natl Acad Sci U S A 2013;110:12006-11.
14. Buijs PR, van Eijck CH, Hofland LJ, Fouchier RA, van den Hoogen BG. Different responses of human pancreatic adenocarcinoma cell lines to oncolytic Newcastle disease virus infection. Cancer Gene Ther 2014;21:24-30.
15. Pasqualini R, Koivunen E, Ruoslahti E. Alpha v integrins as receptors for tumor targeting by circulating ligands. Nature biotechnology 1997;15:542-6.
16. Balvers RK, Belcaid Z, van den Hengel SK, et al. Locally-delivered T-cell-derived cellular vehicles efficiently track and deliver adenovirus delta24-RGD to infiltrating glioma. Viruses 2014;6:3080-96.

17. Galli R, Binda E, Orfanelli U, et al. Isolation and characterization of tumorigenic, stem-like neural precursors from human glioblastoma. Cancer Res 2004;64:7011-21.
18. Gursel DB, Shin BJ, Burkhardt JK, Kesavabhotla K, Schlaff CD, Boockvar JA. Glioblastoma stem-like cells-biology and therapeutic implications. Cancers 2011;3:2655-66.
19. Chou TC, Talalay P. Quantitative analysis of dose-effect relationships: the combined effects of multiple drugs or enzyme inhibitors. Advances in enzyme regulation 1984;22:27-55.
20. Chou TC. Preclinical versus clinical drug combination studies. Leuk Lymphoma 2008;49:2059-80.
21. http://nihclinicalcollection.com/. last visited september 2014.
22. Luo Z, Sheng J, Sun Y, et al. Synthesis and evaluation of multi-target-directed ligands against Alzheimer's disease based on the fusion of donepezil and ebselen. J Med Chem 2013;56:9089-99.
23. Singh N, Halliday AC, Thomas JM, et al. A safe lithium mimetic for bipolar disorder. Nature communications 2013;4:1332.
24. Tsuneizumi T, Babb SM, Cohen BM. Drug distribution between blood and brain as a determinant of antipsychotic drug effects. Biological psychiatry 1992;32:817-24.
25. Wang W, Yang Y, Ying C, et al. Inhibition of glycogen synthase kinase-3beta protects dopaminergic neurons from MPTP toxicity. Neuropharmacology 2007;52:1678-84.
26. Leonard BE. A comparison of the pharmacological properties of the novel tricyclic antidepressant lofepramine with its major metabolite, desipramine: a review. International clinical psychopharmacology 1987;2:281-97.
27. Jiang H, White EJ, Rios-Vicil CI, Xu J, Gomez-Manzano C, Fueyo J. Human adenovirus type 5 induces cell lysis through autophagy and autophagy-triggered caspase activity. J Virol 2011;85:4720-9.
28. Bartlett DL, Liu Z, Sathaiah M, et al. Oncolytic viruses as therapeutic cancer vaccines. Mol Cancer 2013;12:103.
29. Berghauser Pont LM, Spoor JK, Venkatesan S, et al. The Bcl-2 inhibitor Obatoclax overcomes resistance to histone deacetylase inhibitors SAHA and LBH589 as radiosensitizers in patient-derived glioblastoma stem-like cells. Genes Cancer 2014;5:445-59.
30. Berghauser Pont LM, Naipal K, Kloezeman JJ, et al. DNA damage response and anti-apoptotic proteins predict radiosensitization efficacy of HDAC inhibitors SAHA and LBH589 in patient-derived glioblastoma cells. Cancer Lett 2014.
31. Balvers RK, Lamfers ML, Kloezeman JJ, et al. ABT-888 enhances cytotoxic effects of temozolomide independent of *MGMT* status in serum free cultured glioma cells. J Transl Med 2015;13:74.
32. Pollard SM, Yoshikawa K, Clarke ID, et al. Glioma stem cell lines expanded in adherent culture have tumor-specific phenotypes and are suitable for chemical and genetic screens. Cell Stem Cell 2009;4:568-80.
33. Jiang P, Mukthavaram R, Chao Y, et al. Novel anti-glioblastoma agents and therapeutic combinations identified from a collection of FDA approved drugs. J Transl Med 2014;12:13.
34. Alonso MM, Jiang H, Yokoyama T, et al. Delta-24-RGD in combination with RAD001 induces enhanced anti-glioma effect via autophagic cell death. Mol Ther 2008;16:487-93.
35. Lamfers ML, Fulci G, Gianni D, et al. Cyclophosphamide increases transgene expression mediated by an oncolytic adenovirus in glioma-bearing mice monitored by bioluminescence imaging. Mol Ther 2006;14:779-88.

36. Alonso MM, Gomez-Manzano C, Jiang H, et al. Combination of the oncolytic adenovirus ICOVIR-5 with chemotherapy provides enhanced anti-glioma effect *in vivo*. Cancer Gene Ther 2007;14:756-61.
37. Ulasov IV, Sonabend AM, Nandi S, Khramtsov A, Han Y, Lesniak MS. Combination of adenoviral virotherapy and temozolomide chemotherapy eradicates malignant glioma through autophagic and apoptotic cell death *in vivo*. Br J Cancer 2009;100:1154-64.
38. Holzmuller R, Mantwill K, Haczek C, et al. YB-1 dependent virotherapy in combination with temozolomide as a multimodal therapy approach to eradicate malignant glioma. Int J Cancer 2011;129:1265-76.
39. Idema S, Lamfers ML, van Beusechem VW, et al. AdDelta24 and the p53-expressing variant AdDelta24-p53 achieve potent anti-tumor activity in glioma when combined with radiotherapy. J Gene Med 2007;9:1046-56.
40. Geoerger B, Grill J, Opolon P, et al. Potentiation of radiation therapy by the oncolytic adenovirus dl1520 (ONYX-015) in human malignant glioma xenografts. Br J Cancer 2003;89:577-84.
41. McKenzie BA, Zemp FJ, Pisklakova A, et al. In vitro screen of a small molecule inhibitor drug library identifies multiple compounds that synergize with oncolytic myxoma virus against human brain tumor-initiating cells. Neuro Oncol 2015.
42. Diallo JS, Le Boeuf F, Lai F, et al. A high-throughput pharmacoviral approach identifies novel oncolytic virus sensitizers. Mol Ther 2010;18:1123-9.
43. Passer BJ, Cheema T, Zhou B, et al. Identification of the ENT1 antagonists dipyridamole and dilazep as amplifiers of oncolytic herpes simplex virus-1 replication. Cancer Res 2010;70:3890-5.
44. Bieler A, Mantwill K, Dravits T, et al. Novel three-pronged strategy to enhance cancer cell killing in glioblastoma cell lines: histone deacetylase inhibitor, chemotherapy, and oncolytic adenovirus dl520. Hum Gene Ther 2006;17:55-70.
45. Liikanen I, Monsurro V, Ahtiainen L, et al. Induction of interferon pathways mediates *in vivo* resistance to oncolytic adenovirus. Mol Ther 2011;19:1858-66.
46. Jiang H, Gomez-Manzano C, Aoki H, et al. Examination of the therapeutic potential of Delta-24-RGD in brain tumor stem cells: role of autophagic cell death. J Natl Cancer Inst 2007;99:1410-4.
47. Abou El Hassan MA, van der Meulen-Muileman I, Abbas S, Kruyt FA. Conditionally replicating adenoviruses kill tumor cells via a basic apoptotic machinery-independent mechanism that resembles necrosis-like programmed cell death. J Virol 2004;78:12243-51.
48. Baird SK, Aerts JL, Eddaoudi A, Lockley M, Lemoine NR, McNeish IA. Oncolytic adenoviral mutants induce a novel mode of programmed cell death in ovarian cancer. Oncogene 2008;27:3081-90.
49. Kleijn A, Kloezeman J, Treffers-Westerlaken E, et al. The In Vivo Therapeutic Efficacy of the Oncolytic Adenovirus Delta24-RGD Is Mediated by Tumor-Specific Immunity. PLoS One 2014;9:e97495.
50. Schleuning M, Brumme V, Wilmanns W. Growth inhibition of human leukemic cell lines by the phenothiazine derivative fluphenazine. Anticancer Res 1993;13:599-602.
51. Gil-Ad I, Shtaif B, Levkovitz Y, Dayag M, Zeldich E, Weizman A. Characterization of phenothiazine-induced apoptosis in neuroblastoma and glioma cell lines: clinical relevance and possible application for brain-derived tumors. Journal of molecular neuroscience : MN 2004;22:189-98.

52. Hwang MK, Min YK, Kim SH. Calmodulin inhibition contributes to sensitize TRAIL-induced apoptosis in human lung cancer H1299 cells. Biochemistry and cell biology = Biochimie et biologie cellulaire 2009;87:919-26.
53. Lin YK, Leu YL, Yang SH, Chen HW, Wang CT, Pang JH. Anti-psoriatic effects of indigo naturalis on the proliferation and differentiation of keratinocytes with indirubin as the active component. Journal of dermatological science 2009;54:168-74.
54. Hoessel R, Leclerc S, Endicott JA, et al. Indirubin, the active constituent of a Chinese antileukaemia medicine, inhibits cyclin-dependent kinases. Nat Cell Biol 1999;1:60-7.
55. Rahman SH, Bobis-Wozowicz S, Chatterjee D, et al. The nontoxic cell cycle modulator indirubin augments transduction of adeno-associated viral vectors and zinc-finger nuclease-mediated gene targeting. Hum Gene Ther 2013;24:67-77.
56. Mok CK, Kang SS, Chan RW, et al. Anti-inflammatory and antiviral effects of indirubin derivatives in influenza A (H5N1) virus infected primary human peripheral blood-derived macrophages and alveolar epithelial cells. Antiviral research 2014;106:95-104.
57. Hertel L, Chou S, Mocarski ES. Viral and cell cycle-regulated kinases in cytomegalovirus-induced pseudomitosis and replication. PLoS Pathog 2007;3:e6.
58. Hsuan SL, Chang SC, Wang SY, et al. The cytotoxicity to leukemia cells and antiviral effects of Isatis indigotica extracts on pseudorabies virus. Journal of ethnopharmacology 2009;123:61-7.
59. Leclerc S, Garnier M, Hoessel R, et al. Indirubins inhibit glycogen synthase kinase-3 beta and CDK5/p25, two protein kinases involved in abnormal tau phosphorylation in Alzheimer's disease. A property common to most cyclin-dependent kinase inhibitors? J Biol Chem 2001;276:251-60.
60. Benson JM, Shepherd DM. Dietary ligands of the aryl hydrocarbon receptor induce anti-inflammatory and immunoregulatory effects on murine dendritic cells. Toxicol Sci 2011;124:327-38.
61. Yuskaitis CJ, Jope RS. Glycogen synthase kinase-3 regulates microglial migration, inflammation, and inflammation-induced neurotoxicity. Cellular signalling 2009;21:264-73.
62. Samudio I, Harmancey R, Fiegl M, et al. Pharmacologic inhibition of fatty acid oxidation sensitizes human leukemia cells to apoptosis induction. J Clin Invest 2010;120:142-56.
63. Driffort V, Gillet L, Bon E, et al. Ranolazine inhibits NaV1.5-mediated breast cancer cell invasiveness and lung colonization. Mol Cancer 2014;13:264.

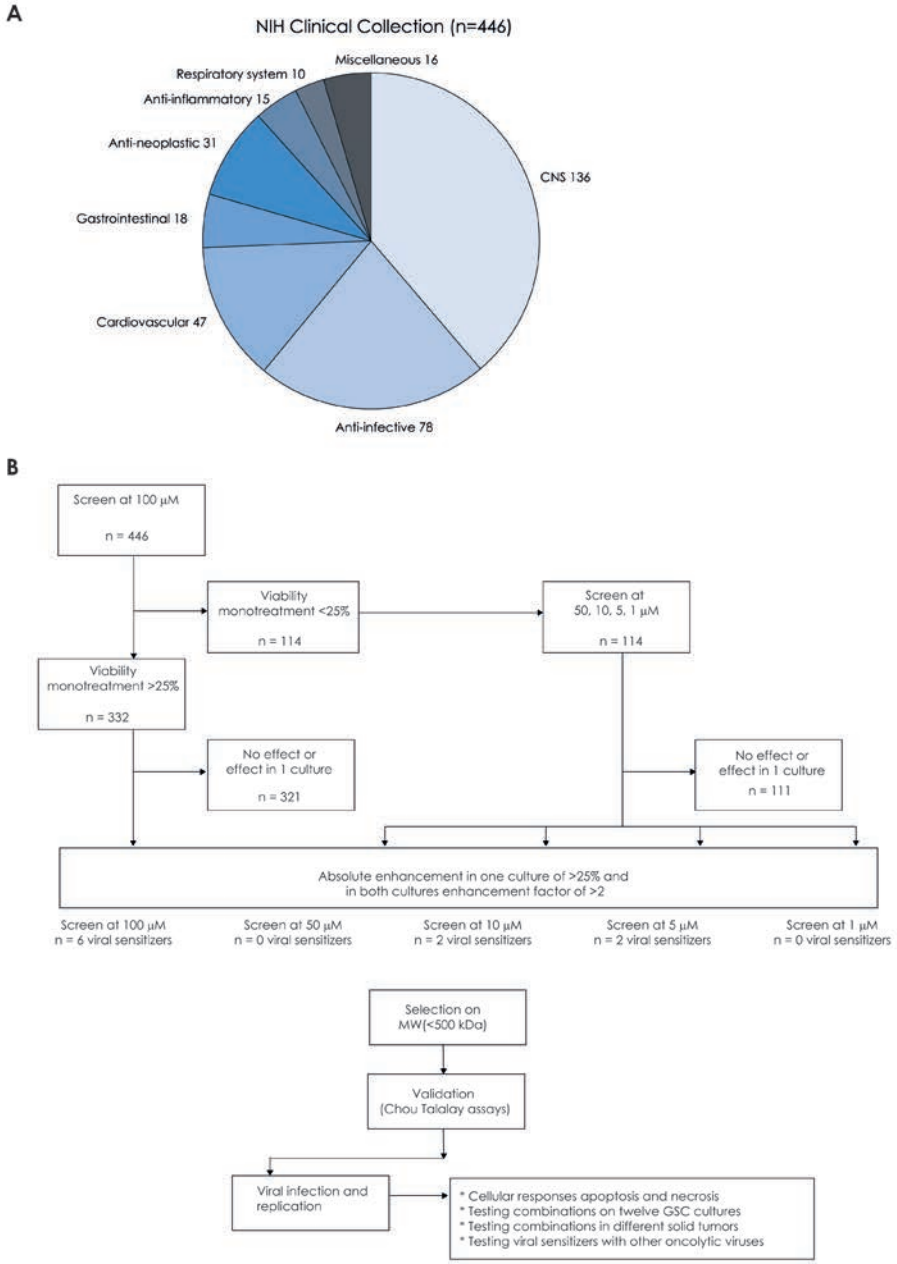

Supplementary Figure 1. The contents of the NIH clinical collection and the drug screening strategy.

(A) The strategy of the compound screening approach is shown schematically. A total of three screens were sequentially performed (first at 100µM, followed by 10 and 1µM, and lastly at 50 and 5µM) using the NIH clinical collection which contains 446 drugs. After these screens, potential viral sensitizers were selected based on enhancement, and ten of the agents were validated using the Chou-Talalay method in the patient-derived GS79 GSC culture. After that, the validated potential viral sensitizers were evaluated for their effects on viral

mechanisms being infection, replication and cellular responses. Finally, four selected compounds were tested on an additional 12 patient-derived GSCs to evaluate their potential use for further *in vivo* studies. **(B)** The NIH clinical collection was used for the compound screen on the patient-derived GSCs. It contains 446 different clinical agents of which 136 were central nervous system (CNS)-related compounds.

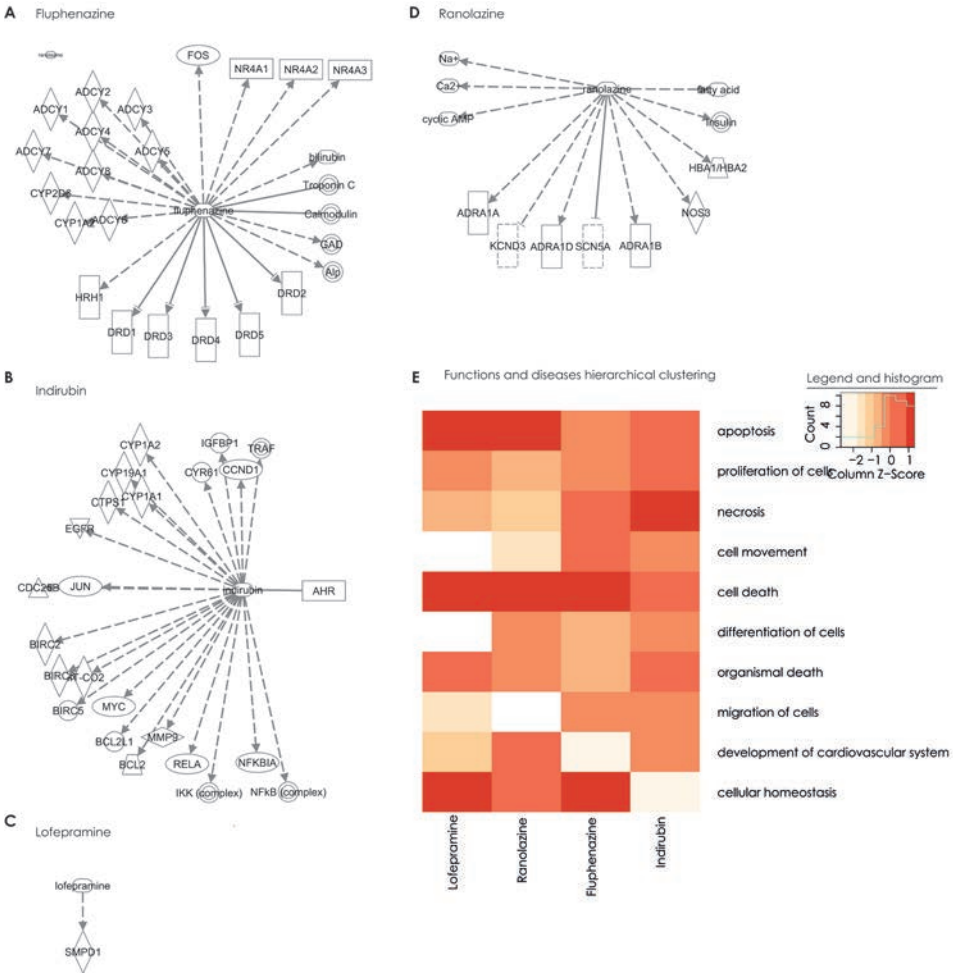

Supplementary Figure 2. In silico analysis confirms viral sensitizers interact with pathways canonical for Delta24-RGD therapeutic outcome.

(A-D) The direct and indirect downstream molecules and proteins (only first order) of the four viral sensitizers (a-d). The dashed arrows indicate indirect relationships whereas the closed arrows show direct relationships with the molecules. **(E)** The common functions and diseases for the four compounds in hierarchical clustered based on p-value of the overlap. All were significant (<0.001), and the data was derived using the IPA September 2014. The top ten of functions and diseases are shown in the heat map. The z-value represents the normalized p-value for each agent.

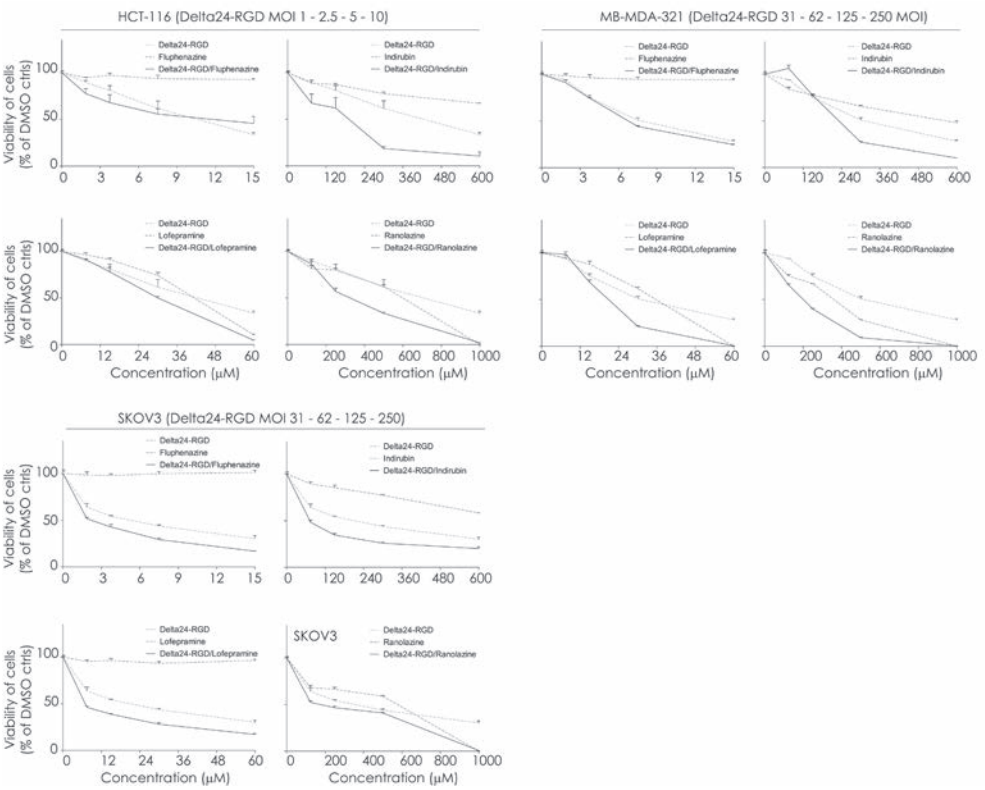

Supplementary Figure 3. Drug/virus combination effects in different solid tumor cell lines.
Dose-response combination assays were performed using Chou-Talalay analysis to study synergy between Delta24-RGD and the four viral sensitizers in three tumor cell lines, being triple negative breast, ovarian and colon carcinoma cells. Viability was measured at day five post-treatment. The dose-response graphs are shown as mean percentage viability compared to DMSO treated controls with the standard deviation.

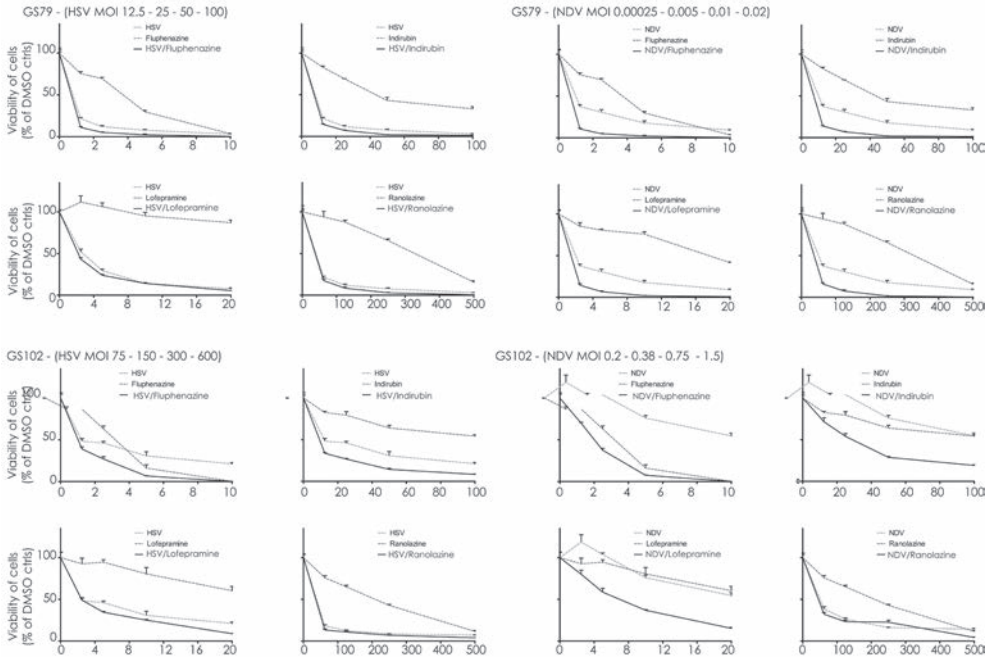

Supplementary Figure 4. Drug/virus combination effects with different OVs.

Dose-response combination assays were performed using Chou-Talalay assays to study synergy between the four viral sensitizers and the HSV-based and NDV oncolytic viruses in the GSCs GS79 and GS102. Viability was measured at day five post-treatment. The dose-response graphs are shown as mean percentage viability compared to DMSO treated controls with the standard deviation.

Chapter 9
General discussion

This general discussion will highlight our most important findings. We discuss the limitations of the studies and the barriers for translation to clinical practice. We will also discuss the next logical steps towards further research.

9.1 Main results

In Part I of this thesis we find a subset of patient derived glioblastoma stem-like cells (GSCs) to be responsive to histone deacetylase inhibitors (HDACi) and radiation. The proteins of pChek2 and Bcl-XL showed to be promising markers for response prediction. We have shown that the latter belongs to a mechanism of resistance. By using the patient-derived GSC model we could identify the large heterogeneity in response to therapy, also for the regimen of HDACi/radiation. We found that the sequence and timing of drug administration is of great importance in combination therapy. We next show that the inhibition of the Bcl-2 family proteins by Obatoclax overcomes the resistance to HDACi, specifically to HDACi as radiosensitizers. This underlines the role of anti-apoptotic proteins in glioblastoma. Again, we found variations in the treatment response among a large panel of cultures. However, we also found that gene expression profiling can provide valuable profiles of prediction. One of the genes we identified as having predictive value, FBXW7, has been reported to be associated to HDACi and Bcl-2 inhibitor therapy response before.

In Part II we show that the anti-epileptic drugs valproic acid, phenytoin and levetiracetam do not negatively interfere with Delta24-RGD oncolysis. The HDACi valproic acid even positively enhanced the oncolytic virus Delta24-RGD in U118 and U373 cell lines. More effective however are the widely-acting HDACi Scriptaid and LBH589, of which the first is an experimental agent. We again find heterogeneity in response between the different GSC cultures in accordance with the first part of this thesis. In this study we have identified only small associations with molecular background including integrin levels and gene expression of retinoblastoma pathway molecules.

In Parts I and II we aimed at circumventing the potential limitations of drug translation to the clinical setting by drug repurposing. We performed a large clinical drug screen to find new agents for glioblastoma that can be used as adjuvants to existing therapies (part I) and that enhance the oncolytic virus Delta24-RGD. We identified various agents including amiodarone, clofazimine and triptolide that provide opportunities for future studies in glioblastoma. Fluphenazine, indirubin, lofepramine and ranolazine show viral sensitizing effects for Delta24-RGD. Our findings also suggest the existence of a general underlying mechanism for these viral sensitizers because the synergy also exists between those drugs and two other oncolytic viruses, as well as with Delta24-RGD in a set of different solid tumor cell lines other than glioblastoma.

9.2 The patient-derived glioblastoma culture model: limitations and future studies

By using the patient-derived GSC model, we were able to study the heterogeneity in response to treatment. This model represents all four subtypes in glioblastoma: neural, proneural, classical and mesenchymal.[1] Moreover, both methylated and unmethylated tumors can be cultured.[2] Preliminary data shows that responses *in vitro* correspond to the response *in vivo*.(unpublished) Others have found that the predictive value of *MGMT* also holds in the *in vitro* patient-derived glioblastoma model in relation to temozolomide response.[3] The GSC model also reflects the original tumors' characteristics in *in vivo* models.[1,4] In our studies we were able to match the molecular characteristics of the tumors at

various levels with the degree of the therapeutic response, including *MGMT* promoter methylation status, DNA repair and apoptotic pathway status and the whole genome expression levels. This has led to identification of potential biomarkers. This is an advantage compared to the conventional models making use of high passage established cell lines cultured in serum supplemented culture medium. Also, because we studied cultures originating from both recurrent and primary glioblastomas, our studies give an indication whether the drugs can be candidate therapeutics for the recurrent glioblastoma as well. These are all advantages compared to the conventional immortalized models.

Whereas this model provides opportunities and a large improvement there are also limitations. The most important is that not all glioblastomas can be cultured.[1,4] Only about 30% of all delivered specimens will grow successfully in neurosphere formation.[1] Literature shows that one of the selection criteria for this feature is the loss of the chromosome 10q on which the PTEN gene is located.[1]

Other possibilities of studying the used therapeutic modalities are using assays in more complex models. Preferably models should be used that exhibit the characteristics of the glioblastoma, including proliferation, migration and invasion.[5] More complex systems can be found in three-dimensional systems. We have studied inhibition of invasion in the three-dimensional invasion neurosphere assay originating from patient-derived GSCs. A next step in complexity is the organotypic spheroid model system. The structure includes tumor cells, but also includes connective tissue, immune cells and moreover capillaries which origin from glioblastoma specimens.[6] These have a life-span of about sixteen weeks.[6] Another option are the organotypic slice cultures which have a shorter life-span.[7] These slices also show heterogeneous responses to therapy.[7] Studying viability in those models requires reliable viability assays which should be feasible for high throughput screenings.[8-10]

Another important step to take is studying the agents in drug delivery systems. The patient-derived GSC model is not suitable for studying drug delivery. New solutions in which lipid vesicles are used as a drug carrier might provide opportunities to handle the blood brain barrier (BBB) passaging problem. Specifically this would be needed in peritumoral areas with intact an blood brain barrier. If drug delivery is a limitation in our identified agents, e.g. the clinical drugs, than there are various manners to overcome this. Currently, an example is provided by the technique of the glutathione PEGylated liposomal particles. There is a phase I/II clinical trial ongoing that delivers doxorubicin to the brain by this method (2B3-101), in solid tumors, brain cancer including glioblastoma and in breast cancer.[11] Such techniques may lead to extensive drug repurposing.

9.3 Drug treatments and molecular profiles

Effects of combination therapies can be ambiguous. On the one hand, drug combination can lead to synergy which allows dose reductions of either agent, subsequently limiting toxicity and potential adverse effects. On the other hand, there is also a risk of induction of adverse effects and toxicity. Importantly, in our studies we indeed found effects of the drug combination of HDACi as radiosensitizers; of Bcl-2 inhibitors and HDACi; of HDACi with Delta24-RGD. In all those studies, we found large heterogeneity in response. The consequences for clinical translation are uncertain: firstly, the response of only subgroups makes drugs less interesting in the first place for large clinical trials. On the other hand,

we have aimed at finding predictors of response. This could be beneficial for trials as only patients that are likely to respond will receive the treatment. Also, tumors that are unlikely to respond to therapy would not be treated with ineffective therapies.

The fact that responses to the tested combination therapies are not determined by *MGMT* promoter methylation status, and show efficacy in GSCs that origin from unmethylated tumor specimens, is promising. For those patients currently no additional effects of concomitantly administered drugs exist.[12] Patients with unmethylated tumors are therefore a logical subject to include in new trials, which is already done in various studies.[11,13,14]

The molecular profiles we have identified as candidate predictors of response need validation *in vivo*, most likely first in retrospect and later prospectively. Since various clinical trials have been performed using HDACi, including VPA, SAHA and LBH589[11], we recommend correlating the molecular tumor markers including anti-apoptotic proteins and DNA damage response proteins, and if cell culture material is available p-Chek2 upon radiation, to treatment response retrospectively.

9.4 Toward precision medicine

We touched upon the concept of precision medicine in the introduction. The research field is shifting towards this approach. This change takes time, but early adopters have already taken steps forward in poor prognostic malignancies such as lung and pancreatic carcinoma.[15-17] These trials focus on subgroups of patients with genotypically or phenotypically defined tumors. These groups can be rather small, which may lead to difficulties regarding analysis, control groups and ethics.[18] In the future, other trials than large randomized cohorts, will be needed to support precision medicine. This may require the n-is-one trial, which includes studying various strategies in one individual, in order to find the best intervention for the patient.[19] As a researcher and as a clinician, one should realize that new trials in a precision medicine setting will require collaboration between centers and moreover collaboration between disciplines.[18] This should facilitate sharing knowledge, increasing comprehensiveness of studies and performing trials at for example mutational level instead of tumor type level (i.e. glioblastoma, lung cancer). This also changes the role of the pharmaceutical industry and provides challenges for this field.

The shift from the concept of 'one drug fits all' to personalized or precision medicine also has great consequences for clinical trial design. However, several experts in the field of trial design in clinical oncology have proposed valuable solutions for this problem.[19-21]

9.5 Oncolytic virotherapy

The finding of lack of interference with anti-epileptics and Delta24-RGD is important, as in the clinical setting usually a scale of medications is prescribed to patients with glioblastoma. For example dexamethasone, which is provided to almost every patient with glioblastoma, has shown to inhibit the viral efficacy.[22] Various studies on oncolytic virus trials now have shown their data and show safety, but also heterogeneity in responses.[23-25] The oncolytic virus Delta24-RGD has ended phase I/II testing in 2014 in glioblastoma patients.[23] There are indications that the initial mode of action is primarily oncolysis caused by the virus, but subsequently the immune response is activated which may eradicate tumor cells.[22,26,27] The advantage of activation of the immune system in glioblastoma is

promising: invaded and migrated tumor cells can then be reached by the immune system, independently of the limited drug penetration.

The therapeutic responses in oncolytic virus trials are encouraging for further development and optimization of this therapeutic strategy. There are many options by which oncolytic virotherapy can be boosted, including increasing infection, replication, oncolysis, by enhancing viral delivery, or by stimulating the immune response.[28-30] Our data provide therapeutic options in four drugs that enhance the viral infection, replication and oncolysis. We also show that the effects of these drugs are not limited to glioblastoma nor to enhancement of Delta24-RGD alone. In terms of future studies, one could thus consider to design new trials including oncolytic virotherapy in combination with clinical drugs that include larger groups of solid tumors. Before this step is taken, more knowledge on the viral sensitizers' behavior on the immune response are desirable. This could be done via the conventional way, treating mice that have an immune system different from the human immune system, or via an unconventional way: studying the immune alterations in patient groups that are already being treated with the clinical drug for another disorder.

9.6 Survival versus outcome

In this thesis, the studies performed in the laboratory setting are focusing on measures of viability, cell death or toxicity. These measures are translated to survival. A clinician should think not only about curing the disease, but also about how to achieve the best quality of life for patients. In the clinical setting, outcome should be viewed as broader, not only including mortality but also quality of life and for example the occurrence of disease related complications.[31,32] The whole set of outcomes at the three levels of survival, short term recovery and sustainability of the provided care to the patient should be taken into account.[33] The three levels of outcome include measures that matter to the patient in the cycle of treatment. For glioma/glioblastoma patients, these measures of course include survival, but also the ability to be independent, the cognitive functioning, the patient-reported quality of life, the level of epilepsy control and the complications experienced during and after treatment (multidisciplinary consensus reached in our center).

We put our research in this context. One way to improve quality of life is to avoid overtreatment of those patients that would not benefit from treatment, or rather to assign the appropriate treatment to the patient that will respond to that treatment. We sought for subgroups of responders and non-responders using the molecular background of the tumor or culture. This has led to identification of both indicators of response, as well as potential predictors of response. (Early) indicators of response can monitor effects and could guide whether to continue treatment or to switch to another therapeutic option. Potential predictors of response can aid in assigning the most effective treatment to a susceptible tumor.

In our studies another possibility to improve outcome in a broader context than survival alone is the use of therapeutic combinations. However, where combination drugs may allow dose reductions of single agents and may increase survival, one should consider the possibility that combination therapies can synergize at the level of side effects. This holds for oncolytic virus therapy as well as for the investigated drugs. Another way that allows dose reductions and increases therapeutic efficacy is the identification of the optimal sequencing and timing of drug combinations. We show this for the HDACi combination

therapies. Clearly, in the radiation setting HDACi efficacy is largest when given 24 hours before radiation is applied. In the setting of viruses, another mechanism is underlying combination effects and the effects are optimal when concomitantly administered.

Lastly, especially in a non-curable disease such as glioblastoma, the quality of life should be centralized in providing health care. Applying the principles of precision medicine in clinical practice could be a step forward in both survival and in improving quality of life in patients with glioblastoma.

References

1. Balvers RK, Kleijn A, Kloezeman JJ, et al. Serum-free culture success of glial tumors is related to specific molecular profiles and expression of extracellular matrix-associated gene modules. Neuro Oncol 2013;15:1684-95.
2. Berghauser Pont LM, Naipal K, Kloezeman JJ, et al. DNA damage response and anti-apoptotic proteins predict radiosensitization efficacy of HDAC inhibitors SAHA and LBH589 in patient-derived glioblastoma cells. Cancer Lett 2014.
3. Fouse SD, Nakamura JL, James CD, Chang S, Costello JF. Response of primary glioblastoma cells to therapy is patient specific and independent of cancer stem cell phenotype. Neuro Oncol 2014;16:361-71.
4. Lee J, Kotliarova S, Kotliarov Y, et al. Tumor stem cells derived from glioblastomas cultured in bFGF and EGF more closely mirror the phenotype and genotype of primary tumors than do serum-cultured cell lines. Cancer Cell 2006;9:391-403.
5. Weber GL, Parat MO, Binder ZA, Gallia GL, Riggins GJ. Abrogation of PIK3CA or PIK3R1 reduces proliferation, migration, and invasion in glioblastoma multiforme cells. Oncotarget 2011;2:833-49.
6. Grill J, Lamfers ML, van Beusechem VW, et al. The organotypic multicellular spheroid is a relevant three-dimensional model to study adenovirus replication and penetration in human tumors *in vitro*. Mol Ther 2002;6:609-14.
7. Merz F, Gaunitz F, Dehghani F, et al. Organotypic slice cultures of human glioblastoma reveal different susceptibilities to treatments. Neuro Oncol 2013;15:670-81.
8. Vinci M, Gowan S, Boxall F, et al. Advances in establishment and analysis of three-dimensional tumor spheroid-based functional assays for target validation and drug evaluation. BMC Biol 2012;10:29.
9. Ivanov DP, Parker TL, Walker DA, et al. Multiplexing spheroid volume, resazurin and acid phosphatase viability assays for high-throughput screening of tumour spheroids and stem cell neurospheres. PLoS One 2014;9:e103817.
10. Gantenbein-Ritter B, Potier E, Zeiter S, van der Werf M, Sprecher CM, Ito K. Accuracy of three techniques to determine cell viability in 3D tissues or scaffolds. Tissue Eng Part C Methods 2008;14:353-8.
11. Health NIo. Www.clinicaltrials.gov. last visited May 2015.
12. Stupp R, Hegi ME, Mason WP, et al. Effects of radiotherapy with concomitant and adjuvant temozolomide versus radiotherapy alone on survival in glioblastoma in a randomised phase III study: 5-year analysis of the EORTC-NCIC trial. Lancet Oncol 2009;10:459-66.
13. Nabors LB, Fink KL, Mikkelsen T, et al. Two cilengitide regimens in combination with standard treatment for patients with newly diagnosed glioblastoma and

unmethylated *MGMT* gene promoter: results of the open-label, controlled, randomized phase II CORE study. Neuro Oncol 2015;17:708-17.
14. Motomura K, Natsume A, Kishida Y, et al. Benefits of interferon-beta and temozolomide combination therapy for newly diagnosed primary glioblastoma with the unmethylated *MGMT* promoter: A multicenter study. Cancer 2011;117:1721-30.
15. Politi K, Herbst RS. Lung Cancer in the Era of Precision Medicine. Clin Cancer Res 2015;21:2213-20.
16. Chantrill LA, Nagrial AM, Watson C, et al. Precision Medicine for Advanced Pancreas Cancer: The Individualized Molecular Pancreatic Cancer Therapy (IMPaCT) Trial. Clin Cancer Res 2015;21:2029-37.
17. Delaloge S, Caron O, Feunteun J. Effect of PALB2 status on breast cancer precision medicine. Lancet Oncol 2015.
18. Hamburg MA, Collins FS. The path to personalized medicine. The New England journal of medicine 2010;363:301-4.
19. Lillie EO, Patay B, Diamant J, Issell B, Topol EJ, Schork NJ. The n-of-1 clinical trial: the ultimate strategy for individualizing medicine? Personalized medicine 2011;8:161-73.
20. Sleijfer S, Bogaerts J, Siu LL. Designing transformative clinical trials in the cancer genome era. J Clin Oncol 2013;31:1834-41.
21. Hayes DF, Markus HS, Leslie RD, Topol EJ. Personalized medicine: risk prediction, targeted therapies and mobile health technology. BMC medicine 2014;12:37.
22. Koks CA, De Vleeschouwer S, Graf N, Van Gool SW. Immune Suppression during Oncolytic Virotherapy for High-Grade Glioma; Yes or No? J Cancer 2015;6:203-17.
23. Lang FF, Conrad C, Gomez-Manzano C, et al. First-in-human phase I clinical trial of oncolytic delta-24-rgd (dnx-2401) with biological endpoints: implications for viroimmunotherapy. Neuro Oncol 2014;16 Suppl 3:iii39.
24. Aghi MK, Chiocca EA. Phase ib trial of oncolytic herpes virus G207 shows safety of multiple injections and documents viral replication. Mol Ther 2009;17:8-9.
25. Pol J, Bloy N, Obrist F, et al. Trial Watch:: Oncolytic viruses for cancer therapy. Oncoimmunology 2014;3:e28694.
26. Kleijn A, Kloezeman J, Treffers-Westerlaken E, et al. The therapeutic efficacy of the oncolytic virus Delta24-RGD in a murine glioma model depends primarily on antitumor immunity. Oncoimmunology 2014;3:e955697.
27. Kleijn A, Kloezeman J, Treffers-Westerlaken E, et al. The *in vivo* therapeutic efficacy of the oncolytic adenovirus Delta24-RGD is mediated by tumor-specific immunity. PLoS One 2014;9:e97495.
28. Ning J, Wakimoto H. Oncolytic herpes simplex virus-based strategies: toward a breakthrough in glioblastoma therapy. Front Microbiol 2014;5:303.
29. Chiocca EA, Rabkin SD. Oncolytic viruses and their application to cancer immunotherapy. Cancer immunology research 2014;2:295-300.
30. Bell J, McFadden G. Viruses for tumor therapy. Cell Host Microbe 2014;15:260-5.
31. Corn BW, Wang M, Fox S, et al. Health related quality of life and cognitive status in patients with glioblastoma multiforme receiving escalating doses of conformal three dimensional radiation on RTOG 98-03. J Neurooncol 2009;95:247-57.
32. Taphoorn MJ, Stupp R, Coens C, et al. Health-related quality of life in patients with glioblastoma: a randomised controlled trial. Lancet Oncol 2005;6:937-44.
33. Porter ME. What is value in health care? New England Journal of Medicine 2010;363:2477-81.

Summary

Glioblastoma is the most malignant primary brain tumor. Glioblastoma is originating from the supportive tissue of the brain, the glial cells. Despite increased research, mortality rates have not decreased significantly. Standard therapy consists of surgical resection, temozolomide and radiation therapy. The survival rate is despite maximum treatment 14.6 months. We are currently learning more about markers that correlate to response to treatment, the most important being the *MGMT* promoter methylation status. One of the issues that prevents treatments from being effective is the multiple escape routes glioblastoma has, to circumvent cell death. We aim to tackle this issue using combination therapies in a representative model, namely the patient-derived glioblastoma stem-like cell (GSC) model. This model reflects the molecular characteristics of the original tumor. This model allows studying novel treatment strategies in the context of heterogeneity in response to therapy, and in the context of analyzing molecular differences underlying response. In this thesis, we apply these concepts in a broad range of treatment modalities including combination therapeutics. We aim at optimizing the treatment with enhancers of radiation and of experimental oncolytic virotherapy. We have also used the approach of clinical drug screening in order to repurpose clinical drugs. We aimed at finding clinically applied drugs that may be candidates for glioblastoma treatment.

Part I of this manuscript describes studies on new therapeutic regimens using HDACi in combination with radiation, and using a large clinical drug screen. In Chapter 3 we show that the histone deacetylase inhibitors (HDACi) SAHA, VPA, MS275, LBH589 and Scriptaid, are radiosensitizers in a significant proportion of GSCs. The observed variations in sensitivity show a relationship with molecular characteristics of the specific cultures. Regarding the clinically most relevant HDACi (SAHA and LBH589), differences in the DNA damage and apoptotic response were found between responsive and resistant cultures. Various identified associated molecules that warrant further exploration as candidate response markers are pChek2 for both SAHA/radiation (RTx) and LBH589/RTx, and in addition Bcl-XL for LBH589/RTx with positive predictive values of 90% and 100%.

In Chapter 4 we emphasize the efficacy of the Bcl-2 family pathway inhibition by Obatoclax to reach sensitization of GSCs to HDACi and HDACi/RTx, circumventing a tumor-related resistance mechanism to treatment. The Bcl-2 family proteins are heterogeneously expressed in glioblastoma and 30% to 60% of tumors shows overexpression. We demonstrate that Obatoclax synergized with HDACi and showed efficacy in a large set of GSCs. This pathway is an adequate target to inhibit, in order to achieve better therapeutic efficacy, also in HDACi/RTx therapy. We identified predictive gene expression profiles for the combination treatments with Obatoclax that are associated with cellular regulatory functions.

In Chapter 5 we screened a large drug collection in order to repurpose clinical drugs for the treatment of glioblastoma. This has led to the identification of three clinical compounds that have potential for treating glioblastoma: amiodarone, clofazimine and triptolide. The drugs were selected based on efficacy in GSCs and lack of toxicity in normal human astrocytes. Twenty GSCs were tested for this purpose. Clofazimine and triptolide have previously been identified as potent inhibitors of immortalized glioma cell lines. Amiodarone is a novel candidate for glioblastoma treatment as a single agent.

Part II of this manuscript describes studies on combination therapeutics for oncolytic virus therapy with Delta24-RGD. Delta24-RGD is a conditionally replicating oncolytic virus that has ended phase I/II testing in patients with glioblastoma. To enhance efficacy of oncolytic virus therapy, combination therapies are needed. First of all we tested whether anti-epileptic drugs interacted with Delta24-RGD efficacy. The three agents valproic acid (a weak HDACi), phenytoin and levetiracetam were studied. HDACi have been reported to alter oncolytic viral activity. In Chapter 6 we illustrate that therapeutic levels of the most frequently prescribed anticonvulsants valproic acid, phenytoin and levetiracetam do not negatively influence the oncolytic activity of Delta24-RGD. In some cells, additive effects between drugs and the virus were observed.

In Chapter 7 we show that the novel pan-HDACi Scriptaid and LBH589, which have stronger HDACi activity than valproic acid, exert enhanced anti-tumor activity in combination with Delta24-RGD in GSCs. These HDACi induced slight up-regulation of cell surface integrins, facilitating adenoviral entry and leading to increased levels of viral gene expression. The HDACi induced cell death pathways in the GSCs, thereby accelerating the virus-induced killing of the infected cells but slightly hampering the viral progeny production. The concerted action of these two treatment modalities leads to improved anti-tumor efficacy and shows limited toxicity in normal human astrocytes. Taken together, Scriptaid and LBH589 offer opportunities as potential candidates for future Delta24-RGD combination studies.

Triggered by the long duration of the process of implementation of novel drugs in clinical practice, we aimed at finding effective viral sensitizers by performing a clinical drug screen. Chapter 8 describes the identification of four effective viral sensitizers for oncolytic virotherapy, including fluphenazine, indirubin, lofepramine and ranolazine. We reveal interaction of the drugs with important viral oncolytic cell death mechanism as shown *in silico* and *in vitro*. These drugs, that are known to pass the blood brain barrier, are not only applicable in glioblastoma but show synergy with Delta24-RGD in multiple cancer types. Moreover, all drugs showed synergistic activity with other oncolytic viruses as well.

Nederlandse samenvatting

Het glioblastoom is de meest kwaadaardige primaire hersentumor. Glioblastomen zijn afkomstig van het steunweefsel van de hersenen, de gliacellen. Ondanks het vele wetenschappelijke onderzoek naar deze ziekte is de mortaliteit niet significant afgenomen. De mediane overleving is 14,6 maanden ondanks maximale behandeling met chirurgische resectie, temozolomide en bestraling. Er wordt steeds meer bekend over markers die respons op behandeling kunnen voorspellen. De belangrijkste is de *MGMT* promoter methylatie status. De effectiviteit van behandeling wordt mede verhinderd door de grote resistentie routes van glioblastomen die celdood kunnen omzeilen. In dit onderzoek benaderen wij dit probleem met het uittesten van combinatietherapieën in een representatief model voor het glioblastoom, het 'patient-derived glioblastoma stem-like cell culture' (GSC) model. Dit model heeft de eigenschappen van de oorspronkelijke tumor. Dit model maakt het mogelijk nieuwe behandelingsstrategieën te bestuderen in de context van heterogeniteit. Dit biedt de mogelijkheid moleculaire verschillen te analyseren die ten grondslag liggen aan de respons op therapie.

Dit proefschrift maakt gebruik van bovenstaande concepten bij het testen van een breed scala aan behandelingen. Het onderzoek richt zich op het optimaliseren van bestaande toegepaste behandeling namelijk bestraling en experimentele behandelingen in de zin van oncolytische virus therapie. Daarbij zochten we naar moleculaire profielen die de respons op behandeling konden voorspellen. We hebben getracht om in het kader van 'drug repurposing' klinische medicijnen te vinden die goede kandidaten zijn voor de behandeling van het glioblastoom, al of niet in combinatietherapie.

Deel I van dit manuscript beschrijft studies naar onder andere nieuwe therapeutische combinatiestrategieën met bestraling en histone deacetylase inhibitors (HDACi) In hoofdstuk 3 laten we zien dat de HDACi SAHA, VPA, MS275, LBH589 en Scriptaid de gevoeligheid voor radiotherapie versterken in een aanzienlijk deel van de GSCs. De verschillen in gevoeligheid hebben een relatie met moleculaire karakteristieken van het specifieke culturen, namelijk met de DNA reparatie eiwitten en met Bcl-2 anti-apoptotische celdood eiwitten. Kandidaat voorspellende markers zijn pChek2 voor de respons op SAHA en LBH589 in combinatie met bestraling en Bcl-XL voor de respons op LBH589 in combinatie met bestraling. De positief voorspellende waardes zijn 90% en 100% respectievelijk.

In hoofdstuk 4 benadrukken we het effect van de remming van Bcl-2 familie eiwitten door Obatoclax op het gevoelig maken van GSCs voor HDACi en bestraling. We omzeilen hiermee een tumor gerelateerd resistentiemechanisme voor HDACi behandeling. De Bcl-2 familie eiwitten komen heterogeen tot expressie in glioblastomen, namelijk in 30% tot 60% van de tumoren. Obatoclax en HDACi tonen effectiviteit en synergie in een panel van verschillende GSCs. Remming van de Bcl-2 eiwitten is daarbij ook effectief om GSCs gevoeliger te maken voor HDACi met bestraling. In deze studie laten we zien dat genexpressieprofielen de combinatiebehandelingen van HDACi, maar ook van bestraling, met Obatoclax mogelijk kunnen voorspellen.

In hoofdstuk 5 is een grote collectie getest van klinische middelen in 20 verschillende GSCs. Dit leidde tot de identificatie van drie klinische toegepaste medicijnen die potentieel werkzaam zijn in glioblastomen, namelijk amiodarone, clofazimine en triptolide. Het voordeel van deze middelen is dat ze reeds goedgekeurd zijn voor klinisch gebruik. Dit kan de weg voor implementatie naar de kliniek voor glioblastomen mogelijk verkorten.

De geneesmiddelen hadden beperkte toxiciteit in normale humane astrocyten. De laatste twee middelen zijn eerder geïdentificeerd als krachtige remmers van geïmmortalizeerde glioomcellijnen. Deze drugs zijn kandidaten voor behandeling van het glioblastoom.

Deel II van dit manuscript beschrijft studies over combinatiebehandelingen in het kader van oncolytische virustherapie met Delta24-RGD. Delta24-RGD is een virus dat specifiek in tumorcellen repliceert. Dit virus is reeds getest in een fase I/II klinische trial. Om de effectiviteit van deze therapie te verbeteren zijn combinatietherapieën nodig. Er is getest of anti-epileptica, die frequent aan patiënten voorgeschreven worden, interactie hebben met de werkzaamheid van Delta24-RGD. De drie middelen zijn valproaat (een zwakke HDACi), fenytoïne en levetiracetam. HDACi kunnen de oncolytische virusactiviteit veranderen in kankercellen. In hoofdstuk 6 laten we dan ook zien dat therapeutische concentraties van de meest voorgeschreven anticonvulsiva valproaat, fenytoïne en levetiracetam de oncolytische activiteit van Delta24-RGD niet nadelig beïnvloeden. In sommige cellen werden additieve effecten tussen drugs en het virus waargenomen.

In hoofdstuk 7 laten we zien dat de nieuwere pan-HDACi Scriptaid en LBH589, die sterker HDACi activiteit hebben, de anti-tumor activiteit van Delta24 RGD in de GSCs versterken. In het algemeen kunnen HDACi zorgen voor verhoogde expressie van integrines die de adenovirale infectie faciliteren. Tevens kunnen HDACi verhoogde virale genexpressie veroorzaken. Dit hebben wij ook geobserveerd. De HDACi induceren celdood, via mechanismen als caspase activatie, necrose en autophagie. Deze mechanismen zijn overeenkomstig met de celdood geïnduceerd door Delta24-RGD. We zien dan ook dat er toename is van celdood door combinatie behandeling, echter, het aantal cellen dat dan nog virus aan kan maken neemt ook af. Dit werd vertaald naar verminderde virale productie. Het combinatie effect van het virus en de HDACi, heeft relatief weinig toxiciteit in normale humane astrocyten en is relatief effectief in een selectie van GSCs. Scriptaid en LBH589 bieden mogelijkheden voor combinatietherapie met Delta24-RGD in de toekomst.

Gedreven door de lange duur van het klinische implementatieproces van nieuwe medicijnen, hebben we ons gericht op het vinden van doeltreffende reeds beschikbare klinische middelen die de virale effectiviteit verhogen. Hoofdstuk 8 beschrijft de identificatie van vier effectieve middelen die de virale oncolytische activiteit significant verhogen. Deze middelen zijn fluphenazine, indirubine, lofepramine en ranolazine. Deze middelen hebben interactie met belangrijke virale mechanismen voor oncolytische celdood, bevestigd met *in silico* en *in vitro* analyses. Deze geneesmiddelen passeren de bloed-hersenbarrière en tonen niet alleen effecten in glioblastomen, maar vertonen ook synergie met Delta24-RGD in diverse andere kankersoorten, namelijk in cellijnen van het mammacarcinoom, het ovariumcarcinoom en het coloncarcinoom. Bovendien vertonen alle drugs synergistische werking met twee andere oncolytische virussen. Deze resultaten zijn veelbelovend voor toekomstige klinische studies met oncolytische virussen.

Manuscripts on which this thesis is based

Manuscripts (this thesis)

Chapter 3 DNA damage response and anti-apoptotic proteins predict radiosensitization efficacy of HDAC inhibitors SAHA and LBH589 in patient-derived glioblastoma cells.

Cancer Letters; *Jan 2015*

Chapter 4 The Bcl-2 inhibitor Obatoclax overcomes resistance to histone deacetylase inhibitors SAHA and LBH589 as radiosensitizers in patient-derived glioblastoma stem-like cells.

Genes & Cancer; *Nov 2014*

Chapter 5 *In vitro* screening of clinical drugs on patient-derived glioblastoma stem-like cells identifies amiodarone, clofazimine and triptolide as potential anti-glioma agents.

Submitted

Chapter 6 Therapeutic concentrations of anti-epileptic drugs do not inhibit the activity of the oncolytic adenovirus Delta24-RGD in malignant glioma.

Journal of Gene Medicine; *April 2013*

Chapter 7 The HDAC inhibitors Scriptaid and LBH589 combined with the oncolytic virus Delta24-RGD exert enhanced anti-tumor efficacy in patient-derived glioblastoma cells.

Plos One; *May 2015*

Chapter 8 *In vitro* screening of clinical drugs identifies enhancers of oncolytic viral therapy in glioblastoma stem-like cells.

Gene Therapy; *July 2015*

Acknowledgements / Dankwoord

Na vier jaar te hebben gewerkt aan dit manuscript, wil ik graag de mensen danken zonder wie dit proefschrift er niet was gekomen of die een bijzondere stempel hebben gedrukt op deze periode.

Allereerst gaat mijn dank uit naar mijn copromotor Martine Lamfers en promotoren Clemens Dirven en Sieger Leenstra.

Martine, mijn dank gaat eerst uit naar jou, voor de ondersteuning die je deze jaren hebt gegeven bij de totstandkoming van dit proefschrift. Jouw secure en kritische blik hebben gezorgd voor kwaliteit, inspiratie om dingen te verfijnen. Jouw adviezen bij het uitdenken van de experimenten en de analyse van de data waren onvervangbaar. Erg leuk dat je me zelfs in Boston nog hebt opgezocht!

Sieger, de vrije manier waarop je mij hebt laten nadenken over mijn proefschrift waardeer ik enorm. Vaak kwam ik met een specifieke vraag naar jouw kantoor en eindigden we in een filosofische discussie over waar het met de wetenschap heen gaat, over de grenzen van het behandelen als arts of over indrukwekkende dingen die je meemaakt als neurochirurg. Je hebt duidelijk een inhoudelijke visie maar ook op menselijk vlak mooie inzichten.

Clemens, zeven jaar geleden kwam ik langs met de wens voor een stage in het kader van onderzoek naar het oncolytische virus, door ons beider enthousiasme resulteerde dat bezoek in lange onderzoeksgeschiedenis en een mooi promotietraject. Dank voor de kans dit boek te maken, de inspiratie die je hebt gegeven om op nieuwe manieren naar organisatie van zorg te kijken. Toen ik besloot van Utrecht naar Rotterdam te reizen voor het CSDH onderzoek leerde ik van Ruben Dammers, Joost Schouten, Hester Hulscher, Diederik Dippel en Hester Lingsma hoe leuk het was om onderzoek te doen en dit was het begin in Rotterdam. Naar jullie gaat mijn dank uit voor de mooie start. Ruben ik weet zeker dat er, na onze mooie papers over een *'niet-zo-fancy-onderwerp'*, maar wel relevant onderwerp ooit een goede trial komt voor level I evidence.

Ik dank de leescommissie voor hun tijd die zij hebben gegeven aan het beoordelen van dit proefschrift. Professor Kanaar, dank voor de fijne samenwerking met uw lab, specifiek met Kishan Naipal, Nicole Verkaik en Dik van Gent. Kishan, naast de foci-analyse vond ik de tripjes in San Diego o.a. naar de coyotes een ware aanvulling op onze PhD tijd! Professor van den Bent, Martin, veel dank voor de kritische en constructieve feedback van de afgelopen jaren tijdens besprekingen. Professor Robe, Pierre, met plezier denk ik aan het moment terug dat wij over het HDAC inhibitor onderzoek discussieerden op de LWNO meetings. Professor van der Spek, dr. Pim French en professor Wesseling, dank voor het lezen van mijn manuscript en het zitting willen nemen in de oppositie tijdens de verdediging. Pim, ook met jou waren de uurtjes nadenken over gene expression zeer waardevol. Je hebt vaak een frisse blik op mijn werk gegeven. Professor van der Spek, de samenwerking met u en uw afdeling, namelijk Sigrid Swagemakers en Andreas Kremer, waren vruchtbaar en hebben het onderzoek een stap verder kunnen brengen. Sigrid, jouw snelheid is onevenaarbaar. Andreas, I am delighted that I have gotten to know you. Thank you for critically reading my manuscripts in your spare time next to your busy job.

Dank gaat uit naar mijn collegae op het lab neurochirurgie. Jenneke, Anne, Wouter, Zineb, Mani, Mariëlle, Tessa en Mircea het was een plezier met jullie te werken. Er was

tijd voor vakinhoudelijke discussies en voor gezelligheid. Jenneke het wordt tijd dat het borrelcadeau aangesproken wordt. Het was mooi teamwerk hoe we de revisies aangepakt hebben! Anne, Wouter en Zineb, ik heb geluk gehad met jullie als medepromovendi. Les 1: vraag in Canada nooit naar een club als je bier wilt drinken en les 2: optimisten schatten tijd nooit goed in, ofwel als je gaat FACS-en moet je eerder pizza bestellen. En als jullie gaan karten doe ik uiteraard graag weer mee! Ik dank de studenten die onder mijn begeleiding aan de projecten hebben gewerkt: Anoek van Leeuwen, Megan van Vooren en Somia Koria.

Anja Onstenk, dank voor jouw inzet bij het regelen van de vele zaken rondom de promotie en mijn werk. De afdeling neurochirurgie van het ErasmusMC dank ik voor de support de afgelopen tijd, dank aan degenen die betrokken waren om het benodigde resectie materiaal aan te leveren alsook aan hen die het begrip hebben dat combineren van promotie en opleiding soms zwaar is.

Dank aan Jeroen de Vrij, Marike Broekman en Niek Maas voor de leuke samenwerking op het lab.

Dr. Lawler and Professor Chiocca, Sean and Nino, I sincerely thank you for the chance you have given me to work in your laboratories and be part of an awesome research group. With great pleasure I think back of this internship. In addition I thank my supervisors in Rotterdam for supporting me during this project. I thank all my collegues in Boston, in specific the Lawler lab (Fong, Marica, Oskar). It has been a great pleasure working with all of you. Thanks for the help with the experiments, making troubles and sharing thoughts with me.

Chrisje, al meer dan tien jaar een dikke maatjes en gelukkig bestaat het Chris-Lot-dagje sinds een tijd omdat je toch soms dingen moet plannen als je druk bent. Jij was er altijd als ik het nodig had en je steun was onvoorwaardelijk!

Leo voor jou geldt dat ook! We verdedigen we binnen 4 weken van elkaar, ik op jouw verjaardag en zijn we elkaars paranimfen. Fantastisch dat je langskwam en mij in liet zien dat NYC echt een must is: cultuurbarbaren in een leuk hostel. JC Kaas, Do, Amy, Daisy, kroonluchters, skivakanties, escape rooms, Vondelpark, dit alles hoorde bij de ontspanning waarvan jullie tijdens mijn promotietijd deel uitmaakten. Noor, onze trip met in 2006 met de Prins van Oranje en in volle vaart de Valentino af was de basis voor veel wijsheid en zotheid als ik Erasmus mag aanhalen. Jij legde contact met een oudhuisgenoot in Boston die me wegwijs maakte, gelukkig kwam je zelf ook nog langs voor een expeditie! Ruth, dank voor je altijd wijze woorden, tripods! Virginie dank voor je hulp bij alle promotievoorbereidingen.

Marnix en Nick, beste maatjes van mijn basis en middelbare school, dank voor jullie relativerende blikken, even een ander ‘onderwerp van gesprek’ en de intellectuele support. Door jullie krijg ik ook mee wat er buiten het ziekenhuis gebeurt. Marcel en Wouter, dank voor de inzet t.a.v. ‘de disco’, zonder deze joint effort had ik nooit meer voldoende slaap gehad om een mooi proefschrift te genereren. Ladies van de Poort, ook jullie hebben aan het begin gestaan van mijn promotieonderzoek, dank voor jullie altijd aanwezige interesse!

Mijn Bostonmaatjes Anil, Guusje, Koen, Rosalie, Lisa, Tobi en Gijs wil ik danken voor de fantastische en onvergetelijke tijd. Anil, ik ben blij bijgedragen te hebben aan de kennis over groente en fruit. Tobi, you still owe me some scrambled eggs. Guus en Koen, dat bijzondere weekend met skiënde clowns zal ik nooit meer vergeten! Caleb, Annelotte, Sara, Pieter and Jean from ICHOM, thanks for the great conversations we had about value based health care. The work you do is an important step in the reforming of health care.

Dank aan de maatjes van de Nationale DenkTank, voor de inspiratie die ik van jullie heb gekregen en krijg: NDT'09 jullie zijn een fantastische groep mensen; Maaike ik heb je leren kennen als een heel goed vriendinnetje en samen delen we de fundering van het NDT alumnibestuur; EJ promotiesupport in de bergen en op de amstel; Jasper, CSO-er in hart en nieren; Harde kern Dr. Bot, Cash en JvT, passie voor de zorg, liefde voor Boston en een heerlijke tijd op de Amstel. Dank aan het alumnibestuur voor jullie energie! Jullie waren een van de weinige teams waar je als voorzitter je nooit druk hoeft te maken. Ik dank het NDT bestuur en Cassandra Hensen voor de flexibiliteit die ze hadden en begrip als ik niet aanwezig kon zijn op een vergadering i.v.m. mijn werk. Het was een groot plezier het lustrum voor te bereiden naast de promotie. Veel dank aan Lotte Wendt en teams vooruitblik, terugblik en alumnidag.

Een master bedrijfskunde is een pittige klus naast een promotie, maar zeker niet af te raden. Mijn dank gaat uit naar alle klasgenootjes van PtMsc16. Maarten, Jasper, Chris, Mignon, Jochem, Casper en Dreamteam Simon, Thomas, Tom, Sasha en Micha, dank voor de flexibiliteit tijdens de Boston-tijd. Programma management: Hannie, Ger, Monique en Myrthe dank voor jullie betrokkenheid. Door jullie heb ik gave start-ups en een groep bijzondere ondernemers in de USA gesproken. Professor Haico Ebbers dank voor de prettige samenwerking en flexibiliteit waardoor ik een manuscript heb kunnen schrijven over Zweedse vergoedingssysteem in de zorg voor wervelkolomchirurgie. Dank aan het COCMA onderwijs fonds, thanks to Fredrik Borgström, Jonas Wohlin and Jens Deerberg-Wittram, without your help and generosity the project would not have been such a great experience.

Dank aan het de eilanders voor het plezierige welkom als ik een weekend kom ontspannen en genieten van de kleine maar belangrijke dingen: golf, Skuumkoppe en Sjans. Ik dank mijn neef Ruben en zijn partner Monique voor het meedenken omtrent de laatste voorbereidingen bij het drukken van dit proefschrift. Geert Jan Jansen, dank voor het beschikbaar stellen van een van jouw werken voor dit proefschrift. Mijn dank gaat uit naar de Stichting STOPhersentumoren, KWF, EUR Trustfonds, Chipsoft, Promega, Zeiss, ABNAMRO en Ruben Dammers, die financiële ondersteuning hebben boden aan ofwel het onderzoek ofwel het drukken van dit proefschrift.

Gijs, heel veel dank gaat uit voor jouw mentale support, je frisse, heldere blik op zaken. Je weet wat men zegt over goede wijn. Deze hebben mij geholpen bij de staart van mijn promotie. Buiten de technische zaken waar je veel bij hebt geholpen, zoals stukken redigeren of de kaft van dit boekje bewerken, wil ik je nog meer danken voor de leuke tijd die we samen hebben en je onvoorwaardelijke geduld. Ook wil ik jouw familie danken voor hun luisterend oor en wijze lessen.

Lieve familie, mam, pap, Margaux, heel veel wil ik jullie danken voor de onvoorwaardelijke steun, luisterend oor, relativeringsvermogen en motiverende houding tijdens de afgelopen jaren. Altijd kon ik bij jullie terecht met ideeën, betere berichten maar ook de mindere berichten en wisten jullie mij de steun te geven die ik nodig had. Mam, pap en Margaux, zoals de paarden altijd iets van ons allen waren, zo is dit boek ook deels van jullie. Ik denk dat er geen woorden zijn om te omschrijven hoe blij ik met jullie ben. Ik ben blij dat jullie altijd achter mijn keuzes staan. Dat maakt dat 'thuiskomen' ook echt thuis is.

PhD Portfolio

PhD Portfolio

Name PhD student:	Lotte M.E. Berghauser Pont
Erasmus MC Dept:	Neurosurgery
Research School:	MolMed
PhD period:	2011-2015
Promotoren:	Prof. dr. C.M.F. Dirven
	Prof. dr. S. Leenstra
Copromotor:	Dr. M.L.M. Lamfers

PhD training

Courses

2013	Course on Animal research
2013	Workshop on BAGE
2012	Workshop on Partek
2012	Biomedical English Writing and Communication

Teaching

2013	Supervising research internship, Megan van Vooren (20 wks)
2013	Supervising research internship, Anoek van Leeuwen (20 wks)
2012	Supervising research internship, Somi Koria (20 wks)

Other activities

2014, 2015	Reviewer for several international journals
2014, 2015	Outcomes in glioma project
2011-2014	Master of Business Administration, Nyenrode Business University
2011-2014	Weekly working group lectures
2011-2014	JNI lectures

Presentations

04/2014	Poster presentation American Association for Cancer Research (AACR) – San Diego (USA)
03/2014	Poster presentation at Neurosciences Interdisciplinary retreat & poster session Brigham and Women's Hospital, Harvard Medical School –Boston (USA) (PhD, CSDH project)
01/2014	Poster presentation Neurosurgery Retreat Harvard Medical School – Harvey Cushing Neuro-Oncology Research Laboratories – Boston (USA)
12/2013	Invited oral presentation Harvard Medical School Department of Neurosurgery – Boston (USA)
11/2013	Poster presentation conference WFO/SNO Scientific Meeting – San Francisco (USA)

10/2013	Oral presentation conference LWNO – Utrecht (NL)
06/2013	Poster presentation conference Replicating Oncolytic Virus Therapy – Quebec (Can)
10/2012	Oral presentation conference LWNO – Utrecht (NL)
09/2012	Poster presentation conference European Association for Neuro-Oncology – Marseille (Fr)
01-03/2010; 04/2011	Oral and poster presentations on research on chronic subdural hematoma: Dutch Neurology and Neurosurgery Study Club, Rotterdam (NL); EANS Annual meeting, Groningen (NL); Winter meeting Dutch Society for Neurosurgery Utrecht.

Conferences (attendance, no presentation)

11/2014	Attendant at the ICHOM Conference in Boston (USA, at Harvard Business School) on value-based health care, a concept founded by Michael Porter.
11/2013	Attendant at the ICHOM Conference in Boston (USA)
10/2014	LWNO national meeting of Neuro-Oncology, Utrecht, The Netherlands
2011	Participant business course at Gupta Strategists, consultant in the health care sector

Manuscripts other than this thesis

Manuscripts (other than this thesis)

2015 Letter to the Editor: Deep venous thrombosis and pulmonary embolism; Volovici V, Dammers R, Berghauser Pont LM. **J Neurosurg**. 2015 Mar.

2015 Management of Chronic Subdural Hematoma: Part II—Treatment and Prognosis; Iris S. C. Verploegh, MD, Victor Volovici, MD, Ruben Dammers, MD, PhD, and Lotte M. E. Berghauser Pont MD. **Contemp Neurosurgery**. 2015 Feb.

2015 Management of Chronic Subdural Hematoma: Part II— Pathogenesis and Diagnosis; Iris S. C. Verploegh, MD, Victor Volovici, MD, Ruben Dammers, MD, PhD, and Lotte M. E. Berghauser Pont MD. **Contemp Neurosurgery**. 2015 Jan.

2015 ABT-888 enhances cytotoxic effects of temozolomide independent of MGMT status in serum free cultured glioma cells; Rutger K Balvers, Martine LM Lamfers, Jenneke J Kloezeman, Anne Kleijn, Lotte ME Berghauser Pont, Clemens MF Dirven, Sieger Leenstra; **Translational medicine**. 2015

2015 Master thesis: Value-based reimbursement in health care. Lotte ME Berghauser Pont, Prof. Dr. H. Ebbers, J. Deerberg-Wittram

2013 Ambivalence among neurologists and neurosurgeons on the treatment of chronic subdural hematoma: a national survey; Berghauser Pont LM, Dippel DW, Verweij BH, Dirven CM, Dammers R.; **Acta Neurol Belg**. 2013 Mar.

2012 The role of corticosteroids in the management of chronic subdural hematoma: a systematic review; Berghauser Pont LM, Dirven CM, Dippel DW, Verweij BH, Dammers R; **Eur J Neurol**. 2012 Nov.

2012 Currarino's triad diagnosed in an adult woman; Berghauser Pont LM, Dirven CM, Dammers R.; **Eur Spine J**. 2012 Jun

2012 Clinical factors associated with outcome in chronic subdural hematoma: a retrospective cohort study of patients on preoperative corticosteroid therapy; Berghauser Pont LM, Dammers R, Schouten JW, Lingsma HF, Dirven CM. **Neurosurgery**. 2012 Apr

2008 Bachelor thesis: interactions of anti-epileptics and drugs for Trimbos-Institute. Lotte ME Berghauser Pont

2007 Tromboprofylaxis for cancer patients (translated from Dutch 'Tromboprofylaxe bij kankerpatiënten´, pharmaceutical literature review). **Pharmaceutical Weekly** the Netherlands. Supervisor Prof. Dr. Schellens.

About the author

About the author

Lotte Marie Elise Berghauser Pont was born on May 5th 1985 in Soest, The Netherlands as a daughter of a healthcare economist and an entrepreneur. At age 15, Lotte left the regular secondary school 'Het Baarnsch Lyceum' to spend her time as a professional horse rider (showjumping) as a member of the juniors and young riders national team. She independently finished 'Gymnasium' in 2003 by central exams in Amsterdam. At this time, Lotte was part of the national team competing in the European Championships for showjumping in San Remo (It).

After another year of international competitions, Lotte got her bachelor's degree in pharmaceutical sciences at Utrecht University in 2007. She continued with fast track Selective Utrecht Medical Master (SUMMA) in 2007 at the University Medical Center Utrecht. In 2008, Lotte encountered an interesting research topic on chronic subdural hematoma, a common neurosurgical condition in the elderly, under supervision of prof.dr. C.M.F. Dirven and dr. R. Dammers at the Erasmus Medical Center (Department of Neurosurgery). During her studies, Lotte took part in a university honors programme, was active in various student society committees and was selected for the National ThinkTank in 2009. Later on, Lotte would become a board member of this organization and co-founded its alumni board.

After graduating cum laude from the medical school in 2011, and inspired by the concept of oncolytic virus therapy, Lotte moved to Rotterdam to research combined therapies and precision medicine for malignant brain tumors. This has resulted in the work described in this thesis under supervision of prof.dr. C.M.F. Dirven and prof.dr. S. Leenstra. Late 2013 she visited the research group of prof.dr. E.A. Chiocca at the Harvard Medical School in Boston for 6 months. Motivated by the dynamics of organizations (including those in health care), Lotte concomitantly graduated cum laude as a Master in Business Administration at Nyenrode University in 2014, having written a thesis about a value-based reimbursement system for Spine Surgery in Sweden. Currently Lotte is a neurosurgical resident at the ErasmusMC.